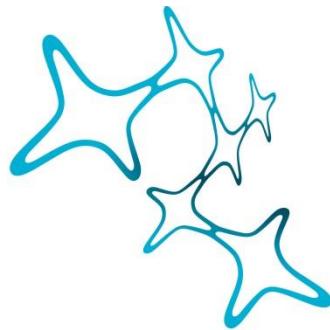


"PHYSICAL ACTIVITY HETEROGENOUSLY MODULATES NG2-GLIA POPULATION BEHAVIOUR, AND IS NECESSARY FOR COGNITIVE ENHANCEMENT"

Jaime Theodore Eugenin von Bernhardt



Graduate School of
Systemic Neurosciences

LMU Munich



Dissertation der
Graduate School of Systemic Neurosciences
der Ludwig-Maximilians-Universität München

June, 2020

Supervisor
Prof. Dr. Leda Dimou
Molecular and Translational Neurosciences
Department of Neurology
Ulm University

First Reviewer: Prof. Dr. Leda Dimou
Second Reviewer: Prof. Dr. Benedikt Grothe
External Reviewer Prof. Dr. Dieter Chichung Lie

Date of Submission: 02nd of June, 2020
Date of Defense: 09th of October, 2020

I would like to dedicate this Ph.D. thesis to the two scientists that have guided my scientific career. My parents: Professor Jaime Eugenin and Professor Rommy von Bernhardi, whose passion for knowledge and science, have been a real inspiration for me. Without their intelligence, support, and love, this thesis would not have been possible to do. If one day, I become half the great scientist and person as they are, my success will be ensured.

Contents

Abstract.....	7
Introduction	8
The end of the neuro-centric view of the world.....	8
The rise of the glia golden age	9
Glial cells in the CNS and their interactions with neurons and circuits	10
Microglia and the “innate immune system” of the CNS	11
Macroglia and their broad spectrum of different glial cells.....	14
Astrocytes, the current “big stars” among glial cells in the CNS.....	15
Oligodendrocytes and myelination, construction of the fast information highway.....	20
NG2-glia, the enigmatic new glial population.....	24
NG2-glia: Solely oligodendrocyte progenitor cells or neural stem cell-like progenitor cells?	25
NG2-glia heterogeneity, are all NG2-glia born equally?	28
Role 1 - Restoring myelin in the CNS	31
Role 2- Surveillance, reaction, and repair	32
Role 3 – Adaptive myelination, a new form of CNS plasticity	34
NG2-glia behavior and dynamics modulated by neuronal activity	36
Talking to NG2-glia through signals and neuron-NG2-glia synapses	38
The million-dollar question: How does myelination induced by modulation of NG2-glia behavior leads to changes in brain plasticity?	40
The aim of this doctoral thesis.....	44
Material and methods	48
Materials	48
Chemical and reagents	48
Homemade solutions recipes	50
Antibodies.....	50

Consumables.....	51
Equipment, devices, and instruments.....	52
Software.....	53
Methods	54
Animals, transgenic lines, housing, and running performance tracking.....	54
DNA extraction and Genotyping.....	57
Tamoxifen induction and BrdU or EdU treatment	59
Histology and Immunofluorescence.....	60
Magnetic associated cell sorting (MACS)	62
Liquid chromatography-mass spectrometry	64
Analysis of cognitive and motoric behavior	65
Statistical analysis.....	68
Results.....	69
Dynamics of proliferation and differentiation of cortical NG2-glia after VPA in the adult mouse brain.....	69
Dynamics in indirect and direct NG2-glia differentiation modalities after VPA in the adult mouse brain.....	76
Proteomic profiling of cortical NG2-glia after VPA by a combined MACS/LC-MS ² approach ..	80
Dynamics of the population of GPR17 ⁺ NG2-glia after VPA in the adult mouse brain.....	87
Differentiation of GPR17 ⁺ NG2-glia after VPA in the adult mouse brain.....	89
Limitations of NG2-glia plasticity after long-lasting VPA	91
Generation and integration of newly generated myelinating oligodendrocytes into the circuit after VPA in the adult mouse brain.....	94
Genetic ablation of proliferating NG2-glia as a model for blocking their differentiation, and its effects in the locomotor activity of adult mice.....	97
Genetic ablation of proliferating NG2-glia, as a model for blocking their differentiation, and effects in cognitive performance of adult mice	101
Genetic ablation of proliferating NG2-glia, as a model for blocking their differentiation, and adult neurogenesis in the mice.....	103
Genetic deletion of Shank3 in the oligodendrocyte lineage and the role of synapses in NG2-glia differentiation in the adult mice	106

Discussion and future perspectives	111
Conceptual and technical dimension of our experimental paradigm for VPA	113
NG2-glia behavior dynamics after VPA	119
Heterogeneous effect of VPA on NG2-glia.....	122
A possible role of GPR17 ⁺ NG2-glia in plasticity and adaptive myelination	126
Oligodendrogenesis promoted by VPA plays a role in exercise-induced cognitive enhancement	128
Possible circuits remodeled by adaptive myelination promoted by VPA.....	132
Possible mechanism of action of VPA.....	135
Exercise and NG2-glia, a target for a possible treatment?	142
Conclusion.....	147
References	149
Acknowledgements.....	172
Appendix	174

Abstract

NG2-glia is a macroglial population, which constitutes about 5-10% of the total cell population in the mammalian brain. These cells have “stem cell-like” features; for instance, they can proliferate and self-renew and they mostly differentiate into oligodendrocytes, a cell type are of great importance as they myelinate axons in the central nervous system, a process essential for the proper function of vertebrates’ nervous system. Although most myelination happens after birth and completed at a young age, it has been shown that it can also occur during adulthood in mammals. Adult myelination can be modulated by experience, but the exact mechanism of this phenomenon remains unclear. Hence, it is thought that neuronal activity could stop the proliferation and promote the differentiation of NG2-glia, and in turn, newly generated oligodendrocytes could provide the new myelin. However, it is still unclear how neuronal activity could lead to changes in NG2-glia behavior in the adult mouse. In this doctoral thesis, I have used a voluntary physical activity (VPA) mouse model to study the effects of experience on NG2-glia, although other mechanism cannot be discarded. Indeed, our results showed an increase in the proliferation and differentiation of NG2-glia in the cerebral cortical grey matter but not in the corresponding white matter after VPA. We also observed that NG2-glia tend to differentiate with two different modalities, and one of them is preferred during VPA. Furthermore, I performed mass spectrometry of sorted NG2-glia to profile them after VPA, and found that the remaining, non-differentiated NG2-glia show less myelin-related proteins. Interestingly, the results of the proteome analysis correlate with the increase in the number of the GPR17⁺ subset of NG2-glia, which is characterized by its slow differentiation rate, and I observed that this population remains mostly unaffected by VPA. Finally, for the first time, I found that newly generated oligodendrocytes integrate into the circuitry of the cortex and this myelin remodeling contributes in cognitive enhancement induced by exercise.

Introduction

The end of the neuro-centric view of the world

The nervous system has the fundamental task of transmitting and processing information. All animals have some kind of nervous system, except distant relatives from the *Porifera phylum*. The ability to perceive our environment, to be self-aware, to run, to fear, to memorize, or, for my dearest readers, to enjoy this thesis, are all results of this complex system.

Mammals' nervous system can be broadly divided into: the central nervous system (CNS) and the peripheral nervous system (PNS). The former is composed of the brain and the spinal cord, and the latter by nerves and ganglia. Thereby, PNS acts as the interface between peripheral tissues, such as the retina, salivary glands, muscles, or stomach, and the CNS. In its turn, the CNS can process afferent input or exert action on the periphery, such as interpretation of visual input, increase saliva secretion in response to the smell of a delicious meal, or to feel stomach butterflies when your loved one passes you by.

The nervous system parenchyma is mainly composed of two cell populations: neurons and glial cells. Neurons are electrically excitable cells with a prototypic morphology: dendrites, soma, axon, and axon terminal. These cells have been the focus of neuroscientists for more than a century, and for good reasons. Any neuroscience textbook would show that an average mouse, and human brain contains $\sim 7 \cdot 10^7$ and $\sim 10^{12}$ neurons, respectively (Ero et al. 2018; von Bartheld, Bahney, and Herculano-Houzel 2016). Neurons are key players for information processing and transmission in the nervous system due to four features. First, their membrane potential is dynamic and modified by a broad spectrum of stimuli provided by other neurons, non-neuronal cells, or directly from external sources (e.g., heat, pain, pH). The depolarization of the membrane potential can trigger an "action potential," which is a discrete, abrupt, and transient reversal of the membrane potential that represents the mechanism of encoding neuronal information. Second, information within a neuron flows from the initial to the terminal axonal segments. This propagation is possible thanks to the depolarization-dependent regeneration of action potentials along the axonal segments, which allows them to travel long

Introduction

distances to depolarize the axon terminal compartment. Third, neurons are connected and transmit information through the “synapses,” which are formed between axon terminals of one neuron and the dendrites of another one, allowing the formation of networks and providing the foundation of information processing. Neurons can also communicate with other cell types to receive a signal when stimulated or deliver a message to execute a function. Fourth, there is an extraordinary variety of neuronal types that can promote or inhibit the networks activity, tuning the circuit and resulting into different outcomes.

These principles give the impression that neurons have monopolized the computational capacities of the nervous system, and thereby, neuroscience research. Nevertheless, it has been shown that neurons cannot regulate several of their cellular processes by themselves, such as energy and neurotransmitters metabolism, homeostasis, repair, as well as sensory reception and information processing. Were scientists overseeing something? Over the last two decades, neuroscientists are turning their heads towards the other major group of cells in the nervous system, the glial cells to search of answers.

The rise of the glia golden age

The term “glial cells” lacks a biological description for this group of cells. Its historical origin is due to misconceptions of researchers at the time. Rudolf Virchow first coined the term “glia” and published it in the article “*Über das granuliert Aussehen der Wandungen des Gehirnaventrikels*” in 1856. In this context, Virchow was pursuing to study the connective tissue of the brain, and initially, he was convinced that a large population of cells composed it. He called them “glial cells,” which derives from the Greek word “glue” because he speculated that their primary function was a structural one: “to keep the nervous tissue together.” Virchow published his textbook “*Cellularpathologie*” in 1858, which became an important starting point to the research of this newly discovered cell population.

For this reason, the term is currently used as a synonym for non-neuronal cells. Notably, it is estimated that the total number of glial cells in CNS is similar to the neuronal population, being $\sim 3 \cdot 10^7$ in mice and $\sim 5 \cdot 10^{11}$ in humans (von Bartheld, Bahney, and Herculano-Houzel

2016; Ero et al. 2018), representing something around 30 – 50% of the total cell population of the CNS. This imprecise number is due to differences in number of glial cells within the various CNS regions in the species that had been studied.

During the last decade considerable efforts have been made to describe the glia identity and their function in-depth, which has provided a roughly coherent classification of the glial cells in the nervous system. In principle, glial cells are divided according to their localization in the nervous system: in the PNS, e.g., Schwann cells, satellite cells, and enteric glial cells, and in the CNS. The latter, in turn, is classified regarding their embryonic origin. **Microglia**, rising from the mesoderm, and **macroglia**, deriving from the neuroectoderm. Macroglia includes astrocytes, ependymal cells, radial glia, oligodendrocytes, and, only recently categorized, NG2-glia.

In this doctoral thesis, the focus will be set mainly in the NG2-glia population and how experience-related events modify their behavior, and, their possible role in information processing in the CNS. In order to describe the intrinsic characteristics of the NG2-glia population and to distinguish this population from the rest of the glia, I will provide a brief description of other glial cells in the CNS. This characterization will evidence their fundamental role in the nervous system function and essential players in regulating neuronal activity and neural network functions.

Glial cells in the CNS and their interactions with neurons and circuits

As mentioned earlier, CNS glial cells can be classified into two major groups: microglia and macroglia. This categorization, mainly given by their different ontogeny, does not reflect on the distinctive functions and morphologies among these cells. Therefore, in the next section of this introduction, I will describe the different glial cells in the CNS, setting our focus solely on the four largest populations present in the adult brain: microglia, astrocytes, oligodendrocytes, and NG2-glia.

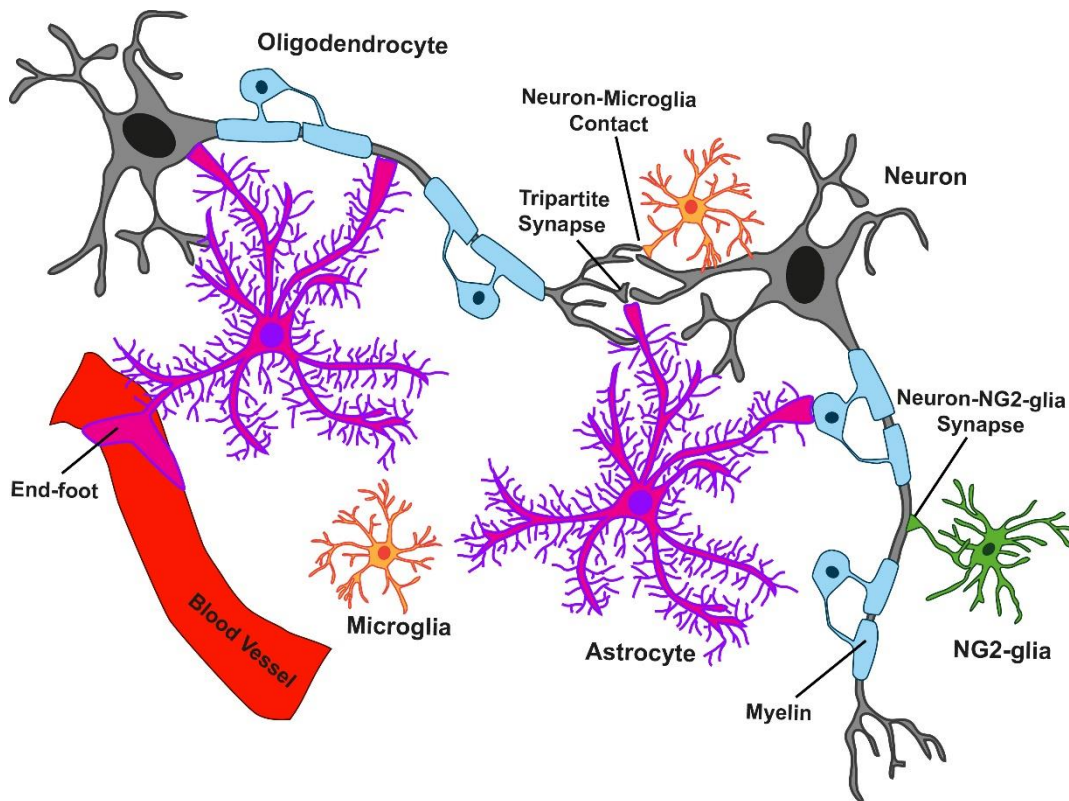


Figure 1. The mammalian CNS has four major glial cell populations: astrocytes, microglia, oligodendrocytes, and NG2-glia. Here I illustrate that all glial cells have physical interaction with neurons. Astrocytes are associated to the soma, axons, and synapses of neurons, the latter known as the tripartite synapse. Additionally, astrocytes are associated to the arterioles by the astrocytic end-foot and they are connected with other astrocytes as well as with oligodendrocytes through gap junctions known as “connexins”. Microglia interact physically with synapses through neuron-microglia contacts. Oligodendrocytes extensive membrane wraps around axons forming the myelin sheath, which provides not only the electrical insulation of axons but also by this structures oligodendrocytes support metabolically neurons. NG2-glia, the cells that generate oligodendrocytes, also interact with axons by forming neuron-NG2-glia synapses. All these structures are important for the regulation of neuronal activity and, in consequence, enable the glial cells to modulate the CNS circuits; therefore, information processing.

Microglia and the “innate immune system” of the CNS

Microglia constitute ~10% of the total cells in the adult mouse CNS (Ero et al. 2018; Lawson et al. 1990). They are the CNS immunocompetent cells having many similarities regarding markers and functions with the monocyte-macrophages family in the periphery (**Fig.1**). Microglia derive from early hematopoietic precursors cells from the yolk sac (Alliot, Godin, and Pessac 1999; Ginhoux et al. 2010), which, in turn, are descending from germinal cells of the mesodermic germ layer. During development, microglia exit the yolk sac and invade the brain at ~E9.5 and rapidly expand in the CNS, reaching ~95% of their final population at postnatal day 2 (P2) in mice (Alliot, Godin, and Pessac 1999). After their expansion, microglia keep constant their population,

Introduction

not requiring additional peripheral progenitors, even after total population depletion (Askew et al. 2017; Bruttger et al. 2015). Once settled in the CNS, microglia constantly surveil and sense the immediate environment through their high dynamic processes (Nimmerjahn, Kirchhoff, and Helmchen 2005; Davalos et al. 2005), thereby, together with their immunogenic origin, researchers have studied the role of microglia in pathology profoundly.

Microglia are the first cells in the frontline and react quickly in a broad spectrum of CNS insults and pathologies. Microglia respond to injuries in CNS by extending their processes and polarizing towards the insult, proliferating, and becoming hypertrophic (Davalos et al. 2005; Nimmerjahn, Kirchhoff, and Helmchen 2005; Simon, Gotz, and Dimou 2011), a process that appears to be regulated by the ATP released from damaged tissue (Davalos et al. 2005). There are many additional molecular signals like danger-associated molecule patterns (DAMPs) and inflammatory cytokines, such as interferon γ (IFN- γ), interleukin (IL-1 α), IL-6, and tumor necrosis factor α (TNF- α) that also participate in this process (Donat et al. 2017). Neurodegenerative diseases in which chronic neuroinflammation is observed, microglia react strongly by changing their morphology and gene expression profile (Salter and Stevens 2017; Song and Colonna 2018). So far goes our understanding, the functions of microglia in pathology appears to be inflammation modulators, providing both pro- and anti-inflammatory cytokines to coordinate various cell populations, to engulf aggregates of protein, debris and dead cells, provide repair signals, etc. (Song and Colonna 2018).

The extensive role of microglia in pathology has caught most of the attention of researchers because of their potential translational and, hence, medical relevance. By comparison, there is less understanding of the microglial role in the healthy brain. Nonetheless, there are significant advances in exploring the different functions that microglial might have in modifying neuronal activity.

One of their most important functions is related to the proper development of neuronal circuits during development. Shortly after birth, microglia engulf multiple synapses, in a process known as “synaptic pruning” and sculpts neuronal dendrites by reducing the number of spines; the structure in which synaptic input is received. The disruption of this biological process leads

to the delay of synaptic maturation of the hippocampus (Paolicelli et al. 2011). The mechanisms and signals for synaptic pruning are not entirely understood, but it appears that fractalkine and complement pathway (especially complement receptor/complement 3 (CR/C3)) are essential (Schafer et al. 2012; Paolicelli et al. 2011) and neuronal activity input seems to be crucial to its proper delivery (Schafer et al. 2012). This unprecedented function has raised the question; how does microglia know where synapses are? And how neuronal activity is transferred to microglia?

Furthermore, in the healthy adult brain, a close structural interaction between microglia processes and neuronal synapses, denominated “microglia contact,” (**Fig. 1**) has been shown by various methods, such as electron microscopy (EM), immunostaining, and *in vivo* two-photon microscopy (Wake et al. 2009; Akiyoshi et al. 2018). Notably, this interaction seems to be experience-dependent. For example, such contacts decrease in the visual pathway by reducing neuronal activity by either deprived visual input by ocular tetrodotoxin (TTX) injection (Wake et al. 2009) or by housing animals in the dark (Tremblay, Lowery, and Majewska 2010).

Little is known about the function of microglia-neuron contacts, but it is tempting to suggest that they represent a mechanism to supervise the neuronal activity. Moreover, microglia do express receptors for different neurotransmitters, such as glutamate, γ -aminobutyric acid (GABA), serotonin, substance P, histamine, purinergic mediators. Their application leads to behavioral changes in microglia, such as process extension, polarization, migration, and changes in intracellular calcium (Davalos et al. 2005; Fontainhas et al. 2011; Seifert et al. 2011). What seems intriguing is that it has been reported that the sudden physical interaction between a microglia process and a dendritic spine leads to an increase in the frequency of local calcium (Ca^{+2}) transients in dendritic spines, promoting local circuitry synchronization (Akiyoshi et al. 2018). Thus, it seems that these contacts are not just for a mere monitoring but also have a modulatory effect on synaptic transmission, neuronal activity, and circuit plasticity by mechanisms that are still poorly understood.

Microglia possess a comprehensive set of skills that allow them to contribute to brain plasticity. For instance, as explained above their ability to engulf and remove synapses during development. Moreover, under pathological conditions, microglia remove synapses in adult mice

after PNS injury, known as synaptic stripping, which makes it a possible mechanism for plasticity (Kettenmann, Kirchhoff, and Verkhratsky 2013). Nonetheless, it was thought that this process does not take place in the healthy adult brain. Only very recently, it has been shown that microglia actively engulf synapses to promote the extinction of fear-related memories by targeting synaptic spines through a complement-dependent mechanism in the adult healthy mouse brain (Wang, Yue, et al. 2020). The inhibition of the complement pathway leads to deteriorated fear-conditioned extinction (Wang, Yue, et al. 2020).

It has also been shown that microglia may have additional mechanisms to modulate brain plasticity. For instance, ablation of microglia leads to deteriorated dendritic spine turn over, and reduced learning or memory capacities (Parkhurst et al. 2013). In this process, researchers found that brain-derived neurotrophic factor (BDNF) secreted by microglia played a significant role (Parkhurst et al. 2013). Furthermore, it has been described that microglia are essential regulators of neurogenesis in the classical neurogenic niches, removing cells undergoing apoptosis through phagocytosis (Sierra et al. 2010), and also provide signals that promote proliferation and differentiation of neural stem cells (NSCs) *in vitro* and *in vivo* (Walton et al. 2006; Battista et al. 2006). Thus, microglia regulate the number of newly generated neurons that would be, later, integrated into the brain circuitry, contributing to a new way of brain plasticity.

Macroglia and their broad spectrum of different glial cells

As previously mentioned, all macroglia in the CNS originate from pseudostratified cells that conform the neural plate, known as neuroepithelial cells, and are sustained by multiple symmetric divisions (Dimou and Gotz 2014; Kriegstein and Alvarez-Buylla 2009). These cells become an apical-basal polarized cells named “**radial glia,**” which in turn proliferate asymmetrically to generate the different cells in the CNS (Kriegstein and Alvarez-Buylla 2009; Dimou and Gotz 2014).

During mice development, after E8, radial glia give rise to neurons, a process known as “neurogenesis” that continues thoroughly after birth and even into adulthood but only in selected regions called “neurogenic niches,” such as the dentate gyrus (DG) of the hippocampus,

the subventricular zone (SVZ, or subependymal zone in adult), and the hypothalamus (Anthony et al. 2004; Kriegstein and Alvarez-Buylla 2009; Dimou and Gotz 2014; Kempermann, Kuhn, and Gage 1997; Knoth et al. 2010). Interestingly, adult neurogenesis is experience-dependent by mechanisms that are still not fully understood (Kempermann, Kuhn, and Gage 1997; van Praag et al. 1999). Radial glia also originates other glial cells later in embryonic development, such as **astrocytes** and **NG2-glia**, the latter also known as oligodendrocyte progenitor cells (OPCs) that eventually will differentiate into **oligodendrocytes**. During development, the generation of glial cells is known as “gliogenesis” (Kriegstein and Alvarez-Buylla 2009).

Astrocytes, the current “big stars” among glial cells in the CNS

Astrocytes are one of the most studied population of glial cells of the CNS (**Fig.1**) (Sierra et al. 2016) and, thereby, they have been bestowed with many functions in the healthy and pathologic CNS. Some estimates suggest that the astrocyte population might represent between ~5 – 20% of the cells in the mouse brain (Ero et al. 2018; Sun et al. 2017) and ~20% in the human brain (Pelvig et al. 2008); however, we still ignore the exact number of astrocytes and studies do not find agreement on the topic.

Astrocytes morphology is commonly described as multiprocessed “stellate-shaped” cells, a description very distant from precise. They indeed have many cytoplasmic projections, with a well-defined arrangement. Close to their cell body are few thicker projections, known as “primary branches” and from these, smaller extensions protrude, which, in turn, even thinner processes arise. Thereby, astrocytes form a very compact dense mesh of projections, having a more spongiform-like morphology (Sofroniew and Vinters 2010; Bushong et al. 2002; Xu, Wang, and Zhou 2014; Ogata and Kosaka 2002).

Astrocytes are impressively heterogeneous. In terms of their morphology, they are classified as “protoplasmic,” which have many short, dense isotropic-distributed processes, and can be found mainly in the cortical grey matter (GM) and hippocampus (Bushong et al. 2002; Ogata and Kosaka 2002).. They establish individual cell-territories in such a way that only ~5% of the volume domain overlaps to each other, providing a homogeneous distribution (Bushong et

al. 2002; Oberheim et al. 2009; Wigley et al. 2007). In contrast, astrocytes in the white matter, specifically in the corpus callosum, have been defined as “fibrous,” having less ramified longer processes, whose distribution is anisotropic (Sofroniew and Vinters 2010; Emsley and Macklis 2006). Nowadays, this early characterization appears to be a huge oversimplification. Not only morphologically variations have been described among different astrocytes, which have a regional specificity, but astrocytes also appear to have a broad spectrum of distinctive electrophysiological properties, differential expression of GFAP, glutamate transporters, receptors, gap junction, and even robust species-specific differences, as it has been described between rodents and humans (Oberheim et al. 2009; Walz and Lang 1998; Matyash and Kettenmann 2010).

Astrocytes are an integral component of the blood-brain barrier (BBB), as well as key to the formation and maintenance (Araya et al. 2008; Janzer and Raff 1987; Kuchler-Bopp et al. 1999). Alteration of astrocyte function leads to BBB malfunction, immune cell infiltration, and leakage from the bloodstream (Araya et al. 2008; Faulkner et al. 2004). Structurally speaking, EM analysis has revealed that astrocytes associate with the blood vessels epithelia by a specialized process known as “astrocytic end-foot” (**Fig.1**) (Araya et al. 2008). Because of this close interaction between blood vessels and astrocytes, it is not surprising that it has been shown that these cells can regulate the cerebral blood flow (CBF). Interestingly, this suggests that astrocytes might act as vascular-neuron intermediaries, and its role is essential for coupling neuronal activity and the CBF to match metabolic demands to network activity (Harder, Zhang, and Gebremedhin 2002).

Glial cells, in general, are fundamental metabolic suppliers of neurons in physiological conditions. The brain requires incredible amounts of energy, and a significant fraction comes from the catabolism of carbohydrates, namely glucose. Among others, astrocytes have been shown to feed neurons by providing glucose directly (Occhipinti, Somersalo, and Calvetti 2009; Dringen, Gebhardt, and Hamprecht 1993) or storing it in the form of glycogen for mid-short usage (Cataldo and Broadwell 1986). Additionally, in anaerobic conditions (diminish or lack of oxygen), astrocytes produce and transport lactate, which is further metabolized by neurons as an

Introduction

alternative source of energy (Suzuki et al. 2011; Walz and Mukerji 1988; van Hall et al. 2009; Wyss et al. 2011).

In the pathologic CNS, astrocytic markers like GFAP, which upregulation is characteristic in activated astrocytes of the GM, has been widely used for the histological and biochemical analysis of nervous tissue during inflammation and damage (Sofroniew and Vinters 2010). Whereas holding some resemblance with the activation of microglia, astrocytes react at later time points than microglia after brain trauma, showing temporally regulated distinctive responses, such as hypertrophy, moderate proliferation, and polarization, which goes together with process extension towards the injury site (Bardehle et al. 2013; Simon, Gotz, and Dimou 2011). Nonetheless, they do not show migratory behaviors towards the insult, like other glial cells do (Dimou and Gotz 2014; Bardehle et al. 2013). Reactive astrocytes have been shown to restrict damage in the CNS, helping in the scar formation, regulating inflammation and immune cells infiltration, and also for BBB repair (Bush et al. 1999; Araya et al. 2008; Voskuhl et al. 2009; Faulkner et al. 2004). Astrocytes have been also shown to participate in various neurodegenerative diseases, like Alzheimer's disease (AD), Parkinson's disease (PD), multiple sclerosis (MS), and amyotrophic lateral sclerosis (ALS) (Sofroniew and Vinters 2010).

Additionally, astrocytes maintain the brain homeostasis and serve essential functions on the modulation of neuronal activity. They uptake extracellular potassium (K^+) mainly by inward rectifying channels, like Kir4.1 (Seifert et al. 2009), which mediates hyperpolarization of the neuronal membrane, preventing the increase of neurons excitability. Additionally, extracellular glutamate is uptaken from the interstitial space by the astrocytic glutamate transporters EAAT1 & 2. This process effectively avoids the increase of tonic activation of glutamate receptors after its release from the presynaptic terminal, and reducing the excitotoxicity glutamate-driven (Rothstein et al. 1996; Tanaka et al. 1997).

The role of astrocytes in preserving CNS homeostasis includes as well the control of pH, through different proton exchange-transporters and pumps, and modulates water movement by aquaporins (AQP), the latter allowing the flow of water by osmotic gradients (Obara, Szeliga, and Albrecht 2008; Simard and Nedergaard 2004). Finally, astrocytes participate in the homeostasis

of neurotransmitters, like glutamate and GABA, by removing them from the extracellular space, synthesizing their molecular precursors in a process known as the “glutamate-GABA-glutamine cycle,” and degradation (Norenberg and Martinez-Hernandez 1979; Zielke et al. 1998; Hertz and Hertz 2003; Ishibashi, Egawa, and Fukuda 2019; Hertz and Zielke 2004).

During the CNS development, astrocytes are critical for the migration of neuronal precursors and the extension of their projections to their target sites within the CNS, both being highly regulated by environmental, cellular, and extracellular molecular cues. Astrocytes provide different signals, additionally to serve as substrate for axon guidance and neurites expansion (Banker 1980; Powell and Geller 1999; Gage, Olejniczak, and Armstrong 1988), an essential feature of the CNS embryonic and postnatal development. In addition, the normal synapse formation, maturation, and stabilization take place under the rigorous modulation of astrocytes, which provides the molecular signals to the proper formation of synapses (Christopherson et al. 2005; Ullian et al. 2001).

In the adult brain, astrocytes have been shown to interact with 80% of neuronal synapses in a highly specialized structure known as the “tripartite synapse” (**Fig.1**) (Perea, Navarrete, and Araque 2009; Halassa et al. 2007). The tripartite synapse has been hypothesized to be the foundation of many functions that astrocytes accomplish in the CNS like glutamate uptake, CBF regulation, and metabolic supply of neurons, etc.

In vitro and *in vivo* experiments have shown that astrocytes express multiple surface receptors, such as glutamatergic, GABAergic, cholinergic, dopaminergic, purinergic receptors, among many others (Shigetomi et al. 2008; Bowser and Khakh 2004; Kang et al. 1998; Araque et al. 2002; Corkrum et al. 2020; Perea, Navarrete, and Araque 2009; Hoft et al. 2014). Notably, astrocytes are electrically non-excitabile cells. Still, their activation leads to the stereotypical response of an increase of their intracellular Ca^{+2} ($[\text{Ca}^{+2}]_i$), which can trigger a signaling cascade and evoke astrocyte responses, including the release of vesicles filled with different molecular signals. In analogy to neurotransmitters, these signals have been named gliotransmitters, with the main ones being D-serine, ATP, and glutamate (Tan et al. 2017; Beltran-Castillo et al. 2017; Gourine et al. 2010; Bezzi et al. 2004; Fiacco and McCarthy 2004). An outstanding feature of

Introduction

astrocytes is that they constitute a syncytium due to the expression of connexins that couples adjacent astrocytes (Xing et al. 2019). The increase of $[Ca^{+2}]_i$ in one cell leads to the activation and subsequent augmentation of $[Ca^{+2}]_i$ in neighboring astrocytes, which allows the propagation of the so-described “calcium wave” (Oberheim et al. 2009; Fiacco and McCarthy 2004). This characteristic provides an extraordinary concept to the field because it suggests that astrocytes not solely react locally but also in a long-range.

The release of gliotransmitters can regulate neuronal circuitries. It has been shown that changes in astrocytes $[Ca^{+2}]_i$ correlate neuronal *N*-methyl-*D*-aspartate (NMDA) receptor slow inward currents by a PAR-1 dependent mechanism (Shigetomi et al. 2008). In the same line, the manipulation of astrocytes $[Ca^{+2}]_i$, by an optogenetic approach, leads to the release of ATP and the activation of purinergic receptors, which simultaneously repress activity of pyramidal neurons by two mechanisms. First, by increasing the membrane hyperpolarization of pyramidal neurons. Second, by increasing the activity of cholecystokinin (CCK) inhibitory interneurons, a superb example of local circuitry modulation (Tan et al. 2017). Additionally, the activation of astrocytes, by hypercapnia (increase in blood carbon dioxide (CO₂) concentration) or diminished pH, augments the firing rate of respiratory motor neurons, increasing respiratory frequency (Gourine et al. 2010; Beltran-Castillo et al. 2017), playing a role of interoceptors.

Another mechanism by which astrocytes could modulate brain plasticity is through the promotion of synaptic scaling by the release of TNF- α (Stellwagen and Malenka 2006), an arrangement in which neurons can detect changes in their firing rate through regulation of their receptor trafficking and scale it to the accumulation of glutamatergic receptors at synapses. Additionally, astrocytes can regulate neurogenesis by modulating NSCs proliferation and progressive maturation *in vitro* and *in vivo* models (Ashton et al. 2012; Song, Stevens, and Gage 2002).

To date, despite the agreement that astrocytes have a modulatory effect on neuronal networks, little is known concerning the contribution of astrocytes in different animal behaviors. A recent study reported astrocyte-dependent synaptogenesis in the striatum, modulated by

GABA release by neighboring neurons, which underlies behaviors including hyperactivity and disrupted attention (Nagai et al. 2019).

Oligodendrocytes and myelination, construction of the fast information highway

The oligodendrocyte lineage remains one of the most mysterious group of glial cells in the CNS. Like for astrocytes, the total amount of oligodendrocytes in the CNS is deceiving. It is estimated that the size of the population ranges from ~15 – 20% (Ero et al. 2018; Valerio-Gomes et al. 2018) and ~40 – 50% (Pelvig et al. 2008) of the total cell population in the mouse and human brain, respectively. Most oligodendrocytes arise shortly after birth, and are generated by the differentiation of NG2-glia, which I have a devoted section to revise these cells later in this introduction. Regarding the distribution of oligodendrocytes, in contrast to other glial cells, this is not homogenous in the CNS, being enriched in areas known as white matter (Tomassy et al. 2014; Ero et al. 2018).

In the current research, it is almost impossible to talk about oligodendrocytes without mentioning, in some fashion, their ability to synthesize myelin in the CNS. In simple terms, myelin is a highly compacted multilayer that is originated by the massive production and extension of the cellular membrane of oligodendrocytes' processes, which wraps around the neuronal axons (**Fig. 2b**). This biological process is known as “myelination,” (**Fig. 2a**) and is critical for the proper function of the CNS as it enables the fast conduction of action potential along the axons. Myelin distribution in the CNS correlates with oligodendrocyte distribution, and it is this biological structure that gives the “white” color in the WM due to the way light scatters because of the molecular composition of the myelin. Just to put on perspective, WM occupies ~44% of the total volume of the CNS (Laughlin and Sejnowski 2003).

From an evolutionary perspective, fast conductivity along the axon was only possible by increasing the axons caliber because it reduces the axial electrical resistance (Hartline and Colman 2007). Well-known examples are the giant squid axon and the axons of the Mauthner cells in the crayfish and goldfish. Although small and big organisms indeed show axonal gigantism, this anyhow limits the number of axons in relation to their size (Hartline and Colman 2007). A

Introduction

brilliant adaptation came with the electrical insulation of axons by myelin, which was developed by members of the subphylum of gnathostome vertebrates and myelin-like structures by some species of invertebrates, such as the shrimp and copepod (Davis et al. 1999; Heuser and Doggenweiler 1966). The latter consist of concentric ensheathment by multiple flattened glial processes and mostly uncompacted sheaths (Salzer and Zalc 2016). Myelinated axons allow smaller caliber axons; therefore, a high number of neurons with high speed conductivity can be packed in an organism. More importantly, myelin accelerates conduction more efficiently than increasing the axon caliber (Tolhurst and Lewis 1992). Notably, within the animal kingdom, myelin and myelin-like structures do not have a common ancestry, but they were independently generated among the different taxa; thus, it represents an astonishing example of convergent adaptation (Hartline and Colman 2007).

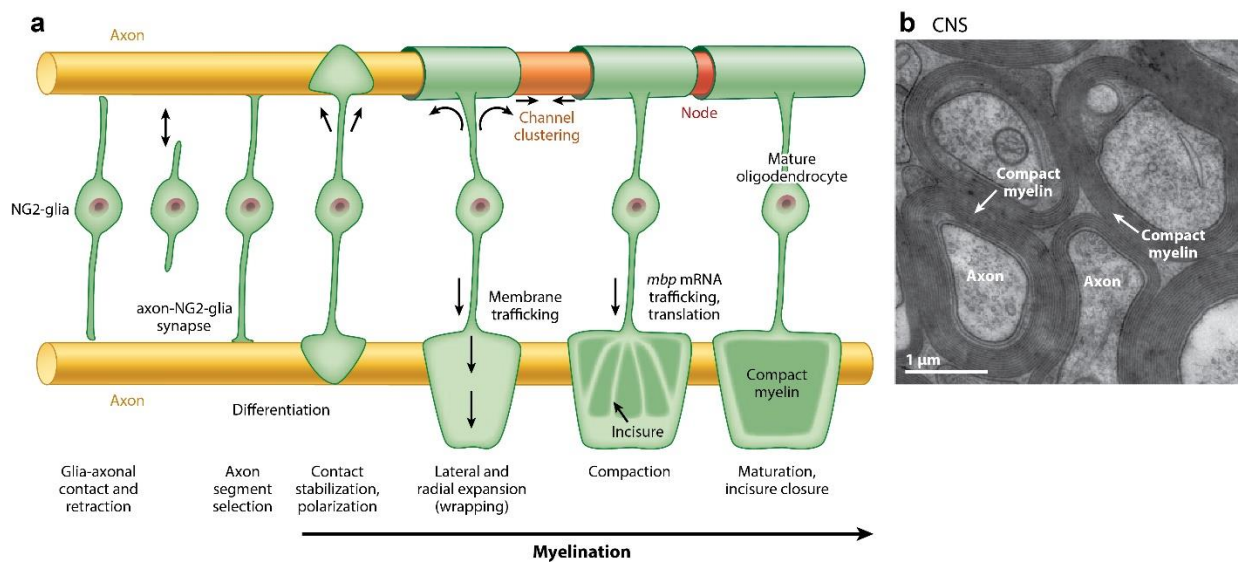


Figure 2. Myelin and myelination. a) Schematic model shows the differentiation of NG2-glia into oligodendrocyte, followed by the synthesis of myelin and its wrapping around axons. NG2-glia extend and retract processes until stabilizing contact with the axon. This event initiates the synthesis and extension of the membrane, originating the myelin sheath. Myelin extends laterally and radially wrapping around the axon, at the same time, voltage-gated ion channels cluster in the segments of the axon that are devoid of myelin, which leads to the formation of the nodes. Myelin transcripts like *mbp* are transported from the soma to the myelin sheath and locally translated, promoting the myelin compaction. The upper part of the illustration shows the myelin wrapping around the axon whereas the lower part shows the appearance of the unfolded myelin on the axon. b) Electron microscopy image of a myelin as a multiple periodic membrane layers (lamellae) wrapping around one axonal segment (adapted from Nave & Werner 2014). Reprinted by permission of Annual Reviews by Copyright Clearance Center's Marketplace™ service. License number 1036331.

Introduction

Axonal myelination has many advantages. Myelin modifies the electrical properties of axons by reducing the capacitance and increasing the resistance of the axonal membrane. Furthermore, myelin sheaths do not cover the entire axon, but they are absent in short segments known as nodes of Ranvier. Within these nodes, sodium voltage-gated sodium channels (Na_v) are densely packed, necessary for the local regeneration of action potentials (Nave and Werner 2014) triggered by depolarization propagated electrotonically from the previous node. Therefore, this particular arrangement of myelin along axons provides the structural basis for the saltatory conduction (Nave and Werner 2014).

As an additional function, it has been postulated that myelin reduces the metabolic cost of neuronal activity. It has been shown that WM has reduced consumption of glucose in comparison to the GM (Sokoloff et al. 1977), in part because myelination minimizes the need for ATP-dependent Na^+/K^+ exchange, to bring back axonal membranes to their resting potential (Wang et al. 2008; Nave and Werner 2014). Nevertheless, it should be considered that the high energy cost of biogenesis and further development of myelin is not pay-back by the saving in membrane potential restoration (Harris and Attwell 2012). In fact, it is calculated that the reduced energetic consumption in the WM is not largely due to long-term compensation but rather due to little metabolic spending because of its diminished synaptic activity (Harris and Attwell 2012; Sokoloff et al. 1977).

In mammals, two cell types have the unique ability to synthesize myelin. SCs in the PNS and oligodendrocytes in the CNS. Despite that both can myelinate axons, they differ enormously in their ontogeny (neural crest and neural plate, respectively), their protein composition, the number of myelinated axonal segments (known as “internodes”) per cell (the ratio internode to myelinating cell is 1:1 in SCs and up to 60:1 in oligodendrocytes), the myelin wrap periodicity (17nm versus 15.5nm, respectively), and substructural differences within the myelin (Nave and Werner 2014). Thus, apparent structural and functional similarity of PNS and CNS myelin is a superb example of convergent cellular evolution within the nervous system.

Myelin is a poorly hydrated structure composed of a mere ~40% of water against ~80% in other brain cellular components (Watanabe, Frahm, and Michaelis 2016). It is highly enriched

Introduction

in lipids, which constitutes up to ~70 – 80% in dry weight (Simons and Nave 2015). Several proteins promote the formation, compaction, assembly, and stability of myelin in the CNS, e.g., proteolipid protein (PLP), myelin basic protein (MBP), cyclic nucleotide phosphodiesterase (CNPase), myelin oligodendrocyte glycoprotein (MOG), myelin-associated glycoprotein (MAG), among others (Nave and Werner 2014). The composition of myelin has provided formidable time stability that has even surpassed researchers' expectations as verified after analyzing myelin samples from the “Tyrolean Ice Man,” who has been dead and preserved in freezing temperatures for over 5000 years (Hess et al. 1998).

The cellular mechanisms that govern myelination (**Fig. 2a**) seem to be influenced by the axon caliber since most thick axons are myelinated (Nave and Werner 2014). After birth, shortly after stabilizing contact with the axon, an oligodendrocyte membrane grows in an impressive rate of $5000\mu\text{m}^2$ per day, requiring around $\sim 10^5$ myelin proteins and other molecules per minute (Pfeiffer, Warrington, and Bansal 1993), by a steady production and trafficking of lipids from the cell body towards the contact point to form the myelin sheath. In a fascinating study done in zebrafish larvae, it has been shown that with increasing size, the membrane starts to expand radially, and the leading edge of the membrane squeezes in between the preceding layer and the axon, a process commonly named as “wrapping.” Simultaneously, myelin sheath expands longitudinally (always in contact with the axon surface), a process that leads to the establishment of the internodes and nodes (Snaidero et al. 2014). Finally, the myelin membrane wraps several times around the axon, the membrane trafficking is terminated, and the mRNA for proteins, like MBP, are transported to the myelin sheaths (Colman et al. 1982), promoting compaction and further maturation of the myelin sheaths (Aggarwal et al. 2013).

In the past decade, new evidence has suggested that oligodendrocytes provide trophic and metabolic support to axons. Deletion of myelin proteins, such as PLP and CNPase, leads to progressive axonal pathology, such as swellings, axonal degeneration, reduction of axonal calibers, and premature death (Lappe-Siefke et al. 2003; Klugmann et al. 1997). Furthermore, oligodendrocytes supply axons with lactate, resembling the function of the lactate-shuffle in astrocytes. It has been demonstrated that the deletion of the *COX10* gene in oligodendrocytes, which is essential for the assembly of the electron transport chain in mitochondria, enhances

their glycolysis. Thereby, oligodendrocytes increase their production of lactate, which, in turn, axons can use as an alternative energy source (Funfschilling et al. 2012). Conversely, the deletion or pharmacological blockade of the monocarboxylate transporter 1 (MCT1), which is solely expressed by oligodendrocytes and allows the transport of lactate into neurons, leads to axonal degeneration (Lee, Morrison, et al. 2012). This metabolic dependency could be due to the physical restrictions that myelin imposes onto axons to uptake extracellular energy resources. Finally, only recently, the function of K⁺ buffering and homeostasis has been attributed to oligodendrocyte (Larson et al. 2018).

Myelination is fundamental for the proper information processing in the CNS because it is essential for the propagation and fast conduction of action potential. It has been shown that abnormal myelination or loss of myelin impoverish motor performance in myelin protein-related mutant animals (Lappe-Siefke et al. 2003; Klugmann et al. 1997). Nonetheless, it could be argued that the problems lie on the degeneration of axons due to lack of metabolic support and not directly in the loss of myelin. Albeit, this theory loses weight in mutants that, at young ages, exhibit mild alterations in myelin, slower propagation of action potentials in the spinal cord, and do not present axonal degeneration. Interestingly, altered behaviors have been also reported, as a deficit in prepulse inhibition of startle response, decreased working and spatial memory, and increased anxiety-like behavior (Tanaka et al. 2009). Additionally, mild myelin disruption results in deficiencies in associative motor learning in mice, which is improved by artificial stimulation of the affected neurons (Kato et al. 2020).

Oligodendrocytes are fundamental to understand production of myelin and their impact on conduction velocity. Nonetheless, to fully understand myelin plasticity in development and adulthood, it is crucial to revise the cells that generate the oligodendrocytes, the NG2-glia.

NG2-glia, the enigmatic new glial population

Oligodendrocytes develop exclusively from a progenitor cell population during late gestational and early postnatal life, known as NG2-glia (Miller 1996), which have earned the title of being the fourth major group of glial cells in the CNS (Dimou and Gallo 2015; Eugenin-von

Introduction

Bernhardi and Dimou 2016). The name NG2-glia derives from the presence of the chondroitin sulfate proteoglycan (CSPG) neuron/glia antigen 2 (NG2) on their cell surface (Dimou and Gotz 2014). To distinguish these from pericytes of the CNS, which also express NG2 (Ozerdem et al. 2001), I prefer to use the term NG2-glia instead of only NG2⁺ cells. NG2-glia can also be found with many different names in the literature. The most often used name oligodendrocyte progenitor cells (OPCs) because their first identified function was the generation and maintenance of the oligodendrocyte population under physiological and pathological conditions. Some of them have been less successful in sticking in the field, such as “polydendrocytes” (Nishiyama, Suzuki, and Zhu 2014), because of their multi-branched and radial morphology, and “synaptocytes” (Xu, Wang, and Zhou 2014), due to their ability to form synapses with neurons.

NG2-glia: Solely oligodendrocyte progenitor cells or neural stem cell-like progenitor cells?

To restrict NG2-glia to be just oligodendrocyte progenitors is inadequate and a misleading concept. The progeny perspective is non-factual because they show neural stem-like properties to a certain extent (**Fig. 3**).

First, NG2-glia proliferate and self-renew their population in the adult brain, representing the primary proliferative cell population (Psachoulia et al. 2009; Simon, Gotz, and Dimou 2011; Dimou and Gotz 2014; Young et al. 2013) outside the neurogenic niches (see above). Second, under physiological conditions, they do not differentiate only into oligodendrocytes. *In vitro* and *in vivo* fate mapping experiments demonstrated that NG2-glia could also give rise to a specific population of astrocytes in the ventrolateral forebrain, striatum, thalamus, and hypothalamus during development (Raff, Miller, and Noble 1983; Zhu, Bergles, and Nishiyama 2008; Huang et al. 2014) and after injury (Alonso 2005; Komitova et al. 2011). A fact suggesting that NG2-glia are not confined to the oligodendrocyte lineage.

An objection to coin them as “neural-stem cell-like” is that they lack multipotency because there is no substantial evidence that they generate neurons. Although NG2-glia have the potential to differentiate into neurons in the adult brain within restricted areas, such as the

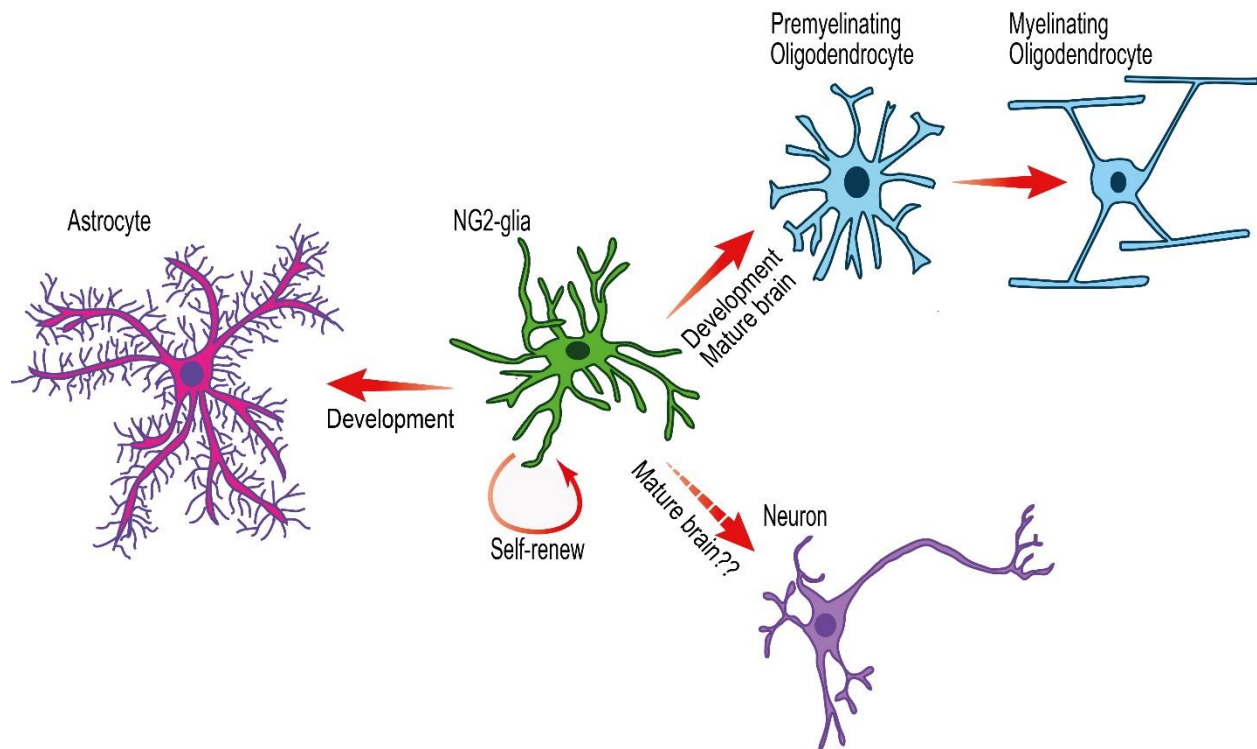


Figure 3. Multiple cell fates of NG2-glia. NG2-glia have the capability to proliferate and differentiate into oligodendrocytes in the immature and mature brain. However, NG2-glia can also differentiate into astrocytes in the ventrolateral forebrain, striatum, thalamus, and hypothalamus during development. Additionally, some studies have suggested that, in adulthood, NG2-glia could also differentiate into neurons, although it remains unclear (adapted from Eugenin-von Bernhardt & Dimou et al. 2016). Figure has been repurposed by the author and reprint permission has been granted by Springer Nature by Copyright Clearance Center’s RightsLink® service. License number 4831841077546.

piriform cortex and the hypothalamus (Guo et al. 2010; Robins et al. 2013; Rivers et al. 2008), the latter being a more convincing study, the neuronal progeny of NG2-glia remains unclear as these results failed to replicate in several other mouse models of fate mapping NG2-glia in the adult (Dimou et al. 2008; Kang et al. 2010; Clarke et al. 2012; Zhu et al. 2011) or embryonic brain (Huang et al. 2019). Therefore, it appears unlikely that NG2-glia have a robust neurogenic potential under physiological conditions.

On the other hand, the pure “oligodendrocyte progenitor” notion of NG2-glia also undermines their functionality. NG2-glia represent around 5 - 10% of the total cells in the adult brain, and they are evenly and widely distributed along the GM and WM of the brain and the spinal cord (Dawson et al. 2003). Histological and *in vivo* imaging analysis has determined that neither NG2-glia processes nor cell bodies overlap significantly, similarly to protoplasmic

Introduction

astrocytes (Wigley et al. 2007; Bushong et al. 2002; Hughes et al. 2013). It is curious that this distribution remains in adulthood, despite that the peak of myelin development already took place at ~P14 (Wright et al. 2010) in mice and during the first year in humans (Snaidero and Simons 2014), culminating at P60 (Wright et al. 2010) and during young adulthood (Snaidero and Simons 2014), respectively. Moreover, there is vast evidence indicating that NG2-glia can proliferate and differentiate into mature oligodendrocytes throughout life, although both their proliferation and differentiation rates depend on the area and decrease with age (Kang et al. 2010; Zhu et al. 2011; Dimou et al. 2008; Young et al. 2013; Dawson et al. 2003; Hughes et al. 2013). Despite proliferation, differentiation, and cell death, the NG2-glia population remains constant during lifetime (Hughes et al. 2013; Schneider et al. 2016). How is this possible?

It has been reported in the healthy brain that NG2-glia have mechanisms that are independent of external molecular signals to maintain their population. In a study made *in vivo* by time-lapse two-photon imaging, it was shown that they can proliferate and migrate short distances within the intact brain parenchyma in a process that is highly regulated by self-repulsion among NG2-glia processes (Hughes et al. 2013). Moreover, it has been described in the mammalian and zebrafish CNS that when a NG2-glia differentiates, dies or is ablated by focal laser, neighboring NG2-glia are triggered to proliferate and migrate into the vacant space to restore the network and keep constant the size of the population (Kirby et al. 2006; Hughes et al. 2013; Birey and Aguirre 2015). Another possible mechanism to keep the NG2-glia population stable was shown by a WM lesion study. In this research, it has been shown that NG2-glia hold the capacity to divide asymmetrically, originating simultaneously one NG2-glia and one oligodendrocyte. This mechanism allows the generation of differentiated cells without altering the number of NG2-glia (Hill et al. 2014), which is another common feature shared between NG2-glia and neural stem cells (Kriegstein and Alvarez-Buylla 2009).

Thus, gathered evidence suggests that the generation of oligodendrocytes is one of the probably further functions of NG2-glia in the healthy CNS. The constant population size and the capability to proliferate and differentiate through life give the impression that NG2-glia might have additional functions. In the pursue of these answers, scientists have adventured in the heterogeneity of these cells.

NG2-glia heterogeneity, are all NG2-glia born equally?

The high diversity of other glial cells, like astrocytes, lead to the suggestion whether NG2-glia represents a homogenous population or whether there is a spectrum of different types within the CNS. Emerging evidence points out that, indeed, the latter might be the case.

During mice development, NG2-glia come in three independent “waves” (**Fig. 4**). In mice, they are generated at E11.5 from the medial ganglionic eminence, followed by a group originated from the lateral ganglionic eminence at E15 and finally developed from the cortical SVZ at P0 (Kessaris et al. 2006). Initially, the three-wave nature of NG2-glia ontogeny suggested that these cells might also have different characteristics and functions in the CNS given that each wave arise from a different niche with a particular expression of transcription factors (Kessaris et al. 2006). Nonetheless, this idea has some inherent weaknesses. Firstly, under physiological conditions, the first wave naturally extinguishes in the CNS and is rapidly replaced by the other two waves (Kessaris et al. 2006). Secondly, and more relevant, the ablation of one wave of NG2-glia is quickly replaced by the other wave (Kessaris et al. 2006). Thus, it seems that NG2-glia are intrinsically redundant during development and this mechanism ensures the generation of oligodendrocytes

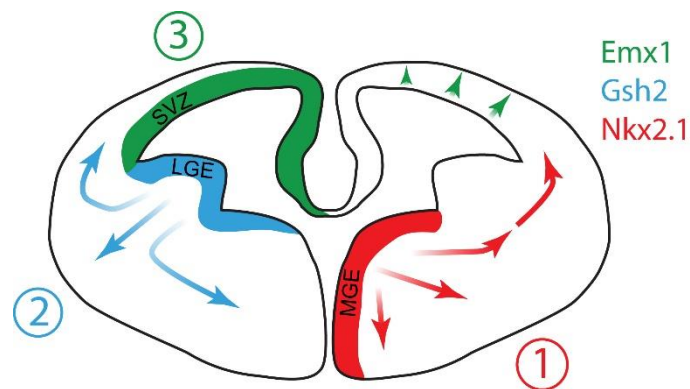


Figure 4. Oligodendrocyte progenitor cells (OPCs) waves during development. 1) The first wave of OPCs (red) are originated from the medial ganglionic eminence (MGE) at E11.5 and they are characterized by expressing the transcription factor NK2 Homeobox 1 (Nkx2.1). The second wave of OPCs (blue) is generated at E15 from the lateral ganglionic eminence (LGE) expressing the GS Homeobox 2 (GSH2) and spreading all over the brain. 3) Finally, at P0, a third wave of OPCs (green) expressing the transcription factor Homeobox protein Emx1 are originated from the ventricular zone. Both second and third wave persist in adulthood whereas the first wave disappears (adapted from Kessaris et al. 2006). Reprinted by permission of Springer Nature by Copyright Clearance Center’s RightsLink® service. License number 4833180838409.

Introduction

and progressive myelination would not be impaired during development, albeit it has not been shown whether have consequences in the adult mice after ablation of any of the waves during development.

Nonetheless, analysis of different areas in the adult brain has confirmed that the heterogeneous nature of NG2-glia resides in their morphology, differentiation and proliferation behavior, their electrophysiological properties, and response to signals.

For instance, WM NG2-glia in the adult corpus callosum (CC) has higher proliferation and differentiation rates than their GM counterparts (Dimou et al. 2008; Vigano et al. 2013; Young et al. 2013). Indeed, when experiments were approached with homo- and heterotopic transplantations of NG2-glia (cells are taken from one adult animal and injected into the same or different area of another adult animal) has revealed that these diverse differentiation properties between white and gray matter NG2-glia are the result of mainly intrinsic properties between these cells (Vigano et al. 2013). Although, transplanted GM cells transplanted into the WM were able to differentiate into oligodendrocyte, they did not become myelinating cells (Vigano et al. 2013). Therefore, the combination of intrinsic and extrinsic factors may control the differentiation and maturation of the oligodendrocyte lineage.

Additionally, when morphology and process distribution show differences between NG2-glia from different regions, i.e., cortical NG2-glia present a radial and isotropic process distribution, in contrast to the ones in the CC, which have an anisotropic distribution of processes and organize in parallel to axons (Young et al. 2013; Vigano et al. 2013). NG2-glia in the WM and GM have also been described to be different regarding their cell cycle length. Even though all NG2-glia can divide, GM cells have a longer cell cycle than WM ones (Young et al. 2013; Psachoulia et al. 2009; Dimou et al. 2008). Their response to extracellular signals is also variable. For example, NG2-glia in the WM show a more robust proliferative response to platelet-derived growth factor (PDGF) than in the GM; regardless that both populations express comparable levels of the PDGFR α (Hill et al. 2013).

Interestingly, in the last years, NG2-glia heterogeneity has been suggested not only between different regions but also within the very same brain area. There is differential

Introduction

expression of proteins solely in subsets of NG2-glia located in the same region. For example, in the cortical GM, only ~50% of NG2-glia express the transcription factor achaete-scute homolog 1/mammalian achaete-scute homolog 1 (*Ascl1/Mash1*), an essential factor for neuronal fate determination (Parras et al. 2007). In the same line, only a subset of the population of hippocampal NG2-glia expresses the “turned on after differentiation 64Kd” (TOAD-64), which is shown in neurons during early development (Belachew et al. 2003). However, it has not been possible to assign any distinctive function to these cell populations.

From an electrophysiological point of view, NG2-glia express Na_vs sensitive to TTX (Karadottir et al. 2008; De Biase, Nishiyama, and Bergles 2010), voltage-gated potassium channels (K_vs), and, on their processes, high voltage-gated calcium channels (Ca_vs), which are downregulated during their differentiation (Verkhatsky and Steinhauser 2000). This broad expression of voltage-gated channels in NG2-glia suggests that they may have dynamic electrical properties. Nonetheless, the electrophysiological properties of NG2-glia have been described to be very variable among the population (Chittajallu, Aguirre, and Gallo 2004; Karadottir et al. 2008; Clarke et al. 2012), and these features vary during different developmental stages in the mouse (Clarke et al. 2012). Thus, theoretically, NG2-glia have all the components needed to generate and propagate action potentials. Notably, GM but not WM NG2-glia showed spiking electrical characteristics (Chittajallu, Aguirre, and Gallo 2004). Additionally, WM NG2-glia in the rat has revealed the existence of spiking and non-spiking NG2-glia (Karadottir et al. 2008). However, data on spiking NG2-glia have been mixed. Some researchers have confirmed their existence (Berret et al. 2017; Karadottir et al. 2008; Chittajallu, Aguirre, and Gallo 2004) whereas others have not reported them (Bergles et al. 2000; Karadottir et al. 2008; De Biase, Nishiyama, and Bergles 2010; Clarke et al. 2012). These differences may suggest that electrophysiological features could be specific for NG2-glia in particular species or during certain developmental stages or both (Clarke et al. 2012).

The recent discovery of the subpopulation of NG2-glia expressing the G-protein coupled receptor 17 (GPR17), a P2Y-like receptor, has supported heterogenic functionality within NG2-glia (Chen et al. 2009; Boda et al. 2011; Vigano et al. 2016). The number of GPR17⁺ NG2-glia increases during development and then decreases to a baseline that remains constant in the

juvenile and adult mice (Chen et al. 2009; Boda et al. 2011). Notably, the dynamics of GPR17⁺ NG2-glia seem to correlate with the dynamics of myelination, both increasing in parallel and reaching a peak around P14. In the same line, the deletion of GPR17 in mice leads to premature myelination during development (Chen et al. 2009). Additionally, in adult mice, GPR17⁺ NG2-glia differentiate very slow in the intact brain in comparison to their GPR17⁻ NG2-glia counterparts (Vigano et al. 2016). However, after sizeable cerebral damage, they proliferate (Boda et al. 2011; Lecca et al. 2008), and undergo rapidly differentiation, suggesting a role as a “reserve pool” of adult progenitors that are maintained for repair processes (Vigano et al. 2016), which still needs to be determined. Because of the importance of this NG2-glia population for my thesis, I will come back later to discuss their role in the brain.

Until now, the evidence presented raises important questions regarding the nature of NG2-glia in the adult brain. Why are NG2-glia widely spread in the CNS after the completion of oligodendrogenesis and developmental myelination? And, why is the distribution even in less myelinated areas as well as in highly myelinated regions? Why is the population size constant, and is this accomplished by some sort of homeostatic control? More importantly, is there a strategic need for NG2-glia to retain the capabilities of proliferation and differentiation in the adult brain? Does NG2-glia heterogeneity play a role? Imagination flies around these questions, and finding answers seems determinant for understanding the fascinating complexity of our CNS. In this thesis, three non-mutually exclusive potential roles have been recapitulated, although the focus will be set on the third one.

Role 1 - Restoring myelin in the CNS

Myelin or oligodendrocytes may lose stability with age, which may affect the integrity of myelin sheaths or the health status of oligodendrocytes. Both would lead to a huge detrimental effect on conduction speed, hence, aberrant information processing. In humans, magnetic resonance imaging (MRI) studies have shown that the WM size decreases with age, affecting more females than males (Guttmann et al. 1998). To support this evidence, MRI and histological studies have shown that the aged rhesus monkey has the same pattern of size declination of the

WM and EM revealed that myelin loses its integrity (Wisco et al. 2008; Peters et al. 1996; Peters 1996). Furthermore, aged oligodendrocytes show swelling and an increased number of inclusions in their processes (Peters 1996), which suggests that aging affects cell viability. Notably, although less frequently, those aberrations can be found in young rhesus monkeys as well (Peters 1996), indicating that either the number of inclusions increases or the repair mechanisms fail with age.

In murine models, it has been shown that internodes shorten during aging (Lasiene et al. 2009). Nonetheless, to our knowledge, no clear relation between either oligodendrocyte swelling or inclusion to internode shortening has been established yet. Interestingly, newly generated oligodendrocytes in older mice display shortened internodes (Young et al. 2013). Therefore, it could be suggested that oligodendrocytes' show senescence changes while aging, leading to internode shortening. The exposed axon might be sensed by NG2-glia that then sequentially differentiates into an oligodendrocyte.

It has been shown that genetically block of NG2-glia differentiation leads to increased nodes and paranodes size, reduced speed conductivity in the CC, and impaired motor behavior (Schneider et al. 2016), reinforcing the notion that oligodendrocyte turnover is necessary during the whole lifespan of an organism.

Role 2- Surveillance, reaction, and repair

The overall distribution of NG2-glia might reflect their function. As microglia and astrocytes, it is conceivable that these progenitors might have a role in overseeing the CNS reaction against any insult or damage caused by trauma or other pathologies. Moreover, it has been described states of different “reactive NG2-glia” exist in different models of injury and demyelination. In hypomyelination, mutant mice, such as the *jimpy* (mutation in Plp) or the *shiverer* (mutation in MBP) mouse lines, display increased proliferation and differentiation of NG2-glia in the spinal cord WM (Wu et al. 2000; Bu et al. 2004). Notably, the transplantation of healthy human NG2-glia into the *shiverer* mouse improves CNS remyelination (Windrem et al. 2008). Additionally, acute lesions of the WM with α -lysophosphatidylcholine (LPC) toxin or by experimental autoimmune encephalomyelitis (EAE), commonly used for multiple sclerosis (MS)

Introduction

studies, result in increased proliferation of NG2-glia and their differentiation into myelinating oligodendrocytes within the lesion (Garay et al. 2011; Hill et al. 2014; Gensert and Goldman 1997; Keirstead, Levine, and Blakemore 1998; Di Bello et al. 1999).

The role of NG2-glia during demyelination and the subsequent remyelination appears to be clear. It is possible that the decrease in myelin, somehow detected, triggers the proliferation and differentiation of NG2-glia in order to recover the loss of myelin, making NG2-glia a prime target for regenerative therapy in MS. However, the picture is not so clear in human. Postmortem analyses of MS patients have revealed that NG2-glia are more abundant in areas where WM is undergoing active inflammatory demyelination, and commonly remyelination occurs, than in chronic lesions (Wilson, Scolding, and Raine 2006). This evidence suggests that NG2-glia are restricted in the long-term pathology, probably due to a hostile environment or exhaustion of the NG2-glia able to differentiate. Remarkably, recent studies in MS patients suggest that proliferation and generation of newly generated oligodendrocytes are uncommon, and remyelination might be due to subtypes of oligodendrocytes that can remyelinate WM injuries rather than repopulation with newly generated oligodendrocytes (Yeung et al. 2019; Jakel et al. 2019). Nonetheless, this topic is far from settled.

In contrast to demyelination, the role of these NG2-glia in other brain insults like acute injury and neurodegeneration is not clear yet. Similarly, to astrocytes and microglia, traumatic brain injuries shown to increase the expression of the NG2 proteoglycan and proliferation, to promote cell body hypertrophy together with process shortening and thickening, migration, and polarization towards the injury site by losing their homeostatic control of the population (Dimou and Gotz 2014; Simon, Gotz, and Dimou 2011; Hughes et al. 2013). As discussed above, the GPR17⁺ NG2-glia that rapidly differentiate after brain injuries. GPR17 is a receptor for uracil nucleotides and cysteine leukotrienes, Cysteinyl leukotriene receptor 1 (cysLTs) (i.e., UDP-glucose and LTD₄), as well as for purines such as ATP (Lecca et al. 2008). Endogenous ligands are secreted after brain injury, suggesting that GPR17 may play the role of damage sensor (Lecca et al. 2008). As already described, GPR17⁺ NG2-glia increase their proliferation and differentiation after stab wound or ischemia (Lecca et al. 2008; Boda et al. 2011; Vigano et al. 2016). NG2-glia together with microglia are known to be the first cells to react to the insult (Simon, Gotz, and

Dimou 2011). Therefore, it is speculated that NG2-glia may participate in the initiation of wound closure, scar formation, and may orchestrate the activation and function of other cells after injury, although it remains still unclear.

The role of NG2-glia in neurodegenerative diseases is also yet unknown. In the model of amyotrophic lateral sclerosis (ALS) in which mice carry a mutation in the superoxide dismutase (SOD) gene, there is an increase in the proliferation and differentiation of NG2-glia. However, newly generated oligodendrocytes do not mature and fail to myelinate (Kang et al. 2013). Furthermore, in the model of APPS1 mice, a mouse model for AD, NG2-glia respond with increased proliferation and differentiation (Behrendt et al. 2013) and become hypertrophic in the GM cerebral cortex (Sirko et al. 2013). It has been described that NG2-glia cluster around the amyloid plaques and, as already suggested for other glial cells, they can engulf the β -amyloid ($A\beta$) indicating a clearing role (Li et al. 2013). Nevertheless, this has not been reported by other groups (Sirko et al. 2013).

Role 3 – Adaptive myelination, a new form of CNS plasticity

In the past, despite the powerful techniques to study myelin, such as EM and immunofluorescence, their steady nature of these results gave the wrong impression that myelin was a static structure and that once myelination is completed, myelin patterns did not suffer significant changes during the lifespan of the individual. Currently, two types of myelination have been distinguished. “Intrinsic” or, as I prefer to call it, “developmental myelination,” consisting of the baseline and programmed blue plan of myelin generation and distribution in the nervous system (Bechler, Swire, and Ffrench-Constant 2018). As a counterpart, “adaptive myelination” is the production of additional myelin that can be modulated through an experience-dependent fashion and that by itself modulate neural circuits (Bechler, Swire, and Ffrench-Constant 2018).

In this context, the term “experience” is used ambiguously. For this thesis, I defined it as “external or internal effects, or influences of events on an individual that are gained through involvement or exposure in a short or long-term to those effects or events.” In the nervous system, experience can generate fast and transient or long-lasting changes in neuronal activity,

Introduction

which in turn have significant effects on the oligodendrocyte lineage. Therefore, it is believed that changes in the myelin pattern and regulation of myelination are essential events for the integration of experiences in the CNS. Such changes are translated into the alteration in cognitive processes, e.g., such as learning and memory. Because of the critical relevance for this doctoral thesis, the topic of adaptive myelination and how NG2-glia may play a role in it will be revised in more detail.

In the first place, it is fundamental to highlight that there is no area of the CNS that is completely myelinated in adulthood, perhaps except for the optic nerve. First of all, in WM structures, such as the CC, not more than 40% of the axons are myelinated in the adult mouse (Sturrock 1976). Moreover, it has been shown that myelinated axons, like the ones from neurons in the layer II-III of the somatosensory cortex, are not fully myelinated along their length. Instead, they instead display different patterns of internodes distributed along the axon, leaving myelin devoid segments (Tomassy et al. 2014). Therefore, unmyelinated axons or their exposed sections represent perfect substrate for myelination to occur, leading to changes in the electrical properties of neurons and the circuits in which they are involved.

The inhibition of action potentials with TTX, Na_vs blocker, leads to a decrease myelination in the mouse optic nerve (Demerens et al. 1996). Conversely, the application of α -scorpion toxin (α ScTX), which delays the inactivation of Na_vs, or stimulation of neurons with an electrode, enhance myelination of axons in mixed oligodendrocyte-neuronal cultures (Demerens et al. 1996; Gary et al. 2012). Although the phenomenon was interesting, adaptive myelination did not gain attention until the first human experiments years later appeared. It could be namely shown by diffusion tensor imaging (DTI) that participants who learned and practiced complex visual-motor tasks, such as juggling or extensive piano playing for weeks, exhibited increased WM size, suggesting an increase in the amount of myelin in this structure (Bengtsson et al. 2005; Scholz et al. 2009). Later on, it could be shown in rodents that social deprivation of juvenile mice led to impaired myelination in the prefrontal cortex (PFC), an area which has been associated with complex emotional and cognitive behavior (Liu et al. 2012; Makinodan et al. 2012). Moreover, it has been shown that optogenetic and pharmacogenetic stimulation of neurons in adult mice led

to increased myelination of the axonal tracts in which neuronal activity was enhanced (Gibson et al. 2014; Mitew et al. 2018; Geraghty et al. 2019).

Interestingly, adaptive myelination does not apply uniquely to mammals but shares an evolutionary trait with other vertebrates. It could be shown in the zebrafish larvae spinal cord that neuronal activity not only enhanced myelination but in addition provides a signal bias for which axons should be myelinated (Hines et al. 2015; Mensch et al. 2015). With time-lapse *in vivo* imaging, it was shown that whereas the first axonal myelin wrapping is axon activity-independent, the stabilization and the longitudinal expansion of prospective myelin sheaths are activity-dependent mediated by the secretion of axonal neurotransmitters and neurotrophic factors as in the mouse (Hines et al. 2015). In contrast, blocking the synaptic vesicle release with tetanus neurotoxin (TeNT) decreases the number of myelinated axons and the total number of myelin sheaths per oligodendrocyte in the zebrafish spinal cord (Mensch et al. 2015). This body of studies has provided the first insights that neuronal activity modulates myelination during development and in adulthood. The current state of the art points out that neuronal activity could potentially modulate the behavior of NG2-glia, enhancing differentiation into newly generated oligodendrocytes, which in turn provide the axons with new myelin (**Fig. 5**). Hence, it is critical to understand how neuronal activity and experience might influence NG2-glia in the healthy CNS.

NG2-glia behavior and dynamics modulated by neuronal activity

Early work showed that intraocular injection of TTX diminished the proliferation of NG2-glia close to axons of the retinal ganglion cells by preventing the neuronal activity-dependent release of mitogens (Barres and Raff 1993). Additionally, *in vivo* studies have shown that high-frequency electrical stimulation applied in the rat medullary pyramids increased the proliferation and differentiation of NG2-glia adjoined to the neurons of the contralateral dorsal corticospinal tract (Li et al. 2010). However, this experimental approach required the implantation of electrodes, generating unavoidably an injury. As I discussed earlier, NG2-glia react to mechanical

insults; thereby, this study presents critical confounding factors to dissect the association between NG2-glia and neuronal activity.

Since then, new strategies have been developed in the last decade to study NG2-glia plasticity. One way has been to study the behavior of NG2-glia *in vivo* in the absence of neuronal activity in sensory deprivation models. The removal and cauterization of whiskers led to an aberrant distribution of NG2-glia in the barrel cortex together with increased proliferation in regions of the barrel that were devoid of NG2-glia (Mangin et al. 2012). However, in another study, trimming of the whiskers led to a decrease in the total number of oligodendrocytes by promoting apoptosis of newly generated oligodendrocytes in the somatosensory cortex (Hill et al. 2014). In contrast, sensory stimulation of whiskers resulted in increased differentiation of NG2-glia in the same cortical region (Hughes et al. 2018). These results suggest that neuronal input is not only important to regulate NG2-glia proliferation and differentiation, but also to enforce distribution and provide survival cues for oligodendrocytes.

The development of new technologies also offered innovative approaches to modulate *in vivo* the behavior of NG2-glia by neuronal activity, such as optogenetics and pharmacogenetics, it has been possible to modulate their firing rate by minimizing the mechanical disturbance of the system. Through these techniques, it was shown that increasing the firing rate of neurons led to the increase of NG2-glia proliferation and differentiation adjoining the stimulated neurons (Gibson et al. 2014; Mitew et al. 2018). Moreover, these newly generated oligodendrocytes myelinate the stimulated axons (Mitew et al. 2018) that further led to an improvement in the behavioral-motor function of stimulated animals (Gibson et al. 2014).

It remains unclear which are the mechanisms and the signals that neurons employ to communicate with NG2-glia. In the following section, I will show different molecules that might contribute to this crosstalk. Additionally, I will review one of the most outstanding structural features that neurons and NG2-glia share: the neuron-NG2-glia synapse.

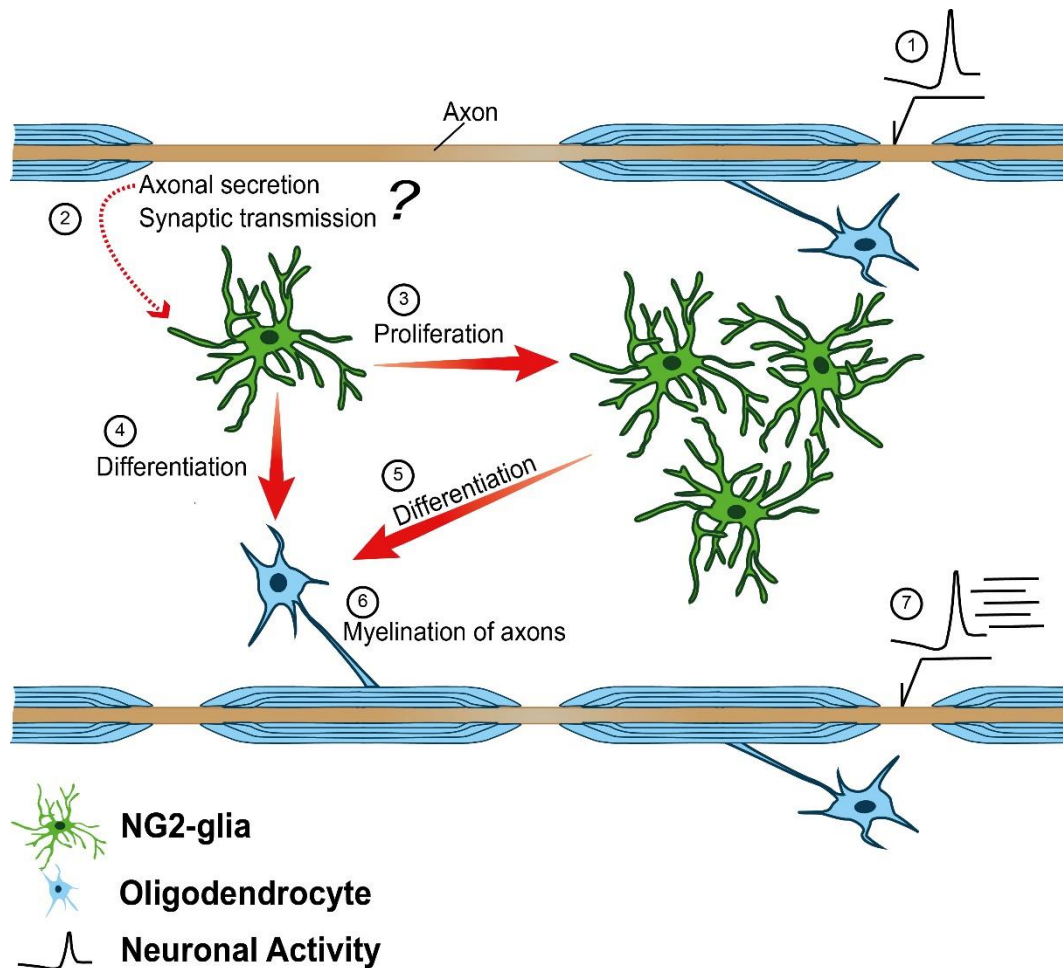


Figure 5. Effect of neuronal activity on NG2-glia behavior. In response to a neuronal activity (1), neurons could release signals secreted from the axon or the soma; or secreted into the synaptic cleft formed between neurons and NG2-glia (2). These signals could manipulate NG2-glia proliferation (3) or differentiation into oligodendrocytes (4). It is also possible that after proliferation the newborn NG2-glia differentiate (5). If new oligodendrocytes are generated, they could potentially myelinate surrounding axons (6) and change the electrical properties of neurons and therefore modify the properties of the neuronal network (7) (adapted from Eugenin-von Bernhardt & Dimou et al. 2016). Figure has been repurposed by the author and reprint permission has been granted by Springer Nature by Copyright Clearance Center's RightsLink® service. License number 4831841077546.

Talking to NG2-glia through signals and neuron-NG2-glia synapses

Most of the cited studies agreed that neuronal signals affecting NG2-glia must be released in an activity-dependent manner. Therefore, it became apparent to think that neurotransmitters may play a role in this communication. Experiments in organotypic cultures of cerebellum slices have shown that the exposition to glutamate receptor agonists, like kainate and *α-amino-3-hydroxy-5-methyl-4-isoxazole propionic acid* (AMPA), decreased NG2-glia proliferation (Yuan et

al. 1998). Contrary, the administration of the antagonist *6,7-dinitroquinoxaline-2,3-dione* (DNQX) led to an increase in cell proliferation (Yuan et al. 1998). Additionally, it has been shown that glutamate increases $[Ca^{+2}]_i$ in NG2-glia (Hamilton et al. 2010); thus, reflecting that neurotransmitters might have the capacity of triggering signal cascades in NG2-glia.

Notably, the expression of receptors in NG2-glia is not limited to just glutamate receptors, such as *N-methyl-D-aspartate* receptor (NMDAR, (Dzamba, Honsa, and Anderova 2013)) and AMPAR, but it extends to a broad spectrum of neurotransmitter receptors, e.g., acetylcholine receptors (De Angelis et al. 2012), *γ-aminobutyric acid* receptors (GABA_AR) (Von Blankenfeld, Trotter, and Kettenmann 1991; Williamson et al. 1998), purinergic receptors (Stevens et al. 2002) and others. Several neurotransmitters have shown a variety of effects on NG2-glia migration, proliferation, and differentiation, but information has been often contradictory. For instance, as described above in *ex vivo* organotypic cultures, glutamate decreases NG2-glia proliferation (Yuan et al. 1998). Nonetheless, in a model in which AMPA receptors have been modified in three different ways, glutamate was inconsistent affecting NG2-glia self-renewal, differentiation, and survival of newly generated oligodendrocytes depending on the modification of the receptor (Kougioumtzidou et al. 2017). Additionally, it has been shown that the responsiveness of NG2-glia towards glutamate is also dependent on molecular switches like BDNF / neuregulin (Lundgaard et al. 2013). This evidence suggests that single neurotransmitters might trigger multiple responses in NG2-glia, depending on the modification of their respective receptors or co-signals.

The way these neurotransmitters are presented to NG2-glia is, indeed, still a matter of debate. Unarguably, the discovery of “true synapses” between neurons and NG2-glia had a profound impact on the field. Initially described in the mouse hippocampus, it showed that the stimulation of neurons located in the CA3 region of the hippocampus triggered an evoked excitatory postsynaptic current (EPSC) in NG2-glia located in the CA1 area (Bergles et al. 2000). Additionally, EM studies revealed that synapses are formed between NG2-glia and unmyelinated axons (or at least in segments devoid of myelin) and also that release vesicles exist on a presynaptic active zone at the axonal membrane adjoining the NG2-glia membrane (Ziskin et al. 2007; Kukley, Capetillo-Zarate, and Dietrich 2007). Nowadays, I know that these synapses exist

Introduction

in different regions of the brain (Bergles et al. 2000; De Biase, Nishiyama, and Bergles 2010; Chittajallu, Aguirre, and Gallo 2004). Besides NG2-glia expression of classic synaptic receptors, it has been shown at mRNA level that they may also express postsynaptic scaffold proteins, such as “postsynaptic density protein 95” (PSD-95) (Sakry, Karram, and Trotter 2011), a standard component of the neuronal postsynaptic density, and it is crucial for synapse formation, maturation, and remodeling (El-Husseini et al. 2000; Marrs, Green, and Dailey 2001).

It is important to highlight that glutamatergic receptors can be functionally expressed in the active synaptic site, extrasynaptically (close to synapses), or ectopically (far away from synapses). Therefore, NG2-glia response to neurotransmitters might not reflect the function of classic synapses per se.

Currently, many questions remain unanswered regarding these neuron-NG2-glia synapses. First, it is not clear whether these synapses are sending unidirectional or bidirectional information. Second, are they present in all or just a subpopulation of NG2-glia? or is it dependent on the maturation of NG2-glia? Most importantly, neither the molecular composition of these synapses nor the potential main functions of these neuron-NG2-glia structures, have been completely elucidated.

The million-dollar question: How does myelination induced by modulation of NG2-glia behavior leads to changes in brain plasticity?

A robust body of information supported that experiences are encoded in the CNS by changing the neuronal activity, which in turn commands NG2-glia to differentiate into oligodendrocytes. In consequence, these newly generated oligodendrocytes synthesize *de novo* myelin to wrap existing axons modifying the properties of the circuits. Albeit, the functional outcome of this process remains less understood. The evidence suggests that increases in myelination are necessary for the integration of new experiences and, hence, could be a potential mechanism for the refinement of cognitive processes, such as learning and memory.

Introduction

It has been shown that the training in complex running wheel induces rapid oligodendrogenesis in mice (McKenzie et al. 2014; Xiao et al. 2016). Conversely, preventing NG2-glia differentiation by knocking down the myelin regulatory factor (Myrf), under an inducible Cre-lox system, led to impaired motor-learning of the task (McKenzie et al. 2014; Xiao et al. 2016). Similarly, it has been shown that the impairment of NG2-glia plasticity by methotrexate, which inhibits BDNF synthesis in neurons, triggers deterioration of working memory (Geraghty et al. 2019). Notably, very recent studies using the same Myrf Cre-lox system as described above show

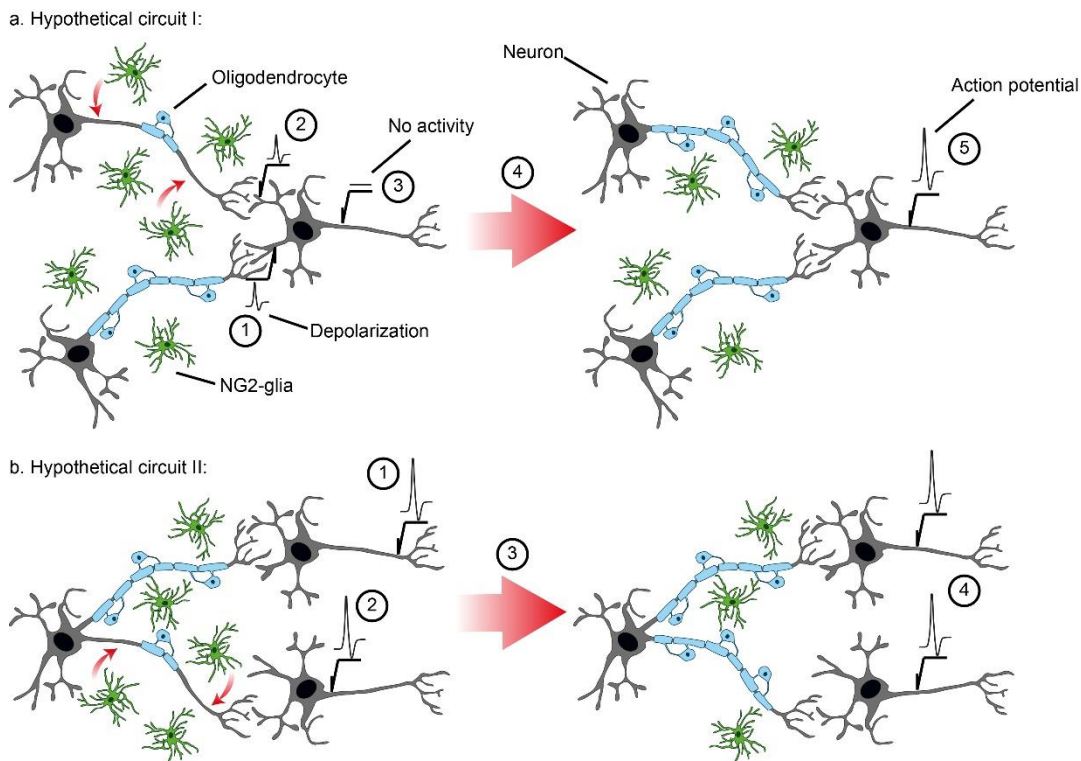


Figure 6. Schematic of how newly generated oligodendrocyte modifies CNS circuitries. The red arrow in the scheme indicates where the newly generated oligodendrocyte will be placed. a) the hypothetical circuit is composed by three neurons. Neuron A and B project and form synapses with neuron C. If neuron B has a shorter axon length or if the axonal length of neuron A and B are equal but B has a higher degree of myelination (as illustrated), neuron C will be depolarized first by neuron B (1), followed by a depolarization of neuron A (2). Nonetheless, both depolarizations by themselves are insufficient to trigger an action potential in neuron C (3). After the differentiation of NG2-glia into oligodendrocytes and myelination of neuron B (4) leads to synchronization of the spike-arrival of neuron A and B to neuron C, triggering an action potential by spatial summation in neuron C (5). b) the hypothetical circuit is composed by three neurons. Neuron D project and form synapses with neuron E and F. The lower branch has a longer length or lower myelination degree than the above branch, leading of the generation of an action potential in neuron E first (1) followed by an action potential in neuron F (2), resulting in asynchronicity of neuron E and F activity. After the differentiation of NG2-glia and myelination of the lower axon (4), the delay in spike-time arrival between the two neurons is reduced, leading to the synchronization of the activity of neuron E and F (4).

Introduction

that spatial and fear-conditioned learning would also require newly generated oligodendrocytes, and its blockage restricts memory formation (Steadman et al. 2020; Pan et al. 2020). Albeit in Steadman et al. results suggested that spatial memory consolidation also required oligodendrogenesis, it could not be shown in the fear-conditioned memory model of Pan et al. Therefore, it could be that oligodendrogenesis play different roles according to the type of memory and cognitive task.

Nonetheless, this does not explain the mechanism by which adaptive myelination contributes in the modulation of cognition. Undoubtedly, it is hard to imagine that solely the increase in conduction velocity of isolated neurons enhance information processing. Hence, the effect should rely upon modulating temporal relations, oscillations, and synchronicity in the interactions of distant brain regions or within local neural networks by adapting spike-timing arrival of action potentials (Pajevic, Basser, and Fields 2014). In this regard, I can take some lessons from the auditory system. Neurons can have anatomical differences, e.g., axonal length, which can be challenging for physiological processes that require the specific or simultaneous arrival of two neuronal signals to properly trigger a response in their target, as it is in the case of sound localization (Seidl 2014). Therefore, the precise tuning of signals is prompt by the sophisticated organization of myelin in axons that deliver the message from the cochlea to the brainstem nuclei for functional sound localization (Ford et al. 2015).

Nonetheless, how can this be translated into adaptive myelination? As described above, within a random circuit (**Fig. 6**), neurons might differ in their axonal length, their degree of myelination, and myelin distribution (Tomassy et al. 2014). If two neurons with different axonal lengths or myelination pattern have one target neuron, their signals may arrive asynchronously, resulting in two independent and time-shifted subthreshold depolarizations on the target neuron without triggering an action potential. If *de novo* myelination occurs on one of the neurons, it could facilitate the simultaneous arrival of signals to the target, and subsequently, generate a higher depolarization for triggering an action potential in the target neuron by spatial summation. Thus, myelination could lead to the formation of coincidence detectors in the CNS. This wild oversimplification illustrates how new myelin derived by NG2-glia differentiation as the result of modulated by neuronal activity could affect brain plasticity. In principle, this mechanism

Introduction

could be extended in a broad variety of different configurations (e.g., a neuron with two neuronal targets providing the bases of two circuits synchronization) and not only in the synchronicity of few signals but of entire circuits or coupling oscillators (Pajevic, Basser, and Fields 2014; Baraban, Mensch, and Lyons 2016).

Unfortunately, there is little evidence for this theoretical framework. Only this year, it has been shown that preventing the proper myelination of thalamocortical axons leads to an increase of asynchronized signals to neurons in the motor cortex, and in consequence, the deterioration of motor learning (Kato et al. 2020). In the same line, blocking oligodendrogenesis induced by fear-conditioned learning, prevented the coupling of cortical and hippocampal oscillators, seemingly crucial for learning and memory consolidation (Steadman et al. 2020).

The aim of this doctoral thesis

A lot of information has been gathered to understand how the modulation of NG2-glia behavior could contribute to adaptive myelination. Nevertheless, there are still gaps in our knowledge regarding the plastic nature of NG2-glia promoted by physiological stimuli.

In an individual's daily life, physical activity represents perhaps the most common experience and it has a dramatic impact on the organism's well-being. Not only it has an essential contribution to our health, such as decreasing the risk of cardiovascular diseases or metabolic-related disorders, but also are the beneficial effects on the development of cognition, enhancement in cognitive performance, and general mental health widely studied (Perez et al. 2019). Unfortunately, together with modernization also has come along physical inactivity, which has been estimated by the world health organization as the fourth leading risk factor for global mortality. With the increased sedentarism of western societies, it is to reverberate on people's health, including mental, and cognition efficiency (Rodriguez-Ayllon et al. 2019; Cunningham et al. 2020).

The knowledge of the effects of physical activity in the oligodendrocyte lineage remains scarce and limited (Tomlinson, Leiton, and Colognato 2016). Our group and others have already shown that increased physical activity lead to enhanced NG2-glia proliferation and differentiation (Simon, Gotz, and Dimou 2011; Mandyam et al. 2007; Ehninger et al. 2011; Tomlinson, Huang, and Colognato 2018). Nevertheless, the narrow scope has been limited to analyzing immediate behaviors of these cells, and most of these studies have utilized methodologies that might undermine the magnitude of the effect, or they inadvertently included confounding factors like those between exercise and enriched environment.

Additionally, these studies have not determined the functional role of these changes in proliferation and differentiation. Exercise promotes improvement in cognitive processes such as learning and memory (Hillman, Erickson, and Kramer 2008). This cognitive enhancement has been historically attributed to the increase of neurogenesis in the dentate gyrus, which in turn

Aim of this doctoral thesis

promotes circuit remodeling, and, as a result, improvement in processes such as learning and memory (van Praag et al. 1999; Olson et al. 2006; Diederich et al. 2017; Voss et al. 2019).

In this doctoral thesis, it has been hypothesized that increased voluntary physical activity (VPA) leads to an augment in the differentiation of NG2-glia, which in turn increases the number of newly generated myelinating oligodendrocytes, thereby participating in the remodeling of the CNS. Although this increase in new oligodendrocytes occurs, the function of them has not been determined; thus, it has been hypothesized that NG2-glia differentiation induced by exercise enables enhancement in cognitive performance promoted by VPA. I also have hypothesized that physical activity promotes the initial differentiation of a subpopulation of NG2-glia but leads to a decrease in the long term plastic behavior of NG2-glia, a phenomenon not described before.

For this, I tested NG2-glia behavior in a VPA paradigm, which primarily consists of providing mice with *ad libitum* running devices and compared them with animals housed in standard cages. VPA has the advantages of inducing increased neuronal activity in a physiological manner, minimizing the manipulation of the mice. Additionally, because of the non-invasive nature of this procedure, the results could have high relevance in translational research. Finally, by tracking the animals running distance, VPA can easily correlate the animal performance to the effects on NG2-glia behavior. Under this simple empirical setup, following objectives were established:

Objective 1. Which modifications does VPA evoke to the behavior of NG2-glia? Which is the time course of this regulation? Are this changes restricted to the motor cortex? Although previous work has shown evidence that the proliferation and differentiation of NG2-glia are modified after physical activity (Simon, Gotz, and Dimou 2011; Mandyam et al. 2007; Ehninger et al. 2011; Tomlinson, Huang, and Colognato 2018), I want to determine whether our model of VPA will sustain similar effects and, most importantly, to deepen our understanding on the dynamics of continuous VPA on time. Also, I want to determine whether this changes happen only in the motor cortex or do they occur in other brain regions. For this, I will analyze the corpus callosum and the piriform cortex as well. For this, *C57Bl/6* wild-type and *NG2-CreERT2 x CAG-GFP* mice

Aim of this doctoral thesis

(Huang et al. 2014) were given *5-bromo-2-deoxyuridine* (BrdU) for the whole duration of the experiment; a thymidine analog which is incorporated into the DNA of dividing nuclei, which allow to track and determine the degree of proliferation and differentiation of NG2-glia. However, as NG2-glia can differentiate without going through proliferation, BrdU-based strategies might undermine the absolute number of newly generated oligodendrocytes, I count direct differentiation of NG2-glia in tamoxifen induced *NG2-CreERT2 x CAG-GFP* mouse line that provide further information on the modalities of differentiation in NG2-glia.

Objective 2. Do NG2-glia conserve the same characteristics they had before VPA? To understand whether NG2-glia identity and characteristics are modified after VPA, I will obtain and analyze their protein profile after VPA, which in turn could lead us to understand: 1) whether the NG2-glia phenotype changes after VPA and determine future plastic abilities, 2) to discover signaling pathways that are activated or inhibited in NG2-glia by VPA, and 3) to give us insights whether VPA leads to an enrichment of specific NG2-glia subpopulation after VPA. To accomplish this, I will use the *Sox10-GFP* animals, house them with or without running wheels, and NG2-glia will be sort out from brains by MACS and analyzed by a mass spectrometry approach. The *Sox10-GFP* mouse line will be use because our group has determined in previous experiments that this strain shows the maximum number and purity of sorted NG2-glia by MACS.

Objective 3. Does VPA similarly affect all NG2-glia populations? Here I want to find out whether the different populations of NG2-glia, namely the GPR17⁺ NG2-glia (Boda et al. 2011; Vigano et al. 2016; Lecca et al. 2008), changed their properties as result of VPA. *Sox10-GFP* mice will be exposed to VPA and the number of GPR17⁺ NG2-glia cells will be determined. Additionally, differentiation of GPR17⁺ NG2-glia will be analyzed by providing free access to running wheels to *GPR17-iCreERT2 x CAG-GFP* animals (Vigano et al. 2016) after induction and count the number of newly generated oligodendrocytes generated from GPR17⁺ NG2-glia.

Objective 4. Do VPA-induced newly generated oligodendrocytes integrate into the circuitry, and do they contribute to exercise-induced enhanced cognitive performance? I am interested in whether oligodendrocytes generated after VPA were able to become mature myelinating oligodendrocytes, providing some hints of adaptive myelination in the CNS. Therefore, utilizing animals from the *NG2-CreER^{T2} x CAG-GFP*, I will count the number of newly generated mature oligodendrocytes after VPA. Additionally, I want to assess the functional role of these cells in cognitive performance enhancement. To achieve this objective, by working with *Sox10-iCreER^{T2} x Esco2-fl x CAG-GFP*, I want to genetically prevent NG2-glia differentiation after induction with tamoxifen. After VPA, I will test the cognitive performance by a novel object recognition test.

Objective 5. Are neuron-glia synapses necessary for NG2-glia differentiation? Neurons can communicate with NG2-glia through synapses (Bergles et al. 2000), and there is a possibility that the action of VPA over NG2-glia is mediated by increased neuronal activity. To analyze the role of synapses and avoid receptor or neurotransmitter-specific effect, I want to modulate the postsynapse by the deletion of scaffolding proteins in the postsynaptic density specifically of NG2-glia in the adult stage. Thereby, I established the *Sox10-iCreER^{T2} x Shank3-fl x CAG-GFP* mouse line that has a deletion in Shank3, an essential scaffold postsynaptic protein (Naisbitt et al. 1999), from the oligodendrocyte lineage in an inducible Cre-lox system. It has been shown that the deletion of Shank3 leads to a decreased number of synapses and diminished AMPAR and NMDAR currents (Arons et al. 2012). I proposed for this doctoral thesis to characterize this mouse line after induction to be used in future projects regarding VPA and as a psychiatric disease mouse model.

Material and methods

Materials

Chemical and reagents

All chemicals and reagents are listed in **table 1**. While working with the various reagents, every necessary security measurement was taken into consideration and implemented for researcher safety.

Table 1. List of chemicals and reagents. All compounds are listed according to their name, formula, or the abbreviation used for this doctoral thesis. Besides, each product's manufacturer and catalog number has been also registered.

Name	Formula / Abbreviation	Company	Catalog
2-propanol (isopropanol)	(CH ₃) ₂ CHOH	VWR	20842.330
4',6-Diamidino-2-phenylindole	DAPI	Sigma-Aldrich	D9564
5-Bromo-2'-deoxyuridine	BrdU	Sigma-Aldrich	B5002
5-ethynyl-2'-deoxyuridine	EdU	Thermo Fisher	E10415
Adult brain dissociation kit		MACS Miltenyi Biotec	130-107-677
Agarose	Alternate polymer of β -D-galactose and 3,6-anhydro-L-galactose	VWR	351020
Aqua-Poly/Mount		Polyscience	18606-5
Betaine solution 5M		Sigma-Aldrich	B0300
Bromophenol blue	C ₁₉ H ₁₀ Br ₄ O ₅ S	Merck	108122
Click-It™ EdU Alexa Fluor® 647		Thermo Fisher	C10340
Corn oil		Sigma-Aldrich	C8267
D (+)-Saccharose	C ₁₂ H ₂₂ O ₁₁	Roth	4621.1
Deoxynucleotide (10Mm)	dNTPs	Sigma-Aldrich	D7295
Double distilled water	ddH ₂ O	Ulm University	
Dulbecco's Phosphate-Buffered Saline with Ca ²⁺ , Mg ²⁺ , pyruvate, and glucose	DPBS	Thermo Fisher	14287080
Ethanol 100%	CH ₃ CH ₂ OH	Honeywell	32205
Ethanol 70%	CH ₃ CH ₂ OH	Roth	T913.3
Ethidium bromide solution (10mg/ml)	C ₂₁ H ₂₀ BrN ₃	Sigma-Aldrich	E1510
Ethylene Glycol	HOCH ₂ CH ₂ OH	Sigma-Aldrich	102466
Ethylenediaminetetraacetic acid disodium salt dihydrate (EDTA)	EDTA-Na ₂ x 2H ₂ O	Sigma-Aldrich	E5134
FcR blocking reagent		MACS Miltenyi Biotec	130-101-547
Ficoll® 400		PanReac AppliChem	A2252
Glacial acetic acid	H ₃ CCOOH	VWR	20104.312
Glutamine 200Mm (100x)		Gibco / Thermo Fisher	25030-024
Glycerol water-free	HOCH ₂ CH(OH)CH ₂ OH	Honeywell	15523

Material and Methods

Goat serum		Gibco / Thermo Fisher	16210072
Hank's balanced salt solution (with Mg ⁺² and Ca ⁺²)	HBSS	Gibco / Thermo Fisher	24020091
Hydrochloric acid 37%	HCl	Sigma-Aldrich	30721
Hydrochloric acid 6N	HCl	Roth	O281.1
Ketamine 10%		Bela-pharm	9089.01.00
MACS Neuro Medium		MACS Miltenyi Biotec	130-093-570
MACS NeuroBrew®-21		MACS Miltenyi Biotec	130-110-916
Magnesium chloride solution (25Mm)	MgCl ₂	Sigma-Aldrich	M8787
Millipore water		University of Ulm	
Paraformaldehyde	PFA	Sigma-Aldrich	P6148
Peroxide solution 30%	H ₂ O ₂	Fischar	27500
Platinum PCR SuperMix High Fidelity		Invitrogen / Thermo Fisher	12532016
Potassium chloride	KCl	Merck Millipore	104936.05
Potassium dihydrogen phosphate	KH ₂ PO ₄	Merck Millipore	104873.1
PreOmics iST kit		PreOmics	PO00001
Primers for Genotyping		Biomers	Self-designed
Proteinase K, lyophilized		Roth	7528.1
Quick-load 100bp DNA ladder		New England Biolabs	N0467S
Rompun 2% (Xylazine)		Bayer	770081
Sodium chloride	NaCl	Sigma-Aldrich	S3014
Sodium chloride (Solution 0.9%)	NaCl	B. Braun	3570350
Sodium dodecyl sulfate (SDS)	CH ₃ (CH ₂) ₁₁ OSO ₃ Na	Sigma-Aldrich	L3771
Sodium hydroxide	NaOH	VWR	28244.295
Sodium phosphate dibasic anhydrous	Na ₂ HPO ₄	Sigma-Aldrich	71642
Sodium phosphate monobasic dehydrate	Na ₂ HPO ₄ x 2H ₂ O	Sigma-Aldrich	71505
Sodium phosphate monobasic dehydrate	NaH ₂ PO ₄ x 2H ₂ O	Sigma-Aldrich	71505
Sodium tetraborate Anhydrous (Borax)	Na ₂ B ₄ O ₇	Sigma-Aldrich	71996
Tamoxifen	C ₆ H ₅ C(C ₂ H ₅)=C(C ₆ H ₅)C ₆ H ₄ OCH ₂ N(CH ₃) ₂	Sigma-Aldrich	T5648
Taq DNA Polymerase		Homemade, kindly provided by Prof. Dr. Götz (LMU)	
Tetramethylrhodamine tyramide amplification kit	TSA® kit	Perkin Elmer	SAT70200IEA
Tissue-Tek® O.C.T.™ compound		Sakura Finetek	4583
Trisodium citrate dehydrate	HOC(COONa)(CH ₂ COONa) ₂ x 2H ₂ O	Sigma-Aldrich	71405
Triton™ X-100	<i>t</i> -Oct-C ₆ H ₄ -(OCH ₂ CH ₂) _x OH, X= 9-10	Sigma-Aldrich	X100
Trizma®	NH ₂ C(CH ₂ OH) ₃	Sigma-Aldrich	T1503
Trypan blue solution		Sigma-Aldrich	T8154
Tween® 20	C ₂₆ H ₅₀ O ₁₀	Roth	9127.1

Homemade solutions recipes

Working and stock solutions prepared in the laboratory are listed in **table 2**.

Table 2. Stock and working solutions recipes. (PBS: Phosphate buffered saline, PBS-T: Phosphate buffered saline with Triton™ X-100, PFA: Paraformaldehyde, PO₄ Buffer: Phosphate Buffer, SDS: Sodium dodecyl sulfate, TAE Buffer: Tris-acetate-EDTA Buffer)

Solution	Composition
Blocking solution	10% goat serum, 0.5% Triton X-100 in 1x PBS
Borate buffer	0.1M Na ₂ B ₄ O ₇ in ddH ₂ O, pH 8.5-8.6
Buffer A	500mM KCl, 100mM Tris-base (Trizma®) in ddH ₂ O; pH 8.7
Citrate buffer	10mM tri-sodium citrate dihydrate, 0.05 % Tween 20 in ddH ₂ O; pH 6.0
Electrophoresis loading dye	20% Ficoll® 400, 0.1M EDTA pH 8.0, 1% SDS, 0.25% Bromophenol blue
Lysis buffer	0.1M Tris HCl pH 8.5, 0.5mM EDTA, 0.02% SDS, 0.2M NaCl in ddH ₂ O, 0.1% Proteinase K
PBS (10x)	137mM NaCl, 8.2mM Na ₂ HPO ₄ x 2 H ₂ O, 2.68mM KCl, 1.47mM KH ₂ PO ₄ ; pH 7.4
PBS-T	0.5% Triton X-100 in 1x PBS; pH 7.4
PFA 20%	0.47 mM HN ₂ PO ₄ x 2 H ₂ O, 20% PFA; pH 7.4
PO ₄ buffer (10x)	1.04M NaH ₂ PO ₄ x 2 H ₂ O, 0.93 M NaOH; pH 7.2-7.4
Re-expression medium	1:50 NeuroBrew®-21, 1:100 L-glutamine 200Mm in MACS neuro medium
SDS (10x)	0.248M Tris-base (Trizma®), 1.918 M Glycine, 35mM SDS, pH 8.3
Storing solution	30% Glycerol, 30% Ethylene glycol, 10% PO ₄ Buffer (10x)
TAE buffer (50x)	2M Tris-base (Trizma), 1M Glacial Acetic Acid, 0.1M Na ₂ -EDTA x 2 H ₂ O in Millipore H ₂ O

Antibodies

The list of all used antibodies is provided in **table 3**.

Table 3. List of primary (1) and secondary (2) antibodies for immunostaining, and magnetic microbeads conjugated antibodies for MACS (3). All antibodies used in this doctoral thesis, displaying the class of antibody, animal host in which the antibody has been produced, and finally the manufacturer together with the catalog number.

1. Primary antibodies:				
Antibody	Isotype	Host	Company	Catalog
αAPC (CC1)	IgG2b	Mouse	Calbiochem (Millipore)	OP80
αBassoon	IgG2ak	Mouse	Enzo Life Sciences	ADI-VAM-PS003-F
αBrdU	IgG	Rat	Abcam	Ab6326
αDCX	IgG	Rabbit	Abcam	ab18723
αGFAP	IgG1	Mouse	Sigma-Aldrich	G3893
αGFP	IgY	Chicken	Aves Labs	GFP-1020
αGPR17	IgG	Rabbit	Homemade (Prof. Rosa)	
αIba1	IgG	Rabbit	Wako Chemicals	019-19741
αKi67 (SP6)	IgG	Rabbit	Thermo Fisher	MA514520
αMAG	IgG1	Mouse	Merck Millipore	MAB1567
αNeuN	IgG1	Mouse	Merck Millipore	MAB377
αNG2	IgG	Rabbit	Merck Millipore	AB5320

Material and Methods

α Olig2	IgG	Rabbit	Merck Millipore	AB9610
α S100 β	IgG1	Mouse	Sigma-Aldrich	S2532
α Shank3	IgG	Rabbit	Homemade (Prof. Böckers)	

2. Secondary antibodies:

Antibody	Isotype	Host	Company	Catalog
α Chicken Alexa Fluor [®] 488	IgG	Goat	Thermo Fisher	A11039
α Mouse IgG Cy [®] 3	IgG	Goat	Dianova	115-165-166
α Mouse IgG2 Alexa Fluor [®] 647	IgG	Goat	Thermo Fisher	A21242
α Mouse IgGak Alexa Fluor [®] 568	IgG	Goat	Thermo Fisher	A21134
α Rabbit Alexa Fluor [®] 488	IgG	Donkey	Thermo Fisher	A21206
α Rabbit biotinylated	IgG	Goat	Vector Laboratories	BA-1000
α Rabbit Cy [®] 3	IgG	Donkey	Dianova	711-17-1525
α Rabbit Cy [®] 5	IgG	Donkey	Dianova	711-17-1525
α Rat Cy [®] 3	IgG	Donkey	Dianova	112-165-167

3. Magnetic beads-associated antibodies for MACS:

Antibody	Isotype	Host	Company	Catalog
α AN2 Microbeads	IgG1	Rat	MACS Miltenyi Biotec	130-097-171
α CD140a (PDGFR α) Microbeads	IgG2b	Rat	MACS Miltenyi Biotec	130-101-547
α O4 Microbeads	IgM	Mouse	MACS Miltenyi Biotec	130-096-670

Consumables

In **table 4**, I have only listed those consumables that were indispensable for our experiments (e.g., genotyping, the sacrifice of animals, immunostainings, cell sorting, and mass spectrometry) and not for regular daily laboratory work.

Table 4. Consumables. Here it has been provided the name of the product, the company that manufactured them, and the catalog number.

Name	Company	Catalog
24-well clear TC-treated multiple wells	Costar	3524
C tubes	MACS Miltenyi Biotec	130-096-334
Conical tubes 15ml	Schubert & Weiss GMBH	352096
Conical tubes 50ml	Schubert & Weiss GMBH	352070
Coverslips, thickness: 1, 24x60mm	Roth	H878.2
Filter papers, type 595 ½, D=240	GE Healthcare Whatman	10311651
Insulin-syringe U-100 (0.5 ml/ 0.3x8mm)	Seidel Medipool	324870
MACS SmartStrainers (70 μ m)	MACS Miltenyi Biotec	130-110-916
MS Columns	MACS Miltenyi Biotec	130-095-823

Material and Methods

Object slide	Roth	H870.1
Pre-Separation Filters (70µm)	MACS Miltenyi Biotec	130-095-823
Reaction tubes 0.5ml	Roth	7060.1
Reaction tubes 1.5ml	Roth	7080.1
Reaction tubes 2.0ml	Roth	7083.1
Reaction tubes 5.0ml	Nerbe plus	04-252-1000
TC Plate 48 well, Standard, F	Sarstedt	83.3923.005
Tissue culture flask T-25 (25cm ²)	Sarstedt	83.3910

Equipment, devices, and instruments

Table 5, only displays the equipment that was fundamental for buffer preparation, VPA performance measurement, sample processing, and data acquisition.

Table 5. Equipment, devices, and instruments utilized for buffer preparation, experiment, sample processing, and data acquisition. It has been provided the name of the equipment and the name of the company, where they were purchased.

Equipment	Company
Beam for motoric assessment	Homemade
Behavior arena	Homemade
Bioruptor® Standard Sonicator System	Diagenode
CM1900 cryostat	Leica
Compact fluorescent microscope BZ-9000 (Bioevo)	Keyence
CS SPE Confocal couple with DMi8 fluorescent microscope	Leica
Digital counter punch proximity switch magnetic induction	Star Eleven
ED open heating water bath	Julabo
EpiShear™ probe sonicator	Active Motif
Eppendorf ThermoMixer® F1.5	Eppendorf
Explorer® analytical electronic balance EX224	OHAUS
Finial steel ends for 19mm curtain poles	Trendy-live
Flying saucer running plate of 17.5cm diameter	Little Family Members (USA)
Gel documentation system with UV transilluminator Smart 3	VWR
gentleMACS™ Octo dissociator	MACS Miltenyi Biotec
Heraeus™ Megafuge™ 40 R centrifuge	Thermo Fisher
Heraeus™ Pico™ 17 microcentrifuge	Thermo Fisher
Inverted light microscope DM IL	Leica
LSM 7 confocal microscope	Zeiss
MACS MultiStand	MACS Miltenyi Biotec
Magnetic hotplate stirrer RCS basic	IKA
Mini centrifuge	Sunlab
MINIPLUS® 3 peristaltic pump	Gilson
Neodym magnets	Kany Store
Neubauer counting chamber (0.1mm depth)	Marienfeld

Material and Methods

OctoMACS™ magnetic separator	MACS Miltenyi Biotec
PCR-thermal cycler advanced® primus 96	Peqlab
pH 525 digital pH-meter	WTW
PowerPac™ HC high-current power supply	Bio-Rad
Precision balance PBS/PBJ	Kern
Q Exactive™ HF Hybrid Quadrupol-Orbitrap™ Mass spectrometer	Thermo Fisher
Rotarod model 47600	Ugo Basile
Running wheels 14cm diameter	Homemade
Standard orbital shaker model 1000	VWR
Stereomicroscope M60	Leica
UltiMate™ 3000 RSLCnano System	Thermo Fisher
Ultrasonic bath sonicator	Thomas Scientific
Vacuum concentrator	H. Saur Laborbedarf
Video camera Toshiba Camileo 200x	Toshiba
Vortem shaking incubator	UniEquip
Vortex-Genie 2	Scientific Industries

Software

In this section, it has been displayed all the software for data acquisition (e.g., microscope imaging, behavior assessment, imaging analysis, proteomic data analysis, image processing, and analysis, data analysis, and figure preparation).

Table 6. Software used for the acquisition and analysis of the data. Together with the software name, it is provided the company or developer of each one.

Software	Developer
Adobe Illustrator	Adobe Systems
BZ Analyzer	Keyence
BZ-II Viewer	Keyence
EthoVision XT	Noldus
GraphPad Prism 7.02	GraphPad Software Inc.
ImageJ	National Institute of Health and the Laboratory for Optical and Computational Instrumentation, USA
LAS X Life Science	Leica
MaxQuant	Computational Systems Biochemistry (Prof. Jürgen Cox, MPI for Biochemistry)
Perseus	Computational Systems Biochemistry (Prof. Jürgen Cox, MPI for Biochemistry)

Methods

Animals, transgenic lines, housing, and running performance tracking

All experiments were performed following the respective authorities' ethical guidelines of the Ludwig Maximilians Universität, Ulm University, and the government of Germany to ensure animal welfare in research. All mice were adult female and male at the 8 – 12 weeks old age (18 – 25g of weight) from the starting point of the experiments. Most of the animal background corresponded to the strain *C57Bl/6* except for the *Sox10-eGFP* mouse, which has an *FVB/N* background. Animals were bred in standard conditions; and given food and water *ad libitum*, including during experimental proceedings. During the experiments, mice were separated and individually caged to follow up on their running performance. During breeding and tests, the light cycle was automatically programmed to implement 12 hours of dark and 12 hours of light cycle.

All running devices consisted of a regular running wheel composed by a metallic grid of 14cm diameter or a flying saucer exercise wheel for small pets made of plastic of 17.5cm width. Running performance was measured by a homemade device, which consisted of two parts: 1) a magnet that was installed on the running apparatus and 2) a magnetic sensor that was connected to a digital clock-like counter. In principle, each time the magnet crossed in front of the sensor, it induced a signal and registered by the digital counter. Thereby, I managed to count the number of rotations of the running wheel or flying saucer made. On a daily base, counters digits were registered for posterior analysis. The conversion of rotations to distance was performed by the following geometric formula: $d * \pi * r = D$, where d is the diameter of the wheel, π is the ratio of a circle's circumference ($d * \pi$) to its diameter (D), and r is the number of rotations. Running performance was defined as D per unit of time (days or weeks).

In this doctoral thesis, the following transgenic mouse lines were used:

1) *NG2-CreERT2 x CAG-GFP* for tamoxifen-inducible GFP expression in NG2-glia (Huang et al. 2014) This mouse model was generated by crossing the *NG2-CreERT²* with the *CAG-GFP* mouse line (Huang et al. 2019; Nakamura, Colbert, and Robbins 2006). The *NG2-CreERT²* was generated by introducing the Cre-recombinase (*CreERT²*) sequence, by a knock-in approach, downstream the promoter of NG2. Thus, Cre-recombinase will be expressed exclusively in those cells, in which

Material and Methods

NG2 promoter has higher strength, such as NG2-glia and pericytes. The expression of CreER^{T2} in multiple cells does not present a problem for our experiments due to the distinctive morphology of the cells. The Cre-recombinase has been fused to the human-estrogen ligand-binding domain, therefore, making the CreER^{T2} only catalytically active under the administration of tamoxifen. Finally, mice have the GFP construct, which upstream has a stop codon flanked by two 34 base-pair loxP sites, all the sequence under the cytomegalovirus- β actin (CMV) promoter (Nakamura, Colbert, and Robbins 2006). Thus, in this mouse line, Cre-recombinase is expressed only in NG2⁺ cells, which application of tamoxifen push for the removal of the stop codon upstream the GFP construct, thereby, constitutively expressing the reporter in NG2⁺ cells, allowing to follow the fate of cells over time.

2) *Sox10-GFP* mouse line was purchased from the Mutant Mouse Resource and Research Center (MMRRC). Mice were generated under the GENSAT project from Nathaniel Heintz of the Rockefeller University in an effort to map the expression of genes in the central nervous system of the mouse (Gong et al. 2003). In this mouse line was introduced a modified bacterial artificial chromosome (BAC) containing inserted GFP upstream of the targeted gene. Because Sox10 is expressed in the whole oligodendrocyte lineage, both NG2-glia and oligodendrocytes constitutively express the reporter.

3) *GPR17-iCreER^{T2} x CAG-GFP* mouse line for tamoxifen-inducible GFP expression in GPR17⁺ NG2-glia was generated by the pairing of the *GPR17-iCreER^{T2}* and the *CAG-GFP* mouse line (Vigano et al. 2016; Nakamura, Colbert, and Robbins 2006). A difference with the *NG2-CreER^{T2} x CAG-GFP* is that in *GPR17-iCreER^{T2}* mice, modified BAC containing the improved CreER^{T2} (iCreER^{T2}) (Shimshek et al. 2002) was introduced under the promoter of GPR17 and, subsequently, BAC was randomly inserted in the mouse genome. Thus, similar to the aforementioned *NG2-CreER^{T2}*, iCreER^{T2} catalytic activity happens solely after tamoxifen induction; thus, constitutively expressing GFP only in GPR17⁺ cells.

4) *Sox10-iCreER^{T2} x Esco2-fl x CAG-GFP* mouse line for tamoxifen-inducible GFP expression and conditional knockout of cohesion acetyltransferase establishment of sister chromatid cohesion 2 (Esco2) in the whole oligodendrocyte lineage (Simon et al. 2012; Schneider et al. 2016;

Material and Methods

Whelan et al. 2012). For this model, three mouse lines have been crossed: The *Sox10-iCreER^{T2}*, the *CAG-GFP*, and the *Esco2-fl*. Similar to the *GPR17-iCreER^{T2}* mouse model, mice were generated by the random insertion of a modified BAC containing the *iCreER^{T2}* under the *Sox10* promoter in the genome. Regarding the *Esco2-fl* mice, two loxp sites have been introduced, flanking exons 2 and 3 of the targeted gene, impairing the expression of *Esco2* in tamoxifen-induced cells. It has been shown that *Esco2* is important for the separation of sister chromatids during mitosis, and its deletion impairs this function, promoting cells to undergo apoptosis (Whelan et al. 2012). Thus, in this mouse line is possible to promote GFP expression and *Esco2* deletion after tamoxifen induction, leading to ablation of proliferating NG2-glia (Schneider et al. 2016). Despite that oligodendrocytes have also a strong *Sox10* promoter; firstly, oligodendrocytes are postmitotic cells; hence, do not proliferate. Secondly, it has been shown that myelin is not affected in these mice (Schneider et al. 2016). Interestingly, it has been shown that, collaterally, these mice present decreased NG2-glia differentiation; thus, it could be used as a model for blocking oligodendrogenesis (Schneider et al. 2016; Fard et al. 2017).

5) *Sox10-iCreER^{T2} x Shank3-fl x CAG-GFP* mouse line for tamoxifen-inducible GFP expression and conditional knockout of the postsynaptic scaffold protein Shank3. Mice were generated by pairing the *Sox10-iCreER^{T2}*, the *CAG-GFP*, and the *Shank3-fl* mouse line (kindly provided by Prof. Dr. Tobias Böckers, not published mice). Shank3 is a member of the Shank family of scaffold proteins, which is important for the structural integrity and assembly of the post synapse (Naisbitt et al. 1999; Arons et al. 2012; Tu et al. 1999). In the *Shank3-fl* mice, two loxp sites have been introduced, flanking the exon 11 of the target gene. Although there is no literature of this mouse model, it has been observed that similar constitutive knockouts show a reduction in the major isoforms of shank3 and decreased number of AMPAR in the postsynaptic density (Schmeisser et al. 2012). Because NG2-glia form synapses with neurons (Bergles et al. 2000; De Biase, Nishiyama, and Bergles 2010), it could be that Shank3 also plays a role in the maintenance of neuron-glia synapses. Thus, in this mouse line is possible to promote GFP expression and Shank3 deletion after tamoxifen induction, possibly impairing communication between NG2-glia and neurons.

DNA extraction and Genotyping

After pups weaning, the tip of the tail or a piece of an ear, removed while ear tagging, was used for DNA extraction. Biological samples were introduced into a 1.5ml reaction tube together with 500µl of lysis buffer containing the proteinase K. Afterwards; the sample was left in a vortem shaking incubator at 55°C and 1300rpm overnight.

On the next day, samples were centrifuged at 12000rpm for 10min. The supernatant was transferred into a fresh 1.5ml reaction tube, and 500µl of isopropanol was added and mixed for 5min on an orbital shaker at room temperature. Samples were centrifuged again at 12000rpm for 10min. Then, the supernatant was discarded carefully, and the pellet was left drying with the reaction tubes leads open and top-down. Finally, 100µl of 10mM Tris-HCl of pH 8.5 was on top of the pellet and incubated in a vortem shaking incubator at 55°C for 2h.

Depending on the DNA sequence, a different protocol was used for sequence amplification (see **table 7**):

Table 7. Specifications for the amplification of the different genes. The table displays the different genes amplified in this doctoral thesis and for each, the reaction buffer, the utilized primers, and the cycle program for the various PCR.

Gene	Reagents and amounts	Primers	Thermocycler program
Esco2	12µl of ddH ₂ O 2µl MgCl ₂ 2µl Buffer A 0.5µl of each primer 0.5µl dNTPs 0.5µl <i>Taq</i> Polymerase 2µl DNA sample	S: ACT TGG GTC CTC ATT CTG CAG AGC AS: GTG CAC ATA CTT ATT GAC AGG TGG	Hot start 94°C 94°C for 3min <u>26 cycles</u> 94°C for 30s 55°C for 30s 72°C for 1min end 72°C for 10min
GFP	12µl of ddH ₂ O 1.5µl MgCl ₂ 2.5µl Buffer A 5µl Betaine 1µl each primer 0.5µl dNTPs 0.5µl <i>Taq</i> Polymerase 1µl DNA sample	S: CTG CTA ACC ATG TTC ATG CC AS: GGT ACA TTG AGC AAC TGA CTG	Hot start 94°C 94°C for 5min <u>29 cycles</u> 94°C for 30s 55°C for 30s 72°C for 1min end 72°C for 10min

Material and Methods

GPR17-iCreERT2	3.5µl of ddH ₂ O 2.5µl MgCl ₂ 2.5µl Buffer A 2.5µl Betaine 0.5µl of each primer 0.5µl dNTPs 0.5µl <i>Taq</i> Polymerase 2µl DNA sample	S: CTT GGC ACC ATA GAT CAG GC AS: TAT GGC AGG AGG CAT GCG CA	Hot start 94°C 94°C for 3min <u>30 cycles</u> 94°C for 30s 55°C for 45s 72°C for 2.5min end 72°C for 5min
NG2-CreERT2	12µl of ddH ₂ O 1.5µl MgCl ₂ 2.5µl Buffer A 5µl Betaine 0.5µl of each primer 0.5µl dNTPs 0.5µl <i>Taq</i> Polymerase 1µl DNA sample	Cre-S: GGC AAA CCC AGA GCC CTG CC WT-AS: GCT GGA GCT GAC AGC GGG Cre-AS: GCC CGG ACC GAC GAT GAA GC	Hot start 94°C 94°C for 3min <u>30 cycles</u> 94°C for 30s 64°C for 30s 72°C for 45s end 72°C for 2min
Shank3	12µl platinum SuperMix 0.5µl of each primer 1µl DNA sample	S: TCTCTGGCCCTGGTTTTATG AS: CAGTGAAGAAGCCCCAGAAG	Hot start 95°C 95°C for 3min <u>36 cycles</u> 95°C for 30s 60°C for 1min 72°C for 2min end 72°C for 10min
Sox10-eGFP	18µl of ddH ₂ O 1.5µl MgCl ₂ 1.5µl Buffer A 0.5µl of each primer 0.5µl dNTPs 0.5µl <i>Taq</i> Polymerase 2µl DNA sample	S: TTC ACC TTG ATG CCG TTC T AS: GCC GCT ACC CCG ACC AC	Hot start 95°C 95°C for 5min <u>30 cycles</u> 95°C for 30s 59°C for 30s 72°C for 20s end 72°C for 3min
Sox10-iCreERT2	11µl of ddH ₂ O 2.5µl MgCl ₂ 2.5µl Buffer A 5µl Betaine 0.5µl of each primer 0.5µl dNTPs 0.5µl <i>Taq</i> Polymerase 5µl DNA sample	S: AAA CAC CCA CAC CTA GAG AC AS: ACC ATT TCC TGT TGT TCA GC	Hot start 94°C 94°C for 3min <u>27 cycles</u> 94°C for 30s 52°C for 30s 72°C for 1min end 72°C for 10min

To analyze the amplified sequences and confirm the product size, the DNA samples were run in an electrophoresis gel. Afterward, the gel was assembled by dissolving 2% agarose in 1x TAE buffer. The solution was heated in a microwave, programmed at 600 W, for a few minutes. After heating, the agarose solution was cooled down with ice and by stirring to avoid the irregular polymerization of the gel. Meanwhile, ethidium bromide was added, depending on the volume

Material and Methods

of the gel (e.g., for 200ml of agarose solution, 10 μ l of ethidium bromide was added). After cooling, the solution was poured in polystyrene electrophoresis running chamber, a plastic comb was placed to generate the sample pockets, and it was left to dry. As soon as the gel polymerized, the running chamber was introduced into a bath chamber filled up with a 1x TAE buffer, and the comb was removed from the gel. Each amplified DNA sample was added with 4 μ l of electrophoresis loading dye, and, subsequently, 15 μ l of each loading dye and DNA mixture was transferred into the gel pockets. The power supply was fixed to 100V, generating an electric field to run the samples for 30 – 50min, depending on the DNA amplification. Each group of probes was run together with a DNA ladder and a positive, a negative, and wild-type control. Finally, the gel was analyzed by a UV transilluminator in a gel documentation system, allowing the visualization of the different DNA fragments.

Tamoxifen induction and BrdU or EdU treatment

All Cre-recombinase mouse lines were induced with tamoxifen, which was diluted initially in 10% ethanol, followed by 90% corn oil to a final concentration of 40mg/ml. To improve the dissolution of tamoxifen, a probe sonicator was implemented for 8min and at 40% intensity. Induction protocol consisted of administering each adult mouse tamoxifen three times for a week, every second day, a dose of 10mg of suspended tamoxifen per 30g of body weight.

The synthetic nucleoside 5-bromo-2'-deoxyuridine (BrdU) or the 5-ethynyl-2'-deoxyuridine (EdU), both analog to the nucleotide thymidine, were administered orally with the drinking water in a concentration of 1mg/ml of BrdU or 0.2mg/ml of EdU and 1% sucrose in tap water. BrdU and EdU were employed to tag dividing cells from its administration until the animal was sacrificed. Hence, providing a marker for proliferation and, together with the CC1 marker, for differentiation. After the preparation of BrdU or EdU, the stock was stored at 4°C for no longer than one week.

Histology and Immunofluorescence

Animals were deeply anesthetized with a drug cocktail containing 3.63% ketamine and 0.175% xylazine diluted in 0.9% NaCl solution. Afterward, transcardial perfusion was performed by pumping 25ml of PBS, followed by 50ml of 4% PFA in PBS as a fixative. Later, brains were extracted and embedded in 4% PFA in PBS for between 30min – 2h. After postfixation completion, brains were transferred to 30% saccharose in PBS overnight, or until sink, for cryoprotection.

Free-floating 30 μ m thick sections of were prepared with the help of a cryostat and kept in PBS at 4°C for short-term storage or in storing solution at -20°C for long-term storage. For staining, slices were blocked and permeabilized in “blocking solution” for 1h. After washing with PBS, sections were incubated in specific combinations of the following primary antibody diluted in blocking solution overnight at 4°C with shaking: rabbit α NG2 (1:500), mouse IgG2b α CC1 (1:50), chicken α GFP (1:500), rabbit α GPR17 (1:1000), mouse IgG1 α MAG (1:300), rabbit α Ki67 (1:100), rabbit α DCX (1:200), mouse IgG1 α GFAP (1:500), rabbit α Iba1 (1:500), mouse IgG1 α NeuN (1:300), rabbit α Olig2 (1:200), mouse IgG1 α S100 β (1:500), rabbit α Shank3 (1:300), and mouse IgG2ak α Bassoon (1:250). Next day, slices were in PBS and incubated in a specific combination of the following secondary antibodies diluted in blocking solution for 2h at room temperature with shaking: α Chicken Alexa Fluor[®] 488 (1:250), α Mouse IgG2b Alexa Fluor[®] 647 (1:250), α Rabbit Alexa Fluor[®] 488 (1:250), α Mouse IgG Cy[®] 3 (1:250), α Mouse IgGak Alexa Fluor[®] 568 (1:250), α Rabbit Cy[®] 3 (1:250), α Rabbit Cy[®] 5 (1:250), and α Rat Cy[®] 3 (1:250). Past this time, slices were washed in PBS.

For the GPR17 immunostaining, slices were first incubated in biotinylated α -rabbit (1:250) and detection made through the signal amplification based on a TSA[®] kit (Perkin Elmer). For this, slices were treated with 1% H₂O₂ in PBS for 30min, followed by washings in PBS. Afterward, incubation in Streptavidin-HRP (1:100, provided by TSA[®] kit) was performed overnight at 4°C. The next day, slices were washed with PBS and incubated in tyramide fluorophore (1:50) in 1x amplification diluent (both provided by TSA[®] kit) for 3 – 10min. Finally, slices were washed in PBS.

Material and Methods

For BrdU immunostaining, initially, other immunostainings were performed. Then the slices were fixated with 4% PFA in PBS, followed by incubation in previously warmed up citrate buffer at 96°C for 15min, followed by a cooling down step for 15min at room temperature and finally washing with PBS. As an alternative to citrate buffer, I incubated the slices in 2N HCl for 1h at room temperature. Afterward, slices were washed in borate buffer two consecutive times for 15min, and subsequently, washing the slices with PBS. After antigen retrieval treatment, BrdU immunostaining was performed as the aforementioned protocol with incubation of the primary antibody rat α BrdU (1:250) and, later on, incubation of the secondary antibody α Rat Cy[®] 3 (1:250) (1:250). For EdU detection, all other stainings were performed before, and slices were treated with a highly-specific click reaction kit (Click-iT™ Alexa Fluor[®] 647).

After immunostaining, slices were counterstained with DAPI (1:1000 in ddH₂O) and mounted on a slide with aqua-poly/mount. To evaluate immunostainings' quality or to generate tile imaging, a compact fluorescent microscope was used, and sequential scanning reconstruction was performed in the BZ-analyzer. Within the same experimental cohort, camera exposure was kept constant for each channel. For high-resolution images and co-localization determination, pictures were taken in a confocal microscope and analyzed through the open-source Java-based image processing software ImageJ and Leica's LAS X Life Science. Settings such as laser intensity, PMT gain, wavelength bandpass filter, and photodetector offset were identical within the same sample cohort.

For cortex analysis, images of a whole column of the cortex, containing each cortical layer. This was done for at least three slices per animal. The advantages of this strategy were, first, to avoid the counting variability among different cortical layers. Second, to analyze and compare the effects among different cortical layers. For CC analysis, three pictures of a different part of the region were taken, and this was performed for at least three slices per animal. For the creation of equally bins size, the cortex was measured, from pia to ventral, and then divided into three equal areas, and named from dorsal to ventral as bin 1 - 3. For counting, only cells containing visible DAPI staining were taken into consideration.

Magnetic associated cell sorting (MACS)

Isolation of NG2-glia was performed by a protocol based on the association of conjugated antibodies with a magnetic bead, which recognizes a specific membrane surface protein on the cells of interest.

Animals were sacrificed after two and four weeks of voluntary physical activity (VPA group) and then sacrificed by cervical dislocation. Control individuals were selected accordingly to the final age of the VPA group. After sacrifice, brains were extracted and embedded in ice-cold Hank's balanced salt solution (HBSS) with Ca^{+2} and Magnesium (Mg^{+2}). Under a stereomicroscope, meninges were removed to diminish contamination from fibroblast or epithelial cells, and the cortical GM was mechanically isolated. The isolated cortices were cut in 4 – 8 smaller sagittal slices and introduced into a c tube (a particular container that is placed in the gentleMAC[®] Octo Dissociator) containing 1900 μl of “buffer Z” (fantasy name from manufacture) until the cell disaggregation step.

For cell dissociation and MACS, I utilized the commercially available “Adult Brain Dissociation Kit” and antibodies conjugated with the magnetic beads from Miltenyi Biotec. Therefore, it must be highlighted that the specific content of the buffers or the enzymes is not available for the public. Thus, I will provide the commercial fantasy names of such products. Already in the buffer Z, the tissues were added 50 μl of “enzyme P” and, subsequently, 30 μl of enzyme mixture was added, which consisted of 20 μl of “buffer Y” and 10 μl of “enzyme A.” Afterward, the lead of the c-tubes was closed and placed upside down (it was made sure that none pieces were stuck on the lead) in an instrument for semi-automated and standardized tissue dissociation/homogenization with heaters named gentleMAC[®] Octo Dissociator. The device's sole purpose is to homogenize samples by steady and smoothly stirring in a temperature-controlled environment.

After dissociation, c tubes were centrifuged at 300g at room temperature for 1min, to make sure that all the homogenized solution was pull to the bottom. For the next step, the homogenate was resuspended and pass through the MACS SmartStrainer[®] (sieve) of 70 μm pore size, previously placed on a 15mL conical tube. Afterward, ice-cold DPBS (with Ca^{+2} , Mg^{2+} ,

Material and Methods

glucose, and pyruvate) was added into the tube, again, through the MACS SmartStrainer[®], to recover cells caught in the filter and, thereby, increasing the number of sorted cells. Then, MACS SmartStrainer[®] was discarded, and the conical tube was centrifuged at 300g for 10min at 4°C, followed by complete removal of the supernatant.

To reduce the probability of clogging the separation column, the debris of produced by myelin and dead cells was removed of the samples. For this, into each conical tube was added 900µl of “debris removal solution,” together with 3100µl DPBS, were mixed with the sieved homogenate. Later, 4000µl of DPBS was slowly and carefully added on top of the previously mixed solution to form two phases. The biphasic solution was centrifuged at 3000g at 4°C for 10min in a full brake and full acceleration mode, resulting in a three-phase solution (above the supernatant, middle debris and bottom the solution and the cell pellet). The upper and middle phases were discarded, and the tube was filled up until 15ml with DPBS.

The conical tube was filled up with cold DPBS to a final volume of 15ml, followed by gently inverting to resuspend the pellet. Afterward, the sample was centrifuged at 1000g at 4°C for 10min, and subsequently, the supernatant was eliminated, leaving the pellet intact.

Cells were resuspended with 2ml of “re-expression medium” and placed in a bain-marie at 37°C with shaking for 30 – 45min. Later, samples were centrifuged at 300g for 10min. The supernatant was discarded and 80µl of DPBS was added on the pellet, subsequently, 10µl of FcR blocking agent was added, mixed, and incubated in the fridge (2°C - 8°C) for 10min.

Meanwhile, a mix of antibodies was prepared, adding 4µl of each antibody of αO4, αCD140 (PDGFRα) and αAN2 (NG2) Microbeads, reaching a final volume of 12µl of antibody solution mixture. Then, 10µl of the antibody solution was added into the sample and incubated for 15min in the fridge (2°C - 8°C). Eventually, cells were washed with 2ml of DPBS and centrifuged at 300g for 10min. Afterward, the supernatant was discarded, and 500µl of DPBS was added.

For sorting, an OctoMACS[™] magnetic separator was coupled to a MACS MultiStand, providing a magnetic field, and a MACS MS column was inserted into the magnet, to retain the labeled cells. A pre-separation filter of 70µm diameter pore was located on top of the column and a conical tube on the bottom, to collect all unlabeled cells. After applying 500µl DPBS, the

Material and Methods

sample was added and passed through the column. Then the column was washed with 500µl DPBS three times. Finally, cells were pushed out of the column, collected, and counted with a Neubauer chamber. Finally, the sample was centrifugated at 300g for 10 min, and the supernatant was discarded. Cells were stored at -80°C until they were processed and run in the mass spectrometer.

Liquid chromatography-mass spectrometry

Cells were processed with the PreOmics Kit as described by the manufacturer. Every reagent and consumables were provided by the manufacturer. For this, cells samples were added 50µl of “lyse buffer” and placed in a heating block at 95°C and 1000rpm for 10min. Afterward, samples were spin down at room temperature and 300g for 10s. Next, samples were sheared in a temperature controlled Bioruptor® sonicator for 10 cycles of 30s intercalating on and off mode. Later, samples were transferred to a cartridge and cool down to room temperature. Then, 50µl of “digest buffer” previously diluted in “resuspend buffer” was applied into the sample and placed in a pre-heated heating block at 37°C and 500rpm for 3h. To stop the proteolysis, 100µl of “stop buffer” was added to the cartridge and placed in a heating block at room temperature and 500rpm for 1min. Afterward, the cartridge was centrifuged at 3800g for 3min and wash two times, each with the same centrifugation configuration. Afterward, 100µl of “elute buffer” was placed and was collected after centrifugation at 3800g for 3min. The collection tube was placed in a vacuum concentrator at 45°C until completely dry. Finally, LC-Load was added, aiming for a final peptide concentration 1g/l. Finally, the collection tube was sonicated in an ultrasonic bath for 5min.

Tryptic peptides corresponding to 1×10^4 cells were injected in an UltiMate™ 3000 RSLCnano System and separated in a 15-cm analytical column (home-packed 75µm ID with ReproSil-Pur C18-AQ 2.4 µm from Dr. Maisch) with a 120-min gradient from 3 to 40% acetonitrile in 0.1% formic acid. The effluent from the HPLC was directly electrosprayed into a Q Exactive™ HF Hybrid Quadrupol-Orbitrap™ mass spectrometer operated in data-dependent mode to switch between full-scan MS and MS/MS acquisition automatically. Survey full-scan MS spectra (from

Material and Methods

m/z 375–1600) were acquired with resolution $R=60,000$ at m/z 400 (AGC target of 3×10^6). The ten most intense peptide ions with charge states between 2 and 5 were sequentially isolated (window 2.0 m/z) to a target value of 1×10^5 and fragmented at 27% normalized collision energy. Typical mass spectrometric conditions were spray voltage, 1.5 kV; no sheath and auxiliary gas flow; heated capillary temperature, 250°C; ion selection threshold, 33,000 counts.

MaxQuant 1.5.2.8 was used to identify proteins and quantify them by LFQ. Conditions were: Database, *Mus musculus* (uniprot_UP000000589 downloaded on the 14.01.2015); MS tol, 10ppm; MS/MS tol, 0.5 Da; Peptide FDR, 0.01; Protein FDR, 0.01 Min. peptide Length, 7; Variable modifications, Oxidation (M); Fixed modifications, Carbamidomethyl (C); Peptides for protein quantitation, razor and unique; Min. peptides, 1; Min. ratio count, 2. Identified proteins were considered differential if the LFQ log₂ p-value were lower than 0.05 (Perseus Multi comparison t-test with default parameters) when 2w VPA vs. control or 4w VPA vs. control groups were compared to each other.

Analysis of cognitive and motoric behavior

Novel Object Recognition (NOR) test:

Our protocol was based on the methods employed in (Leger et al. 2013), which had a total duration of five days. The first three days were for habituation, followed by one-day familiarization to the objects, and on the last day, one of the objects was replaced by a novel object. All sessions were performed in a home-made arena of 36cm wide x 36cm long x 18cm high, and wood shavings were spread on the bottom. After each trial, the arena was cleaned with 70% ethanol to avoid odorant cues from other mice. The objects were placed in one half of the arena, separated 16cm from each other, and 10cm from the arena walls and the middle line.

To have a successful novel object recognition (NOR) test, I needed to eliminate any type of potential stressor. Therefore, I proceeded to take the following precautions. First, to reduce the stress by handling, each mouse was handled for 1min at least two weeks before the test started, twice per week. Second, to reduce stress by novelty (neophobia), animals were exposed to a novel object (different from the used in the test) one week before starting the experiment.

Material and Methods

Third, to reduce environmental stress present in the behavioral room, mice were brought to the place at least 1h before beginning each session. Fourth, three-day habituation to the arena, avoiding any potential neophobic response during the test.

The objects were selected following the suggestions in (Ennaceur 2010) in an effort to maximize differences between the familiar and the novel object. I used two sets of objects. On the one hand, within the set, the objects were completely identical. On the other hand, between sets, the objects were different in color, shape, material, and brightness, although they were similar in their dimensions. Nevertheless, the introduction of several distinctive features between the two sets of objects might inadvertently incline the intrinsic preference of the mice towards one of them. Therefore, to reduce systematic error and interpretation of results due to object preference bias, the set of objects considered familiar or novel, and, as well, its location within the arena was randomly designated for each mouse.

Regarding odor, which could drive the mice's preference towards one of the objects, both object sets were inodorous. Furthermore, before each trial, they were wiped with 70% ethanol to avoid odorant cues from other mice or the researcher and let dry for 3min. In the same line, for each trial, the arena was wiped with 70% ethanol, to reduce odorant references left by other mice, and gloves were changed for a fresh pair.

Regarding the timeline, a three-day habituation protocol was performed not only to reduce potential environmental stressors as mentioned above but to diminish the environmental novelty and promote further exploration towards the objects. Thus, animals were induced to the empty arena for 10min, twice per day, and each time point was at least 6h apart. After each trial, the animal was returned to its cage. For the familiarization protocol, mice were brought to the arena again, albeit this time, they were exposed to two identical objects for 10min. Finalized this session, they were returned to their cages for 24h. On the last day, mice were exposed to one object from the previous day (familiar) and one from the other set (novel) for 10min.

For the analysis, each trial was recorded with a camera and video-tracked by the software Ethovision XT (both provided by Noldus Information Technology). In the software, I established a circular area with a 4cm radius surrounding each object. Explorative behavior of the objects

Material and Methods

was defined as “the amount of time the animal is close to the object showing a sniffing behavior towards the object,” and it was manually counted with the help of the software stop-watch. Recognition index (RI) was calculated by the following formula:

$$RI = \frac{t_{NO} - t_{FO}}{t_{OE}}$$

Where t_{NO} , represent the time exploring the novel object, t_{FO} , time exploring the familiar object, and t_{OE} the total time exploring both objects.

Hindlimbs clasping behavior

Hindlimbs clasping behavior is an observational methodology to analyze neurological motor deficits in mice (Brooks and Dunnett 2009). For this, mice were held from the tail and suspended in the air 3 – 5cm away from the surface about 5min. A healthy physiological response was granted to those animals; which reflex was to stretch the limbs away from the central point of the body. In counterpart, those mice that legs were curling to the middle-point of the body were categorized as clasping behavior.

Beam walk crossing test

Beam walk test consisted of challenging animals to cross a beam from one extreme to the other. The beam was characterized as a wooden round-shaped pole of 1.0cm in diameter and 70cm in length elevated by 18cm from the ground. In healthy physiological conditions, mice have no problems crossing this beam (Schneider et al. 2016). One week before behavioral assessment, animals were daily trained for one week, to habituate the animals to the test. After this training period, the behavior test was monitored by a digital video camera (Toshiba Camileo 200x) and analyzed afterward in a blinded manner.

The score of this test for each mouse was determined by successfully or failing to cross the beam. Animals that stayed on the shaft without walking for more than 30s were also assigned as fail. Mice were enforced to pass the pole three times each trial day with 5min intervals

Material and Methods

between each replicates. The average of the replicates was considered as the final value for further analysis of the motor behavior.

Rotarod performance test

The rotarod test consisted of challenging mice by placing them on a horizontally oriented, rotating cylinder or rod, which is suspended above a chamber. Mice naturally try to stay on top of the rod because the distance between the rod and the floor of the chamber is low enough to avoid injuries from falling but high enough for the animal to prevent them from dropping themselves. The rotation program was set up as within 5 min of the experiment, the speed of rotation linearly increased from 5 to 20rpm. As described in the other test, before the behavioral assessment, mice were daily trained for one week, to habituate the animals to walk on the rotating rod. After this training period, the behavior test was monitored once a week by a digital video camera (Toshiba Camileo 200x) and analyzed afterward in a blinded manner.

By this test, I measured the time to take for the mice to fall from the rod to base. The base has a plank that stops the timer after the mice tumble on it. By stopping the timer, it gave us the time delay that the animals manage to stay on top of the rod. Rotarod test was performed three times per day per animal, and the final value for posterior analysis was taken from the average of the replicates.

Statistical analysis

All graphs were constructed and analyzed in GraphPad Prism except for the proteomic data, which was tested in Perseus. Each figure shows the mean (bar and dots) and the standard error of the mean (S.E.M., error bars). Pie charts show the proportion. Every statistical test used in our experiments is specified in the figures and the text body of the results.

Results

Dynamics of proliferation and differentiation of cortical NG2-glia after VPA in the adult mouse brain

It is well-known that NG2-glia proliferate and differentiate in the physiological adult brain (Simon, Gotz, and Dimou 2011; Dimou et al. 2008; Young et al. 2013; Hughes et al. 2013; Dawson et al. 2003). Physical activity can modulate both proliferation and differentiation *in vivo* (Simon, Gotz, and Dimou 2011; Tomlinson, Huang, and Colognato 2018). Here, I decided to assess if proliferation and differentiation could be modulated through our model of voluntary physical activity (VPA), which consist of providing animals free access to running devices. Because animals innately and voluntary use the running wheels, we can increase their locomotor activity without manipulating them as in the case of forced physical activity models by treadmills. Additionally, I tested the dynamics of these processes by analyzing different time points and by removing the stimulus after a certain period.

The experiments were done in *C57Bl/6* wild-type mice. I split the mice into three groups: 1) animals single housed in standard cages without running wheels (“control group”) for two and four weeks (n= 3 – 7). 2) Mice single housed in cages with running wheels (“VPA group”) for two and four weeks (n = 3 – 7), and 3) Mice single housed with running wheels for two weeks, and afterward, transferred to standard cages for two further weeks (“recovery group”, n = 5) (**Fig. 7a**). Every group was administered BrdU through the drinking water for the duration of the entire experiment (**Fig. 7a**). After each experiment, mice were sacrificed and brains were obtained, sliced, and slices were analyzed by immunostaining.

In most of our experiments, except when mentioned otherwise, I mainly analyzed the GM of the motor cortex (**Fig. 7b**), a decision made in light of two main premises. First, glucose consumption in the rodent motor cortex increases after augmented physical activity (Vissing, Andersen, and Diemer 1996), and the regional CBF is enhanced in the human motor cortex after exercise (Hiura et al. 2018). The local metabolic demand and CBF boost have been associated with an increase in neuronal activity to supply neurons augmented energetic demand. Second, the mouse cortical neurons have differential internode distribution, presenting segments of their

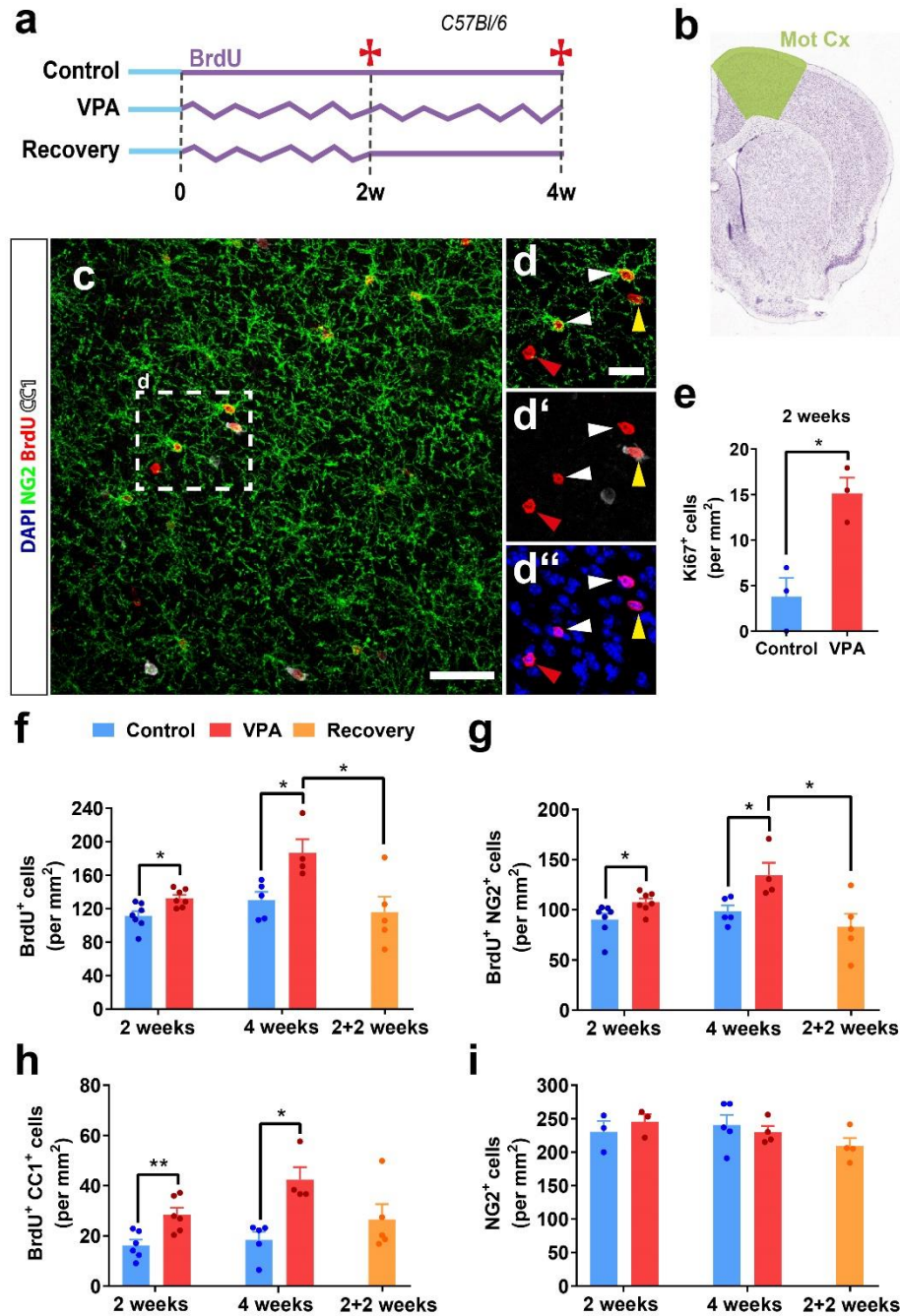


Figure 7. NG2-glia proliferation and differentiation dynamics after VPA in the C57/Bl6 mouse motor cortex. a) Scheme illustrating the experimental protocol. Straight lines indicate mice were housed in standard cages, and crooked ones indicate that they were caged with running wheels. Cyan colored lines represent that pure drinking water was provided, and purple ones that BrdU was given. The red crosses indicate mice sacrifice time points. Time scale: w = weeks. **b)** Coronal brain slice marking the region (motor cortex highlighted with green), where cell counting was performed (bregma: 1.045 to -1.055 mm, modified image from the Allen Institute for Brain Science). **c)** Histological analysis of counterstaining with DAPI (blue), NG2 (green), BrdU (red), and CC1 (white) imaged with 400x optic magnification. Scale bar = 50µm. **d - d'')** Digital magnification of the square area in panel c showing proliferating NG2-glia (white arrow), newly generated oligodendrocytes (yellow arrow), and proliferating cells NG2⁻ and CC1⁻ (red arrow). Scale bar = 20µm. **e)** Quantification of the total number of Ki67⁺ cells in control (blue) and VPA (red) group. **f)** Quantification of the total number of proliferating cells (BrdU⁺) after 2 and 4 weeks in control (blue), VPA (red),

Results

and recovery (orange) groups. g) Quantification of the total number of proliferating NG2-glia (BrdU⁺NG2⁺) after 2 and 4 weeks in control (blue), VPA (red), and recovery (orange) groups. h) Quantification of the total number of newly generated oligodendrocytes (BrdU⁺CC1⁺) after 2 and 4 weeks in control (blue), VPA (red), and recovery (orange) groups. i) Quantification of the total number of NG2-glia (NG2⁺ cells) after 2 and 4 weeks in control (red), VPA (red), and recovery (orange) groups. In all graphs, bar and error bars represent the group mean and the SEM, respectively; and each dot represents a single animal mean (n = 3 - 7). The 2 weeks control vs. 2 weeks VPA data were analyzed by a two-tailed unpaired t-test, and all 4 weeks control vs. 4 weeks VP vs. 2+2 weeks (recovery) data were analyzed through a two-tailed one-way ANOVA and a *post hoc* Newman-Keuls multiple comparison test. P < 0.05 = *, P < 0.01 = **.

axons that remain unmyelinated (Tomassy et al. 2014). Thereby, these exposed segments of the axon represent an excellent substrate for new myelin to be allocated.

Initially, I analyzed whether proliferation was affected by VPA. Hence, I performed immunostaining with an antibody against an epitope of Ki67 protein, in which peak expression occurs during the cell cycle stages S, G2, and M, Ki67-labeled cells that are actively proliferating, albeit, limited to the time point of sacrifice. Already after two weeks of VPA, I observed an ~4 fold increase in the number of Ki67⁺ cells in the VPA compared with the control group (mean ± SEM, control: 3.8 ± 2.04 and VPA: 15.12 ± 1.74; two-tailed unpaired t-test p-value = 0.0134) (**Fig. 7e**), indicating an increase in proliferation due to VPA.

To know whether this proliferation was sustained over time and whether VPA stimulation was constantly necessary for enhancing this behavior, I provided BrdU for two and four weeks and counted the number of BrdU⁺ cells of control, VPA, and recovery animal groups (**Fig. 7a and 7c**). BrdU is incorporated only during the S phase of the cell cycle, which is characterized by the synthesis of new DNA. BrdU incorporation has the advantage over other approaches, such as Ki67 immunostaining, because it allows quantifying all cells proliferating from the time point of BrdU administration until the mice are sacrificed. Because of the way that BrdU incorporates into the DNA, the signal is characterized by its smooth round shape and colocalization with a nuclear counterstainings, like 4',6-diamidino-2-phenylindole (DAPI) (**Fig. 7d**). I found an increase of ~1.2-fold (**Supp. table 1**, two-tailed unpaired t-test p-value = 0.0102) and ~1.4-fold (**Supp. table 1**, two-tailed one-way ANOVA, F-value = 5.548, p-value = 0.0216 followed by Newman-Keuls multiple comparisons *post hoc* test, q-value control vs VPA = 3.594 (statistical analysis was done together with the recovery group)) in the VPA group compared to the control, after two and four

Results

weeks, respectively (**Fig. 7f**). These results confirm that VPA promotes proliferation, which is dependent on the length of the experience or training. It is important to note that the difference between the groups increased over time, which suggests that continuous VPA is necessary and has an additive effect. This notion is reinforced after showing that the removal of the running wheels for two weeks after two weeks of VPA, abolished the increase in the number of BrdU⁺ cells induced by VPA (**Supp. table 1**, two-tailed one-way ANOVA, F-value = 5.548, p-value = 0.0216 followed by Newman-Keuls multiple comparisons *post hoc* test, q-value control vs. recovery = 0.9918 and VPA vs. recovery = 4.529 (statistical analysis was done together with the 4w control and VPA group)) (**Fig. 7f**).

Previous reports have shown that NG2-glia divide in the healthy adult brain, representing the major proliferating cell population outside the neurogenic niches (Simon, Gotz, and Dimou 2011; Young et al. 2013; Kang et al. 2010; Dimou et al. 2008). Thus, to determine whether the BrdU⁺ cells within the oligodendrocyte lineage, I analyzed the colocalization of BrdU with antibodies against either NG2 or *adenomatous polyposis coli* (APC/ CC1) (**Fig. 7c and 7d**). The former is a classic marker for NG2-glia, which, together with BrdU, allows us to estimate the number of proliferating NG2-glia. NG2 antibody signal labels NG2-glia cytoplasm which show long multi-processes with an isotropic radial distribution (**Fig. 7c and 7d**). Although pericytes also express NG2 (Ozerdem et al. 2001), the characteristic multi-processed morphology of NG2-glia (**Fig. 7c and 7d**) made them easily distinguishable from the enlarged shape of CNS pericytes (Ozerdem et al. 2001). On the other hand, CC1 labels exclusively mature oligodendrocytes. The antibody targets an epitope of the APC protein, which function is still largely unknown. The CC1 labeling provides an oval-shaped signal that is localized in the cytoplasm of oligodendrocytes (**Fig. 7c and 7d**). CC1 colocalization with BrdU allows us to determine the number of newly formed oligodendrocytes since the administration of BrdU (Simon, Gotz, and Dimou 2011; Tomlinson, Huang, and Colognato 2018; Gibson et al. 2014; Steadman et al. 2020). This last premise is sustained by the fact that oligodendrocytes are postmitotic cells without the ability to divide. Therefore, the incorporation of BrdU by a proliferating NG2-glia and subsequent differentiation is required to show BrdU⁺ oligodendrocytes.

Results

I observed that in both the control and the VPA groups most BrdU⁺ cells were either NG2⁺ or CC1⁺ (**Fig. 7h and 7i**), indicating that most proliferating cells are from the oligodendrocyte lineage (2w control: BrdU⁺NG2⁺ = 81.33%, BrdU⁺CC1⁺ = 14.62%, 2w VPA: BrdU⁺NG2⁺ = 81.09%, BrdU⁺CC1⁺ = 21.43%, 4w Control: NG2⁺BrdU⁺ = 75.60%, CC1⁺BrdU⁺ = 14.11%, 4w VPA: NG2⁺BrdU⁺ = 72.11%, BrdU⁺CC1⁺ = 22.69%, Recovery: NG2⁺BrdU⁺ = 71.69%, CC1⁺BrdU⁺ = 22.99%). By comparing the VPA group to the control group, I observed that there was a significant increase in the number of NG2⁺BrdU⁺ cells and CC1⁺BrdU⁺ cells by ~1.2-fold (**Supp. table 1**, two-tailed unpaired t-test p-value = 0.0336) and ~1.8-fold (**Supp. table 1**, two-tailed unpaired t-test p-value = 0.0071) after two weeks, respectively, and by ~1.4-fold (**Supp. table 1**, two-tailed one-way ANOVA, F-value = 5.63, p-value = 0.0207 followed by Newman-Keuls multiple comparisons *post hoc* test, q-value control vs. VPA = 3.265 (statistical analysis was done together with the recovery group)) and ~2.3-fold (**Supp. table 1**, two-tailed one-way ANOVA, F-value = 5.634, p-value = 0.0207 followed by Newman-Keuls multiple comparisons *post hoc* test, q-value control vs. VPA = 4.712 (statistical analysis was done together with the recovery group)) after four weeks, respectively (**Fig. 7g and 7h**). In contrast, the recovery group showed a lower number of NG2⁺BrdU⁺ cells with respect to the VPA group at four weeks and similar numbers to the control group at two and four weeks (**Supp. table 1**, two-tailed one-way ANOVA, F-value = 5.63, p-value = 0.0207 followed by Newman-Keuls multiple comparisons *post hoc* test, q-value control vs VPA = 3.265 (statistical test was done together with the 4w control and VPA groups)) (**Fig. 7g**).

Interestingly, although the number of CC1⁺BrdU⁺ cells in the recovery group did not reach statistically significant difference compared to the control and the VPA group, the mean was located between the control and the VPA group (**Supp. table 1**, two-tailed one-way ANOVA, F-value = 5.634, p-value = 0.0207 followed by Newman-Keuls multiple comparisons *post hoc* test, q-value control vs. recovery = 1.71 and VPA vs. recovery = 3.099 (statistical test was done together with the 4w control and VPA group)) (**Fig. 7h**), and was remarkably similar to the mean after two weeks VPA (**Supp. Table 1**). The results suggest that to keep NG2-glia proliferation and differentiation, it is required for the mouse to continuously run, and, along with previous results, the longer the running wheels were provided, the more significant was the increase between the groups. Nonetheless, from the comparison of the recovery group with the two-weeks VPA group,

Results

it is tempting to suggest that the newly generated oligodendrocytes during the VPA remain stable over time, in contrast to the proliferating NG2-glia that decreased again.

Despite the increase in proliferation, I failed to observe changes in the total number of NG2-glia (**Supp. table 1**, for 2 weeks: two-tailed unpaired t-test p-value = 0.5075. For four weeks: two-tailed one-way ANOVA, F-value = 1.534, p-value = 0.2625) (**Fig. 7i**). This result goes in line with previous studies describing that, under physiological conditions, the number of NG2-glia always remains constant (Hughes et al. 2013). Therefore, this data hints at the homeostatic regulation of the NG2-glia population size, even in the VPA condition.

A reasonable question arises from these results. Are these changes specific to the motor cortex or is VPA globally affecting all brain NG2-glia? To answer the question, I analyzed different brain regions after four weeks of VPA (**Fig. 8a**). I focused our analysis in the corpus callosum (CC) ventral to the previously analyzed motor cortex (**Fig. 8b**) as cortical layer V motor cortex neurons project axons within the CC; therefore, it is possible that also in this region NG2-glia are also affected after increased physical activity. By now contradictory results have been shown in regard to NG2-glia proliferation and differentiation induced by neuronal activity in the CC. On the one side, indeed, enhanced neuronal activity of motor cortex neurons by optogenetics increased proliferation of NG2-glia in the CC (Gibson et al. 2014). In contrast, NG2-glia behavior does not change after VPA at the particular selected time point (McKenzie et al. 2014), which could be explained by the different approach to enhance neuronal activity.

Additionally, I analyzed the piriform cortex (**Fig. 8b**) for two reasons. Firstly, it has been prominently associated with odor information processing, which, to our knowledge at least, does not change during physical activity (Hiura et al. 2018). Secondly, I assumed that if VPA systematically changes the NG2-glia behavior, their properties should be similar within different GM areas in comparison to NG2-glia from a WM region, like the CC (Vigano et al. 2013; Dimou et al. 2008; Young et al. 2013).

Notably, I found no differences in the number of BrdU⁺ between the control and VPA group cells after four weeks either in the CC or in the piriform cortex (**Supp. table 1**, two-tailed unpaired t-test CC: p-value = 0.7237, Piriform Cortex: p-value = 0.6347) (**Fig. 8c and 8f**) or in the

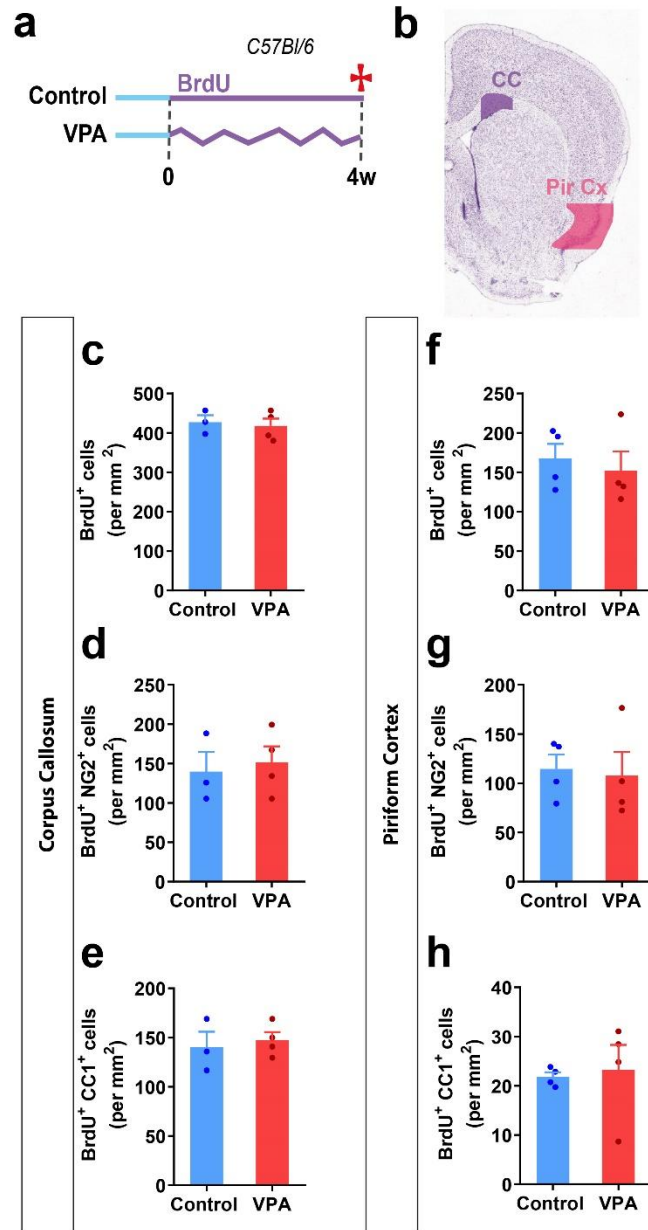


Figure 8. NG2-glia proliferation and differentiation after VPA in *C57/Bl6* mouse corpus callosum and piriform cortex. a) Scheme illustrating the experimental protocol. Straight lines indicate mice that were housed in standard cages, and crooked ones mean that they were caged with running wheels. Cyan colored lines indicate that pure drinking water was provided, and purple ones that BrdU water was given. The red cross indicates mice sacrifice time point. Time scale: w = weeks. b) Coronal brain slice labeling the regions (bregma = 1.045 to -1.055 mm, corpus callosum highlighted in purple and piriform cortex in magenta), where cell counting was performed (modified image from the Allen Institute for Brain Science). Panel c and f) Quantification of the total number of proliferating cells (BrdU⁺) after 4 weeks in control (blue), and VPA (red) groups. d and g) Quantification of the total number of proliferating NG2-glia (BrdU⁺NG2⁺ cells) after 4 weeks in control (blue) and VPA (red) groups. e and g) Quantification of the total number of newly generated oligodendrocytes after 2 and 4 weeks in control (blue), and VPA (red) groups. In all graphs, bar and error bars represent the group mean and SEM, respectively, and each dot represents a single animal mean (n = 4). Data were analyzed by a two-tailed unpaired t-test.

Results

total number of NG2⁺BrdU⁺ cells (**Supp. table 1**, two-tailed unpaired t-test CC: p-value = 0.7285, piriform cortex: p-value = 0.8211) (**Fig. 8d and 8g**) nor the total number of CC1⁺BrdU⁺ cells (**Supp. table 1**, two-tailed unpaired t-test CC: p-value = 0.6934, piriform cortex: p-value = 0.7852) (**Fig. 8e and 8h**). This result suggests that the changes in NG2-glia behavior are rather region-specific and related to local neuronal activity in the motor cortical GM.

Dynamics in indirect and direct NG2-glia differentiation modalities after VPA in the adult mouse brain

So far, I have shown that VPA increase NG2-glia proliferation and differentiation. Even though the quantification of CC1⁺BrdU⁺ cells has been widely used for measuring differentiation of the oligodendrocyte lineage *in vivo* (Simon, Gotz, and Dimou 2011; Tomlinson, Huang, and Colognato 2018; Gibson et al. 2014; Steadman et al. 2020), it requires that NG2-glia proliferated during BrdU administration, and afterward differentiate into oligodendrocytes. This observation represents a limitation in our theoretical framework because NG2-glia can differentiate directly without transiting through proliferation. Moreover, it has been shown by *in vivo* time-lapse live imaging that NG2-glia do not require initial proliferation to become an oligodendrocyte in the adult brain (Hughes et al. 2013; Hughes et al. 2018), at least within the time frame of 40 - 50 days. Therefore, the performed experiments can potentially underestimate the total number of newly generated oligodendrocytes after VPA (**Fig. 9**). To clarify this issue, I took advantage of the tamoxifen-inducible reporter mouse line *NG2-CreER^{T2} x CAG-GFP* that allow us label NG2-glia with a GFP reporter and follow their differentiation by colabelling with oligodendrocyte markers without the aid of BrdU (Huang et al. 2014; Nakamura, Colbert, and Robbins 2006).

NG2-CreER^{T2} x CAG-GFP mice were induced with tamoxifen. Afterward, mice were split into two groups: 1) Mice single housed in a standard cage ("control group," n = 6), and 2) Mice housed in cages with running wheels ("VPA group," n = 9), for six weeks. Control and VPA groups were given BrdU the first four weeks, and then it was replaced with regular BrdU-free water for the last two weeks before the end of the experiment (**Fig. 10a**). By immunolabeling against GFP, CC1, and BrdU, five cell populations were identified. First, cells that were GFP⁺CC1⁺ but BrdU⁻

Results

were classified as “direct newly generated oligodendrocytes” (dNGOLs) (**Fig. 10b, white arrows**). Second, those cells that were $GFP^+CC1^+BrdU^+$ were classified as “indirect newly generated oligodendrocytes” (iNGOLs) (**Fig. 10c, yellow arrows**). Additionally, I identified a small population of $CC1^+BrdU^+$ but GFP^- cells (**Fig. 10d**). These cells could correspond to the incomplete recombination of NG2-glia in our mouse model. Because this population were labeled for BrdU and CC1, they were also classified as iNGOLs (**Fig. 10d, cyan arrows**). Finally, not surprisingly, two populations of cells that were either GFP^+BrdU^+ but $CC1^-$ or GFP^+ but $BrdU^-CC1^-$ were also observed. Those were most likely to be proliferating non-differentiated NG2-glia and NG2-glia that neither proliferated nor differentiated during this time frame (**Fig. 10b – 10d, asterix and hashtag**), respectively.

After quantifying the number of iNGOLs and dNGOLs, I could observe in the control condition that the proportion of both direct and indirect differentiation was similar (iNGOLs = 49.61% vs. dNGOLs = 50.39%) (**Fig. 10e and 10f**). Notably, after VPA, direct, indirect and total differentiation (addition of iNGOLs and dNGOLs) increased by ~ 2.4 -fold, ~ 1.5 -fold, and ~ 2 -fold, respectively, in comparison to the control group (**Supp. table 2**, two-tailed unpaired t-test iNGOLs: p-value = 0.0425, dNGOLs: p-value = 0.0079, total NGOLs p-value = 0.0095) (**Fig. 10e**). In

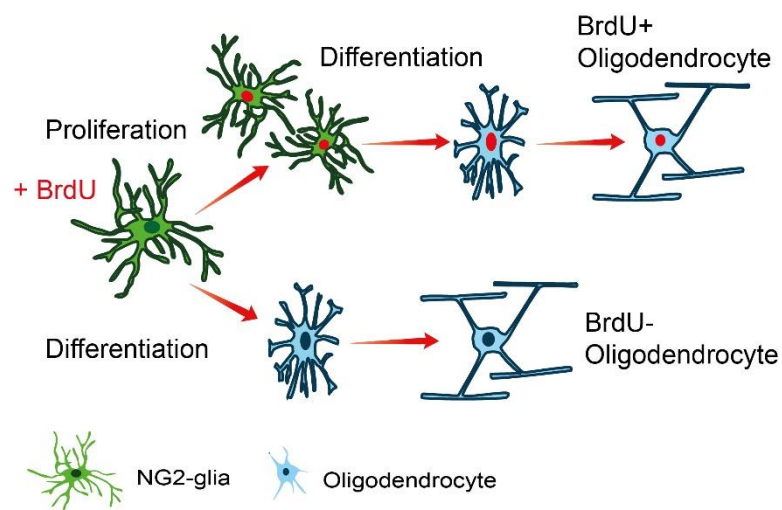


Figure 9. NG2-glia can differentiate into oligodendrocyte by two modalities. In the above part of the scheme, NG2-glia can proliferate, incorporating BrdU and then differentiate. This results in oligodendrocytes label with BrdU. Because oligodendrocytes are postmitotic cells, they cannot incorporate BrdU by themselves. Nonetheless, as shown in the lower part of the illustration, it is possible that NG2-glia differentiates directly into oligodendrocyte, resulting in oligodendrocytes, and therefore, not labelled with BrdU.

Results

contrast, after VPA, the proportion of direct and indirect differentiation shifted mostly in favor of the formation of dNGOLs over iNGOLs (62.30% over 49.61%, respectively) (**Fig. 10e and 10f**). Therefore, it is tempting to think that there is a NG2-glia population exist that is ready to rapidly differentiate into oligodendrocytes in response to VPA (dNGOLs). Conversely, there is another population that is more resistant to differentiation and first prioritizes self-renewal of the population over differentiation. From this experiments, I could confirm that proliferation is not a prerequisite for NG2-glia differentiation, which is supported by previous studies (Hughes et al. 2013; Hughes et al. 2018).

From our initial experiments (**Fig. 7**), differentiation is VPA-duration dependent. The longer the animals run, the bigger the difference between control and VPA groups. Nevertheless, it is not clear whether the physical activity performance, which I have defined as the distance run per unit of time (days or week), within a specific time window had a positive correlation with the magnitude of newly generated oligodendrocytes in the animals. Therefore, I correlated NG2-glia differentiation from each mouse with its VPA performance. Therefore, I correlated the number of indirect, direct, and total NGOLs from each mouse in VPA ($X_{VPA(i)}$) over the mean number of NGOLs in the control group ($\mu_{(x)control}$), and paired it with the number of kilometers per day ran by each mouse.

As expected, I observed that animals that performed poorly had a lower or similar number of NGOLs as the control group compared to their high workout counterparts ($\frac{X_{(i)VPA}}{\mu_{(x)control}} = 1$) (**Fig. 10g**). However, to our surprise, already after a threshold of ~ 1 km per day, differentiation reached rapidly a saturation plateau (best-fit values in a hyperbolic function: maximum plateau value \pm SEM, dNGOLs: $\frac{X_{(i)VPA}}{\mu_{(x)control}} = 3.15 \pm 0.37$, iNGOLs: $\frac{X_{(i)VPA}}{\mu_{(x)control}} = 1.58 \pm 0.14$, and total differentiation: $\frac{X_{(i)VPA}}{\mu_{(x)control}} = 2.38 \pm 0.26$) and differentiation had no correlation to VPA performance anymore (analyzed by a linear correlation, dNGOLs: $r = 0.5609$ and $p\text{-value} = 0.1161$, iNOLs: $r = 0.3535$ and $p\text{-value} = 0.3507$, total differentiation: $r = 0.5162$ and $p\text{-value} = 0.1548$) (**Fig. 10g**). These results revealed that there is a low threshold that needs to reach the maximum

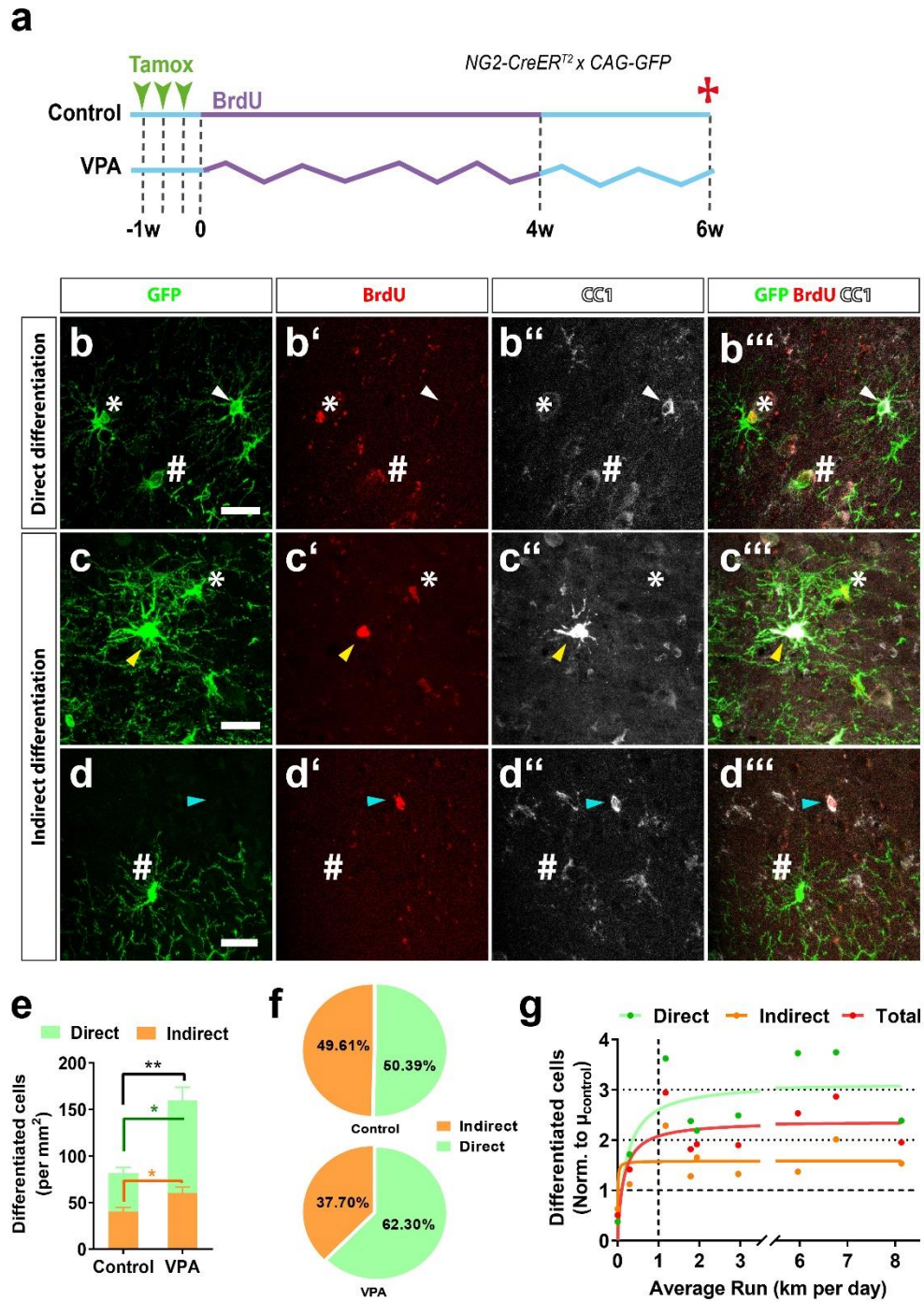


Figure 10. NG2-glia direct and indirect modalities of differentiation and behavior after VPA in *NG2-CreERT2 x CAG-GFP* mouse line. **a)** Scheme illustrating the experimental protocol. Straight lines indicate mice housed in standard cages, and crooked ones indicate that they were caged with running wheels. Cyan colored lines represent that normal drinking water was provided, and purple ones that BrdU water was given. Green arrow head shows the time point for the induction with tamoxifen, and the red cross indicates time point of sacrifice. Time scale: w = weeks. **b-b''')**, **c-c''')**, and **d-d''')** Histological analysis of GFP (green), BrdU (red), and CC1 (white). **b** shows an example of direct differentiation; **c** and **d** present examples of indirect differentiation. In mice, it was possible to find only GFP⁺ (NG2-glia, hashtag #), GFP⁺BrdU⁺ cells (proliferating NG2-glia, asterix *), GFP⁺CC1⁺ (dNGOLs, white arrow), GFP⁺BrdU⁺CC1⁺ cells (iNGOLs, yellow arrow), and BrdU⁺CC1⁺ cells (non-recombined iNGOLs, cyan arrow). Images were taken with

Results

400x optic magnification. Scale bar = 20 μ m. e) Quantification of the total number of newly generated oligodendrocytes by an indirect (orange, bar and asterisk), direct (green, bar and asterisk), and both differentiation modalities (iNGOLs + dNGOLs, black, asterisk) (n = 6 – 9). Bar and error bars represent the group mean and the SEM, respectively. Indirect control vs. indirect VPA, direct control vs. direct VPA, and indirect+direct control vs. both VPA data were analyzed by a two-tailed unpaired t-test. P < 0.05 = *, P < 0.01 = **. f) Pie charts show the proportion of indirect (orange) and direct (green) differentiation in control and VPA groups. g) Dot plot shows the ratio of each VPA mouse over the control mean in indirect (orange), direct (green), and both modalities (red) vs. the average run in km per day. Each dot is a single VPA animal. Dashed lines in axis indicate whether running mice had an equal total number of any differentiation modality to the control group (y=1). Data analyzed was done by a linear correlation and fit a hyperbola function.

differentiation possible by VPA. Nevertheless, the lack of linear correlation suggested that there might be a physiological mechanism that negatively regulates the differentiation of NG2-glia, restricting the total amount of NGOLs induced by VPA. Hence, two questions were raised in light of this evidence. First, do all NG2-glia react identically to VPA, or is there a subpopulation that is more prompt to respond to VPA in comparison to the rest of the population? And second, does the NG2-glia less reactive to VPA expand and take over the total population after VPA? To tackle these questions, I performed a global protein profile description analysis of NG2-glia after VPA.

Proteomic profiling of cortical NG2-glia after VPA by a combined MACS/LC-MS² approach

To profile and analyze molecular changes of NG2-glia after VPA, I employed a two-step approach by specifically obtaining NG2-glia from the adult brain through magnetic-associated cell sorting (MACS) together with liquid chromatography-mass spectrometry (LC-MS²), to analyze the protein expression from sorted NG2-glia after VPA (**Fig. 11a**). For these experiments, animals from the *Sox10-GFP* mice were used as in this mouse line, we obtained the highest number and purity of sorted cells (Nicole Unger's doctoral thesis).

Sox10-GFP mice were divided into three groups: 1) Mice caged in standard cages ("control group," n = 6), 2) mice were caged with a running wheel for two weeks ("2w VPA group," n = 6), and 3) mice housed with a running wheel for four weeks ("4w VPA group," n = 6). All animals were matched by age (14 – 16 weeks old) at the time of sacrifice. The GM was used in the posterior analysis because, as already mentioned, changes of NG2-glia were observed only in this

Results

region and not in the WM. Therefore, MACS and mass spectrometry work flow were performed according to the scheme in Fig. 4a and described more in detail in material and methods (**Fig. 11a**). The number of cells obtained ranged between 5×10^4 – 10×10^4 cells. With this protocol, I retrieved and compared the whole population of NG2-glia in the cortical GM against the population of NG2-glia that did not differentiate and kept proliferating after VPA, giving us an indirect method to identify proteins that might be relevant for differentiation into oligodendrocytes (**Fig. 12**).

As a first step, quality assurance of the probes was done by comparing the linear correlation of each sample to another by retrieving their Pearson's Coefficient. The low coefficients among samples might indicate high disparities, which are likely due to the inadequate processing of the probe. It is crucial to mention that, in this empirical context, the *a priori* assumption was that samples should not differ greatly from each other. By analyzing Pearson's Coefficient among samples, I could observe that the vast majority of the samples had a coefficient between ~ 0.8 - ~ 0.95 (**Fig. 11b**). As expected, Pearson's coefficients are higher when compared within the same group of probes than with another. However, I observed a significant exception in one of the samples from the 2w VPA group (probe 6), whose correlation with other samples ranged from ~ 0.6 - ~ 0.85 , the vast majority being between ~ 0.6 - ~ 0.7 (**Fig. 11b**). Therefore, the probe was excluded from further analysis.

Subsequently, variation in the levels of proteins was determined by a principal component analysis (PCA), and the results were plotted showing the two components with the highest change (Component 1, Component 2) (**Fig. 11c**). I could observe that the probes clustered in similar areas of the PCA plot, nonetheless, it was evident that the samples within the control group showed the greatest variation compared to 2w VPA and the 4w VPA (**Fig. 11c**). Interestingly, PCA suggests that the longer the physical activity, lower was the variation among the probes within the same group (**Fig. 11c**). This data may suggest that increased VPA displaces the NG2-glia population to a more homogeneous one and, therefore, reduced variation in their molecular profile.

Results

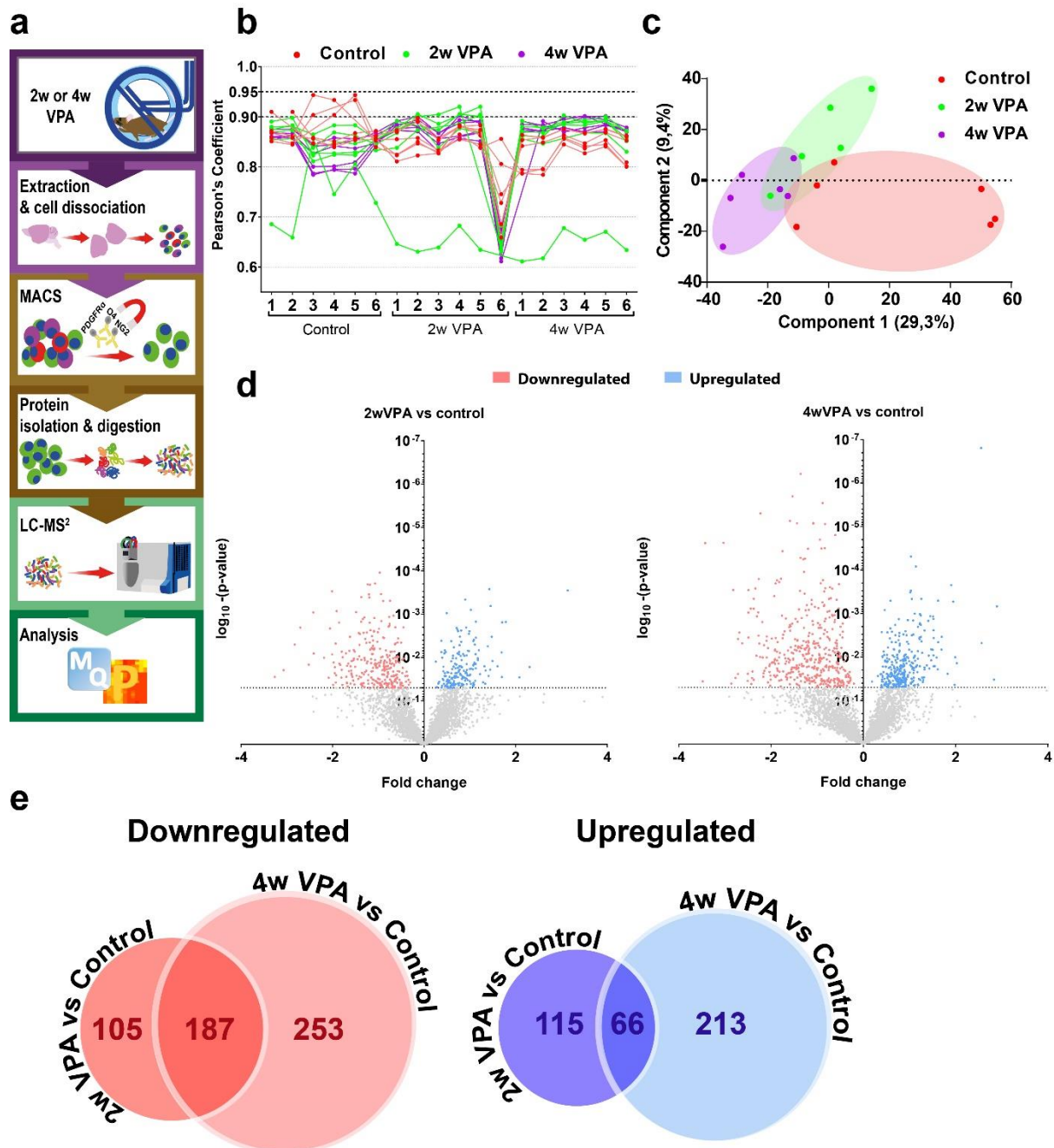


Figure 11. Cortical NG2-glia of the cortex protein profile after the VPA *Sox10-GFP* mouse line. a) Scheme illustrating the experimental protocol. b) Linear correlation (Person's coefficient) comparison among all probes coming from control, 2 weeks VPA (2w VPA), and 4 weeks VPA (4w VPA). c) Principal component analysis of the sample. Each dot is one probe. d) Volcano plot represents the $\log_{10}(-p\text{-value})$ vs. folds change in 2w VPA and 4w VPA in comparison to the control, data analyzed by Perseus software multi comparison t-test ($n = 5 - 6$). The threshold illustrated by the dotted line in the y-axis ($p\text{-value} = 0.05$). The blue dots are single proteins that are upregulated, and red ones are the individual proteins that are downregulated. e) Venn diagram shows downregulated (red) and upregulated (blue) proteins that overlap between 2w VPA vs. control and the 4w VPA vs. control protein group.

Results

To localize specific changes in protein level, I analyzed the global differences between the 2w VPA and the control group, and 4w VPA and the control group (**Fig. 11d**). Considering all proteins above a cut-off in p-value <0.05 , the results showed that after two weeks of VPA, 181 proteins were upregulated, and 292 proteins were downregulated compared with the control group (Perseus multi comparison t-test) (**Fig. 11d**). After four weeks of VPA, the number of proteins upregulated increased to 279 and the proteins downregulated to 440 compared with the control group (**Fig. 11d**). The results show that the increase in VPA duration, increased the number of regulated proteins from 513 to 719 (**Fig. 11e**). Interestingly, by comparing 2w VPA vs. control and 4w VPA vs. control, I appreciated that both groups shared 253 regulated proteins of which 66 proteins were upregulated, and 187 proteins were downregulated (**Fig. 11e**).

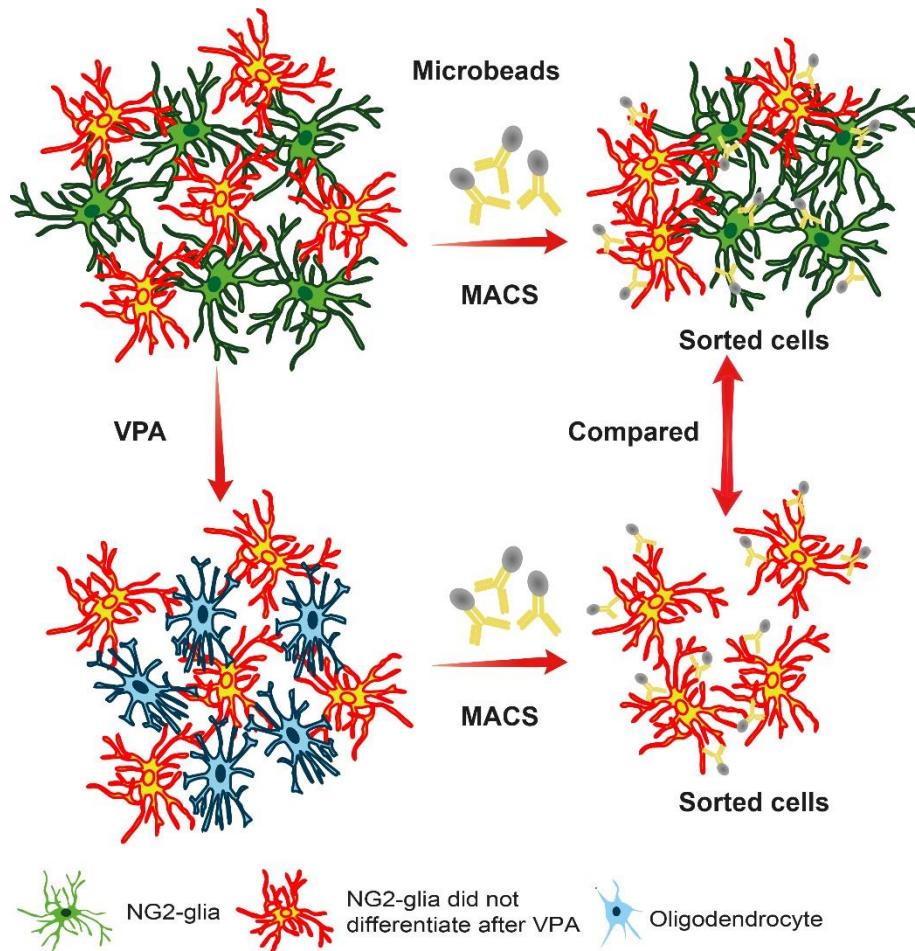


Figure 12. Cells obtained after MACS. Here is illustrated NG2-glia obtained before and after VPA (upper and lower part of the scheme, respectively). Before VPA, different subpopulations of NG2-glia are in the cortical GM. After VPA, NG2-glia differentiate into oligodendrocytes and after MACS, only the cells that did not differentiate are retrieved. Afterward, NG2-glia before and after VPA are compared to each other.

Results

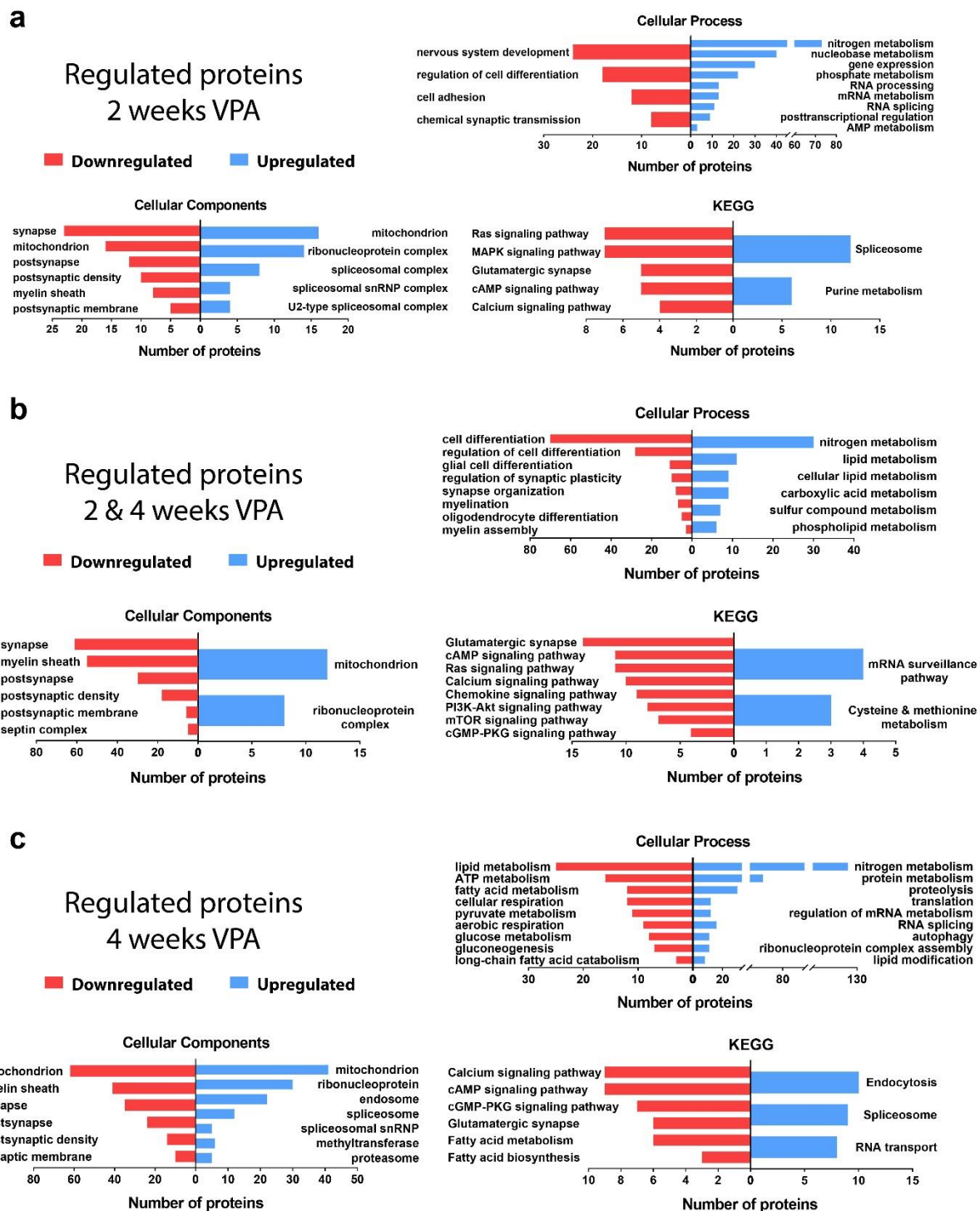


Figure 13. Functional enrichment categorization of downregulated and upregulated proteins after VPA in the *Sox10-GFP* mouse line. Each functional category (e.g., cellular process, cellular components, and KEGG) has been subcategorized in particular global terms (i.e., nervous system development, nitrogen metabolism, etc.). It is shown proteins a) exclusively regulated after 2 weeks VPA, b) shared after 2 weeks and 4 weeks VPA, and c) exclusively regulated at 4 weeks after VPA. In all graphs, the bar represents the accumulative number of proteins for each global term that has been upregulated (blue) and downregulated (red). KEGG database is a collection of manually drawn

Results

pathway maps representing our knowledge on the molecular interaction, reaction, and relation networks for different pathways including, among others, metabolism, genetic information processing, environmental information processing, and cellular processes.

To understand and identify the type of proteins that were regulated by VPA, I took advantage of STRING, an open-source database for protein-protein interaction, which also processes and classifies these interactions by functional enrichment (Szklarczyk et al. 2019) (**Fig. 13**). To facilitate the analysis, I divided the regulated proteins into three groups: 1) Proteins categories exclusively regulated after two weeks VPA (**Fig. 13a**), 2) proteins regulated after both two and four weeks VPA (**Fig. 13b**), and 3) proteins exclusively regulated after four weeks could be observed (**Fig. 13c**).

Interestingly, functional enrichment showed similarities in downregulated proteins in the three groups. The downregulated proteins show that NG2-glia differentiation was affected by VPA. For instance, proteins related to cell differentiation, glial differentiation, oligodendrocyte differentiation, myelination, and myelin assembly were massively downregulated (**Fig. 13b**). In the same line, cellular component proteins related to myelin were strongly reduced in the three groups (**Fig. 13a – 13c**). Interestingly, only after four weeks of VPA, there were robust changes in the metabolism of lipids, such as lipid, and fatty acid metabolism, and long-chain fatty acid catabolism (**Fig. 13c**).

In addition, the “Kyoto encyclopedia of genes and genomes” (KEGG) database identified that fatty acid metabolism and fatty acid biosynthesis-related proteins were downregulated (**Fig. 13c**). This shifted metabolism is arguably crucial for oligodendrocyte lineage maturation because of the massive cellular membrane expansion that takes place in oligodendrocytes during differentiation. Indeed, it has been shown that lipid metabolism proteins are upregulated when NG2-glia undergo differentiation into oligodendrocytes (Swiss et al. 2011), whereas impaired lipid metabolism in NG2-glia led to impaired proliferation, improper oligodendrocyte maturation, and impaired myelination after a WM injury with LPC (Dimas et al. 2019).

Regarding signaling pathways, I could appreciate that proteins related to the phosphoinositide 3-kinases/protein kinase B (PI3k-Akt) and mammalian target of rapamycin

Results

(mTOR) pathways decreased after two and four weeks of VPA (**Fig. 13b**), signaling pathways that are vital for the differentiation of NG2-glia into oligodendrocytes (Yang et al. 2015; Bercury et al. 2014; Zou et al. 2014; Wang, Yang, et al. 2020; Grier et al. 2017). Moreover, I also observed that a high number of proteins from the family of GTP-binding proteins known as septins were downregulated after two and four weeks of VPA (**Fig. 13b**). It has been speculated that septins might play a role in NG2-glia differentiation (Buser et al. 2009), although the data are so far inconclusive.

Unexpectedly, I found that there was a considerable decrease in the abundance of proteins related to synaptic function in the three group (**Fig. 13a – 13c**). For instance, among cellular processes, proteins related to chemical synaptic transmission, regulation of synaptic plasticity, and synapse organization were downregulated. In the same line, among cellular components, synapse, postsynaptic density, and postsynapse related proteins were reduced (**Fig. 13a – 13c**). Furthermore, in the KEGG database, I found that proteins associated with glutamatergic synapses and calcium signaling pathways are downregulated (**Fig. 13a – 13c**). The downregulation of these proteins may be specially significant because NG2-glia respond to neurotransmitters by increasing $[Ca^{+2}]_i$ (Hamilton et al. 2010) and it has been extensively shown that NG2-glia form connections with neurons through synapses (Bergles et al. 2000; De Biase, Nishiyama, and Bergles 2010). These evidences, together with the downregulation of proteins related to the differentiation of NG2-glia, could imply that there is a correlation between synapses and NG2-glia differentiation. NG2-glia forming synapses with neurons may differentiate rapidly after VPA, leaving undifferentiated cells that have fewer or no connections with neurons.

Among the upregulated proteins, I could not identify cellular components, processes, or signaling pathways that associated with specific features of NG2-glia. The ontology of this functional enrichment showed only very general terms as regulation of ribonucleoproteins complex, spliceosome, mRNA metabolism, autophagy, RNA splicing, protein metabolism, proteolysis, endocytosis, among many others (**Fig. 13a – 13c**).

From this protein profiling, it has been shown that the cells that remained undifferentiated after VPA have a less prompt to differentiate molecular signature. Therefore, I

Results

wondered whether a particular subpopulation of NG2-glia, which was more resistant to produce newly generate oligodendrocytes, was overtaking the motor cortex as result of the differentiation of NG2-glia population that responded to VPA (Hughes et al. 2013). Indeed, our group has previously described such subpopulation of NG2-glia that is uniformly distributed and has a much slower differentiation rate, called the GPR17⁺ NG2-glia (Lecca et al. 2008; Chen et al. 2009; Boda et al. 2011; Vigano et al. 2016). Hence, I wanted to test whether VPA led to enrichment of the GPR17⁺ NG2-glia subpopulation.

Dynamics of the population of GPR17⁺ NG2-glia after VPA in the adult mouse brain

Given the characteristics of the protein profile, it could be suggested that after VPA, NG2-glia tends to show a phenotype less prone to differentiate. Therefore, I wondered whether the GPR17⁺ NG2-glia increased their population after VPA and whether these cells respond or not to VPA.

To study the reaction of GPR17⁺ NG2-glia during VPA, I used the *Sox10-GFP* mouse line and split them into two groups: 1) Mice housed in a standard cage (“control group,” n = 3 at two weeks and n = 5 at four weeks), and 2) Mice caged with running wheels (“VPA group,” n = 3 at two weeks and n = 10 at four weeks). Under this experimental setup, I proceed to determine the total number of GFP⁺GPR17⁺ cells after two and four weeks in control or VPA conditions (**Fig. 14a**). In this set of experiments, only animals kept for four weeks on VPA were provided BrdU (**Fig. 14a**). The *Sox10-GFP* mouse line was used to correlate with the results obtained on the proteomic profiling and, also, to identify GPR17⁺ cells quickly with the GFP reporter. As expected from previous reports, not all GFP⁺ cells were GPR17⁺ (**Fig. 14b**).

I observed that after two weeks of VPA, there was a significant increase of ~2.1-fold in the total number of GFP⁺GPR17⁺ cells in the VPA group compared with the control group (**Supp. table 3**, two-tailed unpaired t-test p-value = 0.0368) (**Fig. 14c**). After four weeks of VPA, I observed a significant augmentation of ~1.4-fold in the total number of GFP⁺GPR17⁺ in the VPA group compared with the control group (**Supp. table 3**, two-tailed unpaired t-test p-value = 0.0162) (**Fig. 14c**).

Results

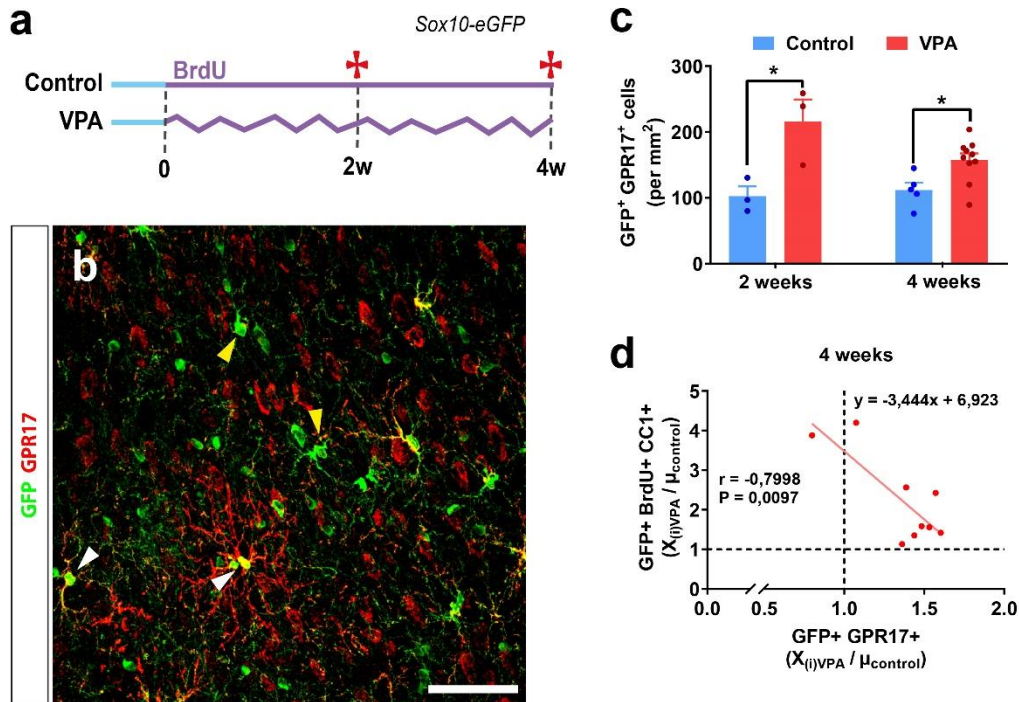


Figure 14. GPR17⁺ NG2-glia behavior after VPA and differentiation in the *Sox10-GFP* mouse line. a) Scheme illustrating the experimental protocol. Straight lines indicate mice housed in standard cages, and crooked ones indicate that they were caged with running wheels. Cyan colored lines represent that pure drinking water was provided, and purple ones that BrdU water was given. Red cross indicates time point of sacrifice. Time scale: w = weeks. b) Histological analysis of GFP (green) and GPR17 (red) imaged with 400x optic magnification. Scale bar = 50 μ m. c) Quantification of the total number of GPR17⁺ NG2-glia (GFP⁺ GPR17⁺ cells). Bar and error bars represent the group mean and SEM, respectively (n = 3 – 10). Each dot represents a single animal. 2w control vs. 2w VPA groups and 4w control vs. 4w VPA groups were independently analyzed by a two-tailed unpaired t-test. P < 0.05 = *. d) Dot plot compares the ratio of each running mouse total number of indirect differentiation (GFP⁺BrdU⁺CC1⁺) over the control group mean to the ratio of each running mouse total number of GPR17⁺ NG2-glia (GFP⁺GPR17⁺) over the control group mean. Dashed lines in axis indicate whether running mice had an equal total number of indirect differentiation than the controls (y-axis = 1) and the equivalent total number of GPR17⁺ NG2-glia than the control group (x-axis = 1). Data was analyzed by a linear correlation (P = 0.0097, r = -0.7998) and fit to a linear regression (y = -3.444x + 6.923) (n = 8).

I wondered whether the increase of GPR17⁺ NG2-glia correlated with a lower global differentiation in the motor cortex. To test this, after four weeks of VPA, I analyzed the correlation between the ratio of the total number of GFP⁺GPR17⁺ cells for each mouse with a running wheel ($Y_{(i)VPA}$) over the mean of GFP⁺GPR17⁺ cells in the control group ($\mu_{(y)control}$) against the ratio of the number of GFP⁺BrdU⁺CC1⁺ cells (iNGOL) for each mouse provided with a running wheel ($Z_{(i)VPA}$) over the mean of GFP⁺BrdU⁺CC1⁺ cells in the control group ($\mu_{(z)control}$) (**Fig. 14d**). In this scenario, a $\frac{Y_{(i)VPA}}{\mu_{(y)control}} = 1$ indicates no changes in the number of GFP⁺GPR17⁺ between

Results

individual running mouse and the control mean, and $\frac{Z_{(i)VPA}}{\mu_{(z)control}} = 1$ indicates no changes in the number of GFP⁺BrdU⁺CC1⁺ cells between each running mouse and the control group mean. Interestingly, a negative correlation between the two variables was observed, where animals that had more GPR17⁺ NG2-glia cells, showed the lower number of newly generated oligodendrocytes (linear correlation GFP⁺BrdU⁺CC1 vs. GFP⁺GPR17⁺: $r = -0.7998$, $r^2 = 0.6397$ and $p\text{-value} = 0.0097$. Linear regression equation: $y = -3.444x + 6.923$) (**Fig. 14d**).

Differentiation of GPR17⁺ NG2-glia after VPA in the adult mouse brain

As mentioned above, the GPR17⁺ NG2-glia is characterized by their slow differentiation (Vigano et al. 2016). My results have shown that there is an increase the number of GPR17⁺ NG2-glia after VPA, therefore, I wondered whether also GPR17⁺ NG2-glia differentiation increased in response to VPA, resembling their abilities in injury models (Vigano et al. 2016; Boda et al. 2011; Lecca et al. 2008).

To study the differentiation abilities of GPR17⁺ NG2-glia, I used the *GPR17-iCreER^{T2} x CAG-GFP* mouse line generated in our group (Vigano et al. 2016). I split the mice into two groups: 1) Mice housed in a standard cage ("control group," $n = 3 - 5$), and 2) Mice caged with running wheels ("VPA group," $n = 3 - 6$), and mice were sacrificed in the time points two, four and six weeks of VPA (**Fig. 15a**).

Most GFP⁺ cells were either NG2⁺ or CC1⁺, which corroborates that all of these cells are part of the oligodendrocyte lineage (**Fig. 15b - 15e**). Additionally, not all NG2⁺ were GFP⁺ (**Fig. 15b and 15c**), reinforcing the heterogeneity of NG2-glia in the brain (Lecca et al. 2008; Boda et al. 2011; Vigano et al. 2016). I did not observe statistically significant differences in the number of GFP⁺NG2⁺ between control and VPA groups at any time point (**Fig. 15f**). but only it appears to be a tendency for higher numbers of GFP⁺NG2⁺ in the VPA groups than in the control groups (**Supp. table 4**, two-tailed unpaired t-test $p\text{-value}$ 2w control vs. 2w VPA = 0.1015, 4w control vs. 4w VPA = 0.3272, and 6w control vs. 6w VPA = 0.1891) (**Fig. 15f**).

Results

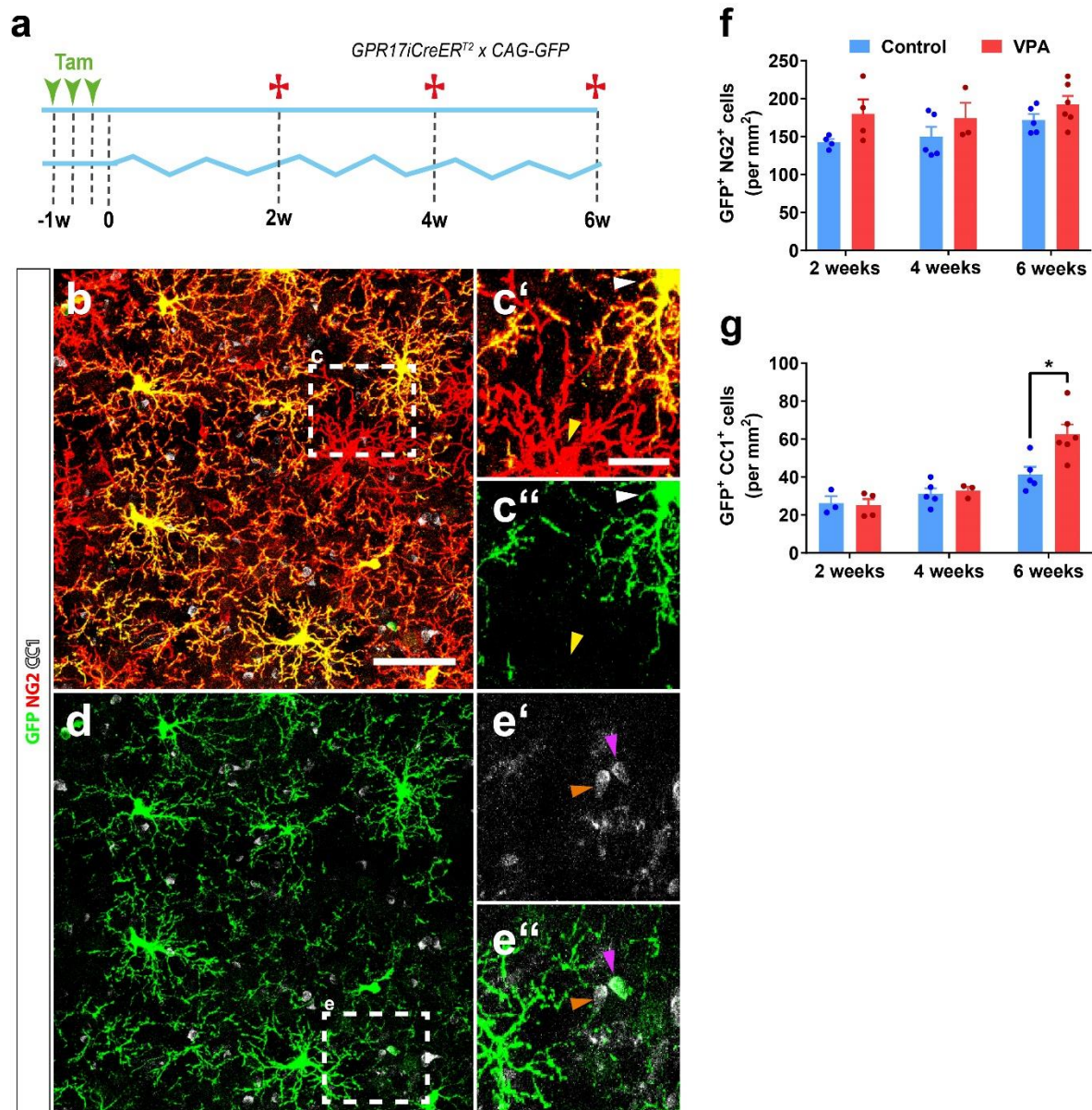


Figure 15. GPR17⁺ NG2-glia differentiation behavior after VPA in the GPR17-iCreERT2 x CAG-GFP mouse line. a) Scheme illustrating the experimental protocol. Straight lines indicate mice housed in standard cages, and crooked ones indicate those caged with running wheels. Cyan colored lines represent indicate that pure drinking water was provided instead. Green arrow head shows time point of induction with tamoxifen, and red cross indicates time point of sacrifice. Time scale: w = weeks. b – e) Histological analysis of GFP (green), NG2-glia (red), and CC1 (white) imaged with 400x optic magnification. b and d scale bar = 50 μ m. c – c') and e – e') digital zoom of the squared area in b and d, respectively. Images show GFP+NG2+ cells (white, arrow), GFP⁻NG2+ cells (yellow arrow), GFP⁺CC1+ cells (magenta arrow), and GFP⁻CC1+ cells (orange arrow). Scale bar = 20 μ m. f) Quantification of the total number of recombined GPR17⁺ NG2-glia (GFP⁺NG2⁺ cells). g) The quantification of newly generated oligodendrocytes generated from recombined GPR17⁺ NG2-glia (GFP⁺CC1⁺ cells). All bar and error bars represent the group mean, and SEM, respectively. Each dot represents a single animal mean (n = 3 – 6). 2w control vs. 2w VPA groups, 4w control vs. 4w VPA groups, and 6w control vs. 6w VPA groups were independently analyzed by a two-tailed unpaired t-test. P < 0.05 = *.

Results

Regarding the differentiation of GPR17⁺ NG2-glia, I could observe that some GFP⁺ cells have differentiated into oligodendrocytes (GFP⁺CC1⁺) (**Fig. 15d and 15e**). I could not observe differences in the number of GFP⁺CC1⁺ cells between control and VPA groups after two or four weeks of running (**Supp. table 4**, two-tailed unpaired t-test p-value 2w control vs. 2w VPA = 0.8400 and p-value 4w control vs. 4w VPA = 0.7077) (**Fig. 15g**). Interestingly, after six weeks of running, I could appreciate an increase in the number of GFP⁺CC1⁺ in the VPA group compare to the control group (**Supp. table 4**, two-tailed unpaired t-test p-value = 0.0130) (**Fig. 15g**), suggesting that GPR17⁺ NG2-glia are prompted to differentiate after VPA, although, they did it at a slower rate or at least in lower numbers compared to the total population of NG2-glia (**compare Fig. 10e with 15g**). These results may suggest that there are subpopulations of NG2-glia that are more prone to differentiate in response to VPA than other populations.

Limitations of NG2-glia plasticity after long-lasting VPA

I have shown that the number of GPR17⁺ NG2-glia increased with VPA and, even if these cells were capable of responding to VPA, their response to the stimulus had a smaller effect compared with the whole NG2-glia population (**compare Fig. 10e with 15g**). Because the number of GPR17⁺ NG2-glia increased and the proteomic data showed that NG2-glia showed a less prone to differentiate phenotype after VPA, it is possible that NG2-glia decreased their response to VPA under prolonged periods of stimulus. To test this, I analyzed the long-term effects of VPA in the *NG2-CreER^{T2} x CAG-GFP* mouse line. Thereby, I divided the animals into three groups: 1) Mice housed in standard cages without running wheels for 19 weeks (“control group,” n = 3), 2) Mice caged without running wheels for 13 weeks and provided with running devices only the last 6 weeks before analysis (“6w VPA group,” n = 4), and 3) Mice housed in standard cages provided with running wheels for 18 weeks (“Extensive or Ext VPA group,” n = 5) (**Fig. 16a**). After 12 weeks, all animals were induced with tamoxifen. Next, all animals received BrdU, followed by two weeks-long BrdU retention before they were sacrificed (**Fig. 16a**). For this experiment, it was essential to ensure that all animals were of the same age at the time point of analysis.

Results

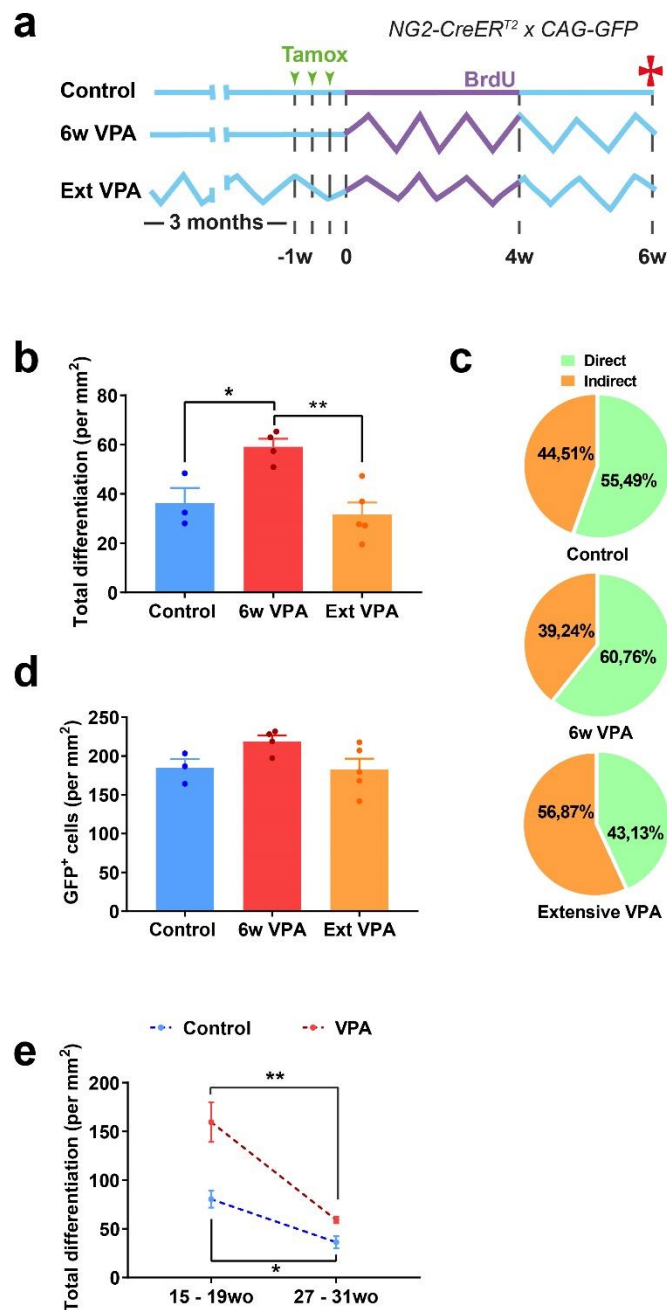


Figure 16. NG2-glia differentiation after extensive VPA treatment in *NG2-CreERT2 x CAG-GFP* mouse line. a) Scheme illustrating the experimental protocol. Straight lines indicate mice that were housed in standard cages, and crooked ones indicate that they were caged with running wheels. Cyan colored lines show that normal drinking water was provided, and purple ones that BrdU water was given. Green arrow head shows time point of induction with tamoxifen, and red cross indicates time points of sacrifice. Time scale: w = weeks. b) Quantification of total differentiation (GFP⁺CC1⁺ plus GFP⁺BrdU⁺CC1⁺ plus BrdU⁺CC1⁺ cells) in the different conditions. c) Pie charts show the proportion of indirect and direct differentiation modality in different conditions. d) Quantification of the total number of recombined cells (GFP⁺ cells) in different conditions. Bars and error bars represent the group mean and the SEM. Each dot represents a single animal mean (n = 3 – 5). Differences between control vs. 6w VPA vs. Ext VPA groups were analyzed by a two-tailed one-way ANOVA and a Tukey's multiple comparison test as *post hoc*. e) Quantification of the total numbers of total differentiation of young (figure 3g) vs. old mice. Symbol and error bars

Results

represent the group mean and SEM, respectively. Each dot represents a single animal mean ($n = 3 - 9$). Differences between young control vs. old control and young VPA vs. old VPA were independently analyzed by a two-tailed unpaired t-test. $P < 0.05 = *$ and $P < 0.001 = **$.

After six weeks of VPA, there was an ~1.6-fold increase in the differentiation of NG2-glia ($GFP^{+}CC1^{+}$, $GFP^{+}BrdU^{+}CC1^{+}$, and $BrdU^{+}CC1^{+}$) even in this higher age. By contrast, in the extensive VPA group, I failed to find differences in the generation of newly generated oligodendrocytes compared with the control group (**Suppl. table 5**, two-tailed one-way ANOVA F-value = 10.02 and p-value = 0.0051 followed by Tukey's multiple comparisons *post hoc* test adjusted p-value control vs. 6w VPA = 0.0283, control vs. extensive VPA = 0.7933, and 6w VPA vs. extensive VPA = 0.0050) (**Fig. 16b**). When I analyzed the fraction of oligodendrocyte generated by a direct or indirect differentiation mechanism, I found that similar to our previous experiment in younger animals (**compare Fig. 16c with 10f**), the 6w VPA showed an increase in the direct differentiation in comparison of the control (control: iNGOLs = 44.51% and dNGOLs = 55.49% vs. 6w VPA: iNGOLs = 39.24% and dNGOLs = 60.76%) (**Fig. 16c**). In contrast, I observed that the extensive VPA group showed a larger proportion of iNGOLs than the 6w VPA or control group (extensive VPA: iNGOLs = 56.87% and dNGOLs = 43.13%) (**Fig. 16c**). Interestingly, the control group in this set of experiments had a higher proportion of NG2-glia undergoing direct differentiation in comparison to our previous experiments in the *NG2-CreER^{T2} x CAG-GFP* mouse line (**compare Fig. 16c with 10f**). These results could be explained by the different ages at the time of analysis. It has been shown that proliferation and differentiation of NG2-glia decrease with aging (Dimou et al. 2008; Dawson et al. 2003; Young et al. 2013); therefore, the probability of finding both processes to be lower in aged animals than in younger ones.

A possible explanation to our findings could be that the number of recombined NG2-glia after tamoxifen induction was lower in the animals that were subjected to extensive VPA than in the 6w VPA and control groups and, therefore, the probability of finding GFP^{+} oligodendrocytes decreased. To test this theory, I counted the number of GFP^{+} cells in the motor cortex of animals from the three studied groups (**Fig. 16d**). In the case of having a lower recombination rate in the extensive VPA group compared with the other groups, I should be able to see less GFP^{+} cells than in the 6w VPA and control animals. However, I did not find statistically significant differences

Results

among the three groups (**Suppl. table 5**, two-tailed one-way ANOVA F-value = 2.897 and p-value = 0.1068) (**Fig. 16d**). The 6w VPA group showed a tendency to increase the number of GFP⁺ compared with the other mice groups, which could be due to the increment of newly generated oligodendrocytes already described in this section (**Fig. 16b and 16d**).

Additionally, I observed that the number of newly generated oligodendrocytes in this set of experiments was significantly diminished in both control and VPA groups (excluding the Extensive VPA group) compared with our previous experiments in the *NG2-CreER^{T2} x CAG-GFP* mouse line (**Fig. 10e**) when animals were categorized by the age in which they were sacrificed (**Suppl. table 2 and 5**, two-tailed unpaired t-test p-value young mice = 0.0128, p-value older mice = 0.0081) (**compare Fig. 16c with 10f and 16e**). Interestingly, despite the reduction in differentiation, I determined that NG2-glia in older mice were also able to differentiate in a proportionally equivalent manner. However, it was slightly reduced in older than in younger mice (~2-fold in young mice versus ~1.6-fold in old mice) (**Fig. 16e**). Thus, I suggest that NG2-glia plasticity modulated by VPA is retained with age, although the total number of newly generated oligodendrocytes is compromised.

Generation and integration of newly generated myelinating oligodendrocytes into the circuit after VPA in the adult mouse brain

I showed that the differentiation of NG2-glia in the motor cortex increased after VPA. Nevertheless, it is not clear whether these newly generated oligodendrocytes myelinate and integrate into the local cortical circuitry. It could be possible that differentiated but non-myelinating oligodendrocytes have a different function that does not involve myelin synthesis. Although such a function has not been described so far. Hence, I wanted to determine whether newly generated oligodendrocytes turned into myelinating cells. Therefore, I used the *NG2-CreERT2 x CAG-GFP* mice and determined the number of GFP⁺ cells that colocalized with the myelin-associated glycoprotein (MAG), a protein that increases its expression in oligodendrocytes during the first stages of axonal ensheathment and myelination (Bartsch, Kirchhoff, and Schachner 1989). With this methodology, I wanted to determine whether the

Results

number of oligodendrocytes that were becoming or were already myelinating axons in the motor cortex were integrating into the local circuit.

After six weeks, I observed that a proportion of the GFP⁺ cells were also MAG⁺ (**Fig. 17a – 17c**), indicating that some NG2-glia differentiated and reached full maturity. However, not all GFP⁺ cells were MAG⁺, meaning that these other cells have either remained NG2-glia or differentiated non-myelinating oligodendrocytes (**Fig. 17a – 17c**). We found that the morphology of the MAG⁺ cells was rather complex (**Fig. 17a-17c**), showing processes which fully colocalized with MAG, suggesting that these oligodendrocytes also developed internode-like structures and could integrate into the motor cortex.

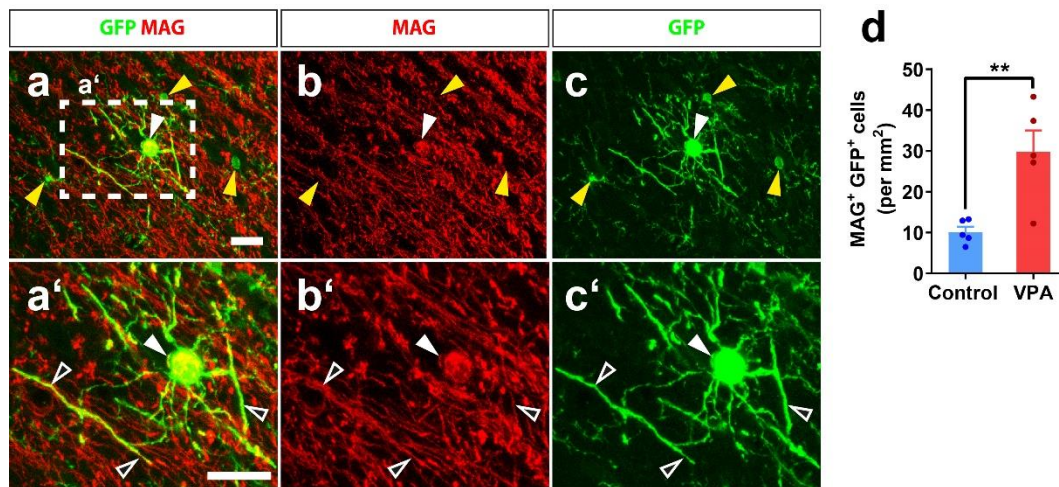


Figure 17. Generation of newly myelinating oligodendrocytes after VPA in *NG2-CreERT2 x CAG-GFP* mouse line. a – c) Histological analysis of GFP (green) and MAG (red) imaged with 630x optical magnification. Image shows myelinating oligodendrocytes (GFP⁺MAG⁺, white arrow) and NG2-glia / non-myelinating oligodendrocytes (GFP⁺MAG⁻). Scale bar = 20µm. a – c) Digital magnification of the squared area in panel a. Here it has been highlighted in GFP+MAG+ the soma (white arrow head) and the processes/internodes (white border and black core arrow head). Scale bar = 20µm. d) Quantification of the total number of newly myelinating oligodendrocyte (GFP⁺MAG⁺). Bar and error bars represent the group mean and the SEM, respectively. Each dot represents a single animal mean (n = 5). Data analyzed by a two-tailed unpaired t-test. P < 0.001 = **.

When I quantified the number of MAG⁺GFP⁺ cells, I observed a ~3-fold increase in the VPA group compared with the control group (**Supp. table 6**, two-tailed unpaired t-test p-value = 0.0068) (**Figure 17d**), suggesting that newly generated oligodendrocytes matured in the motor cortex at a higher or faster degree. Because of the nature of the *NG2-CreERT² x CAG-GFP* mouse line, it was vital to confirm that this signal was specific, and therefore, I analyzed whether

Results

MAG⁺GFP⁺ colocalized with NG2-glia markers, such as NG2. As expected, MAG⁺GFP⁺ cells did not express NG2, and conversely, GFP⁺ cells positive for NG2 labelling were not MAG⁺ (**Figure 18a – 18d**). Thus, I confirmed the specificity of the MAG label and that they were cells more differentiated within the oligodendrocyte lineage.

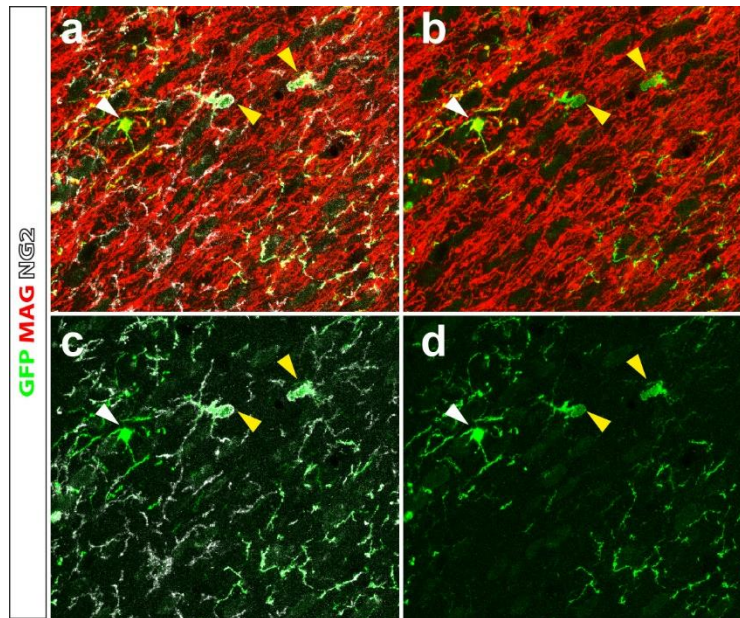


Figure 18. *NG2-CreERT2 x CAG-GFP* mouse shows recombinant NG2⁺ and MAG⁺ cells. a – d) Immunofluorescence of GFP (green), MAG (red), and NG2 (white) was taken with 400x optical magnification. Scale bar = 20 μ m. After recombination, it is possible to appreciate GFP⁺ cells colocalize with NG2 (GFP⁺NG2⁺ cells, yellow arrows) and MAG (GFP⁺MAG⁺ cells, white arrow).

Finally, I evaluated whether the increase in myelinating oligodendrocytes was an overall occurrence in the motor cortex, or it was layer-specific. This distinction could be important because the distribution of myelinating oligodendrocytes could reveal subtle changes in the cortical remodeling, perhaps involving particular layers. Thus, I divided the motor cortex into three equal sized “bins” (**Fig. 19a, and 19b**) and counted the total number of MAG⁺GFP⁺ cells in each bin. I observed that the total number of GFP⁺MAG⁺ cells increase of ~3.4-fold in bin 1, ~1.8-fold in bin 2, and ~5-fold in bin 3 in the VPA group compared with the control group. Although the differences in bin 2 did not reach statistical significance, there was a clear trend in the increase of the total number of newly myelinating oligodendrocytes in the VPA group compared with the control group (**Supp. table 6**, two-tailed unpaired t-test control vs. VPA in bin1 p-value = 0.0154, bin2 p-value = 0.0552, bin3 p-value = 0.0017) (**Fig. 19c**). Therefore, I can conclude that

Results

that maturation of oligodendrocytes happens globally in the motor cortex after VPA, probably promotes overall remodeling in the motor cortex circuitry.

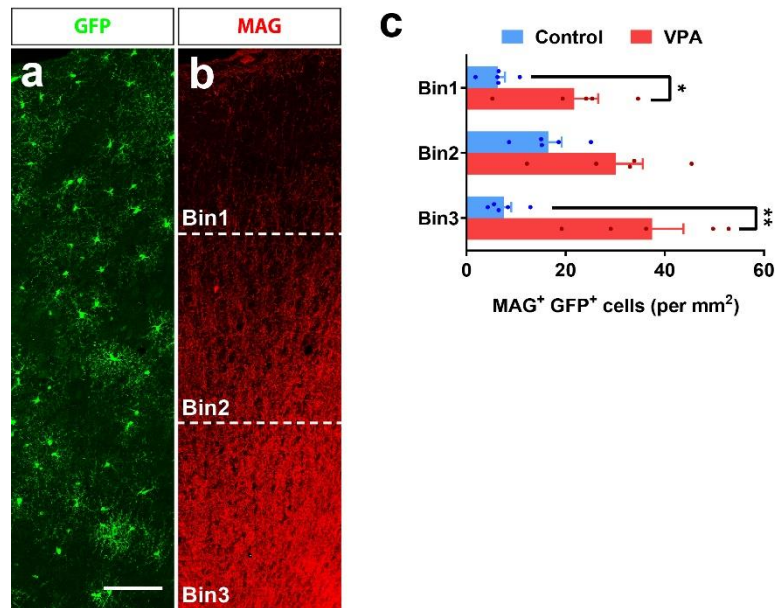


Figure 19. Distribution of newly generated myelinating oligodendrocytes in the motor cortex of the *NG2-CreERT2* x *CAG-GFP* mouse. a and b) Cortical column of the motor cortex immunostaining of GFP (green) and MAG (red). Images were taken with 400x optical magnification. Scale bar = 100µm. Images were independently taken from different regions for posterior stitched to form the column. In b, it is shown how the cortex was divided into three identical areas or bins. c) Quantification of the total number of newly generated oligodendrocytes (GFP⁺MAG⁺) per bin and in control or VPA condition. Bar and error bars represent the group mean and SEM, respectively. Each dot represents a single animal mean (n = 5). Differences between bin1 control vs. bin1 VPA, bin2 control vs. bin 2 VPA, and bin3 control vs. bin 3 VPA groups were independently analyzed by a two-tailed unpaired t-test. P < 0.05 = * and P < 0.001 = **.

Genetic ablation of proliferating NG2-glia as a model for blocking their differentiation, and its effects in the locomotor activity of adult mice

Previous studies have shown that exercise increases the cognitive performance (Hillman, Erickson, and Kramer 2008). Initially, researchers attributed this enhanced cognition to an increased neurogenesis in the hippocampal dentate gyrus (DG) (van Praag et al. 1999; Olson et al. 2006; Diederich et al. 2017; Voss et al. 2019). Robust evidence has shown that these newly generated neurons have the capability to integrate into the existing hippocampal circuitry, leading to the augmented performance of cognitive processes, such as learning and memory (van Praag et al. 1999; Olson et al. 2006; Diederich et al. 2017; Voss et al. 2019). Nevertheless, to our

Results

knowledge, it has never been studied how NG2-glia differentiation enhancement due to physical activity might contribute to improving cognitive performances.

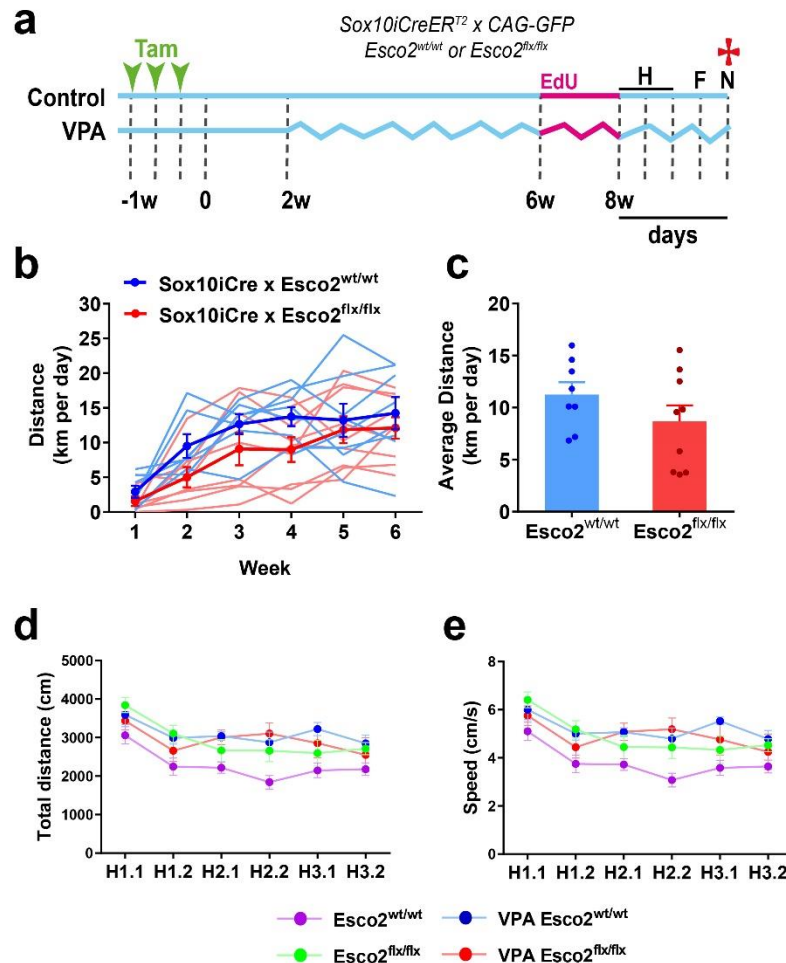


Figure 20. Locomotor activity after genetical ablation of proliferating NG2-glia and decreasing differentiation in the *Sox10-iCreER^{T2} x Esco2-fl x CAG-GFP* mouse under various conditions. a) Scheme illustrating the experimental protocol. Straight lines represent mice that were housed in standard cages, and crooked ones show that they were caged with running wheels. Cyan colored lines represent normal drinking water was provided, and magenta ones that EdU water was administered. Green arrow head show time point of induction with tamoxifen, and red cross indicate time points sacrifice. Time scale: w = weeks. b) The quantification and comparison of the weekly running performance of *Sox10-Esco2^{wt/wt}* (blue) and *Esco2^{flx/flx}* (red) mice. Dots and error bars represent the group mean and the standard error of the mean, and light-colored lines indicate the individual performance of each mouse (n = 8 – 9). Differences between *Esco2^{wt/wt}* and *Esco2^{flx/flx}* were analyzed by a two-way ANOVA. c) The bar graph shows the quantification of the average distance traveled by both genetic conditions. Bars and error bars represent the group mean and the SEM, respectively. Each dot represents a single animal mean (n = 8 – 9). Differences between genetic backgrounds between *Esco2^{wt/wt}* and *Esco2^{flx/flx}* were analyzed by a two-tailed unpaired t-test. d) Total distance traveled and e) speed during the arena exploration in the different conditions. Dots and error bars represent the group mean and SEM, respectively (n = 7 – 10). Differences among conditions were determined by a two-way ANOVA.

Results

So far, I have identified that there is a massive augmentation in the differentiation of NG2-glia in the motor cortex after VPA (**Fig. 7**). Furthermore, these cells appear to mature to form myelin, and might integrate into the local circuitry of the motor cortex (**Fig. 18d and 19c**). Nonetheless, it has not been clarified whether these cells have a relevant function for information processing.

To address this question, I took advantage of the *Sox10-iCreER^{T2} x Esco2-fl x CAG-GFP* mouse line (from now on, Sox10-Esco2^{wt/wt} as control and Sox10-Esco2^{flx/flx} for ablated NG2-glia model), which was already described by our group (Schneider et al. 2016). Similar to other Cre-lox systems described above, this mouse line has a Cre-driver under the promoter of Sox10, leading to the deletion of the Esco2 protein in the whole oligodendrocyte lineage after tamoxifen treatment (Schneider et al. 2016). The deletion promotes active apoptosis in recombined cells attempting to proliferate, which subsequently triggers the reduction of NG2-glia differentiation as a collateral effect (Schneider et al. 2016; Fard et al. 2017). It is believed that the reduction in oligodendrocytes is due to the shift cells from differentiating to proliferating in order to keep the NG2-glia population size stable.

I used the Sox10 Cre-driver line for two main reasons. Firstly, I obtained a high recombination rate of NG2-glia, about ~80% of the total number of NG2-glia (Schneider et al. 2016). Secondly, albeit also oligodendrocytes are recombined, it was assumed that only NG2-glia are affected because oligodendrocytes are postmitotic cells. Hence, they do not proliferate; ergo, they do not undergo apoptosis. Although Esco2 may have other functions, these have not been demonstrated in our knowledge (Schneider et al. 2016). Thus, I used the *Sox10-iCreER^{T2} x Esco2-fl x CAG-GFP* as a model to block differentiation during VPA.

Mice were induced with tamoxifen and kept for two weeks, to ensure the deletion of the Esco2 protein (Schneider et al. 2016). Then, mice were split into four groups: 1) Sox10-Esco2^{wt/wt} (n = 10) and 2) Sox10-Esco2^{flx/flx} (n = 7) mice, which were housed in standard cages, as well as 3) Sox10-Esco2^{wt/wt} (n = 8) and 4) Sox10-Esco2^{flx/flx} (n = 8) mice, which were housed in cages provided with running devices (**Fig. 20a**). After six weeks running (and eight weeks post-induction), I tested the enhancement of long-term memory by using the NOR test based on Leger et al. (2013) (**Fig.**

Results

20a) as this test shows enhancement in the performance of *C57Bl/6* mice after prolonged exercise (Robison et al. 2018).

Our NOR protocol had a duration of 5 consecutive days (**Fig. 20a**). The first three days consisted of a habituation phase, in which animals were exposed to the empty arena for 10 min twice per day, separated by 6h. On the following day, I performed an object familiarization phase for 10min, in which the mice were exposed to two identical objects separated by ~16cm. On the last day, one of the familiar objects was replaced with a novel object, allowing the mouse to explore them for 10min (**Fig. 20a**).

The Sox10-Esco2^{flx/flx}, either housed in standard cages or with running wheels, showed normal behavior after eight weeks post-induction. Nevertheless, it has been described before that some animals might show motor deficits when challenged to walk on a beam or to walk over a metallic grid mesh (Schneider et al. 2016). Thus, to discard that possible changes in the exploration behavior were not due to problems in locomotion, I weekly compared the running performance between the Sox10-Esco2^{wt/wt} and Sox10-Esco2^{flx/flx} mice. I observed no statistically significant difference in the average running performance per week (**Supp. table 7**, each day was analyzed by a two-tailed unpaired t-test p-value week 1 = 0.25, week 2 = 0.0646, week 3 = 0.2352, week 4 = 0.0566, week 5 = 0.6602, and week 6 = 0.4481) (**Fig. 20b**). Additionally, I could not find significance differences in the average distance per day (**Supp. table 7**, two-tailed unpaired t-test p-value = 0.2106) (**Fig. 20c**). It is important to note that Sox10-Esco2^{flx/flx} mice, on average, tended to run less than Sox10-Esco2^{wt/wt} mice (**Fig. 20c**). Nonetheless, every mouse ran over the previously determined threshold of 1Km per day, which was established as necessary to induce newly generated oligodendrocytes in the motor cortex (**Fig. 10g**). Therefore, these slight differences in running performance should not affect the overall differentiation of NG2-glia in the mice of both genotypes.

To further analyze and discard locomotion impairment during the NOR, I quantified the total distances traveled and the speed of the mouse during the habituation phase (**Fig. 20d and 20e, respectively**). During habituation, animals were free to explore the arena without any objects within it. This approach represents a useful measurement because if mobility is

Results

deteriorated, the animals from the Sox10-Esco2^{flx/flx} groups should show less exploration of the arena than their Sox10-Esco2^{wt/wt} counterparts. Each habituation day (X) was executed twice, consisting of an earlier session X.1 and a 6h later session X.2. After analyzing the mouse path automatic tracking, I did not observe statistically significant differences between VPA and no VPA Sox10-Esco2^{wt/wt}, and VPA and no VPA Sox10-Esco2^{flx/flx} mice, either in the total distance traveled (**Suppl. table 9**, each session was analyzed by two-way ANOVA interaction p-value = 0.1449) (**Fig. 20d**) or the average speed (**Suppl. table 9**, each session was analyzed by two-way ANOVA interaction p-value = 0.1093) (**Fig. 20e**). Thus, I concluded that any differences in object exploration could not be explained by motor deficits.

Genetic ablation of proliferating NG2-glia, as a model for blocking their differentiation, and effects in cognitive performance of adult mice

After confirming that the locomotor activity of Sox10-Esco2^{flx/flx} mice was not impaired by the genetic ablation of proliferating NG2-glia, I proceeded to test the changes in cognitive performance of these mice. Therefore, I presented the animals to the familiar objects, to familiarize the mice (**Fig. 20a**) and simultaneously tested whether mice have a preference for any of the two regions where the objects were located. As I described in the material and methods section, the set of familiar and novel objects and their placement were selected randomly to reduce the probability that results were due to object side or object itself preference.

After the familiarization phase, I observed that animals explored the same amount of time both objects (**Supp. table 9**, each group was analyzed by a two-tailed paired t-test p-value for No VPA Sox10-Esco2^{wt/wt} = 0.1849, No VPA Sox10-Esco2^{flx/flx} = 0.4225, VPA Sox10-Esco2^{wt/wt} = 0.3653, and VPA Sox10-Esco2^{flx/flx} = 0.9066) (**Fig. 21a**). Therefore, I concluded that there was no statistically significant side preference. After 24h of retention, I replaced one of the familiar objects with a novel one. I could observe that all groups were able to discriminate the novel object from the familiar object (**Supp. table 10**, each group was analyzed by a two-tailed paired t-test p-value for No VPA Sox10-Esco2^{wt/wt} = 0.0019, No VPA Sox10-Esco2^{flx/flx} = 0.0044, VPA Sox10-Esco2^{wt/wt} = 0.0001, and VPA Sox10-Esco2^{flx/flx} = 0.0224) (**Fig. 21b**), which indicates that

Results

baseline learning and memory consolidation is not affected by the deletion of *Esco2* in the oligodendrocyte lineage. This point was very important for my work because I wanted to find out whether NG2-glia differentiation was important for enhanced cognitive performance induced by increased physical activity and not for the physiological capacity of learning and memory.

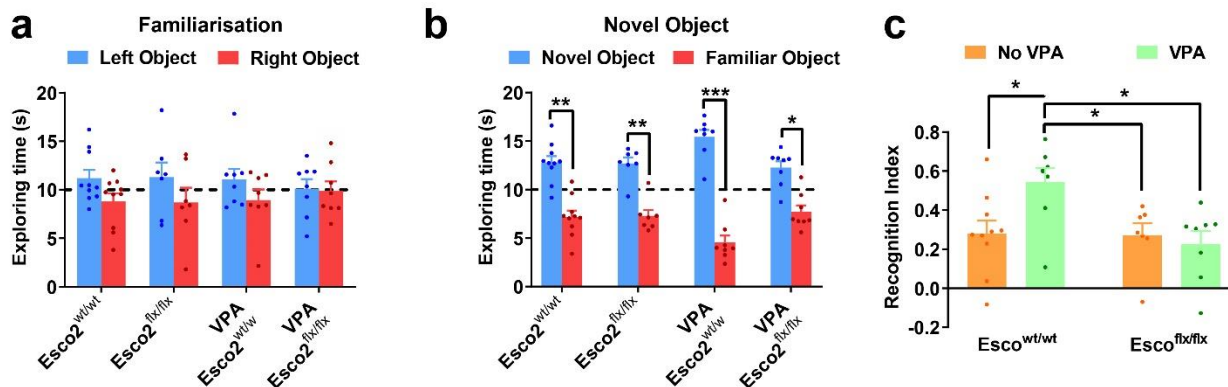


Figure 21. Cognitive performance after genetical ablation of proliferating NG2-glia and decreasing differentiation in the *Sox10-iCreER² x Esco2-fl x CAG-GFP* mouse under different conditions. a) Time spent by mice in object exploration in different conditions during the familiarization phase. b) Time spent by mice in object exploration in different conditions after replacing one familiar object with a novel one. Bars and error bars represent the group mean and SEM, respectively. Each dot represents a single animal mean ($n = 7 - 10$). Dash line indicates that time spent between both objects were equal (y -axis = 10). Differences between the exploration of the left object vs. the right object (familiarization phase) and the novel object vs. familiar object (novel object phase) for each condition were individually analyzed by a two-tailed paired t-test. c) Bar graph with the calculated recognition index for each condition. Bars and error bars represent the group mean and SEM, respectively. Each dot represents a single animal mean ($n = 7 - 10$). Differences among conditions were determined by a two-way ANOVA and a Tukey's multiple comparison test as *post hoc*. $P < 0.05 = *$, $P < 0.01 = **$, and $P < 0.001 = ***$.

To analyze enhanced memory performance, I compared the recognition index (RI) of each group among the groups. RI is the ratio of time spent exploring the novel object subtracted by the time spent with the familiar object over the total time spent exploring both objects (see material and methods). Interestingly, I observed that VPA improved the *Sox10-Esco2^{wt/wt}* mice test performance by ~2 fold in comparison to their counterparts with the same genetic background, which were housed in standard cages (**Fig. 21c**). Albeit, VPA could not improve the recognition index for *Sox10-Esco2^{flx/flx}* mice, which were caged with running devices, in comparison to their respective control group, housed in standard cages (**Supp. table 9**, two-way ANOVA interaction p -value = 0.0302 followed by Tukey's multiple comparisons *post hoc* test adjusted p -value No VPA *Sox10-Esco2^{wt/wt}* vs. VPA *Sox10-Esco2^{wt/wt}* = 0.0343, No VPA *Sox10-*

Results

Esco2^{wt/wt} vs. No VPA Sox10-Esco2^{flx/flx} = 0.9996, No VPA Sox10-Esco2^{wt/wt} vs. VPA Sox10-Esco2^{flx/flx} = 0.9340, VPA Sox10-Esco2^{wt/wt} vs. No VPA Sox10-Esco2^{flx/flx} = 0.0473, VPA Sox10-Esco2^{wt/wt} vs. VPA Sox10-Esco2^{flx/flx} = 0.0128, and No VPA Sox10-Esco2^{flx/flx} vs. VPA Sox10-Esco2^{flx/flx} = 0.9707) (**Fig. 21c**). Altogether, these results suggest that reducing the differentiation of NG2-glia did not affect baseline learning and memory consolidation. Nevertheless, the prevention of augmented newly generated oligodendrocytes, and subsequent myelination by VPA, abolishes cognitive enhancement driven by VPA, highlighting the importance of oligodendrocytes formation for changes in the CNS remodeling.

Genetic ablation of proliferating NG2-glia, as a model for blocking their differentiation, and adult neurogenesis in the mice

Previous results showed the importance of the differentiation of NG2-glia for the remodeling of the CNS for enhanced cognition in increased physical activity conditions. Albeit, as mentioned above, many studies show that increased physical activity leads to enhanced neurogenesis in DG, modifying the hippocampal local circuitry, which might contribute to the increased performance in learning and memory (van Praag et al. 1999; Olson et al. 2006; Diederich et al. 2017; Voss et al. 2019; Wu et al. 2008). For years, this mechanism has been thought to be responsible for the enhancement of cognitive processes by exercise. Henceforth, it is necessary to rule out that, in our *Sox10-iCreER^{T2} x Esco2-fl x CAG-GFP* mice, the Esco2 deletion of the oligodendrocyte lineage affected normal and activity-enhanced neurogenesis. In the same line, NG2-glia are also widely distributed in the mouse hippocampus, where they can proliferate and differentiate (Dawson et al. 2003). Therefore, NG2-glia may play a role in neurogenesis and it is reasonable to think that the newly generated oligodendrocytes provide metabolic support to neuroblasts, improving their chances of survival (Funfschilling et al. 2012; Klugmann et al. 1997; Lappe-Siefke et al. 2003; Lee, Morrison, et al. 2012; Biebl et al. 2000; Kempermann et al. 2003).

To analyze whether neurogenesis is affected in the *Sox10-iCreER^{T2} x Esco2-fl x CAG-GFP* mice, EdU was provided through the drinking water for two weeks prior to starting of the NOR

Results

test (**Fig. 20a**). After NOR, immunolabelling for doublecortin (DCX), a microtubule-associated protein expressed in neuroblast, and staining for EdU, a proliferation marker, was performed. As for BrdU, EdU is incorporated in the S phase of the cell cycle. The main difference resides in the detection method with EdU, being antibody-independent. I observed that Most EdU and all DCX signal was restricted to the subgranular zone and granular layers of the DG (**Fig. 22a – 22d**).

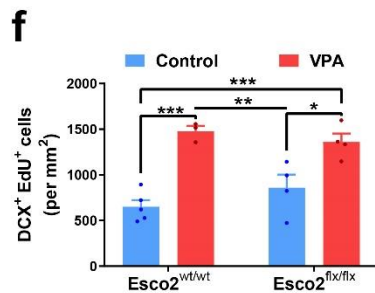
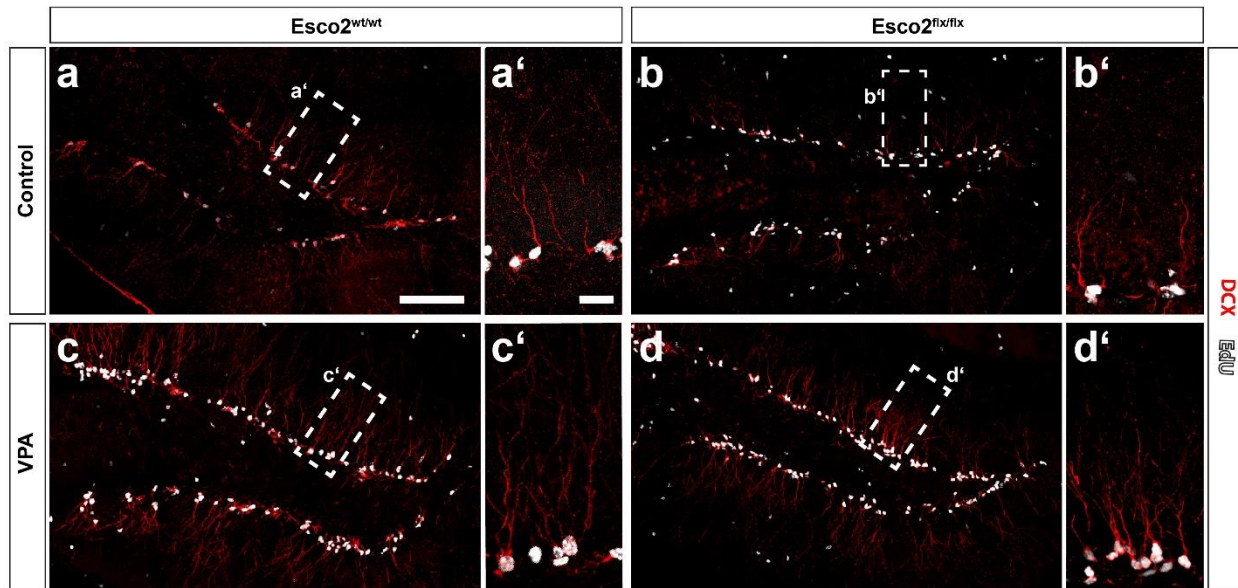


Figure 22. Neurogenesis after genetical ablation of proliferating NG2-glia and decreasing differentiation in the *Sox10-iCreER^{T2} x Esco2-fl x CAG-GFP* mouse line in different conditions. a - d) Histological analysis of hippocampal dentate gyrus immunostaining of DCX (red) and EdU (white) imaged with a 400x magnification lens and posteriorly stitching individual images. Scale bar = 100 μ m. a' – d') Analog magnification in the squared area in a – d, respectively, taken with 630x optical magnification. Scale bar = 20 μ m. f) The quantification of the total number of newly born neurons (DCX⁺EdU⁺ cells) in different conditions. Bars and error bars represent the group mean, and the SEM, respectively. Each dot represents a single animal mean (n = 3 - 5). Differences among conditions were determined by a two-way ANOVA and a Tukey's multiple comparison test *post hoc*. P < 0.05 = *, P < 0.01 = **, and P < 0.001 = ***.

Results

EdU signal, as in the case of BrdU immunostainings, was round-shaped and restricted to the nucleus (**Fig. 22a – 22d**), whereas the DCX label showed a somatic distribution with single or few processes projecting outwards the hippocampal DG hilus (**Fig. 22a – 22d**). These processes branched into one or two smaller processes (**Fig. 22a – 22d**). It is possible to see some of the EdU signal outside the subgranular and granular layer of the DG, which was not the case for the DCX signal (**Fig. 22a – 22d**).

It was possible to observe, in qualitative term, that VPA increased the number of EdU⁺ nuclei in the subgranular zone in both Sox10-Esco2^{wt/wt} and Sox10-Esco2^{flx/flx} (**compare Fig. 22a with 22c and Fig. 22b with 22d, respectively**). This increase in proliferation has been described in previous works (van Praag et al. 1999; Olson et al. 2006; Diederich et al. 2017; Voss et al. 2019; Wu et al. 2008). Another evident feature was that VPA lead to an increased growth and branching of DCX⁺ neurons' processes in both Sox10-Esco2^{wt/wt} and Sox10-Esco2^{flx/flx} after VPA (**compare Fig. 22a with 22c and Fig. 22b with 22d, respectively**) with no apparent differences when comparing the two control or the two VPA groups. It has been shown that increased physical activity results in an increased complexity of the neuroblasts morphology (O'Leary et al. 2019).

To quantify neurogenesis, I counted the number of proliferating neuroblasts, identified as DCX⁺EdU⁺ cells. Both Sox10-Esco2^{wt/wt} and Sox10-Esco2^{flx/flx} mice showed increased after VPA by ~2,3-fold, and ~1,6-fold, respectively, and no statistically significant difference could be observed between the two control or the two VPA groups (**Supp. table 10**, two-way ANOVA interaction p-value = 0.1377 and physical activity condition p-value < 0.0001 followed by Tukey's multiple comparisons *post hoc* test adjusted p-value No VPA Sox10-Esco2^{wt/wt} vs. VPA Sox10-Esco2^{wt/wt} = 0.0005, No VPA Sox10-Esco2^{wt/wt} vs. No VPA Sox10-Esco2^{flx/flx} = 0.4418, No VPA Sox10-Esco2^{wt/wt} vs. VPA Sox10-Esco2^{flx/flx} = 0.001, VPA Sox10-Esco2^{wt/wt} vs. No VPA Sox10-Esco2^{flx/flx} = 0.0077, VPA Sox10-Esco2^{wt/wt} vs. VPA Sox10-Esco2^{flx/flx} = 0.8716, and No VPA Sox10-Esco2^{flx/flx} vs. VPA Sox10-Esco2^{flx/flx} = 0.0183) (**Fig. 22f**). Thus, I concluded that NG2-glia ablation did not impair physiological or exercise-induced neurogenesis, or it does not change the circuitry remodeling of DG mediated by the newly generated neurons promoted by VPA.

Genetic deletion of Shank3 in the oligodendrocyte lineage and the role of synapses in NG2-glia differentiation in the adult mice

Nowadays, there is evidence that neuron-NG2-glia synapses might allow NG2-glia to monitor neuronal activity, which in turn could regulate proliferation and differentiation of NG2-glia (Yuan et al. 1998; Chen et al. 2018; Gautier et al. 2015; Lundgaard et al. 2013). Nonetheless, evidence regarding their function has been, at best, mixed. From our results, simultaneous downregulation of pro-oligodendrogenesis and synaptic proteins suggest that they might play a role in the differentiation of NG2-glia.

I have proposed to target other possible players in synapse formation, maintenance, and function. Therefore, I thought that targeting synaptic scaffold proteins might clarify this issue. In this thesis, I will set a special focus on the Shank3 scaffold protein, which has been shown to be highly expressed in NG2-glia (Zhang et al. 2014).

Shank3 is a novel scaffold protein family that has a relevant role in the assembly of the postsynapse (Naisbitt et al. 1999; Kreienkamp 2008; Tu et al. 1999) and its deletion leads to a decrease in the number of synapses, impairment in the expression and activity of glutamatergic receptors, and an autistic-like behavior in mice (Arons et al. 2012; Schmeisser et al. 2012). Furthermore, haploinsufficiency, caused by deletions of or mutations in Shank3, has been associated with the Phelan-McDermid syndrome, a rare monogenic neurodevelopmental disorder within the autism spectrum disorders (ASD), which is characterized by profound intellectual disability, hypotonia (decreased muscle tone), gait and motor deficits, and delayed or absent speech, among others (De Rubeis et al. 2018; Wilson et al. 2003; Durand et al. 2007). A recent MRI study has shown that mice and Phelan-McDermid human patients with mutations in Shank3 have severe WM alteration (Jesse et al. 2020). Thus, mutations in Shank3 may impair the function of neuron-glia synapses, decreasing the differentiation of NG2-glia and, finally, leading to the reduction of myelin distribution and alteration in the WM.

To study this, I created the *Sox10-iCreERT2 x CAG-GFP x Shank3-fl* (*Shank3^{wt/wt}* refers to the control and *Shank3^{flx/flx}* to the mutant) by crossing our *Sox10-iCreERT2 x CAG-GFP* mice with the *Shank3-fl* mouse line (kindly provided by Prof. Dr. Tobias Böckers, Ulm Universität) (**Fig. 23a**).

Results

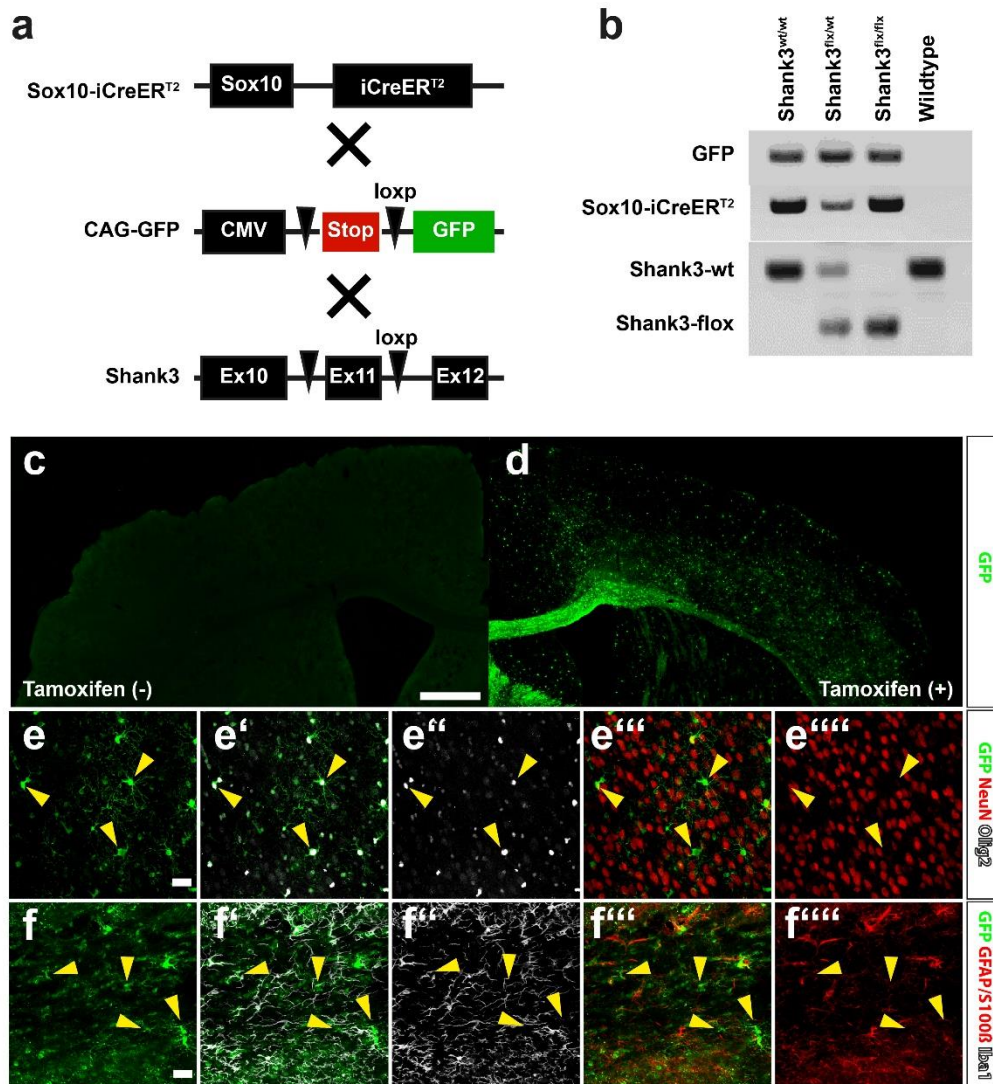


Figure 23. Generation of the *Sox10-iCreER^{T2} x Shank3-fl x CAG-GFP* mouse line. a) Scheme illustrating different mouse lines paired (X) to generate our novel mouse line. *Sox10-iCreER^{T2}* mouse line contains the Sox10 as the promoter sequence, and *iCreER^{T2}* is the sequence for the modified, improved Cre-recombinase fused with the human-estrogen ligand-binding domain. *CAG-GFP* mouse line contains the CMV promoter, a stop codon flanked by two loxp sites (inverted triangle), and a GFP reporter sequence. *Shank3-fl* mouse has the exon (ex) 11 flanked by two loxp sites (inverted triangles). b) The genotype of the mouse line confirming the presence of different transgenes. c and d) Histological analysis of GFP (green) without (-) and with (+) tamoxifen administration imaged with a 100x optical magnification and posterior stitching individual images. Scale bar = 500µm. e - e''''') Immunostaining of GFP (green, yellow arrows), NeuN (red), and Olig2 (white) imaged with 400x optical magnification. Scale bar = 20µm. f - f''''') Immunostaining of GFP (green, yellow arrows), GFAP/S100β (red), and Iba1 (white) imaged with 400x optical magnification. Scale bar = 20µm.

In this mouse model, I expressed GFP and induce the deletion of Exon11 of the Shank3 gene after tamoxifen administration and specifically in the oligodendrocyte lineage (**Fig. 23a**). Additionally, I assumed that the deletion of Shank3 would affect only NG2-glia and not oligodendrocytes due

Results

to the lack of synapses described for the latter. To confirm the presence of the different genes in this novel mouse line, I performed a genomic PCR for GFP, Sox10-iCreER^{T2}, and the Shank3 genes (**Fig. 23b**). I observed that the GFP and the Sox10iCre bands were presented in all the mutant lines and absent in the wild-type control (**Fig. 23b**). Additionally, I found that the wildtype form of Shank3 could be found in the homozygous wildtype Shank3, heterozygous, and wildtype mice but not in the homozygous floxed Shank3 animals, which expressed only the floxed Shank3 form of the gene (**Fig. 23b**).

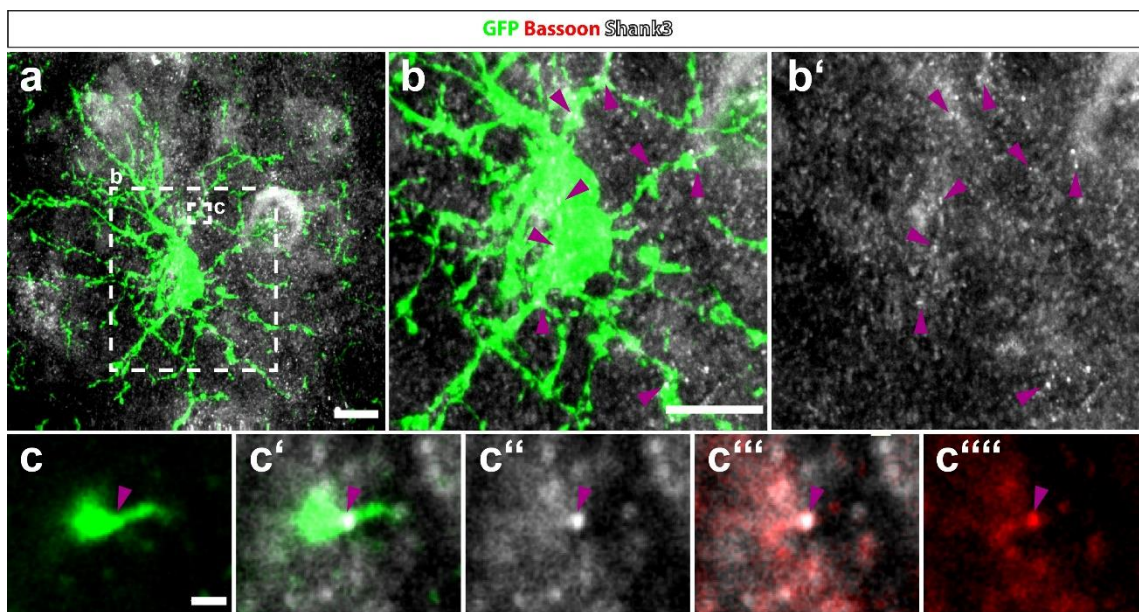


Figure 24. Expression of Shank3 protein in the *Sox10-iCreER^{T2} x Shank3-fl x CAG-GFP* mouse. a) Histological analysis of GFP (green) and Shank3 (white) imaged with 630x optical magnification. Scale bar = 10 μ m. b and b') Digital zoom of squared area b in panel a. Scale bar = 10 μ m. c – c''') Digital zoom of a single Z plane located in the squared area c of panel a. Additionally, qualitative colocalization analysis between GFP and Shank3, and between Shank3 and Bassoon (red). Scale bar = 1 μ m.

Next, I checked whether the oligodendrocyte lineage was recombined and only after tamoxifen administration. I compared the expression of GFP in the adult brain with and without tamoxifen administration. After induction, I observed that GFP reporter was only expressed in the animals treated with tamoxifen (**Fig. 23c and 23d**). Finally, I assessed whether expression of the GFP reporter was restricted to the oligodendrocyte lineage or it was also expressed in other cell types. Thus, we analyzed the colocalization of GFP (**Fig. 23e and 23f, yellow arrows**) with various identity markers, such as Olig2 (for the oligodendrocyte lineage), NeuN (neuronal

Results

marker), GFAP combined with S100 β (astrocyte marker), and Iba1 (microglia marker) (**Fig. 23e and 23f**). I observed that GFP was always in Olig2⁺ cells. Thus, I concluded that the novel mouse line was recombining only after induction with tamoxifen, and the induced mutation recombination would exclusively affect the oligodendrocyte lineage.

So far, the expression of Shank3 in NG2-glia has only been shown at the mRNA level (Zhang et al. 2014). Hence, I decided to check the presence of Shank3 protein by immunolabelling. In the mouse brain cortex, Shank3 was broadly expressed as a punctated signal (**Fig. 24a and 24b**). By colocalizing with the GFP reporter, it was observed several of these puncta distributed in the soma and processes of NG2-glia (**Fig. 24b**), resembling the distribution reported in neurons (Arons et al. 2012); therefore, Shank3 may also be part of NG2-glia neuron-NG2-glia synapses. Furthermore, by single plane analysis, I observed that some of the Shank3 puncta colocalized with bassoon, a neuronal presynaptic marker, suggesting that Shank3 is also part of the molecular structure of the NG2-glia synapse (**Fig. 24c**).

To test a possible role of Shank3 in the oligodendrocyte lineage, I induced the mice with tamoxifen. At 12 weeks post-induction, I performed motor behavioral test with these mice. First, mice were trained in the beam walk crossing and the rotarod for a week. Later, on weekly basis, the behavior was assessed, and then animals were sacrificed (**Fig. 25a**).

Before the training in the motor tasks, I analyzed neurological deficits by checking for claspings. In the physiological condition, mice stretch laterally their hind limbs, as is shown by the Shank3^{wt/wt} mouse (**Fig. 25b**). Nonetheless, the Shank3^{flx/flx} mouse showed hind limb claspings (**Fig. 25c**), a response that has been observed in other mouse models of ASD (Schmeisser et al. 2012; Gemelli et al. 2006) and motor disorders (Auerbach et al. 2001). Furthermore, I observed that the Shank3^{flx/flx} mouse performed considerably worse, and in a progressive fashion, than its control counterparts in the beam walk crossing (**Supp. table 11 and Fig. 25d**) and in the rotarod test (**Supp. table 12 and Fig. 25e**). Our group have shown that the blocking NG2-glia differentiation leads to motor impairment (Schneider et al. 2016). Therefore, deletion of Shank3 may trigger aberrant function of neuron-NG2-glia synapses that are followed by decreased oligodendrogenesis, resulting finally in motor deficits. It is necessary to mention that these

Results

results are still preliminary, and understanding the pathophysiology of this new mouse novel will require more research. Nonetheless, this mouse model could be useful in the future to understand the role of neuro-NG2-glia synapses in development and adulthood, in experience-driven changes of NG2-glia behavior and the role of NG2-glia communication in neurological pathologies, such as ASD.

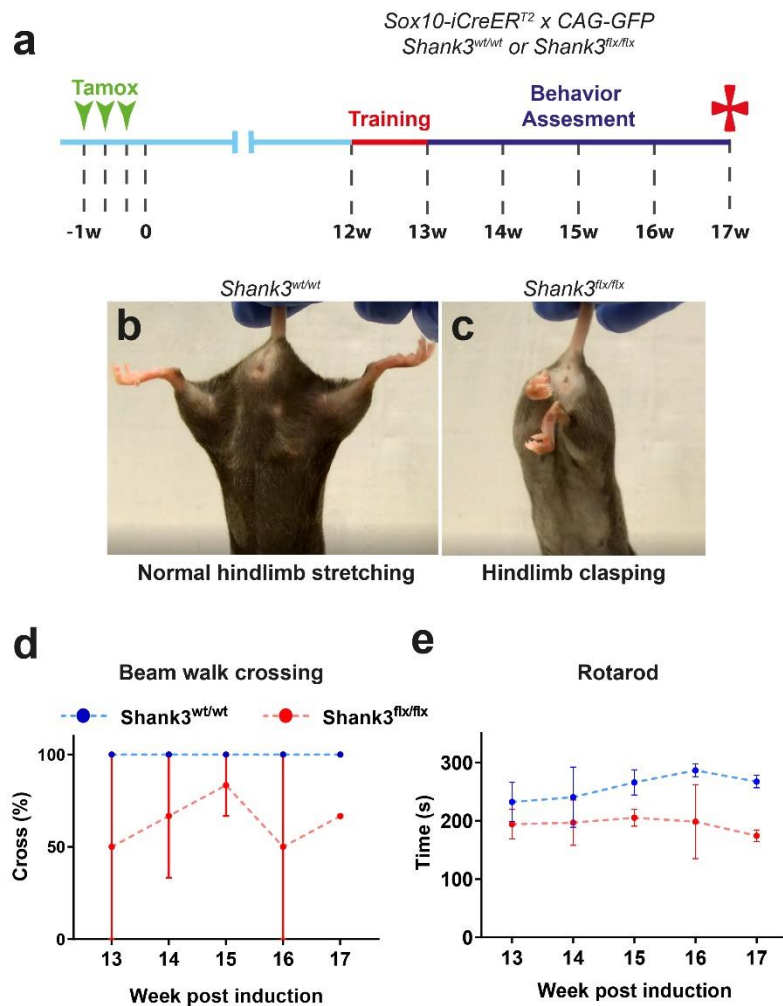


Figure 25. Motoric behavior assessment in the *Sox10-iCreER^{T2} x Shank3-fl x CAG-GFP* mouse. a) Scheme illustrating the experimental protocol. The red-colored line reflects the training period in both motor tasks and dark blue lines during the period of behavioral assessment. Green arrow head shows time point of induction with tamoxifen, and red cross indicate time points of sacrifice. b) and c) Qualitative analysis of neurological deficits by analyzing hindlimb stretching reflex and claspings identification. d) Beam walk crossing analysis between *Shank3^{wt/wt}* (blue) and *Shank3^{flx/flx}* (red). e) Rotarod performance and comparison between *Shank3^{wt/wt}* (blue) and *Shank3^{flx/flx}* (red) (n = 2 – 3). All graphs, dot and error bars represent the group mean and SEM, respectively.

Discussion and future perspectives

Physical activity has been identified as a crucial factor for reducing the risk for metabolic disorders, cardiovascular diseases, hypertension, and even mental disorders (Perez et al. 2019). However, since the industrial revolution, the tendency of modern western societies' lifestyle has been to promote sedentarism (Hallal et al. 2012). In 2012, it was estimated that over ~30% of the world adult population are physically inactive, and USA and Europe, the range is between 30 – 45% (Hallal et al. 2012). It is forecast that in the future to be a major detrimental factor for people's health. Because physical activity has a significant role in cognitive performance (Hillman, Erickson, and Kramer 2008), it is imperative to understand better its effects on the CNS. Nevertheless, we still have a narrow view of the physiological changes triggered by physical activity in the brain. Nowadays, research still has a predominant neuro-centric perspective, and the effect of physical activity on other cell populations, like the oligodendrocyte lineage, with some exception has been poorly described.

With this work, I have increased our understanding of changes in the behavior of NG2-glia and deepen into the role that they might play for circuitry remodeling after physical exercise, being the latter, to our knowledge, studied here for the first time. I have shown that VPA leads to increased proliferation and differentiation of NG2-glia. Interestingly, after increased physical activity, part of the population of NG2-glia less prone to differentiate takes over, in a process I denominated “the GPR17⁺ NG2-glia revolution,” reducing the global plasticity of the oligodendrocyte lineage (**Fig. 26**). GPR17⁺ NG2-glia responded differently to the rest of the NG2-glia population, describing for the first time heterogeneity of NG2-glia in the response to VPA, which might reflect that not all of these cells are participating in experience-dependent circuit remodeling. I also found that the successfully differentiated progenitors were likely to become myelinating cells, which I believed integrated and remodeled the local circuitry. Finally, the increase in newly generated oligodendrocytes was followed up by improved performance in a memory-related task such as the novel object recognition (NOR), effect that was abolished by blocking differentiation of NG2-glia, without affecting the mouse baseline cognitive capability.

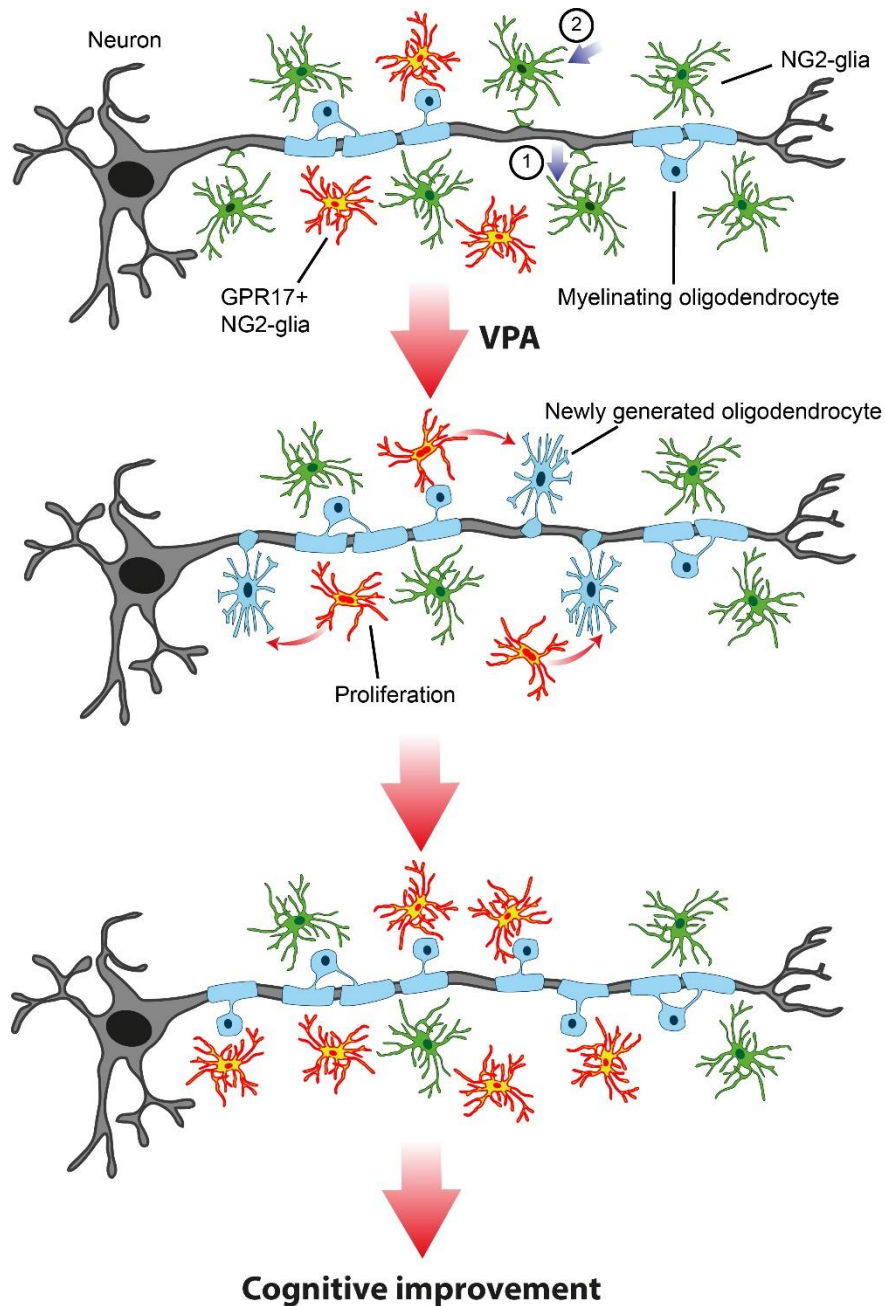


Figure 26. Summary of the effects of VPA in NG2-glia behavior. Here I illustrate that VPA induce the differentiation of NG2-glia by unknown mechanism (blue arrow) that could be axonal secretion or synaptic transmission (1), or a systemic signal (2). Newly generated oligodendrocytes start myelinating the naked segments of the axon, and simultaneously, neighboring GPR17+ NG2-glia start proliferating. The GPR17+ NG2-glia daughter cells migrate to the available space left by the NG2-glia that differentiated after VPA (red curved arrow). Finally, the maturation of oligodendrocytes is completed, forming a new myelin sheath that leads to changes in the axon property, modulating the circuit, and promoting cognitive improved.

In this final part of the thesis, I would like to comment on critical technical points that may have become part of this empirical work and to present arguments to explain our results in the light of the current literature. Furthermore, I include in the last section our vision of how exercise as a treatment could benefit the well-being of patients with various pathologies.

Conceptual and technical dimension of our experimental paradigm for VPA

In this section I would like to comment about the conceptual and experimental advantages and disadvantages of my model for studying the effects of physical activity on the oligodendrocyte lineage. First I will discuss about the VPA model itself and compare it to other models to study physical activity. Then, I will discuss about my approach to assess NG2-glia differentiation and provide reasons why is more accurate than strategies employed by other groups. Finally, I would like to comment on techniques that have been used to study NG2-glia heterogeneity.

In this work, I used VPA as a paradigm for studying the effects of physical activity. The advantage of voluntary over forced physical activity is the reduction of animal manipulation and, accordingly, their stress. This point is fundamental because it has been reported that various stress paradigms induce aberrant NG2-glia behavior, such as decreased proliferation and differentiation, diminished morphological complexity and reduced myelination (Yang et al. 2016; Luo et al. 2019; Banasr et al. 2007). Therefore, stress represents a major confounding factor in exercise-related experiments. This element is important to take in consideration because stress phenotype can be reverse by exercise (Luo et al. 2019), making difficult to interpret the differences between active animals and the control ones under stress conditions.

Another advantage mice running performance can be easily tracked and correlate the behavior of NG2-glia to the running performance due to animals being single-housed. Nonetheless, I must also consider that social isolation has been shown to affect myelination in the prefrontal cortex (Liu et al. 2012; Makinodan et al. 2012). Albeit it should also be pointed out that in my experiments, running and sedentary mice were housed individually. Therefore, social isolation should have affected both groups equally. Additionally, I used 8 – 12 weeks old mice, an age in which myelination is not affected by social isolation (Makinodan et al. 2012). This evidence

suggests the existence of critical time windows for different behaviors, and one may even speculate that also oligodendrocyte progenitors could be more susceptible to specific types of experience at a certain time period. Also, studies on stress differ from the social isolation protocols; therefore, the outcomes may be different. And finally, these results were similar to previous ones obtained by our group in a similar empirical setup but with animals caged in groups (Simon, Gotz, and Dimou 2011). Thus, I think that our experiments did not induce stress by social isolation as a confounding factor.

Conceptually, models for increasing physical activity are two-sided. We are testing animals that have been maintained in captivity their whole life with little space and access for locomotor activity. Therefore, one could argue that I study the consequences of sedentarism rather than the repercussions of enhanced mobility. In my personal view, this conceptual ambiguity does not alter the interpretation or the importance of my results, and, in any case, can be applied and adjusted to the benefit of society.

Additionally, it is important to address that the VPA model, as any *in vivo* model for physical activity, is simple to implement but difficult to fully interpret. Albeit, it is well documented that exercise increases neuronal activity in specific cortical regions; also, many other processes, including metabolic and homeostatic changes, take place simultaneously. For instance, increased physical activity decreases systemic pH by hypercapnia and the release of acidic metabolites from peripheral tissue. Although there is no evidence that NG2-glia express either pH- or CO₂ receptors, it cannot be ruled out, given that other glial cells, like astrocytes, do (Beltran-Castillo et al. 2017; Gourine et al. 2010).

Furthermore, water homeostasis and CBF changes happen after increase physical activity, as well as several molecular mediators, such as glucocorticoids, endorphins, lactate, BDNF, serotonin, etc. are synthesized in response to exercise. Therefore, there are local and systemic changes, and the participation of other cell populations should be also considered. However, at a first glance, that NG2-glia VPA-induced proliferation and differentiation were observed in the motor cortical GM but not in CC and piriform cortex suggests that a local rather than a systemic factor plays a critical role determining NG2-glia reactivity. A local factor may be understood as

the activation of specific neural pathways, the specific activity-dependent area release of active molecules or specific NG2-glia susceptibility in a brain region to a systemic factor. Nonetheless, for complex systems, it is essential to dissect their diverse sides. Exercise has relevant medical applications; hence, understanding its relationship with the oligodendrocyte lineage could be imperative.

Regarding our method for assessing differentiation of NG2-glia, I observed that the use of reporter lines was more accurate in detecting newly generated oligodendrocytes than the most common strategy of analyzing the incorporation of thymine analogues, such as BrdU and EdU, together with typical oligodendrocyte markers, e.g., CC1, GST π , CNPase, etc. (Simon, Gotz, and Dimou 2011; Tomlinson, Huang, and Colognato 2018; Gibson et al. 2014; Steadman et al. 2020). As I reported in this thesis, there is a significant percentage of NG2-glia that directly differentiates without proliferating (Hughes et al. 2013; Hughes et al. 2018); therefore, previous methods have undermined the total number of newly generated oligodendrocytes. Because not every laboratory has access to transgenic mouse lines, a way to overcome this issue is to provide BrdU or EdU for weeks before inducing differentiation of NG2-glia. It has been shown that eventually 80 – 100% of the cell population incorporates the thymine analogs (Simon, Gotz, and Dimou 2011; Young et al. 2013), making it possible to label all NG2-glia and assess the proportion that differentiates after experience exposure. Nonetheless, this strategy unavoidably extends the duration of the experiments, and it could be critically detrimental to those studies that work with concise time windows or in aging and, additionally, NG2-glia keep differentiating while BrdU is provided, making more difficult to distinguish which oligodendrocytes were generated during the physiological conditions and during the experimental conditions.

Another approach for evaluating experience-induced differentiation involve assessing the number of cells expressing novel early oligodendrocyte messenger RNA and proteins, such as Ectonucleotide Pyrophosphatase / Phosphodiesterase 6 (Enpp6) or Breast Carcinoma Amplified Sequence 1 (BCAS1) (Xiao et al. 2016; Fard et al. 2017). However, it is not completely clear whether these markers are also expressed in other stages of the oligodendrocyte lineage or even the time frame in which they are present in newly generated oligodendrocytes. For instance, at P10, BCAS1 seems to be detectable in NG2-glia and in myelinating oligodendrocytes at the

transcriptome level while it could not be found by immunostainings in adult animals (Zhang et al. 2014; Fard et al. 2017). This discordance could reflect differences in the expression of early oligodendrocyte genes in adult and postnatal animals. On the other hand, Enpp6 is detectable at mRNA and protein level in immature and myelinating oligodendrocytes (Zhang et al. 2014; Xiao et al. 2016). It is also feasible that VPA and other conditions could accelerate the maturation of oligodendrocyte progenitors, complicating the design of precise time points for the experimental assessment, i.e., shortening the duration in which cells remain as an immature oligodendrocyte. Therefore, it seems reasonable to evaluate in more detail these markers before their widespread usage.

A weakness of using inducible Cre-lox systems is its recombination rate. Even though it has been shown that a high proportion of NG2-glia expressed the GFP reporter in our mouse lines after recombination, I occasionally observed in our experiments oligodendrocytes that were BrdU⁺ and CC1⁺, but not GFP⁺ (**Fig. 10d**), reflecting a fraction of non-recombined progenitors. This problem can be partially overcome by providing BrdU and counting the number of iNGOLs, although the real absolute numbers of dNGOLs might still be undermined.

The gene or protein expression profiling of NG2-glia is currently becoming a broad approach in an effort to understand the NG2-glia heterogeneity and function in the CNS under a broad variety of conditions (Zhang et al. 2014; Marques et al. 2016; Sharma et al. 2015). In this doctoral thesis, I combined two powerful techniques involving MACS and mass spectrometry to isolate and analyze the molecular signature of NG2-glia exposed and not exposed to VPA. Nonetheless, it is not devoid of restrictions. For instance, concerning our sorting method, I obtained around $5 \times 10^4 - 10 \times 10^4$ cells per mouse cortical GM. These numbers are probably smaller than the total population in the cortex. This issue brings the following questions: am I analyzing a representative sample of cortical NG2-glia? Or am I inadvertently selecting a subpopulation of cells?

One way to overcome this issue might be to increase the yield of cells retrieved by MACS or trying other sorting methodologies, e.g., flow cytometry fluorescence-activated cell sorter (FACS), which would be feasible due to our access to several reporter mouse lines. A second

possibility would be to extensively confirm the differential expression of proteins, found in the mass spectrometry, by histology, combining immunostainings and fluorescence in situ hybridization (FISH). Nevertheless, it is critical to point out that this approach would be immensely dependent on the quality of detection of antibodies and probes, and the former are not necessary always available. Moreover, it is also a strategy that demands a significant amount of work.

I employed mass spectrometry to discover broad changes in the protein profile of NG2-glia. Thereby, I was able to describe and identify changes in the cell population in a qualitative and in a quantitative manner due to the label-free quantification of the peptides contained in our probes. Although a very informative technique, it is limited in the detection of proteins according to their expression in relation to other proteins. Because of the detection system, abundant peptides mask the less abundant ones; therefore, they are overseen in our experiments. This issue could explain why synaptic proteins, like Shank3, were not detected in our proteome analysis.

To improve protein detection in the future, I could process my samples by enriching different subcellular fractions of NG2-glia. In our set of experiments, I took the intact cells and isolated their peptides. On the one hand, this procedure has the advantage of having little variation among replicates, making protein evaluation more consistent. On the other hand, it generates probes with many different proteins, which, as mentioned above, can contribute to highly concentrated peptides, masking the lower abundant ones. By fractioning the cells in the subcellular compartments, e.g., plasmatic membranes, nucleus, and cytoplasm, I would reduce the amount of protein per probe, reducing the risk of masking. Nonetheless, adding extra steps of subcellular fractionation can also affect the replicability of our sampling, by increasing the variability among them.

Another strategy that can be considered is changing the discovery-based approach to a targeted one (Doerr 2013). Typically, mass spectrometer measures and reports the mass-to-charge ratio of the peptide ions. Therefore, in a targeted workflow, it can be programmed to detect specific proteins. Nonetheless, this requires more up-front investment than the discovery-

based strategy because the characteristics of the peptides of interest must be determined beforehand.

Another technique that has a broader output and is being recently implemented in the oligodendrocyte field is single-cell RNA sequencing (sc-RNAseq). It has allowed the characterization of different populations of NG2-glia and oligodendrocytes under various conditions like complex wheel running, demyelination by EAE, and WM lesions of MS patients (Marques et al. 2016; Falcao et al. 2018; Jakel et al. 2019). Such a technique could provide critical insights regarding the behavior of NG2-glia towards neuronal activity and experience. Nonetheless, it contains similar interpretative issues as other techniques. First, it has been a rather general assumption in the field of transcriptomics that increase in messenger RNA necessarily leads to increased protein level. There is a long pathway of regulatory mechanisms in the translation from mRNA to protein, which we generally attribute a biological function regarding signal detection and processing as well as catalytic capacity. Furthermore, only a modest correlation has been reported between transcriptome and proteome analysis in rodents (Ghazalpour et al. 2011). That brings us to the same point, which is the need to corroborate results obtained by sc-RNAseq by other techniques, like immunostainings, FISH, western blot, and even mass spectrometry.

RNAseq has been done by analyzing single time points in the population. Regarding changes in NG2-glia due to experience and neuronal activity, it is relevant to establish critical time windows to define the pathways that are involved in proliferation and differentiation of progenitors. Otherwise, we would detect changes in the population rather than the molecular mechanisms that trigger those responses. This challenge can be addressed with approaches like optogenetics and pharmacogenetics, in which the stimulus can be exquisitely controlled in contrast to indirect stimulation by VPA, or sensorial deprivation, among others. This point also applies to mass spectrometry-based strategies.

A general problem that have most molecular high throughput screening strategies concern the amount of data obtained, and even more important, their processing and

interpretation. Therefore, it is crucial to heavily invest in the development of bioinformatical approaches for the evaluation of the results.

NG2-glia behavior dynamics after VPA

Initially, our results showed that VPA led to increase of proliferation and differentiation of motor cortex NG2-glia (**Fig. 7c – 7h**). This phenomenon had been previously described by other and our groups (Simon, Gotz, and Dimou 2011; Ehninger et al. 2011; Mandyam et al. 2007; Tomlinson, Huang, and Colognato 2018). However, those investigations had conceptual and methodological assumptions, as well as constraints and a different approach to the dynamics of oligodendrocyte progenitors than those used in this work.

First, I mainly focused in the motor cortex (**Fig. 7b**) and not in the prefrontal cortex (Tomlinson, Huang, and Colognato 2018; Mandyam et al. 2007) or the somatosensory cortex (Simon, Gotz, and Dimou 2011). This brain region was selected because the increment of the metabolic demand and the CBF of the motor cortex, as well in other areas, that have been reported after exercise (Vissing, Andersen, and Diemer 1996; Hiura et al. 2018), both affected by local changes in neuronal activity. Additionally, axons in the cortex are not entirely myelinated, having a myelin distribution rather discontinuous (Tomassy et al. 2014). This feature endows cortical axons for possible new myelin incorporation. Because of its paramount importance, I will revisit this topic later in this discussion.

Secondly, this work described the dynamics of the oligodendrocyte progenitors' response to VPA at multiple time points. For instance, I observed increased numbers of proliferating NG2-glia and newly generated oligodendrocytes already after two weeks of VPA, which increased further after four weeks of VPA (**Fig. 7e – 7h**). Therefore, I concluded that the longer of the experience is provided, the more robust is the increase in proliferation and differentiation of NG2-glia. Conversely, the removal of running wheels after two weeks of VPA abolished the effect in cell proliferation and arrested further addition of newly generated oligodendrocytes (**Fig. 7f – 7h**). This initial data set suggests that continuous VPA is necessary to maintain NG2-glia division and differentiation. As soon as the stimuli is removed, the proliferation of NG2-glia dropped,

while the number of oligodendrocytes that have been generated during VPA are the same as in the animals that were directly sacrificed after two weeks of VPA.

Interestingly, the dynamics of the NG2-glia behavior appear to be very similar to neural stem cells (NSC) in the hippocampal DG. It has been shown that increased physical activity increases neurogenesis and it keeps growing as long as the running wheels are available (van Praag et al. 1999; Olson et al. 2006; Diederich et al. 2017; Voss et al. 2019; Wu et al. 2008; Nishijima et al. 2017). As it happened in the oligodendrocyte lineage, NSCs show a negative rebound effect after cessation of physical activity, which leads to a decrease in the number of proliferating NSCs (Nishijima et al. 2017). Therefore, once more, I have provided new evidence that NG2-glia and NSCs shared characteristics in their behavior in response to VPA. Thus, it is possible that exercise-induced oligodendrogenesis and neurogenesis in the adult brain may be ruled by common mechanisms.

In the same line, it has been shown that new neurons are also massively generated without VPA, but most of them do not survive to become mature cells (Kempermann et al. 2003; Biebl et al. 2000). Notably, this fate is overturned by physiological experience, e.g., enriched environment and voluntary physical activity, reducing spontaneous apoptosis of NSCs and providing neuroprotective factors to immature cells (Young et al. 1999; Bouchard-Cannon et al. 2018). Under the light of this evidence, similar situation could be true for the oligodendrocyte lineage. Experiments involving *in vivo* time-lapse 2-photon imaging in adult mice, reports that the number of newly generated oligodendrocytes is higher than expected, albeit, only ~20% of differentiated NG2-glia survive and integrate, which increases with sensorial stimulation of whiskers (Hughes et al. 2018). This phenomenon perhaps explains why I did not observe a strong increase in the number of newly generated oligodendrocytes between the two- and four-weeks control groups (**Fig. 7h**). Therefore, VPA may result in the release of molecules that promote the survival of differentiated NG2-glia and not necessarily lead to increase in differentiation.

Regarding the dynamics of NG2-glia behavior during VPA, it is worth noting that the population of progenitors remains constant despite the increase in their proliferation (**Fig. 7i**). There may be two possible explanations for this observation. First, NG2.glia are regulated by their

physiological homeostatic population control. It could be thinkable that VPA modulates the differentiation of NG2-glia but not their proliferation. Cell division then comes as a byproduct of the increased generation of new oligodendrocytes. It has been shown that NG2-glia regulate their population size by mechanisms of self-repulsion governed by their small projections (Hughes et al. 2013). The differentiation of oligodendrocyte progenitors might leave NG2-glia “free-gap”, thereby promoting the proliferation and later the migration of neighboring cells (Hughes et al. 2013). Hence, proliferation could be subjugated to NG2-glia VPA-induced differentiation and that VPA has not a direct effect on their cell division.

A second possibility is that VPA promotes NG2-glia asymmetric proliferation, a feature that has been widely observed in radial glia cells during development and in the adult, and also in NG2-glia in slices after lysophosphatidylcholine (LPC) damage of the WM (Kriegstein and Alvarez-Buylla 2009; Hill et al. 2014). With this mechanism, NG2-glia can self-renew their population and simultaneously generate new oligodendrocytes. As a result, there is differentiation without affecting the total population of NG2-glia. Although I am reluctant to endorse this alternative, because if asymmetric proliferation was the principal mechanism, the number of BrdU⁺NG2⁺ and BrdU⁺CC1⁺ should be similar. On the contrary, our results show that the proportion of cells that directly differentiate is higher than the one that proliferated before becoming oligodendrocytes (**Fig. 10e**). Therefore, it is more likely that proliferation is driven by homeostatic self-renewal than by asymmetric differentiation, although both phenomena are not mutually exclusive.

Additionally, I showed that NG2-glia can form oligodendrocytes by two modalities. I named them as direct and indirect differentiation, whose distinction is based on the absence or presence of proliferation before the generation of oligodendrocytes, respectively. It is necessary to consider that this concept is framed by the time points when experiments were performed, specifically by the moment I induced the animals and provided BrdU until the time of sacrifice. Most studies do not make this distinction because they tend to choose between two standard methodologies. Either to provide BrdU and observe how many of these labeled progenitors differentiate (Simon, Gotz, and Dimou 2011; Tomlinson, Huang, and Colognato 2018; Gibson et al. 2014; Steadman et al. 2020; Xiao et al. 2016) or to express by transgenic mouse lines a protein

reporter on NG2-glia and check their overlap with oligodendrocyte markers (McKenzie et al. 2014; Young et al. 2013; Huang et al. 2014). Although it has been shown by previous studies done by two photon *in vivo* imaging that these two different modalities exist (Hughes et al. 2013), this doctoral thesis has been the first attempt, in my knowledge, to characterize and quantify them in depth (**Fig. 10e**).

I observed that in animals housed in standard cages, direct and indirect differentiation happened in almost equal proportions. These results can reflect that, under naive physiological conditions, both processes are likely to happen. Nonetheless, VPA increases the likelihood of progenitors to undergo direct differentiation. Those progenitors using the indirect pathway might be cells that proliferated and lately differentiated driven by VPA or by the regular reposition of oligodendrocytes in the system, independent of VPA (Young et al. 2013; Dimou et al. 2008; Hughes et al. 2013; Yeung et al. 2014).

Finally, I found that animals respond differently to VPA depending on their running performance (**Fig. 10**). In mice that run under ~1km per day, NG2-glia differentiation was similar to the controls. Unexpectedly, the maximum increase of newly generated oligodendrocytes was reached immediately after this distance threshold (**Fig. 10**). The explanation for this remains elusive. It could be that optimal effective signaling from neuronal activity was reached immediately after this threshold. Other possibilities could be related to the heterogeneous response of NG2-glia to VPA.

Heterogeneous effect of VPA on NG2-glia

In this doctoral thesis, I have also provided robust evidence that VPA has a differential effect on distinctive populations of NG2-glia in different regions but also within a single one, the latter being the first time that it has been shown that NG2-glia populations have differential responses to VPA or experience.

Notably, the effects of VPA seems to be specific to the GM of the motor cortex, and neither the white matter nor other grey matter areas, like the piriform cortex, show an effect

(Fig. 8c – 8h). This apparent unresponsiveness of the piriform cortex could be due to the lack of changed neuronal activity in that region, given that this area is fundamental in the processing of odorant information, which I assumed remains relatively constant and does not activate after exercise (Hiura et al. 2018). It is worth noting that previous reports have shown that in the prefrontal cortex, NG2-glia presented a similar increase in differentiation, but not the proliferation, after four weeks of increased physical activity (Tomlinson, Huang, and Colognato 2018). These disparities in results could also reflect regional differences in the dynamics of NG2-glia behavior, and particular to this discussion, between the prefrontal and the motor cortex.

The absence of changes in the WM cannot be explained by the lack of neuronal activity given that many neurons of the motor cortex have projections that cross the WM beneath that cortical region. In contrast to our results, it has been described that NG2-glia in the CC increased their differentiation four weeks after a seven-day optogenetic stimulation of pyramidal neurons in layer V of the motor cortex (Gibson et al. 2014). Nevertheless, in these experiments is important to consider differences in the time course of stimulation and that these alterations could be due to the artificial stimulation of these neurons, which would not occur in a physiological context. Our data are reinforced by observations of other groups. It has been reported that physical activity induces WM NG2-glia proliferation after four days of running. However, after ten days of constitutive running, no differences could be observed compared with the control (McKenzie et al. 2014). Also, in juvenile mice, it has been reported that four weeks of running increases the generation of oligodendrocytes in the CC associated with the prefrontal cortex (Tomlinson, Huang, and Colognato 2018), revealing that there may be not only CC regional but also age-dependent differences.

It could be also possible, in regard to our results, that differences in the NG2-glia behavior between the GM and the WM can be due to either intrinsic variation within their populations, making them to react differently to VPA, or environmental disparities, with the WM to be more oligodendrocyte/myelin saturated and, thus, a restrictive environment for NG2-glia differentiation. Furthermore, it has been previously shown by our group and others that oligodendrocyte progenitors in the WM have a distinctive morphology, as well as faster

differentiation and proliferation rates than their counterparts in the GM (Vigano et al. 2013; Young et al. 2013; Dimou et al. 2008).

Interestingly, as discussed above, NG2-glia would take two modalities to differentiate by generating directly or indirectly newly generated oligodendrocytes (**Fig. 10**). I observed that VPA shifted the preference towards the generation of direct over indirect newly generated oligodendrocytes. This preference probably reflects differences within the NG2-glia and their response to VPA, which promotes a part of the population to differentiate rapidly, an event described in other experience-dependent processes (Xiao et al. 2016; McKenzie et al. 2014; Steadman et al. 2020; Pan et al. 2020). In contrast, another fraction remained more resistant to the transition. The idea of two populations differentially responding to VPA gains strength in my study because of five additional pieces of evidence:

First, the differentiation of progenitors by VPA required a low threshold of physical intensity to initiate. After reaching it, the generation of oligodendrocytes lacks a linear correlation, reaching very fast a “saturation plateau”. This differs significantly from the neurogenesis in the hippocampal DG, which shows a positive linear relationship between running performance and the number of newly generated neurons (Diederich et al. 2017). Our interpretation is that the number of NG2-glia that can directly differentiate is limited and thereby restricts the generation of new oligodendrocytes by VPA.

Second, I have shown by NG2-glia protein profiling after VPA that the population shift from a “prompter” to form new oligodendrocytes to a more resistant one (**Fig. 13**). This interpretation raised because initially, after VPA, a part of the NG2-glia population differentiated while another part remains as progenitors. Notably, the total number of NG2-glia in the cortex did not change, regardless of the stimulation by VPA. Therefore, the explanation cannot reside in the fact that fewer cells are recruited after VPA, but, on the contrary, it appears that this population did not manage to differentiate and repopulated the cortex (**Fig. 7i and 14c**). Henceforth, the changes of the protein profile mirror the identity of the “new remained” NG2-glia population after VPA. Finally, I observed by functional enrichment of the remaining population that after VPA there were several downregulated proteins that are involved in the

differentiation of NG2-glia (**Fig. 13**). This data may show the limitations of global NG2-glia plasticity, which will be revised later in this discussion.

Third, I observed that the population GPR17⁺ NG2-glia surpassed the population of progenitors as a higher fraction of NG2-glia expressed GPR17 after VPA (**Fig. 14c**). This shift in the global phenotype was coherent with our findings in the proteome analysis because these cells are known to have a slower differentiation rate than the rest of the NG2-glia (Vigano et al. 2016). Worth noting that I did not observe differences in the total number of NG2-glia after VPA (**Fig. 7i**); thereby, it is reasonable to think that the GPR17⁺ NG2-glia did not increase on top of the pre-existing population but instead replaced it.

Fourth, the behavior of GPR17⁺ NG2-glia after VPA showed significant differences in comparison to the total population of NG2-glia. Moreover, when I compared their differentiation rate with the one of the total population (**compare Fig. 10e with 15g**), I concluded that the magnitude is lower and it is even delayed; thus, despite GPR17⁺ NG2-glia can turn into oligodendrocytes, they do it in a lower rate and scale than other progenitors. Therefore, I suggest that GPR17⁺ cells overtake the NG2-glia population, a fact that might represent a physiological mechanism to break the continuous generation of new oligodendrocytes.

Fifth, extensive VPA failed to generate more oligodendrocytes than those observed in controls (**Fig. 16b**), suggesting that there was a depletion of NG2-glia responsiveness to VPA; thereby, reducing the plasticity capacity of the total population.

From this body of evidence, I concluded that there were at least two populations of NG2-glia that possess a differential reactivity towards VPA, being identified GPR17⁺ NG2-glia as less sensitive to VPA. Recent evidence in zebrafish larvae has shown that only a defined group of NG2-glia was capable of integrating neuronal activity, and that increased activity led to enhanced proliferation and differentiation of oligodendrocyte progenitors (Marisca et al. 2020). These results corroborate that a certain population of oligodendrocyte progenitors might be reactive to VPA and possibly an evolutionary trait shared among vertebrates. Interestingly, in contrast to our data, the same group reported that the NG2-glia population responsive to neuronal activity population in the zebrafish had higher levels the GPR17 mRNA (Marisca et al. 2020). I could

speculate that the role of GPR17⁺ NG2-glia could depend on the animal species and their developmental stage.

These observations corroborate once again the heterogeneous nature of the NG2-glia (Vigano and Dimou 2016). New populations may be discovered in the future at the hand of new methods of mass sequencing at the individual cell level (Falcao et al. 2018; Marques et al. 2016; Vigano and Dimou 2016). Nonetheless, this diversity of NG2-glia is still missing a functional role with the notable exception of the GPR17⁺ NG2-glia, which are differentiating after injury. However, which would be their role in VPA? In the next section, I will attempt to answer this question.

A possible role of GPR17⁺ NG2-glia in plasticity and adaptive myelination

To answer, perhaps it is vital to revise the behavior of this population during development. GPR17⁺ NG2-glia increase shortly after birth of mice and progressively increase with time, reaching a peak in their production at P14, and later decreasing to a baseline level at P24, which is maintained through adulthood (Chen et al. 2009; Boda et al. 2011). Notably, during the same timeline, myelin also reaches a peak of production at P14 as well, and interestingly, deletion of GPR17 protein leads to premature myelination (Chen et al. 2009; Wright et al. 2010). Therefore, it is proposed that the GPR17⁺ NG2-glia function as a physiological brake pedal to restrict the global plasticity of NG2-glia.

I propose that this population share similar functions after VPA. First, I observed that the running mice with the highest number of GPR17⁺ NG2-glia showed the lowest number of indirectly newly generated oligodendrocytes (**Fig. 14d**), suggesting that the promotion of this population possibly limits further oligodendrocyte production. Second, as aforementioned, GPR17⁺ NG2-glia reaction to VPA differs from the rest of the population, and although they differentiate, the magnitude is decreased and delayed compared with the total population, occurring only after six weeks of VPA (**compare Fig. 10e with 15g**). Third, I demonstrated that extensive VPA did not induce the further formation of new oligodendrocytes, suggesting that the system was depleted of VPA sensitive NG2-glia (**Fig. 16b**).

An argument against my third point interpretation may be that NG2-glia from aged animals, appears to have a less plastic phenotype. It has been widely reported that oligodendrocyte progenitors proliferation and differentiation diminishes with aging, as I have also observed in our experiments (**Fig. 16e**) (Dawson et al. 2003; Dimou et al. 2008; Young et al. 2013; Kang et al. 2010). Nonetheless, I demonstrated that aged animals were capable to respond with differentiation after VPA (**Fig. 16b**). Notably, even though NG2-glia in aged animals retain their capacity to respond to VPA, this capacity diminished in older mice compared with the younger ones. Interestingly, differentiation induction by VPA in younger and older animals, approximately double their respective control counterparts (**Fig. 16e**).

To my knowledge, this is the first time shown that changes in NG2-glia plasticity after persistent stimulus have been addressed. These findings bring new questions to the discussion: why are there mechanisms limiting the differentiation of NG2-glia? If newly generated oligodendrocytes are vital for improving the cognition baseline, as aforementioned, why not continue their generation? The answer may be one of the few processes in neurobiology that follows the Occam's razor principle.

First, it is about the finite space that the brain provides. Because NG2-glia guard their own population throughout life by self-regulatory mechanisms (Dawson et al. 2003; Simon, Gotz, and Dimou 2011; Hughes et al. 2013); the pool for oligodendrocytes has a continuum and, in theory, is unlimited.

Second, the substratum available to be myelinated is limited. Axons have a restricted number of segments that allows the integration of new internodes (Tomassy et al. 2014). Moreover, even if there are many naked axonal regions or there are many unmyelinated axons (Sturrock 1976), it is questionable the benefice of additional myelination to information processing. Adaptive myelination is an instrument that has been theorized around the fine-tuning of circuits (Pajevic, Basser, and Fields 2014). Thereby, over-myelination could bring problems of asynchronicity in spike-time arrivals, making some conduction way faster than necessary.

Third, generating new oligodendrocytes that would be unable to myelinate seems like a waste in energetic currency. Although oligodendrogenesis and myelination indeed take place

during the whole lifespan of rodents and humans (Dawson et al. 2003; Dimou et al. 2008; Young et al. 2013; Kang et al. 2010; Yeung et al. 2014), with the human cortex exhibiting an impressive 2.5% turnover per year in adulthood, only a small fraction of them survive to mature and integrate into the cortex (Hughes et al. 2018; Young et al. 2013). Therefore, producing more oligodendrocytes than needed seems to be unfavorable for the organism.

Regarding this last point, VPA could be detrimental for the physiological turnover of oligodendrocytes? It is unlikely to be the case. It has been determined that all NG2-glia can proliferate and differentiate (Simon, Gotz, and Dimou 2011; Vigano et al. 2016). It is possible that other factions of the population, e.g., progenitors expressing GPR17, assume the role of maintaining the production of oligodendrocytes as needed. Furthermore, those myelinating cells that have been integrated during VPA would also be affected by factors such as aging (Lasiene et al. 2009).

Oligodendrogenesis promoted by VPA plays a role in exercise-induced cognitive enhancement

Other studies have reported that increased physical activity induces the differentiation of NG2-glia; however, the question regarding their function after VPA has not been tackled. Hence, to answer this, I asked whether newly generated oligodendrocytes matured into myelinating cells, which could provide insights regarding their incorporation into the cortical circuit. I observed that after six weeks of VPA, the number of MAG⁺GFP⁺ cells increased 3-fold in the motor cortex, and this effect was observed in all cortical layers. This evidence suggests that VPA remodels the cortical circuitry by enhancing myelin availability through newly generated oligodendrocytes.

Do the numbers of newly generated myelinating oligodendrocytes matter? I observed that the number of GFP⁺MAG⁺ cells increased from 10.15 ± 1.30 to 29.78 ± 5.27 per 1mm². Therefore, the question could represent a probable criticism of whether the number of oligodendrocytes that reach full maturity is enough to lead to significant remodeling changes in

the motor cortex, triggering alterations in the cognitive processing of these mice. In principle, it appears to be a legitimate concern. Nonetheless, I believe that it might be unfunded.

First, it has been hypothesized that myelination has a profound effect on the propagation of the action potential, reducing the time delay between the generation of the signal and its arrival. Furthermore, it has been argued that subtle changes in the order of 10% in the distribution and other properties of myelin could lead to substantial changes in the temporal synchrony and oscillations in neuronal firing (Pajevic, Basser, and Fields 2014). Recent experimental evidence supports the theoretical framework that slight enhancement of oligodendrogenesis is sufficient for learning and memory improvement, having tremendous repercussions in hippocampal and prefrontal cortex oscillators synchronicity, which is severely affected by blocking NG2-glia differentiation (Steadman et al. 2020; Pan et al. 2020).

Second, to analyze the contribution of oligodendrocytes to information processing by simply counting cells is misleading. The regulatory power of myelinating cells over circuits depends on the internode associated to the axon and not on their soma. Furthermore, one single oligodendrocyte can form up to 60 internodes (Nave and Werner 2014). Thus, I could estimate from our results that the increase of ~30 newly formed oligodendrocytes after VPA could generate up to a remarkable 1800 new myelin sheaths available to modify propagation speed.

Third, another common misconception is to assume that oligodendrocytes lack selectiveness when choosing the targets to be myelinated. A concept that probably came from *in vitro* experiments. In culture, oligodendrocytes do not require specific signals to initiate myelination. This phenomenon is not only real for mixed cocultures, but also with inert PFA-fixed axons and nanofibers (Rosenberg, Powell, and Chan 2007; Lee, Leach, et al. 2012). Nonetheless, it has been shown *in vivo* that activity-dependent myelination creates a bias on oligodendrocytes to wrap around those neurons that are electrically active (Hines et al. 2015; Mitew et al. 2018). Therefore, those 1800 new internodes might be associated with axons that respond to VPA with increased electrical activity or secreted growth factors (Lundgaard et al. 2013).

Fourth, the amount of newly generated oligodendrocytes may be underestimated due to some limitation that would be worth to consider. In this set of experiments, I used the inducible

Cre-lox system mouse model *NG2-CreER^{T2} x CAG-GFP*, which, as I mentioned, presents incomplete NG2-glia recombination (Huang et al. 2014; Schneider et al. 2016). Therefore, I could oversee part of the population of progenitors that might also be directly differentiating.

The functionality of these new oligodendrocytes is a difficult problem to tackle because of the alleged lack of a measurable behavioral outcome provided by VPA. Nevertheless, we know that increased physical activity leads to cognitive enhancement in tasks related to learning and memory (Hillman, Erickson, and Kramer 2008), a phenomenon, so far, monopolized by neurons and neurogenesis (van Praag et al. 1999; Olson et al. 2006; Diederich et al. 2017; Voss et al. 2019; Wu et al. 2008). The importance of oligodendrocytes has not been approached until now. Previous evidence showed that preventing NG2-glia differentiation impairs motor learning, spatial localization, fear-conditioning, and working memory (McKenzie et al. 2014; Steadman et al. 2020; Pan et al. 2020; Xiao et al. 2016; Geraghty et al. 2019). Hence, following a similar approach like in these studies, I took advantage of our model *Sox10iCreER^{T2} x Esco2^{fl} x CAG-GFP*, which block the formation of newly generated oligodendrocytes (Fard et al. 2017; Schneider et al. 2016). Hence, I induced animals before starting our VPA protocol, to prevent the differentiation of NG2-glia in response to exercise, and later I measured their learning and memory capacity through the novel object recognition task (**Fig. 18**).

I observed that all groups had normal locomotion, and additionally, the baseline ability to recognize the novel object was not impaired (**Fig. 18 and 19**). This last point was fantastic news because I wanted to analyze only the enhancement of cognition due to increased physical activity. Otherwise, if the deletion of *Esco2* from our mutant mouse line had affected the performance in our task, our results would have had a more complicated interpretation. It could be argued that NG2-glia ablation impairs learning and memory and does not relate to cognition enhancement. Interestingly, when I assessed the NOR performance, by retrieving the recognition index, I observed that the improved performance induced by VPA was abolished in the *Sox10-Esco2^{flx/flx}* mice compared with the *Sox10-Esco2^{wt/wt}*. In the same line, *Sox10-Esco2^{flx/flx}* runners showed a performance similar to the *Sox10-Esco2^{wt/wt}* and *Sox10-Esco2^{flx/flx}* housed in standard cages (**Fig. 21**). These results suggest that the formation of new oligodendrocytes is essential for the cognition enhancement induced by VPA.

A question raised along these experiments was whether the ablation of *Esco2* in NG2-glia and the changes in NG2-glia led to impairment of adult neurogenesis and indirectly affect the enhanced generation of neurons also induced by increased locomotion. Therefore, it was imperative for us to show that neurogenesis was not affected by the ablation of NG2-glia. Additionally, the role of newly generated oligodendrocytes could be to metabolically support NSCs that are differentiating into neurons (Funfschilling et al. 2012; Klugmann et al. 1997; Lappe-Siefke et al. 2003; Lee, Morrison, et al. 2012; Biebl et al. 2000; Kempermann et al. 2003).

To tackle this enigma, I analyzed the proliferation of NSCs in the hippocampal DG of *Sox10-Esco2^{wt/wt}* and *Sox10-Esco2^{flx/flx}* with and without VPA. I observed that *Sox10-Esco2^{wt/wt}* and *Sox10-Esco2^{flx/flx}*, showed an increased proliferation of neuroblasts in comparison to their respective sedentary control (**Fig. 21**). Additionally, I failed to find differences between the control groups or the VPA groups. Thus, this data suggests that NG2-glia differentiation is necessary for task performance enhancement but does affect neither baseline memory formation or consolidation, nor hippocampal neurogenesis.

Our work does not pretend to undermine or imply that enhanced neurogenesis by increased physical activity plays no role in cognitive improvement. Conditional depletion or X-ray irradiation of newly born neurons in the DG leads to impairment in spatial memory, novel object recognition, and fear-conditioned memory (Jessberger et al. 2009; Saxe et al. 2006). Moreover, spatial memory deteriorated by X-ray irradiation depletion of DG NSCs can be reversed by forced running exercise, which also increases neurogenesis by brain-derived neurotrophic factor (BDNF)-dependent mechanism (Ji et al. 2014). Thus, I believe that both oligodendrogenesis and neurogenesis are necessary for enhanced cognitive performance induced by exercise, and I forecast that the inhibition of one or the other would lead to the abolishment of augmented cognition.

More and more evidence is gathered supporting the role of oligodendrogenesis in the modulation of cognition. Previous research established that the generation of new oligodendrocytes was a consequence of learning and memory (Steadman et al. 2020; Pan et al. 2020); hence, the experience itself leads to the differentiation of NG2-glia. In this doctoral thesis,

I found that oligodendrogenesis is vital for the integration of increased physical activity and the modulation of cognitive processes. This concept by itself is already a fascinating novelty within the field of NG2-glia, the oligodendrocyte lineage, and adaptive myelination.

There are still questions regarding the participation of adaptive myelination in cognition. Although we know that oligodendrogenesis is necessary for learning and the consolidation of memory, open questions are still unanswered regarding their role in other related processes. For instance, extinction or “forgetting” happens in most forms of memory. In the case of neurons, some mechanisms have been widely described such as reduction of synaptic strength, changes in dendritic spines turnover or their removal, and so on (Luchkina and Bolshakov 2019; Wang, Yue, et al. 2020).

On the other hand, current vision of myelinating oligodendrocytes is that they are persistent in time. Myelinating cells may undergo apoptosis and remove the wrapping around the axon. A second alternative is that the internodes change their properties, such as their length and compaction, or that myelin processes retract undressing their previous targeted axonal segment. However, it could be that myelin does not play a role at all in this process, and only changes at the neuronal level occur.

Possible circuits remodeled by adaptive myelination promoted by VPA

It is known that the distribution of myelin segments along axons of the cortex is heterogenous and discontinuous (Tomassy et al. 2014), providing a suitable substratum for adaptive myelination to occur. It has been shown that myelin impairment of thalamocortical axons, projecting to the motor cortex, has a detrimental effect on motor learning related-tasks (Kato et al. 2020), which has been attributed to asynchronicity of signals arriving at this area.

An important point for these results interpretation is that the motor cortex projects to the retrosplenial cortex (RSC) (Yamawaki, Radulovic, and Shepherd 2016; Jeong et al. 2016), which is an associative cortical area that has been fundamentally related to spatial learning and memory (Vann, Aggleton, and Maguire 2009). It has been reported that object recognition task

adapted for measuring long-term memory is impaired after a lesion in RSC (Haijima and Ichitani 2012). Additionally, by searching in the literature and the Allen Brain Atlas: Mouse Connectivity open-sourced database, I found a possible circuit loop between cortical areas. It has been anatomically described that RSC receives diverse input from the dorsal hippocampus and parahippocampal regions (Sugar et al. 2011) and has monosynaptic projections to the hippocampal DG (Allen Institute, Allen Brain Atlas: Mouse Connectivity). Furthermore, RSC has a feedback loop to the motor cortex (Yamawaki, Radulovic, and Shepherd 2016), emphasizing the reciprocity and codependent function between the RSC and the motor cortex. To advance in the description of the role of adaptive myelination induced by physical activity might have on this circuit, it is important to define whether the motor cortex projections to the RSC are the ones being myelinated. To answer this, it could be informative to inject a retrograde tracer into the RSC of our Cre-lox reporter mouse (e.g., *NG2-CreER^{T2} x CAG-GFP*) and, by histological analysis, evaluate whether these axons have internodes of newly generated oligodendrocytes induced by VPA.

What role is played by newly generate oligodendrocytes in this circuit? With the current evidence, it is difficult to specify the role of NG2-glia and adaptive myelin in the regulation of this circuit. It has been proposed that the purpose of adaptive myelination is to synchronize spike-time arrival and to promote synchronization of signals, circuits, or oscillators (Kato et al. 2020; Steadman et al. 2020). It is tempting to suggest that myelin remodeling might be required to strengthen or synchronize the local corticocortical circuitry between the motor cortex and the RSC. In turn, this could lead to improvement of the strength of the signals from the RSC to the hippocampus or even promote synchronicity among different parts of the circuit. It would be interesting to explore how behaves neuronal activity in these areas and whether they are synchronized before and after increased physical activity. Later, it would be essential to analyze by blocking NG2-glia differentiation during exercise, possibly with Cre-lox systems like our *Esco2-fl* or *Myrf-fl* (key transcription factor in oligodendrogenesis, which deletion impairs the generation of new oligodendrocytes) mice, to assess whether the activity of these areas and their synchronicity changes depending on physical activity.

Interestingly, it has been recently shown that not only long-range excitatory neurons are myelinated but also a large proportion of local inhibitory neurons, mainly the fraction of fast-spiking parvalbumin interneurons (Micheva et al. 2016; Stedehouder et al. 2017; Stedehouder et al. 2019). In addition, myelination of other inhibitory neurons like the somatostatin positive ones has been described, presenting a lower number of internodes than the parvalbumin counterparts (Zonouzi et al. 2019). What seems fascinating is that the degree of myelination in parvalbumin neurons is activity-dependent. It has been shown that by the expression of DREADDs in parvalbumin interneurons, and their subsequent stimulation, the number of internodes associated to them increases together with their arborization complexity (Stedehouder et al. 2018). To understand how new myelin affects these neurons might be of crucial relevance because it is accepted that inhibitory interneurons constitute a significant component in the regulation of behavior (Swanson and Maffei 2019).

Adaptive myelination may regulate local circuits excitation by modifying the spike-time arrival of the cortical interneurons input. For example, new myelination of interneurons allows synchronizing spike-time arrival coming from the inhibitory neuron with the excitatory signal from a pyramidal neuron, resulting in the overall inhibition of the circuit. Nonetheless, it is difficult to imagine how promoting local inhibition could lead to cognitive enhancement. A second possibility is that new myelin “de-synchronizes” the simultaneous spike-time arrival of excitatory and inhibitory neurons inputs, disinhibiting the circuit and promoting overall excitation. Because interneurons can inhibit each other (Pfeffer et al. 2013), interneurons projecting towards other interneurons synchronize their time-spike arrival to inhibit the targeted interneurons and release excitatory neurons from their inhibition.

A simple approach to solve this problem would be to express reporter proteins in different GABAergic neurons (e.g., parvalbumin, somatostatin, and VIP interneurons) and observe whether there is colocalization between internodes of newly generated oligodendrocyte with interneuronal processes. It is possible that newly formed oligodendrocytes might myelinate both excitatory and inhibitory neurons. Nonetheless, to distinguish oligodendrocytes myelinating inhibitory or excitatory neurons is rather simple. It has been shown that oligodendrocytes myelinate either inhibitory or excitatory neurons, but very rarely both (Zonouzi et al. 2019).

However, it is not known the situation after VPA or after other experience-dependent myelination. The reason behind this bias is yet unknown. However, such bias might be related to the recently described heterogeneity of the oligodendrocyte population, suggesting that different cells might have different targets (Marques et al. 2016). Whether this heterogeneity is sustained from different progenitors remains open.

Possible mechanism of action of VPA

The analysis how VPA modifies the behavior of NG2-glia is challenging due to the multiple effects of exercise in the organism (**Fig. 27**). I based our assumption that VPA promotes neuronal activity in the cortex because, after exercise, there is an increased of glucose consumption in the motor cortex and regional CBF (Vissing, Andersen, and Diemer 1996; Hiura et al. 2018). Therefore, the signal released from neurons should be activity-dependent. I have hypothesized that neuronal signals are integrated into NG2-glia through neuron-NG2-glia synapses. It is known that NG2-glia

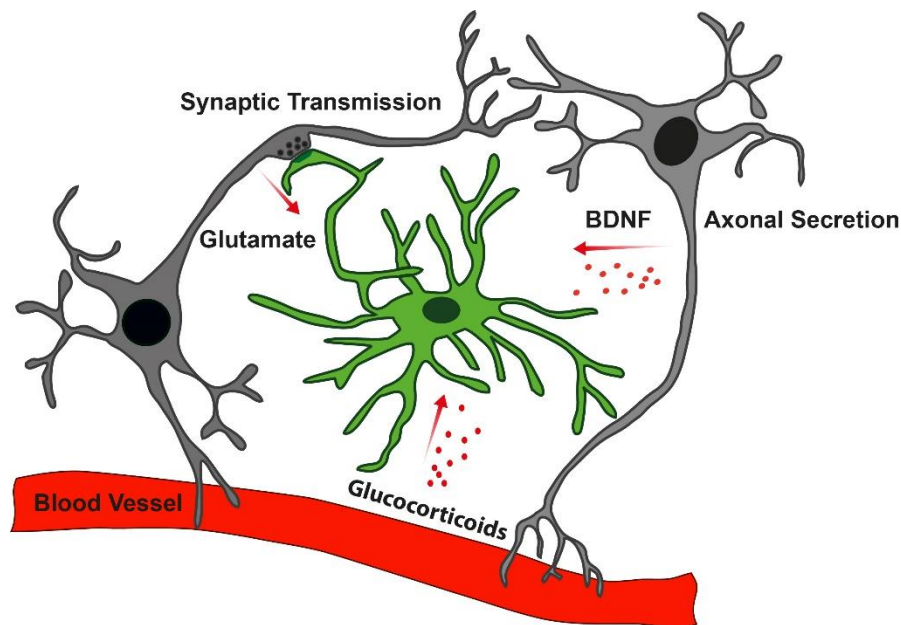


Figure 27. Possible mechanism in which VPA induce changes in NG2-glia behavior. VPA can lead to increase neuronal activity and increase release of neurotransmitters, such as glutamate, which is detected by NG2-glia through the neuron-NG2-glia-synapse. Another mechanism could be involving activity-dependent axonal secretion, such as BDNF, which is independent of synapses. Finally, VPA could increase the release of signals from the blood stream, crossing the blood-brain barrier, and inducing changes in NG2-glia behavior.

form synapses with axons in the adult CNS (Bergles et al. 2000; De Biase, Nishiyama, and Bergles 2010; Kukley, Capetillo-Zarate, and Dietrich 2007; Ziskin et al. 2007). Although the function of these structures remains unknown, synaptic signaling is a suitable mechanism for monitoring neuronal activity and, in turn, commanding the changes in the behavior of NG2-glia in an activity-dependent manner. Notably, it has been shown that NG2-glia downregulate their synapses during their differentiation into myelinating oligodendrocytes, but they conserve them during proliferation (Kukley, Nishiyama, and Dietrich 2010; Kukley et al. 2008). Two conclusions can be extracted from this evidence. First, synapses are required in the lifetime of a NG2-glia. Second, they become dispensable as soon as they become oligodendrocytes.

I have observed that VPA increases the differentiation of NG2-glia, and this process is limited to a population of progenitors, inferred by the lack of correlation between the exercise performance of animals and their capacity to form oligodendrocytes. From our proteome analysis, I proposed that the NG2-glia having a high expression of synaptic-related and glutamatergic signaling pathway-related proteins are the ones responding to VPA by differentiating into oligodendrocytes (**Fig. 13**). Conversely, NG2-glia with low synaptic-related proteins remain as progenitors, and simultaneously they seem to have low levels of proteins related to myelin, myelin assembly, oligodendrogenesis, and cell differentiation (**Fig. 13**). This body of evidence suggest that synapses are essential for NG2-glia differentiation, and those cells that form few synapses or none remain as progenitors.

To my knowledge, it has not been addressed whether all NG2-glia receive synaptic input and, moreover, whether NG2-glia have synapses during every stage of the organism or cell development (**Fig. 14b**). Interestingly, the total number of GPR17⁺ NG2-glia increased, which is a population that is resistant to differentiate under physiological and VPA conditions. Therefore, it would be of interest to describe the electrophysiological properties of these cells and their synaptic inputs. It is feasible that GPR17⁺ NG2-glia do not form synapses with neurons; and thus, they remain unresponsive to the stimulus provided by VPA. In this direction, so far, our group has developed a transcriptome database, through a Cre-lox system involving the ribotag mouse line (Sanz et al. 2009) together with the Cre-driver mouse lines of GPR17i-CreER^{T2} and the NG2-CreER^{T2}. This strategy has been performed in a way to compare the transcriptomic profile of the

GPR17⁺ NG2-glia compared to the total progenitors' population, which might worth the effort to help elucidate further whether there are differences in the expression of synaptic proteins (Nicole Unger's doctoral thesis).

As already mentioned, our proteome analysis revealed a possible relationship between differentiation and synapses. This evidence raised questions about the role of these synapses. Are NG2-glia synapses required only for neuronal activity detection? Or are they necessary for normal physiological differentiation of NG2-glia? These questions have been rather difficult to resolve due to the high functional complexity of the structures. For instance, it has been shown that NG2-glia respond to glutamate by reducing the proliferation and increasing their differentiation of NG2-glia. However, other reports have shown that neuron-NG2-glia synapses function is highly dependent on the specific molecular context like the specific properties of AMPA receptors and activated signaling pathways that turn NG2-glia more sensitive to glutamate (Lundgaard et al. 2013; Chen et al. 2018).

The intricate nature of NG2-glia receptors leads us to look for a different strategy to approach the function of neuron-glia synapses, which might as well provide valuable information to the field. This objective was challenging due to the lack of knowledge in comparison to the neuronal synapses' counterpart. To ensure a successful selection of a protein target, I followed the next assumptions: Firstly, and perhaps most adventurous, I assumed that the structure of neuron-NG2-glia synapses was like the neuronal ones. Secondly, I searched for a structural protein that could be potentially expressed in every NG2-glia synapse. Fourthly, I looked at the available open-sourced transcriptomic data (Zhang et al. 2014), to get insights over the expression of these proteins in NG2-glia, which I were able to corroborate with our adult NG2-glia transcript database generated by the ribotag mouse line (Nicole Unger's doctoral thesis).

Under this premise, I observed that the novel postsynaptic scaffold protein Shank3 was expressed at the transcriptome level in NG2-glia (Zhang et al. 2014). It has been described that this protein is essential for postsynaptic assembly, formation, and maintenance in neurons (Tu et al. 1999; Arons et al. 2012). Taking all this evidence into consideration, with the collaboration of

Prof. Dr. Tobias Böckers at Ulm University, I generated the novel *Sox10-iCreERT2 x Shank3-fl x CAG-GFP* mouse line (**Fig. 23a**).

Initial steps involved the characterization of the mouse line by confirming that genes were in the transgenic model and the functionality of the inducible Cre-lox system. Additionally, I observed that GFP reporter expression was restricted to the oligodendrocyte lineage (**Fig. 23b – 23f**). Furthermore, I found that GFP reporter in *Shank3^{wt/wt}* mice colocalized with Shank3 in a punctated manner and had a wide distribution in processes and soma (**Fig. 24**), resembling the characteristics of the signal in neurons (Arons et al. 2012; Heise et al. 2016). Additionally, I observed that Shank3 puncta signal in NG2-glia colocalized with Bassoon, a presynaptic marker on neurons (**Fig. 24**). This first step might indicate that Shank3 is expressed in NG2-glia and might be a constituent of neuron-NG2-glia synapses. Finally, and most notably, our preliminary data on the affected motor behavior suggest that Shank3 deletion in the oligodendrocyte lineage led to substantial motoric deficits, including clasping behavior and worsen performance in the beam walk and rotarod test (**Fig. 25**). Because of the preliminary nature of this data, all interpretations must be taken carefully at this point, and it is imperative in the future to further characterize this mouse model, albeit it provides fertile ground for future projects.

For instance, autism spectrum disorders (ASD) are thought to be based on synaptopathies; therefore, many of the mouse models have a mutation or deletion of synaptic protein such as the Shank family of scaffold proteins (Monteiro and Feng 2017). Furthermore, haploinsufficiency of Shank3 has been successfully correlated to the Phelan-McDermid syndrome, a rare monogenic neurodevelopmental disorder within ASD (De Rubeis et al. 2018; Wilson et al. 2003; Durand et al. 2007). Nonetheless, it might be wrong to assume that other cell populations are not affected by these genetic modifications. Studies tackling this point are recently developing. The first compelling evidence gathered by MRI has shown that WM aberrations, which might be associated with myelin integrity, occur in Phelan-McDermid patients and Shank3 knockout mice (Jesse et al. 2020). Because NG2-glia synapses had been overlooked in this field, our novel mouse model become attractive to further dissect the role of Shank3 in the oligodendrocyte lineage.

From our early evidence, it is tempting to suggest that the deletion of Shank3 decreases the degree of differentiation of NG2-glia due to impairment in the synaptic communication between neurons and NG2-glia. Our group has shown that preventing the generation and integration of new oligodendrocytes evokes severe motor impairments in mice (Schneider et al. 2016). Additionally, in Shank3 knockout mouse models, minor to critical motor behavior impairments have been observed, depending on the site of gene deletion (Monteiro and Feng 2017). Furthermore, hindlimbs claspings has been described in other models for ASD (Schmeisser et al. 2012; Gemelli et al. 2006), supporting the results observed by the deletion of Shank3 in the oligodendrocyte lineage. Phelan-McDermid patients present neurological deficits as hypotonia, gait disturbance, upper motor neuron dysfunction, motor planning, and gross motor coordination abnormalities (Soorya et al. 2013; Zwanenburg et al. 2016). Thus, it seems that our *Sox10-iCreERT2 x Shank3-fl x CAG-GFP* mice could provide further information of the possible role of the oligodendrocyte lineage in some of the features of the disease.

There is still a long way to have reliable conclusions. Again, the mouse model promises not only to be useful for the study of neuron-NG2-glia synapses but also to understand better the role of the oligodendrocyte lineage in ASD. In future research, I would like to investigate the role of Shank3 in the oligodendrocyte lineage in different developmental stages as well as their synaptic input and synapse integrity. Additionally, it might be of interest to analyze in detail NG2-glia proliferation and differentiation after Shank3 deletion and further analyze the behavioral impairments common in patients and other ASD mouse models.

Leaving neuron-NG2-glia synapse aside, initially on this discussion, I acknowledged that because of the nature of VPA, a wide array of signaling pathways are active that could potentially have robust effects on the brain and NG2-glia. In particular, the BDNF pathway captivated my attention. BDNF is a member of the neurotrophic factor family that activates the tropomyosin receptor kinase B (TrkB), a member of the tyrosine kinase receptors. BDNF has a vast number of functions, such as promoting neurogenesis, synaptic plasticity, cell growth, and survival, just to mention a few of them (Mattson, Maudsley, and Martin 2004).

Interestingly, BDNF is released by exosome from neurons in an activity-dependent manner (Wong et al. 2015), making it a suitable signal for NG2-glia to screen neuronal activity. Impressively, it has been shown that BDNF increases its expression in the brain in running mice, which positively correlates with exercise performance (Neeper et al. 1995). This situation might be the same case in humans as BDNF blood serum levels raise 2 – 3-folds during exercise, which has been estimated that the brain might contribute to 70 – 80% of the total production (Rasmussen et al. 2009). This body of evidence highlights that BDNF possibly has local and systemic targets in the organism.

As briefly mentioned before, BDNF has been widely described as a promoter for neurogenesis, which might represent the link between the formation of newly generated neurons, exercise, and cognitive enhancement (Cefis et al. 2019; Ji et al. 2014). Nonetheless, the first description of a BDNF knockout mouse line revealed that these mice showed a reduction in myelin proteins, and in the number of oligodendrocytes, as well as hypomyelination (Djalali et al. 2005; Cellierino et al. 1997). It has also been described that the complete oligodendrocyte lineage does express the TrkB receptor (Van't Veer et al. 2009; Du et al. 2003), making them a possible target for this neurotrophin. Currently, there is still little knowledge about the effect of BDNF in the oligodendrocyte lineage. Nevertheless, it has been described that it might regulate proliferation and differentiation of NG2-glia, as well as survival and myelin thickness in oligodendrocytes (Du et al. 2003; Fletcher, Murray, and Xiao 2018; Van't Veer et al. 2009; Nicholson et al. 2018; Tshiperson et al. 2015; Cohen et al. 1996).

Notably, I observed in our proteome data that NG2-glia not reactive to VPA showed a downregulation of proteins involved in the BDNF signaling pathway (**Fig. 13**). PI3K/Akt is a classic signaling route activated by the association of BDNF with the TrkB receptor (Chao 2003). This evidence might suggest that BDNF plays a role in NG2-glia differentiation after VPA. It has been previously shown that inducible conditional knockout of the TrkB receptors in NG2-glia abolish their differentiation and myelin plasticity after optogenetic stimuli of neurons (Geraghty et al. 2019). Additionally, the same mouse model showed impairment in working memory, which the authors assumed was due to reduced oligodendrogenesis (Geraghty et al. 2019). Additionally, I observed in our proteome that proteins related to synapses and glutamatergic signaling

pathways seem to be necessary for the formation of newly oligodendrocytes induced by VPA (**Fig. 13**). Previous research has found that BDNF is needed to shift NG2-glia differentiation from being glutamate/NMDAR-independent to –dependent (Lundgaard et al. 2013). Thus, I suggest that VPA requires signals provided by BDNF and the synaptic communication to promote differentiation.

In the future, it would be interesting to test whether the BDNF/TrkB activation in NG2-glia plays a role in their differentiation as well as the oligodendrogenesis-dependent cognitive enhancement by VPA. To analyze BDNF function in oligodendrocyte progenitors, it is feasible to use pharmacological approaches by using the commercially available TrkB agonist, 7,8-dihydroxyflavone (7,8-DHF), and antagonist, ANA-12. Nonetheless, this strategy could lead to confounding factors because neurogenesis is also regulated by BDNF (Cefis et al. 2019; Ji et al. 2014). A more promising experimental approach might be obtaining the commercially available *TrkB-flox* mouse line (MMRRC) (Geraghty et al. 2019) and pair it with our Cre-driver mouse lines such as *Sox10-iCreER^{T2}* or *NG2-CreER^{T2}*. Afterward, I could confirm the role of BDNF by analyzing the differentiation properties of NG2-glia and in behavioral paradigms, e.g., NOR whether cognitive enhancement evoked by VPA is abolished.

As I mentioned earlier, other signals of action might occur at the systemic level. For instance, it has been shown that, after exercise, glucocorticoids significantly augment in the plasma of rodents and even in humans after brief periods of high-intensity of locomotor activity (Borer et al. 1992; Buono, Yeager, and Hodgdon 1986; Coleman et al. 1998). Glucocorticoids are a class of corticosteroids, which are steroid-based hormones that interact with the nuclear receptor, the glucocorticoid receptor (GR). Most of the glucocorticoids are produced in the adrenal gland, and afterward, they can cross the BBB (Mason et al. 2010). Like many other cells, NG2-glia express the GR1, and prolonged treatment to corticosterone lead to a decrease in their proliferation (Alonso 2000; Matsusue et al. 2014). Furthermore, it has been shown that rabbit pups treated with synthetic glucocorticoids, as dexamethasone or betamethasone, showed hypomyelination, reduced oligodendrogenesis, and reduced NG2-glia proliferation, as well as, reactive gliosis (Zia et al. 2015).

Most research in regard to glucocorticoids suggest that they have a detrimental effect on the oligodendrocyte lineage as it has been shown in several stress models (Yang et al. 2016; Luo et al. 2019; Banasr et al. 2007), as these molecules are released under systemic stress conditions. Nonetheless, it could be that in the context of VPA, glucocorticoids promote differentiation of NG2-glia. As a byproduct of this doctoral thesis, I have generated a mouse line that deletes GR explicitly from the oligodendrocyte lineage by paring our *Sox10-iCreER^{T2}* mouse line with the *GR1-fl* mouse line, kindly provided by Prof. Dr. Jan Tuckermann from Ulm University.

Our data suggest that the deletion of GR in the oligodendrocyte lineage enhanced the proliferation and differentiation of NG2-glia (data not shown). Therefore, glucocorticoids might negatively regulate oligodendrogenesis. This evidence provides an exciting insight, whether, the expression and activity of GR are distinct among within the NG2-glia population. Thus, it could bring an interesting point to analyze the response of glucocorticoids in, e.g., GPR17⁺ NG2-glia, which I believe is a cell population less committed to differentiating under VPA conditions.

Exercise and NG2-glia, a target for a possible treatment?

An essential objective in neuroscience is to translate basic purposed research to the benefit of people's well-being. Therefore, this doctoral thesis has a section that aims to contextualize our results in possible therapies that involve exercise and significant aspects to take into consideration for related treatments.

It is widely described that exercise has massive benefits for health and reduces the risk of developing chronic metabolic diseases, such as diabetes, obesity, cardiovascular diseases, and protects mental health (Rodriguez-Ayllon et al. 2019; Booth et al. 2008). Additionally, it is believed that increased physical activity might have not only defensive features but also regenerative ones.

Multiple sclerosis (MS) is an immune-mediated disease which damage is caused by exacerbated inflammation in the CNS, leading to loss of myelin and neurodegeneration (Franklin and Ffrench-Constant 2008). Although, in some cases, remyelination happens naturally at the

early stages of the disease, later in the progression of the disease the formation of new myelin fails and progressively deteriorates. This failure has been attributed to changes in the CNS environment, making it increasingly more hostile or restrictive to ensure successful remyelination. Therefore, it is thought that the manipulation of NG2-glia behavior could help the system to remyelinate and to improve the outcome of the disease. In this work, I have shown that increased physical activity promotes NG2-glia proliferation and differentiation, and possibly myelination in the CNS. Hence, it results naturally to think that exercise could have potential therapeutic properties for treating MS. Unfortunately, although there is promising evidence that training can be beneficial for the rehabilitation of MS patients, it is still inconclusive (Motl et al. 2017), reinforcing the notion that more research has to be done.

There is a downside, nonetheless. Due to the complex heterogeneity of MS, and many features not well understood yet, there is no single model that covers all aspects of the illness. Nevertheless, experimental approaches based on toxin-induced demyelination (cuprizone and LPC) and of the increase of the autoimmune response towards myelin, like in the experimental autoimmune encephalomyelitis (EAE), have provided invaluable insights into the field.

It has been shown that after twenty weeks post-induction of EAE, mice presented cognitive deficits as well as reduction of MBP⁺ and CNPase⁺ cells, probably indicating a decrease in the number of oligodendrocytes. However, after four weeks of forced running, mice improved the lack of both markers for myelinating cells and ameliorated their cognitive impairment (Sung, Lim, and Mao 2003). Similar results have been found in cuprizone models. It has been shown that cuprizone reduces the oligodendrocytes and myelin, which is reversed by forced and voluntary exercise. One of the studies has suggested that this mechanism of recovery might be regulated by the increase in neurotrophins, including BDNF (Naghizadeh et al. 2018; Mandolesi et al. 2019). Nevertheless, these experiments have been performed administering cuprizone and at the same time increased physical activity. Additionally, it has been shown that physical activity before EAE induction is protective by delaying disease onset and reducing clinical score (Le Page, Ferry, and Rieu 1994; Bernardes et al. 2013), making it unclear whether exercise prevented oligodendrocyte death or promoted oligodendrogenesis. Moreover, the participation of NG2-glia in these processes remains uncertain because the empirical framework has been limited to

analyzing only the oligodendrocyte population. Only a recent study has shown that two weeks of increased physical activity improve the demyelinated injury, inflicted by LPC injection in the CC, proposing that it is due to enhanced proliferation and differentiation of NG2-glia, leading to faster remyelination in running animals (Jensen et al. 2018).

Which mechanisms might be promoted by exercise to induce NG2-glia differentiation and convey remyelination? Extrapolating our results and studying the literature, VPA may enhance the neuronal activity, which seems to be a substantial factor for remyelination promoted by NG2-glia differentiation in a glutamate-dependent pathway (Gautier et al. 2015). This can happen together with the exercise-induced synthesis of BDNF in the brain and increment in blood serum (Neeper et al. 1995; Rasmussen et al. 2009), which in turn increases the susceptibility of NG2-glia to neurotransmitters, like glutamate (Lundgaard et al. 2013).

Could it be a remyelination mechanism that is independent of the formation of new oligodendrocytes? Recent evidence in MS patients suggests that progenitors' proliferation and oligodendrogenesis are rather rare events in remyelinating injuries, and the formation of new myelin sheaths come from previously established oligodendrocytes (Jakel et al. 2019; Yeung et al. 2019). This idea has been corroborated to some extent by evidence in the rhesus monkey brains showing that previously integrated oligodendrocytes can form new myelin sheaths (Duncan et al. 2018). Although this is not the newest idea, it defies the strong concept in the field that oligodendrocytes have only a short window of time for myelinating axons (Czopka, Ffrench-Constant, and Lyons 2013). It is possible that exercise mandates oligodendrocytes to form new myelin sheaths. To tackle this question, I propose to use the inducible Cre-lox reporter systems under classic promoters for myelinating oligodendrocytes and analyzing the myelination pattern after VPA by immuno-EM. Albeit, it must be recognized that current technologies and animal models often have severe limitations to answer this question. Moreover, it is also possible that these highly specialized function could be present only in primates.

Exercise could be implemented as a proper therapy for aged individuals. It is known that cognition declines in healthy aging (Gazzaley et al. 2005). Among other things, decreased cognition has been related to diminished WM volume (Garde et al. 2000). This evidence is

supported by the fact that in healthy aging, there is a loss of WM volume and integrity in primates, and reduced oligodendrocyte health (Wisco et al. 2008; Peters et al. 1996; Peters 1996; Guttman et al. 1998).

Interestingly, this deterioration of the WM happens beside the generation of new oligodendrocytes along life. In rodent models, it has been consistently shown that NG2-glia differentiate into oligodendrocytes, forming new myelin, until higher ages, although this process considerably slows down in aged individuals (Dawson et al. 2003; Dimou et al. 2008; Young et al. 2013; Kang et al. 2010; Hill, Li, and Grutzendler 2018; Wang, Ren, et al. 2020). Recent data have shown that increasing the number of newly generated oligodendrocytes by clemastine, a first-generation histamine H1 receptor antagonist, and approved medication for MS treatment (Green et al. 2017), improves cognitive performance in aged mice (Wang, Ren, et al. 2020).

In the context of exercise, it has been shown that increased physical activity reduces the steepness of this deterioration, even in patients presenting dementia (Hillman, Erickson, and Kramer 2008; Heyn, Abreu, and Ottenbacher 2004). Considering our results, I have seen that even in older mice, VPA almost doubled the differentiation of NG2-glia compared with the sedentary mice (**Fig. 16b**). Therefore, it is possible that cognitive decline in running mice could be milder than in non-active mice due to the increments of NG2-glia differentiation. Although it must be considered that generating new oligodendrocytes does not necessarily translate in their incorporation into the brain.

For successful treatments, it must be assessed the beneficial extension of therapies. First, the regenerative impact of exercise could be limited by the locomotor impairing nature of diseases like MS or even healthy aging. On one side, MS patients not only have dysfunctional motility but also very frequently have symptoms as increased fatigue perception and depression (Motl et al. 2017; Wood et al. 2013), which may act in detriment of the motivation for exercising. On the other hand, it has been shown that older individuals tend to have reduced aerobic fitness, stamina, and psychomotor speed (Spirduso 1980). Thus, physical therapies must come together with proper exercise planning and psychological support accordingly with individual patients.

Second, intrinsic changes on oligodendrocyte progenitors, in their CNS environment, must be also taken into consideration. It has been described that the NG2-glia population shifts its expression profile with age (Marques et al. 2016). However, recent data suggest that stiffness of the nervous system surroundings, which is reduced with aging, has a more potent effect over NG2-glia behavior than their inherent properties (Segel et al. 2019). A similar situation happens in disease. In EAE and MS patients, NG2-glia have altered gene expression compared with the healthy individuals (Falcao et al. 2018; Jakel et al. 2019); moreover, the inflammatory activation might provide an extremely hostile environment (Franklin and Ffrench-Constant 2008).

Third, plastic alteration in the NG2-glia population due to exercise might be well considered. I have shown that VPA induced changes in their protein profile that suggested a phenotype more resistant to differentiation (**Fig. 13**), which is coherent with the enrichment of GPR17⁺ NG2-glia in the motor cortex (**Fig. 14**). Most importantly, the persistent stimulus of VPA did not provide a further enhance oligodendrogenesis compared with the animals housed under standard conditions (**Fig. 16**), advocating reduced progenitor plasticity. Therefore, it could be promising to combine exercise therapies with pharmacological approaches. In the same line, it has been shown that combined treatments, e.g., exercise together with clemastine, have a synergistic effect on the improvement of remyelination (Jensen et al. 2018). This evidence reveals that non-VPA reacting NG2-glia retains their capacity to generate new myelinating cells. In our specific situation, it might be helpful to resort to drugs that target the GPR17 receptor, e.g., the P2Y purinergic receptor antagonist cangrelor, which has been shown to promote differentiation of oligodendrocyte progenitors (Lecca et al. 2008). Albeit, its specific pharmacodynamics has been debated during the last years. Thus, in the future, in combination with exercise-based treatments, drugs probably should be applied simultaneously to improve the outcome in patients.

Conclusion

NG2-glia are an exciting cell population that have been very recently accredited as the fourth major glial population. Their distribution in the brain, their long-lasting capacities to proliferate and differentiate, and their reaction towards neuronal activity, experiences, and disease have captivated the attention of many scientists.

In this doctoral thesis, I have explored the response of NG2-glia to VPA, a model to analyze the effect of voluntary incremented physical activity on the progenitor population. Due to my research, I have successfully deepened our knowledge on the dynamics of NG2-glia behavior after VPA. Moreover, I have presented several novel observations in the field of the oligodendrocyte lineage. First, the reaction of NG2-glia appears to be heterogeneous within the progenitors' population, being some cells more sensitive to VPA than others, illustrating the importance of studying the differences within the progenitor population to understand their role in the CNS. Second, I described a mechanism that reduces the global plasticity of NG2-glia by shifting the population towards a less reactive identity after continuous physiological stimuli. This evidence is a significant discovery because limitations to adaptive myelination have not been described previously and could result in severe restrictions to research and to treatments based on myelin plasticity. Finally, for the first time, it has been shown that oligodendrogenesis is necessary for exercise-induced cognitive enhancement. This is unprecedented because it shows for the first time the consequences of the generation of new oligodendrocyte in apparently two unrelated events: the increase of physical activity and the improvement of learning and memory, a process thought to be entirely dependent of neurons.

I regret to finish this thesis with some unanswered questions. In this work, based on our proteome analysis, I have characterized the population of NG2-glia after VPA and compared it to a sedentary group. I could identify that several signaling pathways were downregulated in NG2-glia that did not differentiate after VPA. Among them, I suggested that communication through neuron-glia synapses and the BDNF/TrkB signaling pathway might be the molecular mediators to induce the formation of oligodendrocytes after VPA. As I discussed, it would be exciting to

Conclusion

confirm their role in adaptive myelination influenced by VPA. I also believe that it would be fascinating to describe in more detail the effect of Shank3 deletion in the oligodendrocyte lineage and to comprehend the role of the oligodendrocyte lineage in neurodevelopmental psychiatric disorders like ASD. Finally, it would be interesting to analyze the circuits that are remodeled by myelination after VPA, particularly changes involving the motor cortex. The importance of understanding the myelination pattern of axons in the brain under different conditions might reveal invaluable information regarding the circuit functionality in different brain regions. It would be interesting in the future to have a database with information regarding the distribution of internodes in the CNS under physiological and pathological conditions, the “myelinome.”

Finally, we have seen that in recent years, research of NG2-glia and other glial cells have been gaining ground in the neuroscience field. Hopefully, the significance of each cell population for the proper function of the nervous system makes us think over the popular term for glial cells as “supportive cells.” As Prof. Bruce Ransom suggested, perhaps neuroscientists should start calling glial cells: “partner cells.”

References

- Aggarwal, S., N. Snaidero, G. Pahler, S. Frey, P. Sanchez, M. Zweckstetter, A. Janshoff, A. Schneider, M. T. Weil, I. A. Schaap, D. Gorlich, and M. Simons. 2013. 'Myelin membrane assembly is driven by a phase transition of myelin basic proteins into a cohesive protein meshwork', *PLoS Biol*, 11: e1001577.
- Akiyoshi, R., H. Wake, D. Kato, H. Horiuchi, R. Ono, A. Ikegami, K. Haruwaka, T. Omori, Y. Tachibana, A. J. Moorhouse, and J. Nabekura. 2018. 'Microglia Enhance Synapse Activity to Promote Local Network Synchronization', *eNeuro*, 5.
- Alliot, F., I. Godin, and B. Pessac. 1999. 'Microglia derive from progenitors, originating from the yolk sac, and which proliferate in the brain', *Brain Res Dev Brain Res*, 117: 145-52.
- Alonso, G. 2000. 'Prolonged corticosterone treatment of adult rats inhibits the proliferation of oligodendrocyte progenitors present throughout white and gray matter regions of the brain', *Glia*, 31: 219-31.
- Alonso, G. 2005. 'NG2 proteoglycan-expressing cells of the adult rat brain: possible involvement in the formation of glial scar astrocytes following stab wound', *Glia*, 49: 318-38.
- Anthony, T. E., C. Klein, G. Fishell, and N. Heintz. 2004. 'Radial glia serve as neuronal progenitors in all regions of the central nervous system', *Neuron*, 41: 881-90.
- Araque, A., E. D. Martin, G. Perea, J. I. Arellano, and W. Buno. 2002. 'Synaptically released acetylcholine evokes Ca²⁺ elevations in astrocytes in hippocampal slices', *J Neurosci*, 22: 2443-50.
- Araya, R., M. Kudo, M. Kawano, K. Ishii, T. Hashikawa, T. Iwasato, S. Itohara, T. Terasaki, A. Oohira, Y. Mishina, and M. Yamada. 2008. 'BMP signaling through BMPRIA in astrocytes is essential for proper cerebral angiogenesis and formation of the blood-brain-barrier', *Mol Cell Neurosci*, 38: 417-30.
- Arons, M. H., C. J. Thynne, A. M. Grabrucker, D. Li, M. Schoen, J. E. Cheyne, T. M. Boeckers, J. M. Montgomery, and C. C. Garner. 2012. 'Autism-associated mutations in ProSAP2/Shank3 impair synaptic transmission and neurexin-neurologin-mediated transsynaptic signaling', *J Neurosci*, 32: 14966-78.
- Ashton, R. S., A. Conway, C. Pangarkar, J. Bergen, K. I. Lim, P. Shah, M. Bissell, and D. V. Schaffer. 2012. 'Astrocytes regulate adult hippocampal neurogenesis through ephrin-B signaling', *Nat Neurosci*, 15: 1399-406.
- Askew, K., K. Li, A. Olmos-Alonso, F. Garcia-Moreno, Y. Liang, P. Richardson, T. Tipton, M. A. Chapman, K. Riecken, S. Beccari, A. Sierra, Z. Molnar, M. S. Cragg, O. Garaschuk, V. H. Perry, and D. Gomez-Nicola. 2017. 'Coupled Proliferation and Apoptosis Maintain the Rapid Turnover of Microglia in the Adult Brain', *Cell Rep*, 18: 391-405.
- Auerbach, W., M. S. Hurlbert, P. Hilditch-Maguire, Y. Z. Wadghiri, V. C. Wheeler, S. I. Cohen, A. L. Joyner, M. E. MacDonald, and D. H. Turnbull. 2001. 'The HD mutation causes progressive lethal neurological disease in mice expressing reduced levels of huntingtin', *Hum Mol Genet*, 10: 2515-23.
- Banasr, M., G. W. Valentine, X. Y. Li, S. L. Gourley, J. R. Taylor, and R. S. Duman. 2007. 'Chronic unpredictable stress decreases cell proliferation in the cerebral cortex of the adult rat', *Biol Psychiatry*, 62: 496-504.

References

- Banker, G. A. 1980. 'Trophic interactions between astroglial cells and hippocampal neurons in culture', *Science*, 209: 809-10.
- Baraban, M., S. Mensch, and D. A. Lyons. 2016. 'Adaptive myelination from fish to man', *Brain Res*, 1641: 149-61.
- Bardehle, S., M. Kruger, F. Buggenthin, J. Schwausch, J. Ninkovic, H. Clevers, H. J. Snippert, F. J. Theis, M. Meyer-Luehmann, I. Bechmann, L. Dimou, and M. Gotz. 2013. 'Live imaging of astrocyte responses to acute injury reveals selective juxtavascular proliferation', *Nat Neurosci*, 16: 580-6.
- Barres, B. A., and M. C. Raff. 1993. 'Proliferation of oligodendrocyte precursor cells depends on electrical activity in axons', *Nature*, 361: 258-60.
- Bartsch, U., F. Kirchhoff, and M. Schachner. 1989. 'Immunohistological localization of the adhesion molecules L1, N-CAM, and MAG in the developing and adult optic nerve of mice', *J Comp Neurol*, 284: 451-62.
- Battista, D., C. C. Ferrari, F. H. Gage, and F. J. Pitossi. 2006. 'Neurogenic niche modulation by activated microglia: transforming growth factor beta increases neurogenesis in the adult dentate gyrus', *Eur J Neurosci*, 23: 83-93.
- Bechler, M. E., M. Swire, and C. Ffrench-Constant. 2018. 'Intrinsic and adaptive myelination-A sequential mechanism for smart wiring in the brain', *Dev Neurobiol*, 78: 68-79.
- Behrendt, G., K. Baer, A. Buffo, M. A. Curtis, R. L. Faull, M. I. Rees, M. Gotz, and L. Dimou. 2013. 'Dynamic changes in myelin aberrations and oligodendrocyte generation in chronic amyloidosis in mice and men', *Glia*, 61: 273-86.
- Belachew, S., R. Chittajallu, A. A. Aguirre, X. Yuan, M. Kirby, S. Anderson, and V. Gallo. 2003. 'Postnatal NG2 proteoglycan-expressing progenitor cells are intrinsically multipotent and generate functional neurons', *J Cell Biol*, 161: 169-86.
- Beltran-Castillo, S., M. J. Olivares, R. A. Contreras, G. Zuniga, I. Llona, R. von Bernhardi, and J. L. Eugenin. 2017. 'D-serine released by astrocytes in brainstem regulates breathing response to CO2 levels', *Nat Commun*, 8: 838.
- Bengtsson, S. L., Z. Nagy, S. Skare, L. Forsman, H. Forssberg, and F. Ullen. 2005. 'Extensive piano practicing has regionally specific effects on white matter development', *Nat Neurosci*, 8: 1148-50.
- Bercury, K. K., J. Dai, H. H. Sachs, J. T. Ahrendsen, T. L. Wood, and W. B. Macklin. 2014. 'Conditional ablation of raptor or rictor has differential impact on oligodendrocyte differentiation and CNS myelination', *J Neurosci*, 34: 4466-80.
- Bergles, D. E., J. D. Roberts, P. Somogyi, and C. E. Jahr. 2000. 'Glutamatergic synapses on oligodendrocyte precursor cells in the hippocampus', *Nature*, 405: 187-91.
- Bernardes, D., O. C. Oliveira-Lima, T. V. Silva, C. C. Faraco, H. R. Leite, M. A. Juliano, D. M. Santos, J. R. Bethea, R. Brambilla, J. M. Orian, R. M. Arantes, and J. Carvalho-Tavares. 2013. 'Differential brain and spinal cord cytokine and BDNF levels in experimental autoimmune encephalomyelitis are modulated by prior and regular exercise', *J Neuroimmunol*, 264: 24-34.
- Berret, E., T. Barron, J. Xu, E. Debner, E. J. Kim, and J. H. Kim. 2017. 'Oligodendroglial excitability mediated by glutamatergic inputs and Nav1.2 activation', *Nat Commun*, 8: 557.

References

- Bezzi, P., V. Gundersen, J. L. Galbete, G. Seifert, C. Steinhauser, E. Pilati, and A. Volterra. 2004. 'Astrocytes contain a vesicular compartment that is competent for regulated exocytosis of glutamate', *Nat Neurosci*, 7: 613-20.
- Biebl, M., C. M. Cooper, J. Winkler, and H. G. Kuhn. 2000. 'Analysis of neurogenesis and programmed cell death reveals a self-renewing capacity in the adult rat brain', *Neurosci Lett*, 291: 17-20.
- Birey, F., and A. Aguirre. 2015. 'Age-Dependent Netrin-1 Signaling Regulates NG2+ Glial Cell Spatial Homeostasis in Normal Adult Gray Matter', *J Neurosci*, 35: 6946-51.
- Boda, E., F. Vigano, P. Rosa, M. Fumagalli, V. Labat-Gest, F. Tempia, M. P. Abbracchio, L. Dimou, and A. Buffo. 2011. 'The GPR17 receptor in NG2 expressing cells: focus on in vivo cell maturation and participation in acute trauma and chronic damage', *Glia*, 59: 1958-73.
- Booth, F. W., M. J. Laye, S. J. Lees, R. S. Rector, and J. P. Thyfault. 2008. 'Reduced physical activity and risk of chronic disease: the biology behind the consequences', *Eur J Appl Physiol*, 102: 381-90.
- Borer, K. T., L. L. Bestervelt, M. Mannheim, M. B. Brosamer, M. Thompson, U. Swamy, and W. N. Piper. 1992. 'Stimulation by voluntary exercise of adrenal glucocorticoid secretion in mature female hamsters', *Physiol Behav*, 51: 713-8.
- Bouchard-Cannon, P., C. Lowden, D. Trinh, and H. M. Cheng. 2018. 'Dexas1 is a homeostatic regulator of exercise-dependent proliferation and cell survival in the hippocampal neurogenic niche', *Sci Rep*, 8: 5294.
- Bowser, D. N., and B. S. Khakh. 2004. 'ATP excites interneurons and astrocytes to increase synaptic inhibition in neuronal networks', *J Neurosci*, 24: 8606-20.
- Brooks, S. P., and S. B. Dunnett. 2009. 'Tests to assess motor phenotype in mice: a user's guide', *Nat Rev Neurosci*, 10: 519-29.
- Bruttger, J., K. Karram, S. Wortge, T. Regen, F. Marini, N. Hoppmann, M. Klein, T. Blank, S. Yona, Y. Wolf, M. Mack, E. Pinteaux, W. Muller, F. Zipp, H. Binder, T. Bopp, M. Prinz, S. Jung, and A. Waisman. 2015. 'Genetic Cell Ablation Reveals Clusters of Local Self-Renewing Microglia in the Mammalian Central Nervous System', *Immunity*, 43: 92-106.
- Bu, J., A. Banki, Q. Wu, and A. Nishiyama. 2004. 'Increased NG2(+) glial cell proliferation and oligodendrocyte generation in the hypomyelinating mutant shiverer', *Glia*, 48: 51-63.
- Buono, M. J., J. E. Yeager, and J. A. Hodgdon. 1986. 'Plasma adrenocorticotropin and cortisol responses to brief high-intensity exercise in humans', *J Appl Physiol (1985)*, 61: 1337-9.
- Buser, A. M., B. Erne, H. B. Werner, K. A. Nave, and N. Schaeren-Wiemers. 2009. 'The septin cytoskeleton in myelinating glia', *Mol Cell Neurosci*, 40: 156-66.
- Bush, T. G., N. Puvanachandra, C. H. Horner, A. Polito, T. Ostenfeld, C. N. Svendsen, L. Mucke, M. H. Johnson, and M. V. Sofroniew. 1999. 'Leukocyte infiltration, neuronal degeneration, and neurite outgrowth after ablation of scar-forming, reactive astrocytes in adult transgenic mice', *Neuron*, 23: 297-308.
- Bushong, E. A., M. E. Martone, Y. Z. Jones, and M. H. Ellisman. 2002. 'Protoplasmic astrocytes in CA1 stratum radiatum occupy separate anatomical domains', *J Neurosci*, 22: 183-92.
- Cataldo, A. M., and R. D. Broadwell. 1986. 'Cytochemical identification of cerebral glycogen and glucose-6-phosphatase activity under normal and experimental conditions. II. Choroid plexus and ependymal epithelia, endothelia and pericytes', *J Neurocytol*, 15: 511-24.

References

- Cefis, M., A. Prigent-Tessier, A. Quirie, N. Pernet, C. Marie, and P. Garnier. 2019. 'The effect of exercise on memory and BDNF signaling is dependent on intensity', *Brain Struct Funct*, 224: 1975-85.
- Cellerino, A., P. Carroll, H. Thoenen, and Y. A. Barde. 1997. 'Reduced size of retinal ganglion cell axons and hypomyelination in mice lacking brain-derived neurotrophic factor', *Mol Cell Neurosci*, 9: 397-408.
- Chao, M. V. 2003. 'Neurotrophins and their receptors: a convergence point for many signalling pathways', *Nat Rev Neurosci*, 4: 299-309.
- Chen, T. J., B. Kula, B. Nagy, R. Barzan, A. Gall, I. Ehrlich, and M. Kukley. 2018. 'In Vivo Regulation of Oligodendrocyte Precursor Cell Proliferation and Differentiation by the AMPA-Receptor Subunit GluA2', *Cell Rep*, 25: 852-61 e7.
- Chen, Y., H. Wu, S. Wang, H. Koito, J. Li, F. Ye, J. Hoang, S. S. Escobar, A. Gow, H. A. Arnett, B. D. Trapp, N. J. Karandikar, J. Hsieh, and Q. R. Lu. 2009. 'The oligodendrocyte-specific G protein-coupled receptor GPR17 is a cell-intrinsic timer of myelination', *Nat Neurosci*, 12: 1398-406.
- Chittajallu, R., A. Aguirre, and V. Gallo. 2004. 'NG2-positive cells in the mouse white and grey matter display distinct physiological properties', *J Physiol*, 561: 109-22.
- Christopherson, K. S., E. M. Ullian, C. C. Stokes, C. E. Mullen, J. W. Hell, A. Agah, J. Lawler, D. F. Mosher, P. Bornstein, and B. A. Barres. 2005. 'Thrombospondins are astrocyte-secreted proteins that promote CNS synaptogenesis', *Cell*, 120: 421-33.
- Clarke, L. E., K. M. Young, N. B. Hamilton, H. Li, W. D. Richardson, and D. Attwell. 2012. 'Properties and fate of oligodendrocyte progenitor cells in the corpus callosum, motor cortex, and piriform cortex of the mouse', *J Neurosci*, 32: 8173-85.
- Cohen, R. I., R. Marmur, W. T. Norton, M. F. Mehler, and J. A. Kessler. 1996. 'Nerve growth factor and neurotrophin-3 differentially regulate the proliferation and survival of developing rat brain oligodendrocytes', *J Neurosci*, 16: 6433-42.
- Coleman, M. A., T. Garland, Jr., C. A. Marler, S. S. Newton, J. G. Swallow, and P. A. Carter. 1998. 'Glucocorticoid response to forced exercise in laboratory house mice (*Mus domesticus*)', *Physiol Behav*, 63: 279-85.
- Colman, D. R., G. Kreibich, A. B. Frey, and D. D. Sabatini. 1982. 'Synthesis and incorporation of myelin polypeptides into CNS myelin', *J Cell Biol*, 95: 598-608.
- Corkrum, M., A. Covelo, J. Lines, L. Bellocchio, M. Pisansky, K. Loke, R. Quintana, P. E. Rothwell, R. Lujan, G. Marsicano, E. D. Martin, M. J. Thomas, P. Kofuji, and A. Araque. 2020. 'Dopamine-Evoked Synaptic Regulation in the Nucleus Accumbens Requires Astrocyte Activity', *Neuron*.
- Cunningham, C., O' Sullivan R, P. Caserotti, and M. A. Tully. 2020. 'Consequences of physical inactivity in older adults: A systematic review of reviews and meta-analyses', *Scand J Med Sci Sports*.
- Czopka, T., C. Ffrench-Constant, and D. A. Lyons. 2013. 'Individual oligodendrocytes have only a few hours in which to generate new myelin sheaths in vivo', *Dev Cell*, 25: 599-609.
- Davalos, D., J. Grutzendler, G. Yang, J. V. Kim, Y. Zuo, S. Jung, D. R. Littman, M. L. Dustin, and W. B. Gan. 2005. 'ATP mediates rapid microglial response to local brain injury in vivo', *Nat Neurosci*, 8: 752-8.

References

- Davis, A. D., T. M. Weatherby, D. K. Hartline, and P. H. Lenz. 1999. 'Myelin-like sheaths in copepod axons', *Nature*, 398: 571.
- Dawson, M. R., A. Polito, J. M. Levine, and R. Reynolds. 2003. 'NG2-expressing glial progenitor cells: an abundant and widespread population of cycling cells in the adult rat CNS', *Mol Cell Neurosci*, 24: 476-88.
- De Angelis, F., A. Bernardo, V. Magnaghi, L. Minghetti, and A. M. Tata. 2012. 'Muscarinic receptor subtypes as potential targets to modulate oligodendrocyte progenitor survival, proliferation, and differentiation', *Dev Neurobiol*, 72: 713-28.
- De Biase, L. M., A. Nishiyama, and D. E. Bergles. 2010. 'Excitability and synaptic communication within the oligodendrocyte lineage', *J Neurosci*, 30: 3600-11.
- De Rubeis, S., P. M. Siper, A. Durkin, J. Weissman, F. Muratet, D. Halpern, M. D. P. Trelles, Y. Frank, R. Lozano, A. T. Wang, J. L. Holder, Jr., C. Betancur, J. D. Buxbaum, and A. Kolevzon. 2018. 'Delineation of the genetic and clinical spectrum of Phelan-McDermid syndrome caused by SHANK3 point mutations', *Mol Autism*, 9: 31.
- Demerens, C., B. Stankoff, M. Logak, P. Anglade, B. Allinquant, F. Couraud, B. Zalc, and C. Lubetzki. 1996. 'Induction of myelination in the central nervous system by electrical activity', *Proc Natl Acad Sci U S A*, 93: 9887-92.
- Di Bello, I. C., M. R. Dawson, J. M. Levine, and R. Reynolds. 1999. 'Generation of oligodendroglial progenitors in acute inflammatory demyelinating lesions of the rat brain stem is associated with demyelination rather than inflammation', *J Neurocytol*, 28: 365-81.
- Diederich, K., A. Bastl, H. Wersching, A. Teuber, J. K. Strecker, A. Schmidt, J. Minnerup, and W. R. Schabitz. 2017. 'Effects of Different Exercise Strategies and Intensities on Memory Performance and Neurogenesis', *Front Behav Neurosci*, 11: 47.
- Dimas, P., L. Montani, J. A. Pereira, D. Moreno, M. Trotsmuller, J. Gerber, C. F. Semenkovich, H. C. Kofeler, and U. Suter. 2019. 'CNS myelination and remyelination depend on fatty acid synthesis by oligodendrocytes', *Elife*, 8.
- Dimou, L., and V. Gallo. 2015. 'NG2-glia and their functions in the central nervous system', *Glia*, 63: 1429-51.
- Dimou, L., and M. Gotz. 2014. 'Glial cells as progenitors and stem cells: new roles in the healthy and diseased brain', *Physiol Rev*, 94: 709-37.
- Dimou, L., C. Simon, F. Kirchhoff, H. Takebayashi, and M. Gotz. 2008. 'Progeny of Olig2-expressing progenitors in the gray and white matter of the adult mouse cerebral cortex', *J Neurosci*, 28: 10434-42.
- Djalali, S., M. Holtje, G. Grosse, T. Rothe, T. Stroh, J. Grosse, D. R. Deng, R. Hellweg, R. Grantyn, H. Hortnagl, and G. Ahnert-Hilger. 2005. 'Effects of brain-derived neurotrophic factor (BDNF) on glial cells and serotonergic neurones during development', *J Neurochem*, 92: 616-27.
- Doerr, A. 2013. 'Mass spectrometry-based targeted proteomics', *Nat Methods*, 10: 23.
- Donat, C. K., G. Scott, S. M. Gentleman, and M. Sastre. 2017. 'Microglial Activation in Traumatic Brain Injury', *Front Aging Neurosci*, 9: 208.
- Dringen, R., R. Gebhardt, and B. Hamprecht. 1993. 'Glycogen in astrocytes: possible function as lactate supply for neighboring cells', *Brain Res*, 623: 208-14.
- Du, Y., T. Z. Fischer, L. N. Lee, L. D. Lercher, and C. F. Dreyfus. 2003. 'Regionally specific effects of BDNF on oligodendrocytes', *Dev Neurosci*, 25: 116-26.

References

- Duncan, I. D., A. B. Radcliff, M. Heidari, G. Kidd, B. K. August, and L. A. Wierenga. 2018. 'The adult oligodendrocyte can participate in remyelination', *Proc Natl Acad Sci U S A*, 115: E11807-E16.
- Durand, C. M., C. Betancur, T. M. Boeckers, J. Bockmann, P. Chaste, F. Fauchereau, G. Nygren, M. Rastam, I. C. Gillberg, H. Anckarsater, E. Sponheim, H. Goubran-Botros, R. Delorme, N. Chabane, M. C. Mouren-Simeoni, P. de Mas, E. Bieth, B. Roge, D. Heron, L. Burglen, C. Gillberg, M. Leboyer, and T. Bourgeron. 2007. 'Mutations in the gene encoding the synaptic scaffolding protein SHANK3 are associated with autism spectrum disorders', *Nat Genet*, 39: 25-7.
- Dzamba, D., P. Honsa, and M. Anderova. 2013. 'NMDA Receptors in Glial Cells: Pending Questions', *Curr Neuropharmacol*, 11: 250-62.
- Ehninger, D., L. P. Wang, F. Klempin, B. Romer, H. Kettenmann, and G. Kempermann. 2011. 'Enriched environment and physical activity reduce microglia and influence the fate of NG2 cells in the amygdala of adult mice', *Cell Tissue Res*, 345: 69-86.
- El-Husseini, A. E., E. Schnell, D. M. Chetkovich, R. A. Nicoll, and D. S. Bredt. 2000. 'PSD-95 involvement in maturation of excitatory synapses', *Science*, 290: 1364-8.
- Emsley, J. G., and J. D. Macklis. 2006. 'Astroglial heterogeneity closely reflects the neuronal-defined anatomy of the adult murine CNS', *Neuron Glia Biol*, 2: 175-86.
- Ennaceur, A. 2010. 'One-trial object recognition in rats and mice: methodological and theoretical issues', *Behav Brain Res*, 215: 244-54.
- Ero, C., M. O. Gewaltig, D. Keller, and H. Markram. 2018. 'A Cell Atlas for the Mouse Brain', *Front Neuroinform*, 12: 84.
- Eugenin-von Bernhardt, J., and L. Dimou. 2016. 'NG2-glia, More Than Progenitor Cells', *Adv Exp Med Biol*, 949: 27-45.
- Falcao, A. M., D. van Bruggen, S. Marques, M. Meijer, S. Jakel, E. Agirre, Samudyata, E. M. Floriddia, D. P. Vanichkina, C. Ffrench-Constant, A. Williams, A. O. Guerreiro-Cacais, and G. Castelo-Branco. 2018. 'Disease-specific oligodendrocyte lineage cells arise in multiple sclerosis', *Nat Med*, 24: 1837-44.
- Fard, M. K., F. van der Meer, P. Sanchez, L. Cantuti-Castelvetri, S. Mandad, S. Jakel, E. F. Fornasiero, S. Schmitt, M. Ehrlich, L. Starost, T. Kuhlmann, C. Sergiou, V. Schultz, C. Wrzos, W. Bruck, H. Urlaub, L. Dimou, C. Stadelmann, and M. Simons. 2017. 'BCAS1 expression defines a population of early myelinating oligodendrocytes in multiple sclerosis lesions', *Sci Transl Med*, 9.
- Faulkner, J. R., J. E. Herrmann, M. J. Woo, K. E. Tansey, N. B. Doan, and M. V. Sofroniew. 2004. 'Reactive astrocytes protect tissue and preserve function after spinal cord injury', *J Neurosci*, 24: 2143-55.
- Fiacco, T. A., and K. D. McCarthy. 2004. 'Intracellular astrocyte calcium waves in situ increase the frequency of spontaneous AMPA receptor currents in CA1 pyramidal neurons', *J Neurosci*, 24: 722-32.
- Fletcher, J. L., S. S. Murray, and J. Xiao. 2018. 'Brain-Derived Neurotrophic Factor in Central Nervous System Myelination: A New Mechanism to Promote Myelin Plasticity and Repair', *Int J Mol Sci*, 19.

References

- Fontainhas, A. M., M. Wang, K. J. Liang, S. Chen, P. Mettu, M. Damani, R. N. Fariss, W. Li, and W. T. Wong. 2011. 'Microglial morphology and dynamic behavior is regulated by ionotropic glutamatergic and GABAergic neurotransmission', *PLoS One*, 6: e15973.
- Ford, M. C., O. Alexandrova, L. Cossell, A. Stange-Marten, J. Sinclair, C. Kopp-Scheinflug, M. Pecka, D. Attwell, and B. Grothe. 2015. 'Tuning of Ranvier node and internode properties in myelinated axons to adjust action potential timing', *Nat Commun*, 6: 8073.
- Franklin, R. J., and C. Ffrench-Constant. 2008. 'Remyelination in the CNS: from biology to therapy', *Nat Rev Neurosci*, 9: 839-55.
- Funfschilling, U., L. M. Supplie, D. Mahad, S. Boretius, A. S. Saab, J. Edgar, B. G. Brinkmann, C. M. Kassmann, I. D. Tzvetanova, W. Mobius, F. Diaz, D. Meijer, U. Suter, B. Hamprecht, M. W. Sereda, C. T. Moraes, J. Frahm, S. Goebbels, and K. A. Nave. 2012. 'Glycolytic oligodendrocytes maintain myelin and long-term axonal integrity', *Nature*, 485: 517-21.
- Gage, F. H., P. Olejniczak, and D. M. Armstrong. 1988. 'Astrocytes are important for sprouting in the septohippocampal circuit', *Exp Neurol*, 102: 2-13.
- Garay, L., V. Tungler, M. C. Deniselle, A. Lima, P. Roig, and A. F. De Nicola. 2011. 'Progesterone attenuates demyelination and microglial reaction in the lysolecithin-injured spinal cord', *Neuroscience*, 192: 588-97.
- Garde, E., E. L. Mortensen, K. Krabbe, E. Rostrup, and H. B. Larsson. 2000. 'Relation between age-related decline in intelligence and cerebral white-matter hyperintensities in healthy octogenarians: a longitudinal study', *Lancet*, 356: 628-34.
- Gary, D. S., M. Malone, P. Capestany, T. Houdayer, and J. W. McDonald. 2012. 'Electrical stimulation promotes the survival of oligodendrocytes in mixed cortical cultures', *J Neurosci Res*, 90: 72-83.
- Gautier, H. O., K. A. Evans, K. Volbracht, R. James, S. Sitnikov, I. Lundgaard, F. James, C. Lao-Peregrin, R. Reynolds, R. J. Franklin, and R. T. Karadottir. 2015. 'Neuronal activity regulates remyelination via glutamate signalling to oligodendrocyte progenitors', *Nat Commun*, 6: 8518.
- Gazzaley, A., J. W. Cooney, J. Rissman, and M. D'Esposito. 2005. 'Top-down suppression deficit underlies working memory impairment in normal aging', *Nat Neurosci*, 8: 1298-300.
- Gemelli, T., O. Berton, E. D. Nelson, L. I. Perrotti, R. Jaenisch, and L. M. Monteggia. 2006. 'Postnatal loss of methyl-CpG binding protein 2 in the forebrain is sufficient to mediate behavioral aspects of Rett syndrome in mice', *Biol Psychiatry*, 59: 468-76.
- Gensert, J. M., and J. E. Goldman. 1997. 'Endogenous progenitors remyelinate demyelinated axons in the adult CNS', *Neuron*, 19: 197-203.
- Geraghty, A. C., E. M. Gibson, R. A. Ghanem, J. J. Greene, A. Ocampo, A. K. Goldstein, L. Ni, T. Yang, R. M. Marton, S. P. Pasca, M. E. Greenberg, F. M. Longo, and M. Monje. 2019. 'Loss of Adaptive Myelination Contributes to Methotrexate Chemotherapy-Related Cognitive Impairment', *Neuron*, 103: 250-65 e8.
- Ghazalpour, A., B. Bennett, V. A. Petyuk, L. Orozco, R. Hagopian, I. N. Mungrue, C. R. Farber, J. Sinsheimer, H. M. Kang, N. Furlotte, C. C. Park, P. Z. Wen, H. Brewer, K. Weitz, D. G. Camp, 2nd, C. Pan, R. Yordanova, I. Neuhaus, C. Tilford, N. Siemers, P. Gargalovic, E. Eskin, T. Kirchgesner, D. J. Smith, R. D. Smith, and A. J. Lusis. 2011. 'Comparative analysis of proteome and transcriptome variation in mouse', *PLoS Genet*, 7: e1001393.

References

- Gibson, E. M., D. Purger, C. W. Mount, A. K. Goldstein, G. L. Lin, L. S. Wood, I. Inema, S. E. Miller, G. Bieri, J. B. Zuchero, B. A. Barres, P. J. Woo, H. Vogel, and M. Monje. 2014. 'Neuronal activity promotes oligodendrogenesis and adaptive myelination in the mammalian brain', *Science*, 344: 1252304.
- Ginhoux, F., M. Greter, M. Leboeuf, S. Nandi, P. See, S. Gokhan, M. F. Mehler, S. J. Conway, L. G. Ng, E. R. Stanley, I. M. Samokhvalov, and M. Merad. 2010. 'Fate mapping analysis reveals that adult microglia derive from primitive macrophages', *Science*, 330: 841-5.
- Gong, S., C. Zheng, M. L. Doughty, K. Losos, N. Didkovsky, U. B. Schambra, N. J. Nowak, A. Joyner, G. Leblanc, M. E. Hatten, and N. Heintz. 2003. 'A gene expression atlas of the central nervous system based on bacterial artificial chromosomes', *Nature*, 425: 917-25.
- Gourine, A. V., V. Kasymov, N. Marina, F. Tang, M. F. Figueiredo, S. Lane, A. G. Teschemacher, K. M. Spyer, K. Deisseroth, and S. Kasparov. 2010. 'Astrocytes control breathing through pH-dependent release of ATP', *Science*, 329: 571-5.
- Green, A. J., J. M. Gelfand, B. A. Cree, C. Bevan, W. J. Boscardin, F. Mei, J. Inman, S. Arnow, M. Devereux, A. Abounasr, H. Nobuta, A. Zhu, M. Friessen, R. Gerona, H. C. von Budingen, R. G. Henry, S. L. Hauser, and J. R. Chan. 2017. 'Clemastine fumarate as a remyelinating therapy for multiple sclerosis (ReBUILD): a randomised, controlled, double-blind, crossover trial', *Lancet*, 390: 2481-89.
- Grier, M. D., K. L. West, N. D. Kelm, C. Fu, M. D. Does, B. Parker, E. McBrier, A. H. Lagrange, K. C. Ess, and R. P. Carson. 2017. 'Loss of mTORC2 signaling in oligodendrocyte precursor cells delays myelination', *PLoS One*, 12: e0188417.
- Guo, F., Y. Maeda, J. Ma, J. Xu, M. Horiuchi, L. Miers, F. Vaccarino, and D. Pleasure. 2010. 'Pyramidal neurons are generated from oligodendroglial progenitor cells in adult piriform cortex', *J Neurosci*, 30: 12036-49.
- Guttmann, C. R., F. A. Jolesz, R. Kikinis, R. J. Killiany, M. B. Moss, T. Sandor, and M. S. Albert. 1998. 'White matter changes with normal aging', *Neurology*, 50: 972-8.
- Haijima, A., and Y. Ichtani. 2012. 'Dissociable anterograde amnesic effects of retrosplenial cortex and hippocampal lesions on spontaneous object recognition memory in rats', *Hippocampus*, 22: 1868-75.
- Halassa, M. M., T. Fellin, H. Takano, J. H. Dong, and P. G. Haydon. 2007. 'Synaptic islands defined by the territory of a single astrocyte', *J Neurosci*, 27: 6473-7.
- Hallal, P. C., L. B. Andersen, F. C. Bull, R. Guthold, W. Haskell, U. Ekelund, and Group Lancet Physical Activity Series Working. 2012. 'Global physical activity levels: surveillance progress, pitfalls, and prospects', *Lancet*, 380: 247-57.
- Hamilton, N., S. Vayro, R. Wigley, and A. M. Butt. 2010. 'Axons and astrocytes release ATP and glutamate to evoke calcium signals in NG2-glia', *Glia*, 58: 66-79.
- Harder, D. R., C. Zhang, and D. Gebremedhin. 2002. 'Astrocytes function in matching blood flow to metabolic activity', *News Physiol Sci*, 17: 27-31.
- Harris, J. J., and D. Attwell. 2012. 'The energetics of CNS white matter', *J Neurosci*, 32: 356-71.
- Hartline, D. K., and D. R. Colman. 2007. 'Rapid conduction and the evolution of giant axons and myelinated fibers', *Curr Biol*, 17: R29-35.
- Heise, C., J. C. Schroeder, M. Schoen, S. Halbedl, D. Reim, S. Woelfle, M. R. Kreutz, M. J. Schmeisser, and T. M. Boeckers. 2016. 'Selective Localization of Shanks to VGLUT1-Positive Excitatory Synapses in the Mouse Hippocampus', *Front Cell Neurosci*, 10: 106.

References

- Hertz, L., and E. Hertz. 2003. 'Cataplerotic TCA cycle flux determined as glutamate-sustained oxygen consumption in primary cultures of astrocytes', *Neurochem Int*, 43: 355-61.
- Hertz, L., and H. R. Zielke. 2004. 'Astrocytic control of glutamatergic activity: astrocytes as stars of the show', *Trends Neurosci*, 27: 735-43.
- Hess, M. W., E. Kirschning, K. Pfaller, P. L. Debbage, H. Hohenberg, and G. Klima. 1998. '5000-year-old myelin: uniquely intact in molecular configuration and fine structure', *Curr Biol*, 8: R512-3.
- Heuser, J. E., and C. F. Doggenweiler. 1966. 'The fine structural organization of nerve fibers, sheaths, and glial cells in the prawn, *Palaemonetes vulgaris*', *J Cell Biol*, 30: 381-403.
- Heyn, P., B. C. Abreu, and K. J. Ottenbacher. 2004. 'The effects of exercise training on elderly persons with cognitive impairment and dementia: a meta-analysis', *Arch Phys Med Rehabil*, 85: 1694-704.
- Hill, R. A., A. M. Li, and J. Grutzendler. 2018. 'Lifelong cortical myelin plasticity and age-related degeneration in the live mammalian brain', *Nat Neurosci*, 21: 683-95.
- Hill, R. A., K. D. Patel, C. M. Goncalves, J. Grutzendler, and A. Nishiyama. 2014. 'Modulation of oligodendrocyte generation during a critical temporal window after NG2 cell division', *Nat Neurosci*, 17: 1518-27.
- Hill, R. A., K. D. Patel, J. Medved, A. M. Reiss, and A. Nishiyama. 2013. 'NG2 cells in white matter but not gray matter proliferate in response to PDGF', *J Neurosci*, 33: 14558-66.
- Hillman, C. H., K. I. Erickson, and A. F. Kramer. 2008. 'Be smart, exercise your heart: exercise effects on brain and cognition', *Nat Rev Neurosci*, 9: 58-65.
- Hines, J. H., A. M. Ravanelli, R. Schwandt, E. K. Scott, and B. Appel. 2015. 'Neuronal activity biases axon selection for myelination in vivo', *Nat Neurosci*, 18: 683-9.
- Hiura, M., T. Nariai, M. Sakata, A. Muta, K. Ishibashi, K. Wagatsuma, T. Tago, J. Toyohara, K. Ishii, and T. Maehara. 2018. 'Response of Cerebral Blood Flow and Blood Pressure to Dynamic Exercise: A Study Using PET', *Int J Sports Med*, 39: 181-88.
- Hoft, S., S. Griemsmann, G. Seifert, and C. Steinhauser. 2014. 'Heterogeneity in expression of functional ionotropic glutamate and GABA receptors in astrocytes across brain regions: insights from the thalamus', *Philos Trans R Soc Lond B Biol Sci*, 369: 20130602.
- Huang, W., Q. Guo, X. Bai, A. Scheller, and F. Kirchhoff. 2019. 'Early embryonic NG2 glia are exclusively gliogenic and do not generate neurons in the brain', *Glia*, 67: 1094-103.
- Huang, W., N. Zhao, X. Bai, K. Karam, J. Trotter, S. Goebbels, A. Scheller, and F. Kirchhoff. 2014. 'Novel NG2-CreERT2 knock-in mice demonstrate heterogeneous differentiation potential of NG2 glia during development', *Glia*, 62: 896-913.
- Hughes, E. G., S. H. Kang, M. Fukaya, and D. E. Bergles. 2013. 'Oligodendrocyte progenitors balance growth with self-repulsion to achieve homeostasis in the adult brain', *Nat Neurosci*, 16: 668-76.
- Hughes, E. G., J. L. Orthmann-Murphy, A. J. Langseth, and D. E. Bergles. 2018. 'Myelin remodeling through experience-dependent oligodendrogenesis in the adult somatosensory cortex', *Nat Neurosci*, 21: 696-706.
- Ishibashi, M., K. Egawa, and A. Fukuda. 2019. 'Diverse Actions of Astrocytes in GABAergic Signaling', *Int J Mol Sci*, 20.

References

- Jakel, S., E. Agirre, A. Mendanha Falcao, D. van Bruggen, K. W. Lee, I. Knuesel, D. Malhotra, C. Ffrench-Constant, A. Williams, and G. Castelo-Branco. 2019. 'Altered human oligodendrocyte heterogeneity in multiple sclerosis', *Nature*, 566: 543-47.
- Janzer, R. C., and M. C. Raff. 1987. 'Astrocytes induce blood-brain barrier properties in endothelial cells', *Nature*, 325: 253-7.
- Jensen, S. K., N. J. Michaels, S. Ilyntskyy, M. B. Keough, O. Kovalchuk, and V. W. Yong. 2018. 'Multimodal Enhancement of Remyelination by Exercise with a Pivotal Role for Oligodendroglial PGC1alpha', *Cell Rep*, 24: 3167-79.
- Jeong, M., Y. Kim, J. Kim, D. D. Ferrante, P. P. Mitra, P. Osten, and D. Kim. 2016. 'Comparative three-dimensional connectome map of motor cortical projections in the mouse brain', *Sci Rep*, 6: 20072.
- Jessberger, S., R. E. Clark, N. J. Broadbent, G. D. Clemenson, Jr., A. Consiglio, D. C. Lie, L. R. Squire, and F. H. Gage. 2009. 'Dentate gyrus-specific knockdown of adult neurogenesis impairs spatial and object recognition memory in adult rats', *Learn Mem*, 16: 147-54.
- Jesse, S., H. P. Muller, M. Schoen, H. Asoglu, J. Bockmann, H. J. Huppertz, V. Rasche, A. C. Ludolph, T. M. Boeckers, and J. Kassubek. 2020. 'Severe white matter damage in SHANK3 deficiency: a human and translational study', *Ann Clin Transl Neurol*, 7: 46-58.
- Ji, J. F., S. J. Ji, R. Sun, K. Li, Y. Zhang, L. Y. Zhang, and Y. Tian. 2014. 'Forced running exercise attenuates hippocampal neurogenesis impairment and the neurocognitive deficits induced by whole-brain irradiation via the BDNF-mediated pathway', *Biochem Biophys Res Commun*, 443: 646-51.
- Kang, J., L. Jiang, S. A. Goldman, and M. Nedergaard. 1998. 'Astrocyte-mediated potentiation of inhibitory synaptic transmission', *Nat Neurosci*, 1: 683-92.
- Kang, S. H., M. Fukaya, J. K. Yang, J. D. Rothstein, and D. E. Bergles. 2010. 'NG2+ CNS glial progenitors remain committed to the oligodendrocyte lineage in postnatal life and following neurodegeneration', *Neuron*, 68: 668-81.
- Kang, S. H., Y. Li, M. Fukaya, I. Lorenzini, D. W. Cleveland, L. W. Ostrow, J. D. Rothstein, and D. E. Bergles. 2013. 'Degeneration and impaired regeneration of gray matter oligodendrocytes in amyotrophic lateral sclerosis', *Nat Neurosci*, 16: 571-9.
- Karadottir, R., N. B. Hamilton, Y. Bakiri, and D. Attwell. 2008. 'Spiking and nonspiking classes of oligodendrocyte precursor glia in CNS white matter', *Nat Neurosci*, 11: 450-6.
- Kato, D., H. Wake, P. R. Lee, Y. Tachibana, R. Ono, S. Sugio, Y. Tsuji, Y. H. Tanaka, Y. R. Tanaka, Y. Masamizu, R. Hira, A. J. Moorhouse, N. Tamamaki, K. Ikenaka, N. Matsukawa, R. D. Fields, J. Nabekura, and M. Matsuzaki. 2020. 'Motor learning requires myelination to reduce asynchrony and spontaneity in neural activity', *Glia*, 68: 193-210.
- Keirstead, H. S., J. M. Levine, and W. F. Blakemore. 1998. 'Response of the oligodendrocyte progenitor cell population (defined by NG2 labelling) to demyelination of the adult spinal cord', *Glia*, 22: 161-70.
- Kempermann, G., D. Gast, G. Kronenberg, M. Yamaguchi, and F. H. Gage. 2003. 'Early determination and long-term persistence of adult-generated new neurons in the hippocampus of mice', *Development*, 130: 391-9.
- Kempermann, G., H. G. Kuhn, and F. H. Gage. 1997. 'More hippocampal neurons in adult mice living in an enriched environment', *Nature*, 386: 493-5.

References

- Kessaris, N., M. Fogarty, P. Iannarelli, M. Grist, M. Wegner, and W. D. Richardson. 2006. 'Competing waves of oligodendrocytes in the forebrain and postnatal elimination of an embryonic lineage', *Nat Neurosci*, 9: 173-9.
- Kettenmann, H., F. Kirchhoff, and A. Verkhratsky. 2013. 'Microglia: new roles for the synaptic stripper', *Neuron*, 77: 10-8.
- Kirby, B. B., N. Takada, A. J. Latimer, J. Shin, T. J. Carney, R. N. Kelsh, and B. Appel. 2006. 'In vivo time-lapse imaging shows dynamic oligodendrocyte progenitor behavior during zebrafish development', *Nat Neurosci*, 9: 1506-11.
- Klugmann, M., M. H. Schwab, A. Puhlhofer, A. Schneider, F. Zimmermann, I. R. Griffiths, and K. A. Nave. 1997. 'Assembly of CNS myelin in the absence of proteolipid protein', *Neuron*, 18: 59-70.
- Knoth, R., I. Singec, M. Ditter, G. Pantazis, P. Capetian, R. P. Meyer, V. Horvat, B. Volk, and G. Kempermann. 2010. 'Murine features of neurogenesis in the human hippocampus across the lifespan from 0 to 100 years', *PLoS One*, 5: e8809.
- Komitova, M., D. R. Serwanski, Q. R. Lu, and A. Nishiyama. 2011. 'NG2 cells are not a major source of reactive astrocytes after neocortical stab wound injury', *Glia*, 59: 800-9.
- Kougioumtzidou, E., T. Shimizu, N. B. Hamilton, K. Tohyama, R. Sprengel, H. Monyer, D. Attwell, and W. D. Richardson. 2017. 'Signalling through AMPA receptors on oligodendrocyte precursors promotes myelination by enhancing oligodendrocyte survival', *Elife*, 6.
- Kreienkamp, H. J. 2008. 'Scaffolding proteins at the postsynaptic density: shank as the architectural framework', *Handb Exp Pharmacol*: 365-80.
- Kriegstein, A., and A. Alvarez-Buylla. 2009. 'The glial nature of embryonic and adult neural stem cells', *Annu Rev Neurosci*, 32: 149-84.
- Kuchler-Bopp, S., J. P. Delaunoy, J. C. Artault, M. Zaepfel, and J. B. Dietrich. 1999. 'Astrocytes induce several blood-brain barrier properties in non-neural endothelial cells', *Neuroreport*, 10: 1347-53.
- Kukley, M., E. Capetillo-Zarate, and D. Dietrich. 2007. 'Vesicular glutamate release from axons in white matter', *Nat Neurosci*, 10: 311-20.
- Kukley, M., M. Kiladze, R. Tognatta, M. Hans, D. Swandulla, J. Schramm, and D. Dietrich. 2008. 'Glial cells are born with synapses', *FASEB J*, 22: 2957-69.
- Kukley, M., A. Nishiyama, and D. Dietrich. 2010. 'The fate of synaptic input to NG2 glial cells: neurons specifically downregulate transmitter release onto differentiating oligodendroglial cells', *J Neurosci*, 30: 8320-31.
- Lappe-Siefke, C., S. Goebbels, M. Gravel, E. Nicksch, J. Lee, P. E. Braun, I. R. Griffiths, and K. A. Nave. 2003. 'Disruption of Cnp1 uncouples oligodendroglial functions in axonal support and myelination', *Nat Genet*, 33: 366-74.
- Larson, V. A., Y. Mironova, K. G. Vanderpool, A. Waisman, J. E. Rash, A. Agarwal, and D. E. Bergles. 2018. 'Oligodendrocytes control potassium accumulation in white matter and seizure susceptibility', *Elife*, 7.
- Lasiene, J., A. Matsui, Y. Sawa, F. Wong, and P. J. Horner. 2009. 'Age-related myelin dynamics revealed by increased oligodendrogenesis and short internodes', *Aging Cell*, 8: 201-13.
- Laughlin, S. B., and T. J. Sejnowski. 2003. 'Communication in neuronal networks', *Science*, 301: 1870-4.

References

- Lawson, L. J., V. H. Perry, P. Dri, and S. Gordon. 1990. 'Heterogeneity in the distribution and morphology of microglia in the normal adult mouse brain', *Neuroscience*, 39: 151-70.
- Le Page, C., A. Ferry, and M. Rieu. 1994. 'Effect of muscular exercise on chronic relapsing experimental autoimmune encephalomyelitis', *J Appl Physiol (1985)*, 77: 2341-7.
- Lecca, D., M. L. Trincavelli, P. Gelosa, L. Sironi, P. Ciana, M. Fumagalli, G. Villa, C. Verderio, C. Grumelli, U. Guerrini, E. Tremoli, P. Rosa, S. Cuboni, C. Martini, A. Buffo, M. Cimino, and M. P. Abbracchio. 2008. 'The recently identified P2Y-like receptor GPR17 is a sensor of brain damage and a new target for brain repair', *PLoS One*, 3: e3579.
- Lee, S., M. K. Leach, S. A. Redmond, S. Y. Chong, S. H. Mellon, S. J. Tuck, Z. Q. Feng, J. M. Corey, and J. R. Chan. 2012. 'A culture system to study oligodendrocyte myelination processes using engineered nanofibers', *Nat Methods*, 9: 917-22.
- Lee, Y., B. M. Morrison, Y. Li, S. Lengacher, M. H. Farah, P. N. Hoffman, Y. Liu, A. Tsingalia, L. Jin, P. W. Zhang, L. Pellerin, P. J. Magistretti, and J. D. Rothstein. 2012. 'Oligodendroglia metabolically support axons and contribute to neurodegeneration', *Nature*, 487: 443-8.
- Leger, M., A. Quiedeville, V. Bouet, B. Haelewyn, M. Boulouard, P. Schumann-Bard, and T. Freret. 2013. 'Object recognition test in mice', *Nat Protoc*, 8: 2531-7.
- Li, Q., M. Brus-Ramer, J. H. Martin, and J. W. McDonald. 2010. 'Electrical stimulation of the medullary pyramid promotes proliferation and differentiation of oligodendrocyte progenitor cells in the corticospinal tract of the adult rat', *Neurosci Lett*, 479: 128-33.
- Li, W., Y. Tang, Z. Fan, Y. Meng, G. Yang, J. Luo, and Z. J. Ke. 2013. 'Autophagy is involved in oligodendroglial precursor-mediated clearance of amyloid peptide', *Mol Neurodegener*, 8: 27.
- Liu, J., K. Dietz, J. M. DeLoyht, X. Pedre, D. Kelkar, J. Kaur, V. Vialou, M. K. Lobo, D. M. Dietz, E. J. Nestler, J. Dupree, and P. Casaccia. 2012. 'Impaired adult myelination in the prefrontal cortex of socially isolated mice', *Nat Neurosci*, 15: 1621-3.
- Luchkina, N. V., and V. Y. Bolshakov. 2019. 'Mechanisms of fear learning and extinction: synaptic plasticity-fear memory connection', *Psychopharmacology (Berl)*, 236: 163-82.
- Lundgaard, I., A. Luzhynskaya, J. H. Stockley, Z. Wang, K. A. Evans, M. Swire, K. Volbracht, H. O. Gautier, R. J. Franklin, Ffrench-Constant Charles, D. Attwell, and R. T. Karadottir. 2013. 'Neuregulin and BDNF induce a switch to NMDA receptor-dependent myelination by oligodendrocytes', *PLoS Biol*, 11: e1001743.
- Luo, Y., Q. Xiao, J. Wang, L. Jiang, M. Hu, Y. Jiang, J. Tang, X. Liang, Y. Qi, X. Dou, Y. Zhang, C. Huang, L. Chen, and Y. Tang. 2019. 'Running exercise protects oligodendrocytes in the medial prefrontal cortex in chronic unpredictable stress rat model', *Transl Psychiatry*, 9: 322.
- Makinodan, M., K. M. Rosen, S. Ito, and G. Corfas. 2012. 'A critical period for social experience-dependent oligodendrocyte maturation and myelination', *Science*, 337: 1357-60.
- Mandolesi, G., S. Bullitta, D. Fresegna, F. De Vito, F. R. Rizzo, A. Musella, L. Guadalupi, V. Vanni, M. Stampanoni Bassi, F. Buttari, M. T. Viscomi, D. Centonze, and A. Gentile. 2019. 'Voluntary running wheel attenuates motor deterioration and brain damage in cuprizone-induced demyelination', *Neurobiol Dis*, 129: 102-17.
- Mandyam, C. D., S. Wee, A. J. Eisch, H. N. Richardson, and G. F. Koob. 2007. 'Methamphetamine self-administration and voluntary exercise have opposing effects on medial prefrontal cortex gliogenesis', *J Neurosci*, 27: 11442-50.

References

- Mangin, J. M., P. Li, J. Scafidi, and V. Gallo. 2012. 'Experience-dependent regulation of NG2 progenitors in the developing barrel cortex', *Nat Neurosci*, 15: 1192-4.
- Marisca, R., T. Hoche, E. Agirre, L. J. Hoodless, W. Barkey, F. Auer, G. Castelo-Branco, and T. Czopka. 2020. 'Functionally distinct subgroups of oligodendrocyte precursor cells integrate neural activity and execute myelin formation', *Nat Neurosci*, 23: 363-74.
- Marques, S., A. Zeisel, S. Codeluppi, D. van Bruggen, A. Mendanha Falcao, L. Xiao, H. Li, M. Haring, H. Hochgerner, R. A. Romanov, D. Gyllborg, A. Munoz Machado, G. La Manno, P. Lonnerberg, E. M. Floriddia, F. Rezayee, P. Ernfors, E. Arenas, J. Hjerling-Leffler, T. Harkany, W. D. Richardson, S. Linnarsson, and G. Castelo-Branco. 2016. 'Oligodendrocyte heterogeneity in the mouse juvenile and adult central nervous system', *Science*, 352: 1326-29.
- Marrs, G. S., S. H. Green, and M. E. Dailey. 2001. 'Rapid formation and remodeling of postsynaptic densities in developing dendrites', *Nat Neurosci*, 4: 1006-13.
- Mason, B. L., C. M. Pariante, S. Jamel, and S. A. Thomas. 2010. 'Central nervous system (CNS) delivery of glucocorticoids is fine-tuned by saturable transporters at the blood-CNS barriers and nonbarrier regions', *Endocrinology*, 151: 5294-305.
- Matsusue, Y., N. Horii-Hayashi, T. Kirita, and M. Nishi. 2014. 'Distribution of corticosteroid receptors in mature oligodendrocytes and oligodendrocyte progenitors of the adult mouse brain', *J Histochem Cytochem*, 62: 211-26.
- Mattson, M. P., S. Maudsley, and B. Martin. 2004. 'BDNF and 5-HT: a dynamic duo in age-related neuronal plasticity and neurodegenerative disorders', *Trends Neurosci*, 27: 589-94.
- Matyash, V., and H. Kettenmann. 2010. 'Heterogeneity in astrocyte morphology and physiology', *Brain Res Rev*, 63: 2-10.
- McKenzie, I. A., D. Ohayon, H. Li, J. P. de Faria, B. Emery, K. Tohyama, and W. D. Richardson. 2014. 'Motor skill learning requires active central myelination', *Science*, 346: 318-22.
- Mensch, S., M. Baraban, R. Almeida, T. Czopka, J. Ausborn, A. El Manira, and D. A. Lyons. 2015. 'Synaptic vesicle release regulates myelin sheath number of individual oligodendrocytes in vivo', *Nat Neurosci*, 18: 628-30.
- Micheva, K. D., D. Wolman, B. D. Mensch, E. Pax, J. Buchanan, S. J. Smith, and D. D. Bock. 2016. 'A large fraction of neocortical myelin ensheathes axons of local inhibitory neurons', *Elife*, 5.
- Miller, R. H. 1996. 'Oligodendrocyte origins', *Trends Neurosci*, 19: 92-6.
- Mitew, S., I. Gobius, L. R. Fenlon, S. J. McDougall, D. Hawkes, Y. L. Xing, H. Bujalka, A. L. Gundlach, L. J. Richards, T. J. Kilpatrick, T. D. Merson, and B. Emery. 2018. 'Pharmacogenetic stimulation of neuronal activity increases myelination in an axon-specific manner', *Nat Commun*, 9: 306.
- Monteiro, P., and G. Feng. 2017. 'SHANK proteins: roles at the synapse and in autism spectrum disorder', *Nat Rev Neurosci*, 18: 147-57.
- Motl, R. W., B. M. Sandroff, G. Kwakkel, U. Dalgas, A. Feinstein, C. Heesen, P. Feys, and A. J. Thompson. 2017. 'Exercise in patients with multiple sclerosis', *Lancet Neurol*, 16: 848-56.
- Nagai, J., A. K. Rajbhandari, M. R. Gangwani, A. Hachisuka, G. Coppola, S. C. Masmanidis, M. S. Fanselow, and B. S. Khakh. 2019. 'Hyperactivity with Disrupted Attention by Activation of an Astrocyte Synaptogenic Cue', *Cell*, 177: 1280-92 e20.

References

- Naghizadeh, M., R. Ranjbar, M. R. Tabandeh, and A. Habibi. 2018. 'Effects of Two Training Programs on Transcriptional Levels of Neurotrophins and Glial Cells Population in Hippocampus of Experimental Multiple Sclerosis', *Int J Sports Med*, 39: 604-12.
- Naisbitt, S., E. Kim, J. C. Tu, B. Xiao, C. Sala, J. Valtschanoff, R. J. Weinberg, P. F. Worley, and M. Sheng. 1999. 'Shank, a novel family of postsynaptic density proteins that binds to the NMDA receptor/PSD-95/GKAP complex and cortactin', *Neuron*, 23: 569-82.
- Nakamura, T., M. C. Colbert, and J. Robbins. 2006. 'Neural crest cells retain multipotential characteristics in the developing valves and label the cardiac conduction system', *Circ Res*, 98: 1547-54.
- Nave, K. A., and H. B. Werner. 2014. 'Myelination of the nervous system: mechanisms and functions', *Annu Rev Cell Dev Biol*, 30: 503-33.
- Neeper, S. A., F. Gomez-Pinilla, J. Choi, and C. Cotman. 1995. 'Exercise and brain neurotrophins', *Nature*, 373: 109.
- Nicholson, M., R. J. Wood, J. L. Fletcher, M. van den Buuse, S. S. Murray, and J. Xiao. 2018. 'BDNF haploinsufficiency exerts a transient and regionally different influence upon oligodendroglial lineage cells during postnatal development', *Mol Cell Neurosci*, 90: 12-21.
- Nimmerjahn, A., F. Kirchhoff, and F. Helmchen. 2005. 'Resting microglial cells are highly dynamic surveillants of brain parenchyma in vivo', *Science*, 308: 1314-8.
- Nishijima, T., Y. Kamidozono, A. Ishiizumi, S. Amemiya, and I. Kita. 2017. 'Negative rebound in hippocampal neurogenesis following exercise cessation', *Am J Physiol Regul Integr Comp Physiol*, 312: R347-R57.
- Nishiyama, A., R. Suzuki, and X. Zhu. 2014. 'NG2 cells (polydendrocytes) in brain physiology and repair', *Front Neurosci*, 8: 133.
- Norenberg, M. D., and A. Martinez-Hernandez. 1979. 'Fine structural localization of glutamine synthetase in astrocytes of rat brain', *Brain Res*, 161: 303-10.
- O'Leary, J. D., A. E. Hoban, A. Murphy, O. F. O'Leary, J. F. Cryan, and Y. M. Nolan. 2019. 'Differential effects of adolescent and adult-initiated exercise on cognition and hippocampal neurogenesis', *Hippocampus*, 29: 352-65.
- Obara, M., M. Szeliga, and J. Albrecht. 2008. 'Regulation of pH in the mammalian central nervous system under normal and pathological conditions: facts and hypotheses', *Neurochem Int*, 52: 905-19.
- Oberheim, N. A., T. Takano, X. Han, W. He, J. H. Lin, F. Wang, Q. Xu, J. D. Wyatt, W. Pilcher, J. G. Ojemann, B. R. Ransom, S. A. Goldman, and M. Nedergaard. 2009. 'Uniquely hominid features of adult human astrocytes', *J Neurosci*, 29: 3276-87.
- Occhipinti, R., E. Somersalo, and D. Calvetti. 2009. 'Astrocytes as the glucose shunt for glutamatergic neurons at high activity: an in silico study', *J Neurophysiol*, 101: 2528-38.
- Ogata, K., and T. Kosaka. 2002. 'Structural and quantitative analysis of astrocytes in the mouse hippocampus', *Neuroscience*, 113: 221-33.
- Olson, A. K., B. D. Eadie, C. Ernst, and B. R. Christie. 2006. 'Environmental enrichment and voluntary exercise massively increase neurogenesis in the adult hippocampus via dissociable pathways', *Hippocampus*, 16: 250-60.

References

- Ozerdem, U., K. A. Grako, K. Dahlin-Huppe, E. Monosov, and W. B. Stallcup. 2001. 'NG2 proteoglycan is expressed exclusively by mural cells during vascular morphogenesis', *Dev Dyn*, 222: 218-27.
- Pajevic, S., P. J. Basser, and R. D. Fields. 2014. 'Role of myelin plasticity in oscillations and synchrony of neuronal activity', *Neuroscience*, 276: 135-47.
- Pan, S., S. R. Mayoral, H. S. Choi, J. R. Chan, and M. A. Kheirbek. 2020. 'Preservation of a remote fear memory requires new myelin formation', *Nat Neurosci*.
- Paolicelli, R. C., G. Bolasco, F. Pagani, L. Maggi, M. Scianni, P. Panzanelli, M. Giustetto, T. A. Ferreira, E. Guiducci, L. Dumas, D. Ragozzino, and C. T. Gross. 2011. 'Synaptic pruning by microglia is necessary for normal brain development', *Science*, 333: 1456-8.
- Parkhurst, C. N., G. Yang, I. Ninan, J. N. Savas, J. R. Yates, 3rd, J. J. Lafaille, B. L. Hempstead, D. R. Littman, and W. B. Gan. 2013. 'Microglia promote learning-dependent synapse formation through brain-derived neurotrophic factor', *Cell*, 155: 1596-609.
- Parras, C. M., C. Hunt, M. Sugimori, M. Nakafuku, D. Rowitch, and F. Guillemot. 2007. 'The proneural gene Mash1 specifies an early population of telencephalic oligodendrocytes', *J Neurosci*, 27: 4233-42.
- Pelvig, D. P., H. Pakkenberg, A. K. Stark, and B. Pakkenberg. 2008. 'Neocortical glial cell numbers in human brains', *Neurobiol Aging*, 29: 1754-62.
- Perea, G., M. Navarrete, and A. Araque. 2009. 'Tripartite synapses: astrocytes process and control synaptic information', *Trends Neurosci*, 32: 421-31.
- Perez, E. C., D. R. Bravo, S. P. Rodgers, A. R. Khan, and J. L. Leasure. 2019. 'Shaping the adult brain with exercise during development: Emerging evidence and knowledge gaps', *Int J Dev Neurosci*.
- Peters, A. 1996. 'Age-related changes in oligodendrocytes in monkey cerebral cortex', *J Comp Neurol*, 371: 153-63.
- Peters, A., D. L. Rosene, M. B. Moss, T. L. Kemper, C. R. Abraham, J. Tigges, and M. S. Albert. 1996. 'Neurobiological bases of age-related cognitive decline in the rhesus monkey', *J Neuropathol Exp Neurol*, 55: 861-74.
- Pfeffer, C. K., M. Xue, M. He, Z. J. Huang, and M. Scanziani. 2013. 'Inhibition of inhibition in visual cortex: the logic of connections between molecularly distinct interneurons', *Nat Neurosci*, 16: 1068-76.
- Pfeiffer, S. E., A. E. Warrington, and R. Bansal. 1993. 'The oligodendrocyte and its many cellular processes', *Trends Cell Biol*, 3: 191-7.
- Powell, E. M., and H. M. Geller. 1999. 'Dissection of astrocyte-mediated cues in neuronal guidance and process extension', *Glia*, 26: 73-83.
- Psachoulia, K., F. Jamen, K. M. Young, and W. D. Richardson. 2009. 'Cell cycle dynamics of NG2 cells in the postnatal and ageing brain', *Neuron Glia Biol*, 5: 57-67.
- Raff, M. C., R. H. Miller, and M. Noble. 1983. 'A glial progenitor cell that develops in vitro into an astrocyte or an oligodendrocyte depending on culture medium', *Nature*, 303: 390-6.
- Rasmussen, P., P. Brassard, H. Adser, M. V. Pedersen, L. Leick, E. Hart, N. H. Secher, B. K. Pedersen, and H. Pilegaard. 2009. 'Evidence for a release of brain-derived neurotrophic factor from the brain during exercise', *Exp Physiol*, 94: 1062-9.

References

- Rivers, L. E., K. M. Young, M. Rizzi, F. Jamen, K. Psachoulia, A. Wade, N. Kessarar, and W. D. Richardson. 2008. 'PDGFRA/NG2 glia generate myelinating oligodendrocytes and piriform projection neurons in adult mice', *Nat Neurosci*, 11: 1392-401.
- Robins, S. C., E. Trudel, O. Rotondi, X. Liu, T. Djogo, D. Kryzskaya, C. W. Bourque, and M. V. Kokoeva. 2013. 'Evidence for NG2-glia derived, adult-born functional neurons in the hypothalamus', *PLoS One*, 8: e78236.
- Robison, L. S., D. L. Popescu, M. E. Anderson, S. I. Beigelman, S. M. Fitzgerald, A. E. Kuzmina, D. A. Lituma, S. Subzwari, M. Michaelos, B. J. Anderson, W. E. Van Nostrand, and J. K. Robinson. 2018. 'The effects of volume versus intensity of long-term voluntary exercise on physiology and behavior in C57/Bl6 mice', *Physiol Behav*, 194: 218-32.
- Rodriguez-Ayllon, M., C. Cadenas-Sanchez, F. Estevez-Lopez, N. E. Munoz, J. Mora-Gonzalez, J. H. Migueles, P. Molina-Garcia, H. Henriksson, A. Mena-Molina, V. Martinez-Vizcaino, A. Catena, M. Lof, K. I. Erickson, D. R. Lubans, F. B. Ortega, and I. Esteban-Cornejo. 2019. 'Role of Physical Activity and Sedentary Behavior in the Mental Health of Preschoolers, Children and Adolescents: A Systematic Review and Meta-Analysis', *Sports Med*, 49: 1383-410.
- Rosenberg, S. S., B. L. Powell, and J. R. Chan. 2007. 'Receiving mixed signals: uncoupling oligodendrocyte differentiation and myelination', *Cell Mol Life Sci*, 64: 3059-68.
- Rothstein, J. D., M. Dykes-Hoberg, C. A. Pardo, L. A. Bristol, L. Jin, R. W. Kuncl, Y. Kanai, M. A. Hediger, Y. Wang, J. P. Schielke, and D. F. Welty. 1996. 'Knockout of glutamate transporters reveals a major role for astroglial transport in excitotoxicity and clearance of glutamate', *Neuron*, 16: 675-86.
- Sakry, D., K. Karram, and J. Trotter. 2011. 'Synapses between NG2 glia and neurons', *J Anat*, 219: 2-7.
- Salter, M. W., and B. Stevens. 2017. 'Microglia emerge as central players in brain disease', *Nat Med*, 23: 1018-27.
- Salzer, J. L., and B. Zalc. 2016. 'Myelination', *Curr Biol*, 26: R971-R75.
- Sanz, E., L. Yang, T. Su, D. R. Morris, G. S. McKnight, and P. S. Amieux. 2009. 'Cell-type-specific isolation of ribosome-associated mRNA from complex tissues', *Proc Natl Acad Sci U S A*, 106: 13939-44.
- Saxe, M. D., F. Battaglia, J. W. Wang, G. Malleret, D. J. David, J. E. Monckton, A. D. Garcia, M. V. Sofroniew, E. R. Kandel, L. Santarelli, R. Hen, and M. R. Drew. 2006. 'Ablation of hippocampal neurogenesis impairs contextual fear conditioning and synaptic plasticity in the dentate gyrus', *Proc Natl Acad Sci U S A*, 103: 17501-6.
- Schafer, D. P., E. K. Lehrman, A. G. Kautzman, R. Koyama, A. R. Mardinly, R. Yamasaki, R. M. Ransohoff, M. E. Greenberg, B. A. Barres, and B. Stevens. 2012. 'Microglia sculpt postnatal neural circuits in an activity and complement-dependent manner', *Neuron*, 74: 691-705.
- Schmeisser, M. J., E. Ey, S. Wegener, J. Bockmann, A. V. Stempel, A. Kuebler, A. L. Janssen, P. T. Udvardi, E. Shiban, C. Spilker, D. Balschun, B. V. Skryabin, St Dieck, K. H. Smalla, D. Montag, C. S. Leblond, P. Faure, N. Torquet, A. M. Le Sourd, R. Toro, A. M. Grabrucker, S. A. Shoichet, D. Schmitz, M. R. Kreutz, T. Bourgeron, E. D. Gundelfinger, and T. M. Boeckers. 2012. 'Autistic-like behaviours and hyperactivity in mice lacking ProSAP1/Shank2', *Nature*, 486: 256-60.

References

- Schneider, S., A. Gruart, S. Grade, Y. Zhang, S. Kroger, F. Kirchhoff, G. Eichele, J. M. Delgado Garcia, and L. Dimou. 2016. 'Decrease in newly generated oligodendrocytes leads to motor dysfunctions and changed myelin structures that can be rescued by transplanted cells', *Glia*, 64: 2201-18.
- Scholz, J., M. C. Klein, T. E. Behrens, and H. Johansen-Berg. 2009. 'Training induces changes in white-matter architecture', *Nat Neurosci*, 12: 1370-1.
- Segel, M., B. Neumann, M. F. E. Hill, I. P. Weber, C. Viscomi, C. Zhao, A. Young, C. C. Agle, A. J. Thompson, G. A. Gonzalez, A. Sharma, S. Holmqvist, D. H. Rowitch, K. Franze, R. J. M. Franklin, and K. J. Chalut. 2019. 'Niche stiffness underlies the ageing of central nervous system progenitor cells', *Nature*, 573: 130-34.
- Seidl, A. H. 2014. 'Regulation of conduction time along axons', *Neuroscience*, 276: 126-34.
- Seifert, G., K. Huttmann, D. K. Binder, C. Hartmann, A. Wyczynski, C. Neusch, and C. Steinhauser. 2009. 'Analysis of astroglial K⁺ channel expression in the developing hippocampus reveals a predominant role of the Kir4.1 subunit', *J Neurosci*, 29: 7474-88.
- Seifert, S., M. Pannell, W. Uckert, K. Farber, and H. Kettenmann. 2011. 'Transmitter- and hormone-activated Ca(2+) responses in adult microglia/brain macrophages in situ recorded after viral transduction of a recombinant Ca(2+) sensor', *Cell Calcium*, 49: 365-75.
- Sharma, K., S. Schmitt, C. G. Bergner, S. Tyanova, N. Kannaiyan, N. Manrique-Hoyos, K. Kongi, L. Cantuti, U. K. Hanisch, M. A. Philips, M. J. Rossner, M. Mann, and M. Simons. 2015. 'Cell type- and brain region-resolved mouse brain proteome', *Nat Neurosci*, 18: 1819-31.
- Shigetomi, E., D. N. Bowser, M. V. Sofroniew, and B. S. Khakh. 2008. 'Two forms of astrocyte calcium excitability have distinct effects on NMDA receptor-mediated slow inward currents in pyramidal neurons', *J Neurosci*, 28: 6659-63.
- Shimshak, D. R., J. Kim, M. R. Hubner, D. J. Spergel, F. Buchholz, E. Casanova, A. F. Stewart, P. H. Seeburg, and R. Sprengel. 2002. 'Codon-improved Cre recombinase (iCre) expression in the mouse', *Genesis*, 32: 19-26.
- Sierra, A., F. de Castro, J. Del Rio-Hortega, J. Rafael Iglesias-Rozas, M. Garrosa, and H. Kettenmann. 2016. 'The "Big-Bang" for modern glial biology: Translation and comments on Pio del Rio-Hortega 1919 series of papers on microglia', *Glia*, 64: 1801-40.
- Sierra, A., J. M. Encinas, J. J. Deudero, J. H. Chancey, G. Enikolopov, L. S. Overstreet-Wadiche, S. E. Tsirka, and M. Maletic-Savatic. 2010. 'Microglia shape adult hippocampal neurogenesis through apoptosis-coupled phagocytosis', *Cell Stem Cell*, 7: 483-95.
- Simard, M., and M. Nedergaard. 2004. 'The neurobiology of glia in the context of water and ion homeostasis', *Neuroscience*, 129: 877-96.
- Simon, C., M. Gotz, and L. Dimou. 2011. 'Progenitors in the adult cerebral cortex: cell cycle properties and regulation by physiological stimuli and injury', *Glia*, 59: 869-81.
- Simon, C., H. Lickert, M. Gotz, and L. Dimou. 2012. 'Sox10-iCreERT2 : a mouse line to inducibly trace the neural crest and oligodendrocyte lineage', *Genesis*, 50: 506-15.
- Simons, M., and K. A. Nave. 2015. 'Oligodendrocytes: Myelination and Axonal Support', *Cold Spring Harb Perspect Biol*, 8: a020479.
- Sirko, S., G. Behrendt, P. A. Johansson, P. Tripathi, M. Costa, S. Bek, C. Heinrich, S. Tiedt, D. Colak, M. Dichgans, I. R. Fischer, N. Plesnila, M. Staufienbiel, C. Haass, M. Snapyan, A. Saghatelian, L. H. Tsai, A. Fischer, K. Grobe, L. Dimou, and M. Gotz. 2013. 'Reactive glia in

References

- the injured brain acquire stem cell properties in response to sonic hedgehog. [corrected]', *Cell Stem Cell*, 12: 426-39.
- Snaidero, N., W. Mobius, T. Czopka, L. H. Hekking, C. Mathisen, D. Verkleij, S. Goebbels, J. Edgar, D. Merkler, D. A. Lyons, K. A. Nave, and M. Simons. 2014. 'Myelin membrane wrapping of CNS axons by PI(3,4,5)P3-dependent polarized growth at the inner tongue', *Cell*, 156: 277-90.
- Snaidero, N., and M. Simons. 2014. 'Myelination at a glance', *J Cell Sci*, 127: 2999-3004.
- Sofroniew, M. V., and H. V. Vinters. 2010. 'Astrocytes: biology and pathology', *Acta Neuropathol*, 119: 7-35.
- Sokoloff, L., M. Reivich, C. Kennedy, M. H. Des Rosiers, C. S. Patlak, K. D. Pettigrew, O. Sakurada, and M. Shinohara. 1977. 'The [14C]deoxyglucose method for the measurement of local cerebral glucose utilization: theory, procedure, and normal values in the conscious and anesthetized albino rat', *J Neurochem*, 28: 897-916.
- Song, H., C. F. Stevens, and F. H. Gage. 2002. 'Astroglia induce neurogenesis from adult neural stem cells', *Nature*, 417: 39-44.
- Song, W. M., and M. Colonna. 2018. 'The identity and function of microglia in neurodegeneration', *Nat Immunol*, 19: 1048-58.
- Soorya, L., A. Kolevzon, J. Zweifach, T. Lim, Y. Dobry, L. Schwartz, Y. Frank, A. T. Wang, G. Cai, E. Parkhomenko, D. Halpern, D. Grodberg, B. Angarita, J. P. Willner, A. Yang, R. Canitano, W. Chaplin, C. Betancur, and J. D. Buxbaum. 2013. 'Prospective investigation of autism and genotype-phenotype correlations in 22q13 deletion syndrome and SHANK3 deficiency', *Mol Autism*, 4: 18.
- Spiriduso, W. W. 1980. 'Physical fitness, aging, and psychomotor speed: a review', *J Gerontol*, 35: 850-65.
- Steadman, P. E., F. Xia, M. Ahmed, A. J. Mocle, A. R. A. Penning, A. C. Geraghty, H. W. Steenland, M. Monje, S. A. Josselyn, and P. W. Frankland. 2020. 'Disruption of Oligodendrogenesis Impairs Memory Consolidation in Adult Mice', *Neuron*, 105: 150-64 e6.
- Stedehouder, J., D. Brizee, G. Shpak, and S. A. Kushner. 2018. 'Activity-Dependent Myelination of Parvalbumin Interneurons Mediated by Axonal Morphological Plasticity', *J Neurosci*, 38: 3631-42.
- Stedehouder, J., D. Brizee, J. A. Slotman, M. Pascual-Garcia, M. L. Leyrer, B. L. Bouwen, C. M. Dirven, Z. Gao, D. M. Berson, A. B. Houtsmuller, and S. A. Kushner. 2019. 'Local axonal morphology guides the topography of interneuron myelination in mouse and human neocortex', *Elife*, 8.
- Stedehouder, J., J. J. Couey, D. Brizee, B. Hosseini, J. A. Slotman, C. M. F. Dirven, G. Shpak, A. B. Houtsmuller, and S. A. Kushner. 2017. 'Fast-spiking Parvalbumin Interneurons are Frequently Myelinated in the Cerebral Cortex of Mice and Humans', *Cereb Cortex*, 27: 5001-13.
- Stellwagen, D., and R. C. Malenka. 2006. 'Synaptic scaling mediated by glial TNF-alpha', *Nature*, 440: 1054-9.
- Stevens, B., S. Porta, L. L. Haak, V. Gallo, and R. D. Fields. 2002. 'Adenosine: a neuron-glia transmitter promoting myelination in the CNS in response to action potentials', *Neuron*, 36: 855-68.

References

- Sturrock, R. R. 1976. 'Changes in neurologia and myelination in the white matter of aging mice', *J Gerontol*, 31: 513-22.
- Sugar, J., M. P. Witter, N. M. van Strien, and N. L. Cappaert. 2011. 'The retrosplenial cortex: intrinsic connectivity and connections with the (para)hippocampal region in the rat. An interactive connectome', *Front Neuroinform*, 5: 7.
- Sun, W., A. Cornwell, J. Li, S. Peng, M. J. Osorio, N. Aalling, S. Wang, A. Benraiss, N. Lou, S. A. Goldman, and M. Nedergaard. 2017. 'SOX9 Is an Astrocyte-Specific Nuclear Marker in the Adult Brain Outside the Neurogenic Regions', *J Neurosci*, 37: 4493-507.
- Sung, B., G. Lim, and J. Mao. 2003. 'Altered expression and uptake activity of spinal glutamate transporters after nerve injury contribute to the pathogenesis of neuropathic pain in rats', *J Neurosci*, 23: 2899-910.
- Suzuki, A., S. A. Stern, O. Bozdagi, G. W. Huntley, R. H. Walker, P. J. Magistretti, and C. M. Alberini. 2011. 'Astrocyte-neuron lactate transport is required for long-term memory formation', *Cell*, 144: 810-23.
- Swanson, O. K., and A. Maffei. 2019. 'From Hiring to Firing: Activation of Inhibitory Neurons and Their Recruitment in Behavior', *Front Mol Neurosci*, 12: 168.
- Swiss, V. A., T. Nguyen, J. Dugas, A. Ibrahim, B. Barres, I. P. Androulakis, and P. Casaccia. 2011. 'Identification of a gene regulatory network necessary for the initiation of oligodendrocyte differentiation', *PLoS One*, 6: e18088.
- Szklarczyk, D., A. L. Gable, D. Lyon, A. Junge, S. Wyder, J. Huerta-Cepas, M. Simonovic, N. T. Doncheva, J. H. Morris, P. Bork, L. J. Jensen, and C. V. Mering. 2019. 'STRING v11: protein-protein association networks with increased coverage, supporting functional discovery in genome-wide experimental datasets', *Nucleic Acids Res*, 47: D607-D13.
- Tan, Z., Y. Liu, W. Xi, H. F. Lou, L. Zhu, Z. Guo, L. Mei, and S. Duan. 2017. 'Glia-derived ATP inversely regulates excitability of pyramidal and CCK-positive neurons', *Nat Commun*, 8: 13772.
- Tanaka, H., J. Ma, K. F. Tanaka, K. Takao, M. Komada, K. Tanda, A. Suzuki, T. Ishibashi, H. Baba, T. Isa, R. Shigemoto, K. Ono, T. Miyakawa, and K. Ikenaka. 2009. 'Mice with altered myelin proteolipid protein gene expression display cognitive deficits accompanied by abnormal neuron-glia interactions and decreased conduction velocities', *J Neurosci*, 29: 8363-71.
- Tanaka, K., K. Watase, T. Manabe, K. Yamada, M. Watanabe, K. Takahashi, H. Iwama, T. Nishikawa, N. Ichihara, T. Kikuchi, S. Okuyama, N. Kawashima, S. Hori, M. Takimoto, and K. Wada. 1997. 'Epilepsy and exacerbation of brain injury in mice lacking the glutamate transporter GLT-1', *Science*, 276: 1699-702.
- Tolhurst, D. J., and P. R. Lewis. 1992. 'Effect of myelination on the conduction velocity of optic nerve fibres', *Ophthalmic Physiol Opt*, 12: 241-3.
- Tomassy, G. S., D. R. Berger, H. H. Chen, N. Kasthuri, K. J. Hayworth, A. Vercelli, H. S. Seung, J. W. Lichtman, and P. Arlotta. 2014. 'Distinct profiles of myelin distribution along single axons of pyramidal neurons in the neocortex', *Science*, 344: 319-24.
- Tomlinson, L., P. H. Huang, and H. Colognato. 2018. 'Prefrontal cortex NG2 glia undergo a developmental switch in their responsiveness to exercise', *Dev Neurobiol*, 78: 687-700.
- Tomlinson, L., C. V. Leiton, and H. Colognato. 2016. 'Behavioral experiences as drivers of oligodendrocyte lineage dynamics and myelin plasticity', *Neuropharmacology*, 110: 548-62.

References

- Tremblay, M. E., R. L. Lowery, and A. K. Majewska. 2010. 'Microglial interactions with synapses are modulated by visual experience', *PLoS Biol*, 8: e1000527.
- Tsiperson, V., Y. Huang, I. Bagayogo, Y. Song, M. W. VonDran, E. DiCicco-Bloom, and C. F. Dreyfus. 2015. 'Brain-derived neurotrophic factor deficiency restricts proliferation of oligodendrocyte progenitors following cuprizone-induced demyelination', *ASN Neuro*, 7.
- Tu, J. C., B. Xiao, S. Naisbitt, J. P. Yuan, R. S. Petralia, P. Brakeman, A. Doan, V. K. Aakalu, A. A. Lanahan, M. Sheng, and P. F. Worley. 1999. 'Coupling of mGluR/Homer and PSD-95 complexes by the Shank family of postsynaptic density proteins', *Neuron*, 23: 583-92.
- Ullian, E. M., S. K. Sapperstein, K. S. Christopherson, and B. A. Barres. 2001. 'Control of synapse number by glia', *Science*, 291: 657-61.
- Valerio-Gomes, B., D. M. Guimaraes, D. Szczupak, and R. Lent. 2018. 'The Absolute Number of Oligodendrocytes in the Adult Mouse Brain', *Front Neuroanat*, 12: 90.
- Van't Veer, A., Y. Du, T. Z. Fischer, D. R. Boetig, M. R. Wood, and C. F. Dreyfus. 2009. 'Brain-derived neurotrophic factor effects on oligodendrocyte progenitors of the basal forebrain are mediated through trkB and the MAP kinase pathway', *J Neurosci Res*, 87: 69-78.
- van Hall, G., M. Stromstad, P. Rasmussen, O. Jans, M. Zaar, C. Gam, B. Quistorff, N. H. Secher, and H. B. Nielsen. 2009. 'Blood lactate is an important energy source for the human brain', *J Cereb Blood Flow Metab*, 29: 1121-9.
- van Praag, H., B. R. Christie, T. J. Sejnowski, and F. H. Gage. 1999. 'Running enhances neurogenesis, learning, and long-term potentiation in mice', *Proc Natl Acad Sci U S A*, 96: 13427-31.
- Vann, S. D., J. P. Aggleton, and E. A. Maguire. 2009. 'What does the retrosplenial cortex do?', *Nat Rev Neurosci*, 10: 792-802.
- Verkhatsky, A., and C. Steinhauser. 2000. 'Ion channels in glial cells', *Brain Res Brain Res Rev*, 32: 380-412.
- Vigano, F., and L. Dimou. 2016. 'The heterogeneous nature of NG2-glia', *Brain Res*, 1638: 129-37.
- Vigano, F., W. Mobius, M. Gotz, and L. Dimou. 2013. 'Transplantation reveals regional differences in oligodendrocyte differentiation in the adult brain', *Nat Neurosci*, 16: 1370-2.
- Vigano, F., S. Schneider, M. Cimino, E. Bonfanti, P. Gelosa, L. Sironi, M. P. Abbracchio, and L. Dimou. 2016. 'GPR17 expressing NG2-Glia: Oligodendrocyte progenitors serving as a reserve pool after injury', *Glia*, 64: 287-99.
- Vissing, J., M. Andersen, and N. H. Diemer. 1996. 'Exercise-induced changes in local cerebral glucose utilization in the rat', *J Cereb Blood Flow Metab*, 16: 729-36.
- von Bartheld, C. S., J. Bahney, and S. Herculano-Houzel. 2016. 'The search for true numbers of neurons and glial cells in the human brain: A review of 150 years of cell counting', *J Comp Neurol*, 524: 3865-95.
- Von Blankenfeld, G., J. Trotter, and H. Kettenmann. 1991. 'Expression and Developmental Regulation of a GABA_A Receptor in Cultured Murine Cells of the Oligodendrocyte Lineage', *Eur J Neurosci*, 3: 310-16.
- Voskuhl, R. R., R. S. Peterson, B. Song, Y. Ao, L. B. Morales, S. Tiwari-Woodruff, and M. V. Sofroniew. 2009. 'Reactive astrocytes form scar-like perivascular barriers to leukocytes during adaptive immune inflammation of the CNS', *J Neurosci*, 29: 11511-22.
- Voss, M. W., C. Soto, S. Yoo, M. Sodoma, C. Vivar, and H. van Praag. 2019. 'Exercise and Hippocampal Memory Systems', *Trends Cogn Sci*, 23: 318-33.

References

- Wake, H., A. J. Moorhouse, S. Jinno, S. Kohsaka, and J. Nabekura. 2009. 'Resting microglia directly monitor the functional state of synapses in vivo and determine the fate of ischemic terminals', *J Neurosci*, 29: 3974-80.
- Walton, N. M., B. M. Sutter, E. D. Laywell, L. H. Levkoff, S. M. Kearns, G. P. Marshall, 2nd, B. Scheffler, and D. A. Steindler. 2006. 'Microglia instruct subventricular zone neurogenesis', *Glia*, 54: 815-25.
- Walz, W., and M. K. Lang. 1998. 'Immunocytochemical evidence for a distinct GFAP-negative subpopulation of astrocytes in the adult rat hippocampus', *Neurosci Lett*, 257: 127-30.
- Walz, W., and S. Mukerji. 1988. 'Lactate production and release in cultured astrocytes', *Neurosci Lett*, 86: 296-300.
- Wang, C., H. Yue, Z. Hu, Y. Shen, J. Ma, J. Li, X. D. Wang, L. Wang, B. Sun, P. Shi, L. Wang, and Y. Gu. 2020. 'Microglia mediate forgetting via complement-dependent synaptic elimination', *Science*, 367: 688-94.
- Wang, F., S. Y. Ren, J. F. Chen, K. Liu, R. X. Li, Z. F. Li, B. Hu, J. Q. Niu, L. Xiao, J. R. Chan, and F. Mei. 2020. 'Myelin degeneration and diminished myelin renewal contribute to age-related deficits in memory', *Nat Neurosci*.
- Wang, L., H. Yang, C. Zang, Y. Dong, J. Shang, J. Chen, Y. Wang, H. Liu, Z. Zhang, H. Xu, X. Bao, and D. Zhang. 2020. 'CXCR2 antagonism promotes oligodendrocyte precursor cell differentiation and enhances remyelination in a mouse model of multiple sclerosis', *Neurobiol Dis*, 134: 104630.
- Wang, S. S., J. R. Shultz, M. J. Burish, K. H. Harrison, P. R. Hof, L. C. Towns, M. W. Wagers, and K. D. Wyatt. 2008. 'Functional trade-offs in white matter axonal scaling', *J Neurosci*, 28: 4047-56.
- Watanabe, T., J. Frahm, and T. Michaelis. 2016. 'In Vivo Brain MR Imaging at Subnanoliter Resolution: Contrast and Histology', *Magn Reson Med Sci*, 15: 11-25.
- Whelan, G., E. Kreidl, G. Wutz, A. Egner, J. M. Peters, and G. Eichele. 2012. 'Cohesin acetyltransferase *Esco2* is a cell viability factor and is required for cohesion in pericentric heterochromatin', *EMBO J*, 31: 71-82.
- Wigley, R., N. Hamilton, A. Nishiyama, F. Kirchhoff, and A. M. Butt. 2007. 'Morphological and physiological interactions of NG2-glia with astrocytes and neurons', *J Anat*, 210: 661-70.
- Williamson, A. V., J. R. Mellor, A. L. Grant, and A. D. Randall. 1998. 'Properties of GABA(A) receptors in cultured rat oligodendrocyte progenitor cells', *Neuropharmacology*, 37: 859-73.
- Wilson, H. C., N. J. Scolding, and C. S. Raine. 2006. 'Co-expression of PDGF alpha receptor and NG2 by oligodendrocyte precursors in human CNS and multiple sclerosis lesions', *J Neuroimmunol*, 176: 162-73.
- Wilson, H. L., A. C. Wong, S. R. Shaw, W. Y. Tse, G. A. Stapleton, M. C. Phelan, S. Hu, J. Marshall, and H. E. McDermid. 2003. 'Molecular characterisation of the 22q13 deletion syndrome supports the role of haploinsufficiency of SHANK3/PROSAP2 in the major neurological symptoms', *J Med Genet*, 40: 575-84.
- Windrem, M. S., S. J. Schanz, M. Guo, G. F. Tian, V. Washco, N. Stanwood, M. Rasband, N. S. Roy, M. Nedergaard, L. A. Havton, S. Wang, and S. A. Goldman. 2008. 'Neonatal chimerization with human glial progenitor cells can both remyelinate and rescue the otherwise lethally hypomyelinated shiverer mouse', *Cell Stem Cell*, 2: 553-65.

References

- Wisco, J. J., R. J. Killiany, C. R. Guttmann, S. K. Warfield, M. B. Moss, and D. L. Rosene. 2008. 'An MRI study of age-related white and gray matter volume changes in the rhesus monkey', *Neurobiol Aging*, 29: 1563-75.
- Wong, Y. H., C. M. Lee, W. Xie, B. Cui, and M. M. Poo. 2015. 'Activity-dependent BDNF release via endocytic pathways is regulated by synaptotagmin-6 and complexin', *Proc Natl Acad Sci U S A*, 112: E4475-84.
- Wood, B., I. A. van der Mei, A. L. Ponsonby, F. Pittas, S. Quinn, T. Dwyer, R. M. Lucas, and B. V. Taylor. 2013. 'Prevalence and concurrence of anxiety, depression and fatigue over time in multiple sclerosis', *Mult Scler*, 19: 217-24.
- Wright, J., G. Zhang, T. S. Yu, and S. G. Kernie. 2010. 'Age-related changes in the oligodendrocyte progenitor pool influence brain remodeling after injury', *Dev Neurosci*, 32: 499-509.
- Wu, C. W., Y. T. Chang, L. Yu, H. I. Chen, C. J. Jen, S. Y. Wu, C. P. Lo, and Y. M. Kuo. 2008. 'Exercise enhances the proliferation of neural stem cells and neurite growth and survival of neuronal progenitor cells in dentate gyrus of middle-aged mice', *J Appl Physiol (1985)*, 105: 1585-94.
- Wu, Q., R. H. Miller, R. M. Ransohoff, S. Robinson, J. Bu, and A. Nishiyama. 2000. 'Elevated levels of the chemokine GRO-1 correlate with elevated oligodendrocyte progenitor proliferation in the jimpy mutant', *J Neurosci*, 20: 2609-17.
- Wyss, M. T., R. Jolivet, A. Buck, P. J. Magistretti, and B. Weber. 2011. 'In vivo evidence for lactate as a neuronal energy source', *J Neurosci*, 31: 7477-85.
- Xiao, L., D. Ohayon, I. A. McKenzie, A. Sinclair-Wilson, J. L. Wright, A. D. Fudge, B. Emery, H. Li, and W. D. Richardson. 2016. 'Rapid production of new oligodendrocytes is required in the earliest stages of motor-skill learning', *Nat Neurosci*, 19: 1210-17.
- Xing, L., T. Yang, S. Cui, and G. Chen. 2019. 'Connexin Hemichannels in Astrocytes: Role in CNS Disorders', *Front Mol Neurosci*, 12: 23.
- Xu, G., W. Wang, and M. Zhou. 2014. 'Spatial organization of NG2 glial cells and astrocytes in rat hippocampal CA1 region', *Hippocampus*, 24: 383-95.
- Yamawaki, N., J. Radulovic, and G. M. Shepherd. 2016. 'A Corticocortical Circuit Directly Links Retrosplenial Cortex to M2 in the Mouse', *J Neurosci*, 36: 9365-74.
- Yang, H. J., L. Wang, M. Wang, S. P. Ma, B. F. Cheng, Z. C. Li, and Z. W. Feng. 2015. 'Serine/threonine-protein kinase PFTK1 modulates oligodendrocyte differentiation via PI3K/AKT pathway', *J Mol Neurosci*, 55: 977-84.
- Yang, Y., Y. Zhang, F. Luo, and B. Li. 2016. 'Chronic stress regulates NG2(+) cell maturation and myelination in the prefrontal cortex through induction of death receptor 6', *Exp Neurol*, 277: 202-14.
- Yeung, M. S. Y., M. Djelloul, E. Steiner, S. Bernard, M. Salehpour, G. Possnert, L. Brundin, and J. Frisen. 2019. 'Dynamics of oligodendrocyte generation in multiple sclerosis', *Nature*, 566: 538-42.
- Yeung, M. S., S. Zdunek, O. Bergmann, S. Bernard, M. Salehpour, K. Alkass, S. Perl, J. Tisdale, G. Possnert, L. Brundin, H. Druid, and J. Frisen. 2014. 'Dynamics of oligodendrocyte generation and myelination in the human brain', *Cell*, 159: 766-74.
- Young, D., P. A. Lawlor, P. Leone, M. Dragunow, and M. J. During. 1999. 'Environmental enrichment inhibits spontaneous apoptosis, prevents seizures and is neuroprotective', *Nat Med*, 5: 448-53.

References

- Young, K. M., K. Psachoulia, R. B. Tripathi, S. J. Dunn, L. Cossell, D. Attwell, K. Tohyama, and W. D. Richardson. 2013. 'Oligodendrocyte dynamics in the healthy adult CNS: evidence for myelin remodeling', *Neuron*, 77: 873-85.
- Yuan, X., A. M. Eisen, C. J. McBain, and V. Gallo. 1998. 'A role for glutamate and its receptors in the regulation of oligodendrocyte development in cerebellar tissue slices', *Development*, 125: 2901-14.
- Zhang, Y., K. Chen, S. A. Sloan, M. L. Bennett, A. R. Scholze, S. O'Keeffe, H. P. Phatnani, P. Guarnieri, C. Caneda, N. Ruderisch, S. Deng, S. A. Liddel, C. Zhang, R. Daneman, T. Maniatis, B. A. Barres, and J. Q. Wu. 2014. 'An RNA-sequencing transcriptome and splicing database of glia, neurons, and vascular cells of the cerebral cortex', *J Neurosci*, 34: 11929-47.
- Zhu, X., D. E. Bergles, and A. Nishiyama. 2008. 'NG2 cells generate both oligodendrocytes and gray matter astrocytes', *Development*, 135: 145-57.
- Zhu, X., R. A. Hill, D. Dietrich, M. Komitova, R. Suzuki, and A. Nishiyama. 2011. 'Age-dependent fate and lineage restriction of single NG2 cells', *Development*, 138: 745-53.
- Zia, M. T., G. Vinukonda, L. R. Vose, B. B. Bhimavarapu, S. Iacobas, N. K. Pandey, A. M. Beall, P. Dohare, E. F. LaGamma, D. A. Iacobas, and P. Ballabh. 2015. 'Postnatal glucocorticoid-induced hypomyelination, gliosis, and neurologic deficits are dose-dependent, preparation-specific, and reversible', *Exp Neurol*, 263: 200-13.
- Zielke, H. R., R. M. Collins, Jr., P. J. Baab, Y. Huang, C. L. Zielke, and J. T. Tildon. 1998. 'Compartmentation of [14C]glutamate and [14C]glutamine oxidative metabolism in the rat hippocampus as determined by microdialysis', *J Neurochem*, 71: 1315-20.
- Ziskin, J. L., A. Nishiyama, M. Rubio, M. Fukaya, and D. E. Bergles. 2007. 'Vesicular release of glutamate from unmyelinated axons in white matter', *Nat Neurosci*, 10: 321-30.
- Zonouzi, M., D. Berger, V. Jokhi, A. Kedaigle, J. Lichtman, and P. Arlotta. 2019. 'Individual Oligodendrocytes Show Bias for Inhibitory Axons in the Neocortex', *Cell Rep*, 27: 2799-808 e3.
- Zou, Y., W. Jiang, J. Wang, Z. Li, J. Zhang, J. Bu, J. Zou, L. Zhou, S. Yu, Y. Cui, W. Yang, L. Luo, Q. R. Lu, Y. Liu, M. Chen, P. F. Worley, and B. Xiao. 2014. 'Oligodendrocyte precursor cell-intrinsic effect of Rheb1 controls differentiation and mediates mTORC1-dependent myelination in brain', *J Neurosci*, 34: 15764-78.
- Zwanenburg, R. J., S. A. Ruiter, E. R. van den Heuvel, B. C. Flapper, and C. M. Van Ravenswaaij-Arts. 2016. 'Developmental phenotype in Phelan-McDermid (22q13.3 deletion) syndrome: a systematic and prospective study in 34 children', *J Neurodev Disord*, 8: 16.

Acknowledgements

Despite the fact that this Ph.D. thesis has been written in a first-personal singular pronoun, I must thank a large number of people for the success of this project, because it would not be possible without them.

First of all, I would like to thank **Leda Dimou** for the opportunity to perform my Ph.D. thesis in her laboratory and introducing me to the fascinating NG2-glia. I sincerely appreciate her supervision and both technical and theoretical advice for the completion of this project. Also, I would like to thank her for her support and mentorship not only in my academic life but also in my personal one. Thanks for being a good mentor, I am truly honored to become her first Ph.D. student as a Professor.

I would also like to thank **Benedikt Grothe** for being in my 2nd TAC member and for being 2nd reviewer of this dissertation. I am grateful for the time he takes to assist to my TAC meetings, the great comments, discussion, and suggestions. Additionally, I would like to thank him for coordinating the GSN and being one of the interviewers that allowed me to be part of this great program.

I would like to thank **Martin Kerschensteiner** for being my 3rd TAC member and his great suggestions in each meeting.

I would like to thank **Dirk Dietrich** for being my 4th TAC member and for accepting to be part of the examination of the defense. I am very grateful that he took his time to travel from Bonn to Munich whenever it is necessary, always open to give excellent advice, comments, and suggestions.

I would like to thank the **administration body and the faculty members of the GSN** for their help concerning the bureaucracy along my Ph.D. and for the many opportunities of interesting courses that they offer. Also I truly appreciate their incredible effort to form interactions among the different students of the program, and their commitment to run a great graduate school.

I would like to thank **Magdalena Götz** very much for the excellent collaboration between our laboratories back in Munich. I will always appreciate her comments and suggestions in the lab

Acknowledgements

meetings during the initial steps of my Ph.D. thesis, her enthusiasm, energy, and knowledge of science. Additionally, I would like to thank her for accepting to be my examiner for my defense. I would also like to thank **her group** for the support and the incredible work environment.

I would like to thank **Jan Deussing** for accepting to be my examiner for my defense.

I would like to thank **Dietrich Chichung Lie** for accepting to be my external reviewer of this manuscript.

I would like to thank **Thomas Wirth, Bernd Knöll, and all the members of the Institute for Physiological Chemistry** for welcoming our group to Ulm, for the support in our research, the many parties, fun moments, and the scientific collaborations. Moving to a new city and university is a hard task, but their warm welcome made things much more easy.

I would like to thank **Tobias Böckers and the members of his group** for the support and the collaborations to make possible this project.

I would like to thank the **animal caretakers from Munich and from Ulm** for their important role in keeping my animals happy.

I cannot express enough gratitude to the **old and new members of the NG2-glia group**. Thanks for the fun, the support, the scientific discussion, for making this laboratory a great working environment.

Finally, I would like to thank **my friends and family** for their mental support and company, which made my Ph.D. thesis a bit less hard.

Appendix

Supplemental Table 1. Absolute numbers of proliferating cells (BrdU⁺ cells), NG2-glia (NG2⁺ cells), proliferating NG2-glia (NG2⁺BrdU⁺ cells), and newly generated oligodendrocyte (CC1⁺BrdU⁺ cells) in *C57Bl/6* wildtype mice in cerebral GM motor cortex and piriform cortex, and WM at different time points after VPA. Data are presented as mean \pm SEM.

Brain Region	Marker	2w control [cells/mm ²]	2w VPA [cells/mm ²]	4w control [cells/mm ²]	4w VPA [cells/mm ²]	Recovery [cells/mm ²]
GM Motor Cortex	BrdU ⁺	111.20 \pm 5.81	132.60 \pm 3.95	130.30 \pm 9.82	186.60 \pm 16.27	115.60 \pm 41.56
	NG2 ⁺	230.50 \pm 16.08	245.00 \pm 11.82	240.90 \pm 15.11	230.20 \pm 9.18	209.40 \pm 11.91
	NG2 ⁺ BrdU ⁺	90.46 \pm 6.03	107.50 \pm 3.77	98.51 \pm 5.88	24.77 \pm 12.38	82.91 \pm 13.11
	CC1 ⁺ BrdU ⁺	16.26 \pm 2.22	28.41 \pm 2.84	18.40 \pm 3.21	42.34 \pm 5.11	26.59 \pm 6.09
Corpus Callosum	BrdU ⁺	-	-	427.50 \pm 17.20	417.70 \pm 18.37	-
	NG2 ⁺ BrdU ⁺	-	-	139.90 \pm 24.94	151.60 \pm 20.31	-
	CC1 ⁺ BrdU ⁺	-	-	140.50 \pm 15.3	147.30 \pm 8.37	-
GM Piriform Cortex	BrdU ⁺	-	-	167.40 \pm 18.59	152.1 \pm 24.29	-
	NG2 ⁺ BrdU ⁺	-	-	114.50 \pm 14.62	107.90 \pm 23.95	-
	CC1 ⁺ BrdU ⁺	-	-	21.79 \pm 0.95	23.25 \pm 5.03	-

Supplemental table 2. Absolute number of iNGOLs (GFP⁺CC1⁺BrdU⁺ and CC1⁺BrdU⁺ cells), dNGOLs (GFP⁺CC1⁺ but BrdU⁻ cells), and total NGOLs (iNGOLs + dNGOLs) in *NG2-CreER^{T2} x CAG-GFP* mice in the cerebral GM motor cortex after VPA. Data are presented as mean \pm SEM.

	6w control [cells/mm ²]	6w VPA [cells/mm ²]
iNGOLs	40.37 \pm 4.28	60.12 \pm 6.52
dNGOLs	41.01 \pm 6.35	99.39 \pm 14.45
Total NGOLs	80.46 \pm 8.68	159.50 \pm 20.22

Supplemental table 3. Absolute number of GPR17⁺ NG2-glia (GFP⁺GPR17⁺ cells) in *Sox10-GFP* mice in the cerebral GM motor cortex at different time points after VPA. Data are presented as mean \pm SEM.

	2w control [cells/mm ²]	2w VPA [cells/mm ²]	4w control [cells/mm ²]	4w VPA [cells/mm ²]
GFP ⁺ GPR17 ⁺	102.50 \pm 14.82	215.80 \pm 33.59	112.00 \pm 11.17	157.50 \pm 10.17

Supplemental table 4. Absolute number of recombined (GFP+ cells) GPR17+ NG2-glia that remain NG2-glia (GFP+NG2+ cells) or differentiated (GFP+CC1+ cells) in GPR17iCreER^{T2} x CAG-GFP at different time points after VPA. Data presented as mean ± SEM.

	2w control [cells/mm ²]	2w VPA [cells/mm ²]	4w control [cells/mm ²]	4w VPA [cells/mm ²]	6w control [cells/mm ²]	6w VPA [cells/mm ²]
GFP+NG2 ⁺	142.80 ± 4.28	180.10 ± 18.84	149.90 ± 13.06	174.30 ± 20.19	171.80 ± 7.99	192.40 ± 11.35
GFP+CC1 ⁺	26.29 ± 3.65	25.25 ± 3.20	31.19 ± 2.90	32.82 ± 2.08	41.41 ± 3.94	62.45 ± 5.26

Supplemental table 5. Absolute number of recombined (GFP⁺) cells and the total number of newly generated oligodendrocytes (total differentiation = GFP+CC1⁺ and CC1+BrdU⁺ cells) in *NG2-CreER^{T2}* x *CAG-GFP* mice in cerebral GM motor cortex after different time points after VPA. Data are presented as mean ± SEM.

	Control [cells/mm ²]	6w VPA [cells/mm ²]	Extensive VPA [cells/mm ²]
GFP ⁺	184.80 ± 11.38	219.10 ± 7.69	182.90 ± 13.65
Total differentiation	36.26 ± 6.17	59.12 ± 3.21	31.72 ± 4.78

Supplemental table 6. Absolute number of newly generated myelinating oligodendrocytes (MAG⁺GFP⁺ cells) in *NG2-CreER^{T2}* x *CAG-GFP* mice in the cerebral GM motor cortex after VPA. Data are presented as mean ± SEM.

	6w Control [cells/mm ²]	6w VPA [cells/mm ²]
Bin 1	6.38 ± 1.41	21.76 ± 4.81
Bin 2	16.53 ± 2.69	30.13 ± 5.44
Bin 3	7.54 ± 1.50	37.44 ± 6.30
Average whole cortex	10.15 ± 1.30	29.78 ± 5.27

Supplemental table 7. Weekly average and total average of the running performance (km/d) of *Sox10-Esco2^{wt/wt}* and *Sox10-Esco2^{fix/fix}* mice. Data are presented as mean ± SEM.

	<i>Sox10-Esco2^{wt/wt}</i> [km/d]	<i>Sox10-Esco2^{fix/fix}</i> [km/d]
Week 1	2.92 ± 0.88	1.57 ± 0.71
Week 2	9.51 ± 1.70	5.02 ± 1.46
Week 3	12.66 ± 1.45	9.09 ± 2.36
Week 4	13.72 ± 1.40	8.99 ± 1.77
Week 5	13.21 ± 2.37	11.85 ± 1.94
Week 6	14.24 ± 2.32	12.10 ± 1.57
Average per day (whole period)	11.26 ± 1.76	8.68 ± 1.54

Supplemental table 8. Total distance traveled (cm) and average speed achieved (cm/s) of *Sox10-Esco2^{wt/wt}* and *Sox10-Esco2^{flx/flx}* mice with and without VPA during the habituation phase. Data are presented as mean \pm SEM.

	No VPA Sox10- Esco2 ^{wt/wt} [cm]	No VPA Sox10- Esco2 ^{flx/flx} [cm]	VPA Sox10- Esco2 ^{wt/wt} [cm]	VPA Sox10- Esco2 ^{flx/flx} [cm]
Habituation 1.1	3060.0 \pm 226.1	3845.0 \pm 196.3	3595.0 \pm 254.7	3441.0 \pm 240.7
Habituation 1.2	2249.0 \pm 219.7	3106.0 \pm 218.2	2994.0 \pm 161.7	2661.0 \pm 271.8
Habituation 2.1	2220.0 \pm 143.9	2668.0 \pm 287.5	3038.0 \pm 110.5	3008.0 \pm 189.6
Habituation 2.2	1842.0 \pm 547.0	2661.0 \pm 282.8	2877.0 \pm 264.9	3107.0 \pm 276.9
Habituation 3.1	2150.0 \pm 190.0	2598.0 \pm 336.4	3222.0 \pm 170.5	2855.0 \pm 382.9
Habituation 3.2	2183.0 \pm 162.0	2716.0 \pm 158.3	2854.0 \pm 604.1	2550.0 \pm 442.6

	No VPA Sox10- Esco2 ^{wt/wt} [cm/s]	No VPA Sox10- Esco2 ^{flx/flx} [cm/s]	VPA Sox10- Esco2 ^{wt/wt} [cm/s]	VPA Sox10- Esco2 ^{flx/flx} [cm/s]
Habituation 1.1	5.10 \pm 0.38	6.41 \pm 0.33	6.00 \pm 0.42	5.76 \pm 0.41
Habituation 1.2	3.75 \pm 0.37	5.18 \pm 0.37	5.01 \pm 0.27	4.44 \pm 0.45
Habituation 2.1	3.72 \pm 0.25	4.45 \pm 0.48	5.07 \pm 0.18	5.09 \pm 1.07
Habituation 2.2	3.08 \pm 0.29	4.44 \pm 0.47	4.80 \pm 0.44	5.19 \pm 0.46
Habituation 3.1	3.59 \pm 0.32	4.33 \pm 0.56	5.53 \pm 0.16	4.76 \pm 0.64
Habituation 3.2	3.64 \pm 0.27	4.53 \pm 0.26	4.78 \pm 0.36	4.25 \pm 0.74

Supplemental table 9. Average exploration time (s) spent by objects of *Sox10-Esco2^{wt/wt}* and *Sox10-Esco2^{flx/flx}* mice with and without VPA during familiarization and novel object recognition phases. Average recognition index score obtained of *Sox10-Esco2^{wt/wt}* and *Sox10-Esco2^{flx/flx}* mice. Data are presented as mean \pm SEM.

	No VPA Sox10- Esco2 ^{wt/wt} [s]	No VPA Sox10- Esco2 ^{flx/flx} [s]	VPA Sox10- Esco2 ^{wt/wt} [s]	VPA Sox10- Esco2 ^{flx/flx} [s]
Familiarization phase				
Left object	11.21 \pm 0.84	11.30 \pm 1.51	11.06 \pm 1.10	10.12 \pm 0.98
Right object	8.79 \pm 0.84	8.70 \pm 1.51	8.94 \pm 1.10	9.88 \pm 0.98
Novel object recognition phase				
Familiar object	7.19 \pm 0.65	7.28 \pm 0.61	4.56 \pm 0.71	7.72 \pm 0.65
Novel object	12.81 \pm 0.65	12.72 \pm 0.61	15.44 \pm 0.71	12.28 \pm 0.65

	No VPA Sox10- Esco2 ^{wt/wt}	No VPA Sox10- Esco2 ^{flx/flx}	VPA Sox10- Esco2 ^{wt/wt}	VPA Sox10- Esco2 ^{flx/flx}
Recognition index	0.28 \pm 0.07	0.27 \pm 0.06	0.54 \pm 0.07	0.23 \pm 0.06

Supplemental table 10. Absolute number of proliferating neuroblasts (DCX⁺EdU⁺ cells) in *Sox10-Esco2*^{wt/wt} and *Sox10-Esco2*^{flx/flx} mice with and without VPA in the hippocampal subgranular zone of the dentate gyrus. Data are presented as mean ± SEM.

	No VPA Sox10- Esco2 ^{wt/wt} [cells/mm ²]	No VPA Sox10- Esco2 ^{flx/flx} [cells/mm ²]	VPA Sox10- Esco2 ^{wt/wt} [cells/mm ²]	VPA Sox10- Esco2 ^{flx/flx} [cells/mm ²]
DCX+EdU+	650.80 ± 73.09	858.80 ± 144.3	1477.00 ± 61.02	1361.00 ± 92.49

Supplemental table 11. Percentage of successful beam crossing from the total number of crossings (%) in *Shank3*^{wt/wt} and *Shank3*^{flx/flx} mice. Data are presented as mean ± SEM.

	<i>Shank3</i> ^{wt/wt} [%]	<i>Shank3</i> ^{flx/flx} [%]
Week 13	100.00 ± 0.00	50.00 ± 50.00
Week 14	100.00 ± 0.00	66.67 ± 33.33
Week 15	100.00 ± 0.00	83.33 ± 16.57
Week 16	100.00 ± 0.00	50.00 ± 50.00
Week 17	100.00 ± 0.00	66.67 ± 0.00

Supplemental table 12. Time of *Shank3*^{wt/wt} and *Shank3*^{flx/flx} mice spent on an accelerating rotarod. Data are presented as mean ± SEM.

	<i>Shank3</i> ^{wt/wt} [s]	<i>Shank3</i> ^{flx/flx} [s]
Week 13	232.20 ± 33.92	194.20 ± 25.54
Week 14	240.40 ± 51.58	196.80 ± 38.83
Week 15	265.50 ± 11.18	205.20 ± 14.50
Week 16	286.50 ± 11.18	198.50 ± 63.50
Week 17	267.30 ± 10.81	174.20 ± 10.17

Curriculum Vitae

Personal details:

Birth name: Jaime Theodore Eugenín von Bernhardt

Date and place of birth: September 9th 1989, Santiago, Chile

Education:

03.2004 – 10.2007: High school studies, Colegio Internacional SEK-Chile.

03.2008– 08.2012: Studies in Biology Licentiate, Pontificia Universidad Católica de Chile.

10.2013 – 10.2015: Master in Neuroscience Program, Graduate School of Systemic Neurosciences, Ludwig-Maximilians Universität, Munich, Germany. Supervisor: Dr. Leda Dimou.

10.2015 – present: PhD candidate in Systemic Neuroscience, Graduate School of Systemic Neurosciences, Ludwig-Maximilians Universität, Munich, Germany. Supervisor: Prof. Dr. Leda Dimou. (Currently working in Ulm Universität, Ulm)

Previous Research Experience:

12.2008 – 02.2009: Dr. Jaime Eugenín, Neural Systems Laboratory, Department of Biology, Universidad de Santiago de Chile. Research Project: “Quantal slowing of the respiratory rhythm of mouse neonates induced by somatostatin”

Techniques: Extracellular recordings of fictive respiration from ventral cervical roots originating the phrenic nerve in brainstem-spinal cord (“en bloc”) preparations obtained from mouse neonates.

01. - 02.2009: Dr. Juan Larraín, Center for Aging & Regeneration & Millenium Nucleus in Regenerative Biology, Department of Cellular and Molecular Biology, Pontificia Universidad Católica de Chile. Research Project: “Expression & Distribution of Syndecan-4 in mice during embryonic development”

Techniques: PCR for genomic determination, Immunohistochemistry, Transgenic Mice handling.

03 – 12.2010: Bachelor Thesis (tutor: Dr. Katia Gysling), Molecular and Cell Biology of Addiction Laboratory, Department of Cellular and Molecular Biology, Pontificia Universidad Católica de Chile. Research Project: “Expression, Activity & Histologic Distribution of PKM ζ after cocaine treatment in CA1 & CA3 regions of hippocampus”

Techniques: Western Blot, Animal handling (work with rats), reverse transcriptase PCR, In situ hybridization, enzymatic activity measure.

02.2011 – 05.2012: Dr. Katia Gysling, Research Project: “PKM ζ expression regulated by dopaminergic receptors in CA1 & CA3 regions of hippocampus”.

Techniques: Western Blot, Animal management (work with rats), Estereotaxis, Neuron and glia cultures, reverse transcriptase PCR, Neurobehavioral evaluations tests: “Conditional Place Preference”, Immunofluorescence and Confocal Microscopy, *In situ* hybridization.

07. – 08.2013: Drs. Larry Cohen, John Nicholls, Kenneth Muller & Jaime Eugenin. Marine Biological Laboratory (MBL), Woods Hole, Massachusetts, USA. Research project: “In vivo optical recording of calcium signal from pacemaker neurons in the respiratory column of the Brainstem”
Techniques: Extracellular recordings of fictive respiration from ventral cervical roots originating the phrenic nerve in brainstem-spinal cord (“en bloc”) preparations obtained from mouse neonates and two-photon Microscopy.

03. – 04.2014: Master’s Research Project with Prof. Dr. Michael Kiebler, Department of Anatomy III and Cell Biology, Faculty of Medicine, Ludwig-Maximilians Universität, Research Proposal: “Role of 3’UTR in the sub-cellular localization of CalM3 mRNA in Neurons”.
Techniques: Neuron cultures, Fluorescent *In situ* hybridization (FISH), plasmid cloning, Confocal Microscopy.

08. – 11.2014: Master’s Research Project with Dr. Leda Dimou, Department of Physiological Genomics, Faculty of Medicine, Ludwig-Maximilians Universität. Research Proposal: “Characterization of the Glia Composition of the 1 β -Integrin conditional Knock-out Mice”
Techniques: Mutants Mice management, immunohistochemistry, Epifluorescent & Confocal Microscopy.

10.2014 – 02.2015: Master’s Research Project with Dr. Mario Wullmann, Department of Neurobiology, Ludwig-Maximilians Universität. Research project: “Distribution of Tyrosine Hydroxylase and Orthopedia transcription factor in the zebra fish’s brain”
Techniques: Animal Management (Zebrafish), Immunohistochemistry, Epifluorescent & Confocal Microscopy.

03 – 08-2015: Master Thesis: Dr. Leda Dimou Department of Physiological Genomics, Faculty of Medicine, Ludwig-Maximilians Universität. Research project: “How does neuronal activity modify the behavior of NG2-glia”
Techniques: Immunohistochemistry, Epifluorescent & Confocal Microscopy.

Extracurricular Activities Relevant for the Field:

10. – 11.2010: IBRO’s Course in Neuroscience. Universidad de Santiago de Chile.

07.-08.2011: “Techniques in Neuroscience I: Electrophysiology” theoretical/practical course for the PhD Program in Neuroscience. Universidad de Santiago de Chile.

03.2012: “Workshop: Advance Methods for the Study of Neuronal Systems applied for the Olfative System” theoretical workshop. Universidad de Chile.

11.2012: “II International Workshop: Motivated Behavior Stress and Addiction: From molecules to behavior”. Universidad Técnica Federico Santa María de Valparaíso.

Awards:

07.10.2015: 2nd place for the best poster in the GSN Symposium Fall, Munich, Germany.

31.09.2016: YoungGlia Gold Award for young scientist, Homburg, Germany.

Scientific Congress Presentations (last 5 years):

Speaker:

30.10.2015: SFB 870 Symposium. Monastery in Seeon, Germany

31.05.2016: 2nd YoungGlia Meeting, SPP1757 for Glial heterogeneity. Homburg, Germany

Posters:

12.12.2016: SFB 870 Symposium. Monastery in Seeon, Germany

31.05.2016: 2nd YoungGlia Meeting, Sponsors: SPP1757 for Glial heterogeneity and Glial Assembly. Homburg, Germany.

03.11.2016: <interact> student conference for interdisciplinary exchange

02.03.2017: Myelin-Netzwerk's meeting in Current Topics in Myelin Research. Kassel, Germany.

16.01.2018: 3rd YoungGlia Meeting, Sponsors: SPP1757 for Glial heterogeneity and Glial Assembly. Atami, Japan.

19.01.2018: Glial assembly: a new regulatory machinery of brain function, Tokyo, Japan

10.07.2019: XIV European Meeting on Glial Cells in Health and Disease. Porto, Portugal.

Participation in scientific public outreach:

11.2014, 07.2015 & 03.2016: Participation and organization of the project: "GSN's Kid's Brain Day" promotion of neuroscience for students from kindergarten to high school. Funded by the Graduate School in Systemic Neuroscience of the Ludwig-Maximilians Universität.

03.2016: Organization of the event: Pint of science in Munich.

09.2020: Organization of the event: Pint of Science in Ulm.

Relevant skills:

Use of programs: Prisma[®] (statistics), ImagJ[®] (image analysis), Basic skills in Matlab[®] and Python[®].

Languages: Spanish (native), English (Fluent), and German (Basic)

Publication list

- 1) von Bernhardt R, **Eugenin-von Bernhardt J**, Flores B, Eugenin J (2016) "Glial Cells and Integrity of the Nervous System". *Adv. Exp. Med. Biol.* (949) p1-24
- 2) **Eugenin-von Bernhardt J**, Dimou L (2016) "NG2-glia, More Than Progenitor Cells". *Adv. Exp. Med. Biol.* (949) p27-45.
- 3) **Eugenin-von Bernhardt J, Dimou L** (2019) "Recent Advances in Live Imaging of Cells of the Oligodendrocyte Lineage". *Methods Mol Biol.* (1936) p275-294.

Eidesstattliche Versicherung/Affidavit

Hiermit versichere ich an Eides statt, dass ich die vorliegende Dissertation „**Physical activity heterogeneously modulates NG2-glia population behavior and is necessary for cognitive enhancement**“ selbstständig angefertigt habe, mich außer der angegebenen keiner weiteren Hilfsmittel bedient und alle Erkenntnisse, die aus dem Schrifttum ganz oder annähernd übernommen sind, als solche kenntlich gemacht und nach ihrer Herkunft unter Bezeichnung der Fundstelle einzeln nachgewiesen habe.

I hereby confirm that the dissertation “**Physical activity heterogeneously modulates NG2-glia population behavior and is necessary for cognitive enhancement**” is the result of my own work and that I have only used sources or materials listed and specified in the dissertation.

Ulm, den 19.11.2020
Ulm, date 19.11.2020

Jaime Eugenin von Bernhardi
Unterschrift signature

Author contributions

Jaime Eugenin von Bernhardt, Nicole Unger, Ignasi Forné, Tobias Böckers, Axel Imhoff, Leda Dimou

For this doctoral thesis, I (JEvB), contributed in the design and performed all experiments, analyzed and discussed the data with exception of the MACS and LC-MS² done by NU, who supported me with the extraction of the cortical GM and the sample preparation for proteome analysis, and IF and AI, who did the mass spectrometry on my samples and did the initial proteome analysis. TB provided us with the *Shank3^{flx/flx}* mice, which was used for the generation of the *Sox10iCreERT² x Shank3^{flx/flx} x CAG-GFP* mouse line. Finally, LD conceived and supervised the project, participated in the design of the experiments, and discussed the data.

Place, date

Signature Ph.D. candidate

Jaime Theodore Eugenin von Bernhardt

Signature Head of the Lab

Professor Dr. Leda Dimou